frontiers | Research Topics

Biomarkers of peripheral and central auditory system integrity and function

Edited by
Stefan Weder, Stephen O'Leary and
Christo William Bester

Published in
Frontiers in Neurology

ISSN 1664-8714
ISBN 978-2-8325-4493-8
DOI 10.3389/978-2-8325-4493-8

About Frontiers

Frontiers is more than just an open access publisher of scholarly articles: it is a pioneering approach to the world of academia, radically improving the way scholarly research is managed. The grand vision of Frontiers is a world where all people have an equal opportunity to seek, share and generate knowledge. Frontiers provides immediate and permanent online open access to all its publications, but this alone is not enough to realize our grand goals.

Frontiers journal series

The Frontiers journal series is a multi-tier and interdisciplinary set of open-access, online journals, promising a paradigm shift from the current review, selection and dissemination processes in academic publishing. All Frontiers journals are driven by researchers for researchers; therefore, they constitute a service to the scholarly community. At the same time, the *Frontiers journal series* operates on a revolutionary invention, the tiered publishing system, initially addressing specific communities of scholars, and gradually climbing up to broader public understanding, thus serving the interests of the lay society, too.

Dedication to quality

Each Frontiers article is a landmark of the highest quality, thanks to genuinely collaborative interactions between authors and review editors, who include some of the world's best academicians. Research must be certified by peers before entering a stream of knowledge that may eventually reach the public - and shape society; therefore, Frontiers only applies the most rigorous and unbiased reviews. Frontiers revolutionizes research publishing by freely delivering the most outstanding research, evaluated with no bias from both the academic and social point of view. By applying the most advanced information technologies, Frontiers is catapulting scholarly publishing into a new generation.

What are Frontiers Research Topics?

Frontiers Research Topics are very popular trademarks of the *Frontiers journals series*: they are collections of at least ten articles, all centered on a particular subject. With their unique mix of varied contributions from Original Research to Review Articles, Frontiers Research Topics unify the most influential researchers, the latest key findings and historical advances in a hot research area.

Find out more on how to host your own Frontiers Research Topic or contribute to one as an author by contacting the Frontiers editorial office: frontiersin.org/about/contact

Biomarkers of peripheral and central auditory system integrity and function

Topic editors

Stefan Weder — University Hospital of Bern, Switzerland

Stephen O'Leary — The University of Melbourne, Australia

Christo William Bester — The University of Melbourne, Australia

Citation

Weder, S., O'Leary, S., Bester, C. W., eds. (2024). *Biomarkers of peripheral and central auditory system integrity and function*. Lausanne: Frontiers Media SA. doi: 10.3389/978-2-8325-4493-8

Table of contents

frontiers | Frontiers in Neurology

TYPE Editorial
PUBLISHED 05 February 2024
DOI 10.3389/fneur.2024.1374844

OPEN ACCESS

EDITED AND REVIEWED BY
Michael Strupp,
Ludwig Maximilian University of Munich, Germany

*CORRESPONDENCE
Stefan Weder
✉ stefan.weder@insel.ch

RECEIVED 22 January 2024
ACCEPTED 23 January 2024
PUBLISHED 05 February 2024

CITATION
Weder S, Bester CW and O'Leary S (2024) Editorial: Biomarkers of peripheral and central auditory system integrity and function. *Front. Neurol.* 15:1374844. doi: 10.3389/fneur.2024.1374844

Editorial: Biomarkers of peripheral and central auditory system integrity and function

Stefan Weder[1]*, Christo William Bester[2] and Stephen O'Leary[2]

[1]Department of Otorhinolaryngology, Head and Neck Surgery, Inselspital, Bern University Hospital, Bern, Switzerland, [2]Department of Otolaryngology, The University of Melbourne, Melbourne, VIC, Australia

KEYWORDS

auditory system, diagnostic and therapeutic applications, patient-centered approaches, biomarkers, technological advances

Editorial on the Research Topic
Biomarkers of peripheral and central auditory system integrity and function

Objective biomarkers of auditory system integrity and function are becoming increasingly indispensable in the diagnostic, therapeutic, and rehabilitative aspects of hearing impairments. This Research Topic compiles pioneering studies on such biomarkers and measurement methods. Ranging from sophisticated genetic sequencing to advanced electrophysiological recordings and imaging methods. These techniques aim to enhance our understanding of auditory pathways, improve therapeutic indications, and provide refined patient counseling and monitoring throughout treatment.

Here, we present 10 studies that epitomize the progress in this field:

- The study by Sun et al. on the genetic etiology of Auditory Neuropathy Spectrum Disorder offers significant insights into the disorder's genetic diversity, paving the way for personalized therapy.
- Mushtaq et al.'s work demonstrates the potential for cochlear implant users to self-assess cochlear health, indicating a shift toward more autonomous patient monitoring.
- Han et al. investigate the unique cortical activation patterns in individuals with single-sided deafness, enhancing our understanding of speech processing in challenging environments.
- The research by Caldas et al. evaluates a novel assessment tool for cochlear implants, proposing enhancements in cochlear implant fittings' accuracy.
- Haggerty et al. focus on the complexities of cochlear synaptopathy, advocating for sophisticated diagnostic methods.
- The study by Chen et al. highlights the crucial impact of treatment timing on sudden sensorineural hearing loss recovery, emphasizing rapid intervention.
- Schuerch et al. employ deep learning algorithms to improve the objectivity and reliability of intracochlear electrocochleography.
- Schraivogel et al. reveal the potential of impedance subcomponents in cochlear implants as specific biomarkers for residual hearing.
- Kadowaki et al. present an objective measure for auditory temporal resolution, paving the way for improved assessments of auditory processing.

- The comparative study by Gawliczek et al. on Auditory Brainstem Response and Extracochlear Electrocochleography in evaluating coupling efficiency in middle ear implant surgery offers valuable normative data for surgical precision.

Conclusion

The studies featured in this Research Topic highlight the importance of objective biomarkers of auditory system integrity and function in enhancing the diagnosis, treatment indications, and monitoring of hearing impairments. These findings advocate for nuanced, patient-centered approaches and emphasize the significance of integrating these biomarkers into clinical practice. The continued exploration and application of these objective measures promise to enhance the lives of individuals with hearing impairments and deepen our overall understanding of the auditory system.

Author contributions

SW: Writing—original draft. CB: Writing—review & editing. SO'L: Writing—review & editing.

Funding

The author(s) declare that no financial support was received for the research, authorship, and/or publication of this article.

Conflict of interest

The authors declare that the research was conducted in the absence of any commercial or financial relationships that could be construed as a potential conflict of interest.

Publisher's note

frontiers | Frontiers in Neurology

TYPE Original Research
PUBLISHED 16 November 2022
DOI 10.3389/fneur.2022.1042408

OPEN ACCESS

EDITED BY
Stefan Weder,
Bern University Hospital, Switzerland

REVIEWED BY
P. Ashley Wackym,
Rutgers Robert Wood Johnson School of Medicine, New Brunswick, United States
Daniel John Brown,
Curtin University, Australia

*CORRESPONDENCE
Faizah Mushtaq
faizahmushtaq1@gmail.com

SPECIALTY SECTION
This article was submitted to Neuro-Otology, a section of the journal Frontiers in Neurology

RECEIVED 12 September 2022
ACCEPTED 25 October 2022
PUBLISHED 16 November 2022

CITATION
Mushtaq F, Soulby A, Boyle P, Nunn T and Hartley DEH (2022) Self-assessment of cochlear health by cochlear implant recipients. *Front. Neurol.* 13:1042408. doi: 10.3389/fneur.2022.1042408

Self-assessment of cochlear health by cochlear implant recipients

Faizah Mushtaq[1,2,3]*, Andrew Soulby[4], Patrick Boyle[5], Terry Nunn[4] and Douglas E. H. Hartley[1,2,3,6]

[1]National Institute for Health Research (NIHR) Nottingham Biomedical Research Centre (BRC), Nottingham, United Kingdom, [2]Hearing Sciences, Division of Clinical Neuroscience, School of Medicine, University of Nottingham, Nottingham, United Kingdom, [3]Rinri Therapeutics Ltd., Innovation Centre, Sheffield, United Kingdom, [4]St. Thomas' Hearing Implant Centre, St. Thomas' Hospital, London, United Kingdom, [5]Advanced Bionics GmbH, European Research Center, Hannover, Germany, [6]Nottingham University Hospitals National Health Service (NHS) Trust, Queen's Medical Centre, Nottingham, United Kingdom

Recent technological advances in cochlear implant (CI) telemetry have enabled, for the first time, CI users to perform cochlear health (CH) measurements through self-assessment for prolonged periods of time. This is important to better understand the influence of CH on CI outcomes, and to assess the safety and efficacy of future novel treatments for deafness that will be administered as adjunctive therapies to cochlear implantation. We evaluated the feasibility of using a CI to assess CH and examined patterns of electrode impedances, electrically-evoked compound action potentials (eCAPs) and electrocochleography (ECochGs), over time, in a group of adult CI recipients. Fifteen subjects were trained to use the Active Insertion Monitoring tablet by Advanced Bionics, at home for 12 weeks to independently record impedances twice daily, eCAPs once weekly and ECochGs daily in the first week, and weekly thereafter. Participants also completed behavioral hearing and speech assessments. Group level measurement compliance was 98.9% for impedances, 100% for eCAPs and 99.6% for ECochGs. Electrode impedances remained stable over time, with only minimal variation observed. Morning impedances were significantly higher than evening measurements, and impedances increased toward the base of the cochlea. eCAP thresholds were also highly repeatable, with all subjects showing 100% measurement consistency at, at least one electrode. Just over half of all subjects showed consistently absent thresholds at one or more electrodes, potentially suggesting the existence of cochlear dead regions. All subjects met UK NICE guidelines for cochlear implantation, so were expected to have little residual hearing. ECochG thresholds were, unsurprisingly, highly erratic and did not correlate with audiometric thresholds, though lower ECochG thresholds showed more repeatability over time than higher thresholds. We conclude that it is feasible for CI users to independently record CH measurements using their CI, and electrode impedances and eCAPs are promising measurements for objectively assessing CH.

KEYWORDS

cochlear implant, hearing loss, electrode impedance, electrocochleography, electrically-evoked compound action potential, neural response telemetry

Introduction

Hearing loss is principally caused by sensory hair cell death or dysfunction, and, subsequently, auditory neuron degeneration (1). Cochlear implants (CIs) are often considered the gold standard treatment for severe hearing loss and although most recipients receive benefit, outcomes vary widely (2–4). Cochlear health (CM) can be broadly defined as a cochlea free from disease, illness or injury as evidenced by good hair cell and spiral ganglion function, aligned with a lack of evidence of inflammation. Consequently, variations in CM could account for some of the variability observed in CI outcomes (5, 6). Indeed, there is a worldwide effort to develop novel biological treatments to address the deficiencies of hearing devices, such as pharmacological treatments, and stem cell and gene-based approaches (7, 8). These aim to restore natural hearing by repairing or replacing damaged cells within the inner ear. The privileged location of the inner ear creates a challenge for the delivery of such treatments and for their safety and efficacy assessments. Therefore, it is anticipated that many early-phase human trials will involve delivery of novel therapeutics as an adjunct to cochlear implantation. Until fairly recently, it has been notoriously difficult to measure CH. However, due to technological advances, an additional advantage of an adjunctive approach is that post-operative monitoring of CH can be performed telemetrically using the CI electrode (9). Unlike other assessment methods, the CI electrode provides direct access to the cochlea, enabling CH parameters to be continuously recorded.

A number of established biomarkers can be used to evaluate CH, including electrode impedances, electrically-evoked compound action potentials (eCAPs) and electrocochleography (ECochGs) (9–11). Electrode impedances are used to evaluate the interface between the intra-cochlear electrode array and the tissue surrounding it, and are sensitive to inflammatory changes within the cochlea (6, 12, 13). Whilst a direct comparison between electrode impedances and the intra-cochlear inflammatory response in human listeners is difficult, animal models have shown that inflammatory tissue growth around an electrode array in guinea pigs is positively correlated with intra-cochlear electrode impedances measurements (10). Electrode impedances have been shown to stabilize after the first few weeks and months post-implantation in functioning electrodes (14, 15).

The eCAP is a direct measurement of a synchronized neural response generated by auditory nerve fibers that makes it feasible to evaluate the health status of the auditory nerve (9, 16). It is sensitive to electrode impedances, electrode placement and the health status of auditory nerve fibers near the recording electrode (17, 18). Recent literature has focused on using the eCAP to evaluate neural survival (19–21). Although a direct comparison between eCAP responses and spiral ganglion cell density in human listeners is not feasible, animal studies have shown that spiral-ganglion nerve survival in guinea pigs is positively correlated with eCAP responses (22, 23).

An EcochG enables the non-invasive monitoring of residual acoustic auditory function, including hair cell responses, that strongly correlates with audiometric thresholds (11). Importantly, our study involved adults who fit the UK National Institute for Health and Care Excellence (NICE) criteria for cochlear implantation (24), so we expected to record few EcochG responses. The EcochG was included in the test paradigm due to the exploratory nature of this study.

Together, electrode impedances, eCAPs and ECochGs provide a multi-faceted snapshot of the health status of the cochlea. To date, these measurements have not been assessed repeatedly over time due to the reliance on patients attending clinics, making regular, long-term measurements impractical. However, recent technological advances now enable participants to take recordings themselves (25). Therefore, we sought to (i) evaluate the feasibility of using a CI to measure CH through participant self-assessment and (ii) examine the pattern of CH measurements over time. We hypothesized that our group of adult CI recipients would show stable impedances and eCAPs over time, indicating no change in the intra-cochlear inflammatory response and sensory nerve survival, respectively. We also hypothesized that (i) ECochGs would only be recorded in subjects with residual hearing, measured using Pure Tone Audiometry (PTA), (ii) that lower ECochG thresholds would show more repeatability compared with higher thresholds, and that (iii) thresholds would be lower at lower frequencies, compared to higher frequencies, of the cochlea, as that pattern of hearing loss is typically observed in deaf individuals (26).

Materials and methods

Subjects

Fifteen adult CI recipients (mean age 57.8 years; age range 33–75 years, 8 males) with a unilateral CI from Advanced Bionics for >1 year volunteered to participate in the study. All subjects could read and understand English. At the time of recruitment, no subjects had any known neurocognitive impairments likely to impact their ability to participate in the research activities or any known cochlear abnormalities likely to influence their CH measurements. Subjects were recruited from the National Institute of Health Research (NIHR) Nottingham Biomedical Research Center (BRC) Hearing Sciences participant database, the Nottingham Auditory Implant Programme and online advertisements. Written informed consent was obtained from all subjects and the study was approved by the University of Nottingham Faculty of Medicine and Health Sciences Research Ethics Committee and the West Midlands—Black Country Research Ethics Committee.

FIGURE 1
AIM system components. (1) AIM tablet; (2) CI sound processor; (3) CI headpiece magnet and cable; (4) programming cable; (5) AIM insert earphone connector; and (6) acoustic tube with yellow foam ear tip.

Equipment

Active insertion monitoring (AIM) system

The AIM system takes the form of an electronic tablet with pre-programmed CH measurement software "OM Suite" (Advanced Bionics LLC, Santa Clarita, CA) installed, enabling recordings to be made with ease (25). Typically, the AIM system is used by clinicians during CI surgery for real-time CH monitoring. Specifically, intraoperative monitoring during the insertion of the electrode array into the cochlea aims to evaluate any associations between these objective measures of CH and loss of residual acoustic hearing (27, 28). In this project, we repurposed this technology for post-implantation CH self-assessment. All participants received an AIM device, on loan to the University of Nottingham from Advanced Bionics, in order to take their own CH recordings themselves at home. A charger, connection cables, acoustic tubes and foam ear tips were also provided. Each participant also received a separate CI processor and headpiece/magnet so that they did not need to use their own clinical processors to perform the recordings. A photograph of the components of the AIM system is displayed in Figure 1. In addition to the AIM equipment, participants were also sent a memory stick to save data onto and some subjects requested a touchscreen pen. Each AIM system was stored in a carry case also provided by Advanced Bionics.

Behavioral assessments

Unaided PTA was performed using a Siemens Unity 2 Diagnostic Audiometer in a soundproof room following the procedure outlined in BSA (29). Participants did not wear their CIs or any other listening devices during this test.

Speech test stimuli were programmed in Python (Python Software Foundation, Beaverton, OR) on a Lenovo Thinkpad laptop and presented in the free field through a Genelec 8030A loudspeaker *via* an external Focusrite sound card. Participants were seated comfortably directly in front of a loudspeaker at a listening distance of 1.5 m with their CIs (and any other contralateral listening devices if usually worn) turned on. Auditory stimuli were calibrated to an average level of 70 dBA, measured at the participant's listening position without the subject present using a sound level meter (Type 2250, Brüel & Kjær, Nærum, Denmark).

Speech test stimuli included 2 Bamford-Kowal-Bench (BKB) sentence lists (30), comprised of 16 sentences in each list, and 3 Arthur Boothroyd (AB) short word lists (31), comprised of 10 words in each list, both presented in quiet and recited by a male speaker. Each BKB list has 50 key words, and each AB short word list has 30 phonemes. In both speech tests, participants were instructed to listen carefully and repeat the sentence/word heard back to the experimenter to the best of their ability. Participants were scored on their ability to correctly identify the pre-determined key words/phonemes.

CH measurements

The three CH measures were pre-programmed in OM Suite on the AIM tablet. A description of each measurement is provided below. It is important to highlight that the research team used the pre-programmed measurements as pre-set on the AIM devices and did not manipulate the coding of the measurements (beyond selecting some stimulation parameters, which are highlighted as appropriate). Also note that in Advanced Bionics CIs, electrode 1 (e1) is the most apically located electrode and e16 is positioned closest to the base of the cochlea. All measurements were performed on the implanted ear.

Electrode impedances

Electrode impedances are recorded by creating a circuit between the intra-cochlear electrode to be measured, and both the ring and case ground electrodes. A biphasic pulse with a current of 32 μA and a phase duration of 18 μs (36 μs in total) is delivered. The voltage on the intra-cochlear contacts with respect to the ground electrodes is recorded using an amplifier inside the implant. This value is digitized and transmitted using the back telemetry function to the sound processor, and then to the software application being used to make the impedance measurement. The voltage is recorded ~7 μs into the current pulse, so it primarily represents the access resistance component of the impedance. The same process is repeated for all 16 of the intra-cochlear electrode contacts and the resulting recorded voltages are used to calculate the impedance, using Ohm's Law. Dividing each recorded voltage by the 32 μA stimulation current

provides the impedance value. In this study, impedance data from all 16 electrodes was recorded.

eCAPs

Neural Response Imaging is the technique used to record eCAPs *via* the Advanced Bionics CI system (16). In order to record an eCAP threshold, current is delivered between one intra-cochlear electrode contact and the case ground electrode. A biphasic pulse with a phase duration of 32 μs is used for stimulation. Typically, the current used starts at a low level and is increased in steps until a recognizable response is obtained. In this study, the minimum eCAP stimulation level was fixed across the cohort at 100 current units (cu), but the maximum level varied from 250 to 350 cu depending on an individual's comfort level. The recording amplifier is typically configured to record from an electrode contact two positions away from the stimulating contact. This is to avoid the charge and stimulation artifact present at the stimulating contact, yet to record from the same part of the cochlea to which stimulation has been delivered. The recording amplifier is referenced to the ring ground electrode. By separating the case and ring grounds for eCAP measurements, the noise is reduced and the small neural response can be better identified. In order to reject the remaining stimulus artifact, opposite polarity, cathodic leading and anodic leading pulses are used, with the recorded voltages from each being summed. This cancels the artifact but sums the physiological response. Some 64 of these pairs of responses are averaged when recording eCAPs. In this study, eCAP thresholds were only measured at e1, e5, e9 and e13 to gain an insight into auditory nerve function from several regions along the length of the cochlear duct, whilst ensuring the measurement duration was a reasonable length for participants.

ECochGs

The ECochG recording capability of the Advanced Bionics CI system records the cochlear microphonic component of ECochG for acoustic stimulation of the cochlea. A burst of acoustic stimulation of 50 ms in duration is delivered *via* an insert earphone. Since CI recipients are typically severe-to-profoundly deaf, the level used for monitoring during insertion of the electrode array is quite high, usually ∼100–115 dB SPL. Note that the algorithm used by Advanced Bionics is: Threshold = S – 20 × log10 (C/0.25) where S is the stimulus level in dB SPL and C is the cochlear microphonic amplitude. The software then uses a single stimulus level from which to plot a linear regression. While acoustic stimulation is delivered, the potentials inside the cochlea are recorded from the most apical electrode contact, contact 1. Pairs of acoustic stimuli are delivered with opposite phases. These two recordings are then subtracted to isolate the cochlear microphonic signal. A number of subtracted pairs are averaged, typically 20, after which a data point is plotted on a cochlear microphonic vs. time plot if the signal-to-noise criterion is met (2:1 in this study). In order to estimate the cochlear microphonic amplitude, a fast-Fourier transform is performed on the time domain data, with the bins in the region of the stimulation frequency used to calculate the response amplitude. During clinical use of the AIM system, the intention is to provide real-time feedback to the surgeon, which requires a rapid measurement, producing up to 8 points per second. In this study, EcochG thresholds were recorded at 125, 250, 500, 750, 1,000, 1,500, 2,000, 3,000, and 4,000 Hz using a 115 dB HL tone-burst stimulus.

Experimental procedure

Initial set-up and AIM training

Once each eligible subject had consented and was enrolled onto the study, they were issued an AIM system. Relevant measurement settings were loaded onto each AIM tablet and the performance of the system checked by a researcher prior to being sent to subjects. Once received, participants completed at least one virtual training session with a researcher. They were instructed on how to safely perform their CH measurements and shown how to electronically share data with the research team. Maximum eCAP stimulation levels were also set for each subject during their initial training session. A minimum level of 250 cu was pre-programmed onto the AIM system by the research team and, if necessary, increased to either 300 or 350 cu during the training depending on how comfortable each participant found the stimuli to be. Subjects were also taught how to check certain settings (e.g., ECochG stimulation level and electrodes selected for eCAPs) and advised to perform these checks at the start of each week throughout the study. Note that there were no reported instances of any participant having to change any settings and all data files received were as expected, showing no indication of altered or inconsistent measurement settings. Practice measurement runs were performed during the training session and repeated until both the participant and researcher were confident that all the relevant steps had been learned. Subsequent training sessions were offered on a case-by-case basis as and when required throughout the project.

CH measurement period

CH measurements were made by participants themselves at home over a 12-week period, including electrode impedances, eCAPs and ECochGs. Electrode impedances were performed twice a day in order to examine whether recordings remained consistent throughout the day. Subjects were asked to perform the morning (denoted as AM) impedance measurements as close to the start of their day as reasonably possible and to perform the evening (denoted as PM) impedance measurements as close to the end of their day as reasonably possible. eCAPs and ECochGs

were performed less frequently in order to minimize participant burden and increase measurement compliance as they were more time consuming for subjects to perform than impedances. eCAPs were performed once a week (i.e., on day 1 of each week) and ECochGs were performed daily in the first week and weekly thereafter (i.e., on days 1–7 during week 1 and then on day 1 of each week from week 2 onwards). Each data collection session lasted ∼5–10 min in total, depending on which measurements were performed. AIM systems were returned to the research group after the testing period was completed.

Behavioral assessments

In order to investigate the correlation between CI outcomes and CH, subjects were invited to attend an in-person research appointment to complete a hearing test and speech assessments upon completion of their 12-week testing period. Note that behavioral assessments were conducted for descriptive purposes (i.e., to contrast against ECochG data) and not intended for formal data analyses. Due to the global coronavirus (COVID-19) pandemic that was ongoing throughout the study, the research appointment took place soon after the end of the testing period for some participants, whereas for others it was not carried out until several months later. This variation is not deemed remarkable since participants were experienced CI users who were expected to have stable hearing (losses). Importantly, only 13 out of the 15 participants agreed to attend the face-to-face appointment so behavioral data is not available for 2 subjects.

Data analysis

AIM data file conversion

Raw electrode impedance, eCAP and ECochG data files were converted from JSON to Microsoft Excel files using conversion software provided by Advanced Bionics. Data from Excel files were extracted using MATLAB (Mathworks, Natick, MA) and analyses were carried out in IBM SPSS Statistics for Windows Version 28.0 software (IBM Corp., Armonk, New York).

Electrode impedances

Scatter graphs of each individual's impedance measurements for all electrodes were generated, and standard deviations calculated to assess variation. In order to examine whether impedances differed between morning and evening recordings, and between different cochlear regions, eight electrode impedance values were generated per subject and entered in a repeated measures analysis of variance (RM- ANOVA). Specifically, mean individual impedance values (from the entire dataset) for e1-e4, e5-e8, e9-e12, and e13-e16 were calculated for AM and PM separately. The first within-subject factor was "timing" which had two levels (AM and PM) and the second was "cochlear region" which had four levels (e1-e4, e5-e8, e9-e12, and e13-e16).

eCAPs

Individual eCAP thresholds were plotted for the entire testing period in order to visually assess the data and identify potential cochlear dead regions. Measurement variation at each recording electrode was assessed using boxplots. Importantly, cochlear dead regions refer to parts of the cochlea where auditory neurons and/or inner hear cells are damaged or dysfunctional (32). Assessing cochlear dead regions is of great scientific and clinical importance as they inform hearing device programming and decisions (32, 33), and influence clinical outcomes (32, 34). Furthermore, changes in cochlear dead regions following administration of hearing loss treatments which aim to restore hair cell and/or auditory neuron function (e.g., 7) could help assess the success of such solutions.

ECochGs

Average thresholds were calculated for each individual at each frequency at which a successful threshold was derived. The relationship between measurement consistency and ECochG threshold was assessed with a correlation and boxplots were produced to investigate the spread of ECochG thresholds at each frequency across the group.

Behavioral assessments

A series of correlations were performed between AB phoneme scores vs. impedances and eCAPs to investigate the relationship between CI outcome vs. impedance variability and potential dead regions, respectively. A single standard deviation value was calculated from all impedances (across the entire electrode array and across all 12 weeks) for each individual and correlated against AB scores. Four mean eCAP thresholds per subject, one for each recording electrode (e1, e5, e9, and e13) were also calculated (absent thresholds were excluded), as well as the total number of successful thresholds (out of a maximum of 48 per subject). These values were then entered into five correlations with corrections made for multiple comparisons as appropriate.

Results

Participant compliance

Participant compliance was exceptionally high. A total of 27 impedances were missing out of a possible 2,520 recordings across the cohort. Specifically, compliance with twice-daily impedance recordings was either 99 or 100% in 10 subjects, and did not drop below 96% across all 15 participants in the study.

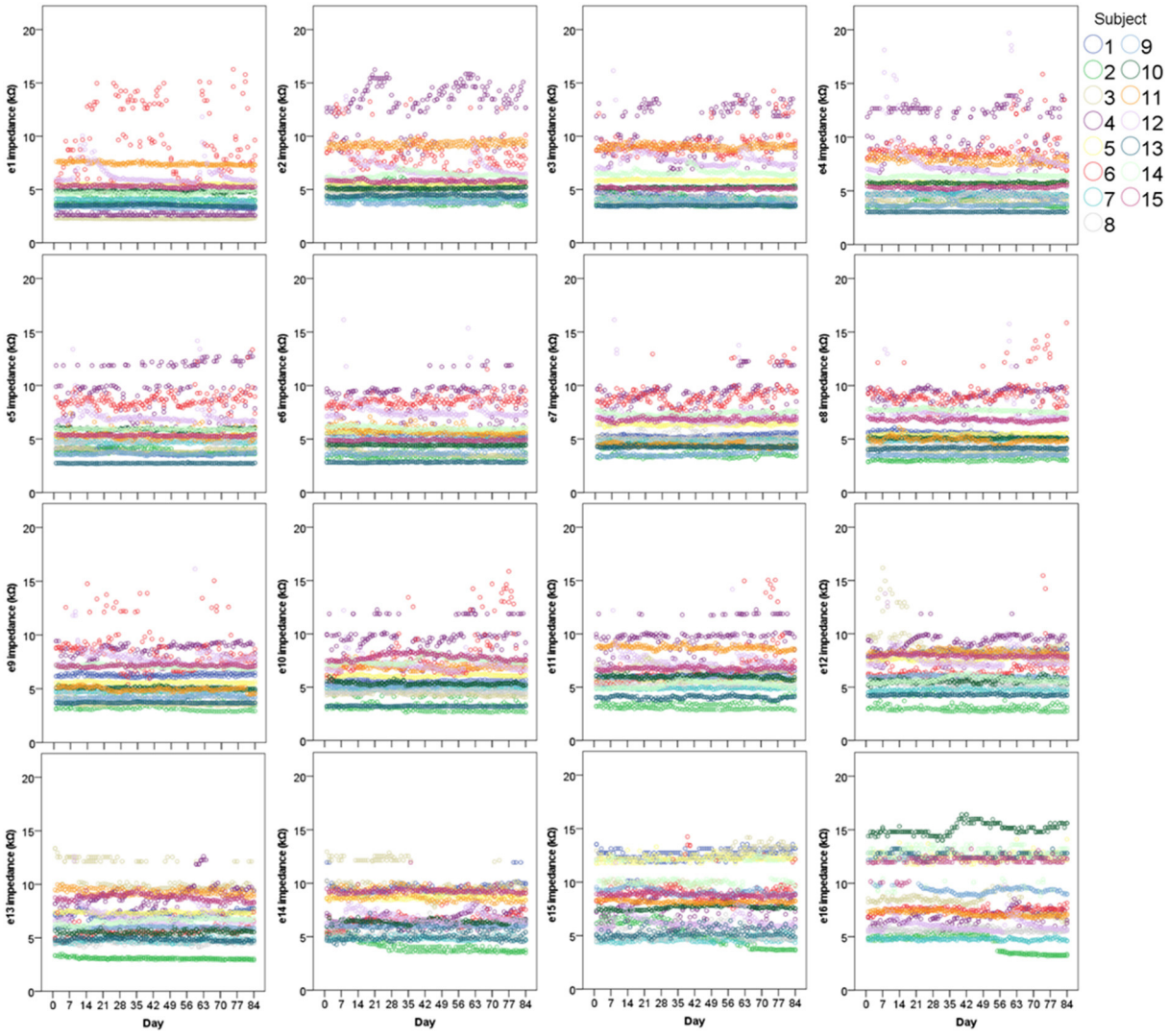

FIGURE 2
Scatter graphs displaying individual electrode impedances at all 16 electrodes over 12 weeks ($N = 15$). Two points (both AM and PM) are plotted for each day.

Only 1 ECochG recording was missed from a possible 270 across the entire group and no eCAP measurements were missed by any participant. Group level compliance with recordings was 98.9% for impedances, 100% for eCAPs and 99.6% for ECochGs.

Data exclusion

Electrode impedances from e16 in subject 1 and e14 in subject 14 were excluded from data analyses. These anomalous results were removed as they were consistently abnormally high (65 kΩ in subject 1 and ~30 kΩ in subject 14) throughout the testing period, indicating that the electrode contacts in question may be sitting in an extracochlear location and/or switched off.

CH measurements

Electrode impedances

Scatter graphs showing individual measurements over time are displayed in Figure 2. As hypothesized, impedances remained very stable over time in the majority of cases across all 16 electrodes. Importantly, even the most varied data still generally fell within the accepted normal clinical range of 2–15 kΩ (T Nauwelaers 2022, personal communication, 17 Oct).

To investigate measurement stability across the electrode array, standard deviations were calculated and plotted for each electrode contact, for each subject (see Figure 3). Variation was minimal across the electrode array for the majority of participants, with only four cases in which the

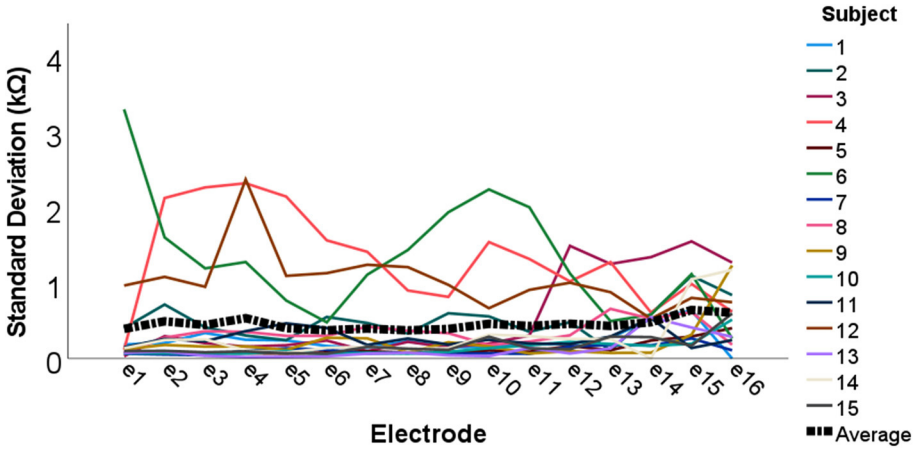

FIGURE 3
Individual and group level electrode impedance standard deviations plotted across the electrode array. Colored lines represent each individual participant ($N = 15$), and the black dotted line shows group average standard deviations.

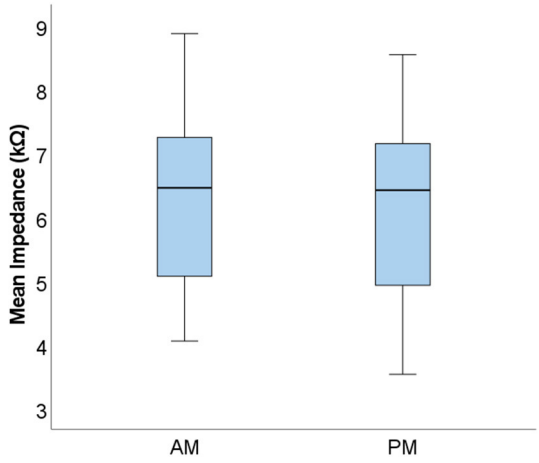

FIGURE 4
Boxplots displaying group level mean AM and PM impedances. Mean values calculated from the four electrode groupings are shown ($N = 15$).

standard deviation appeared noticeably higher, though all these measurements still fell within the clinically accepted range (T Nauwelaers 2022, personal communication, 17 Oct). Mean group level standard deviations at each electrode suggested highly stable impedances across the subject group, with a slight increase in variation at either end of the array, particularly toward the basal end of the cochlea (e15 and e16). An RM-ANOVA was performed to investigate morning vs. evening and cochlear region (e1-e4, e5-e8, e9-e12, and e13-e16) differences. There was a statistically significant main effect of timing [$F_{(1,14)} = 5.808$, $p = 0.030$] and cochlear region (F(1.316, 18.419) = 9.565, $p = 0.004$), however there was no significant interaction between the two [$F_{(3,42)} = 0.864$, $p = 0.467$]. On average, impedances were 0.111 kΩ higher ($p = 0.030$) in AM compared to PM recordings (see Figure 4). Pairwise comparisons with Bonferroni-adjusted alpha levels revealed that impedances were the highest in the most basal electrode grouping (e13-e16). Specifically, they were 2.182 kΩ ($p = 0.045$), 2.236 kΩ ($p = 0.025$) and 1.688 kΩ ($p = 0.026$) higher than the e1-e4, e5-e8, and e9-12 groupings, respectively. No other pairwise comparisons were statistically significantly different.

eCAPs

Individual eCAP thresholds across the testing period are displayed in Figure 5. In all subjects, a successful eCAP threshold was consistently derived every week from a minimum of one electrode. In the majority of cases, each subject's thresholds appeared stable and highly repeatable over time, as hypothesized. There appeared to be greater variation in responses where thresholds were higher compared to lower thresholds, which seemed to be more consistent over time. In some cases, a threshold was consistently absent over all 12 weeks at a particular electrode, as indicated by missing bars in Figure 5, which was suggestive of potential cochlear dead region(s) in the subjects in question.

The spread of the data across at each recording electrode is visualized in boxplots displayed in Figure 6 (only successful thresholds are included). Although the greatest number of outliers are found in thresholds derived from e1, these data also have the tightest interquartile range. Conversely, eCAPs from e5 are the most spread out. Furthermore, eCAP thresholds did not significantly change from the base (e13) to the apex (e1) of the cochlea.

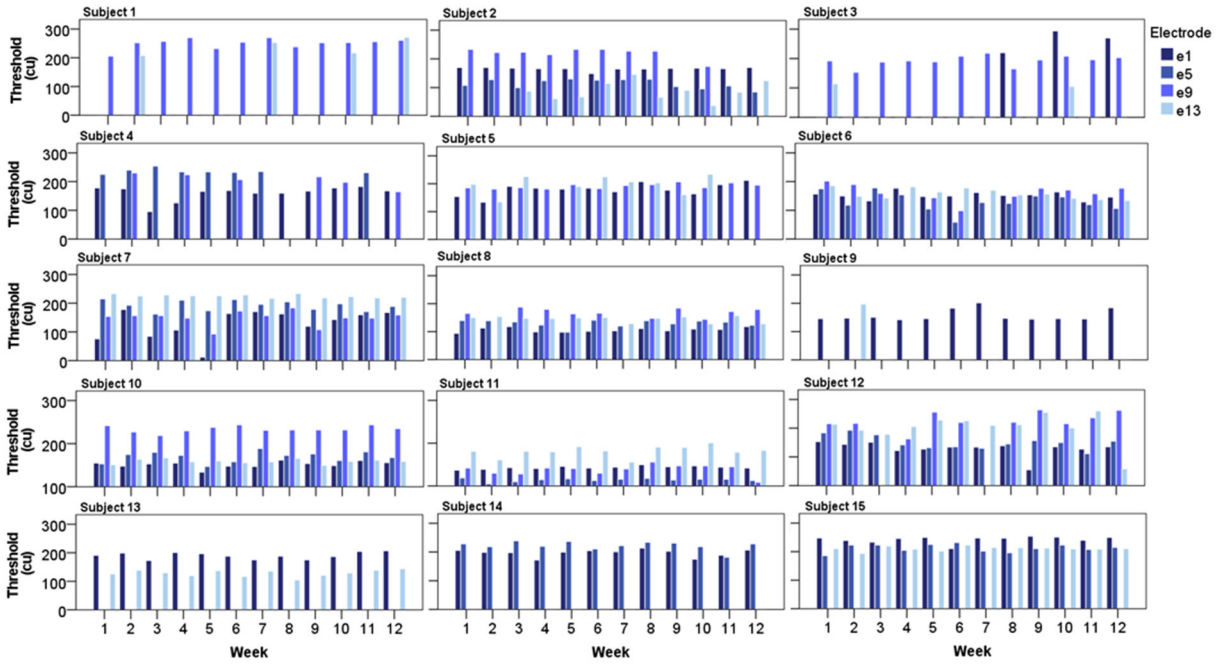

FIGURE 5
Bar charts displaying each subject's eCAP threshold from all four recording electrodes over the 12-week testing period ($N = 15$).

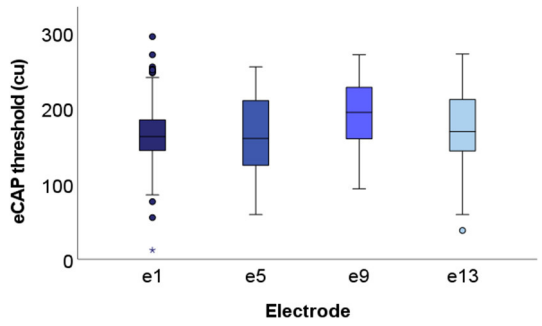

FIGURE 6
Boxplots displaying group level eCAP data at each of the four recording electrodes. All successful thresholds from the entire cohort ($N = 15$) are included. Specifically, 159, 116, 117, and 122 thresholds (out of a maximum of 180) are included from e1, e5, e9, and e13, respectively. Median values fell within the range of 150–200 cu across all four electrodes.

ECochGs

Table 1 summarizes each subject's ECochG thresholds. The number of valid thresholds varied considerably, and, in most cases, were low, though high consistency was observed in a handful of subjects. The number of hearing frequencies the thresholds were recorded at also varied extensively from subject to subject, with some individuals only showing a successful response at 2 of the frequencies recorded at, and others at all 9. In order to assess whether measurement consistency (i.e., the number of valid thresholds) was higher when the ECochG thresholds were lower, a correlation was performed between valid and average thresholds. As hypothesized, a statistically significant negative correlation was observed ($\tau b = -0.160$, $n = 75$, $p = 0.030$), indicating that lower (i.e., better) ECochG thresholds showed more repeatability over time compared with higher thresholds.

Figure 7 illustrates the spread of ECochG thresholds at each frequency across the subject group. The two lowest frequencies display the greatest variation, whereas the mid-frequencies (750–2,000 Hz) are the most consistent. As expected, ECochG thresholds overall worsen from 125 to 750 Hz after which they generally fall within the profound hearing loss range. However, since the overall number of successful thresholds recorded in the group differed quite considerably at each frequency, the ECochG data must be interpreted with this caveat in mind.

Behavioral assessments

BKB sentence test and AB short word mean test scores from the 13 subjects who completed behavioral assessments are displayed in Table 2. Most participants demonstrated high levels of sentence recognition, as indicated by the high BKB scores. As expected, AB phoneme identification scores were lower in

TABLE 1 Summary of each subject's ECochG threshold ($N = 15$).

		Frequency (Hz)								
Subject	**Threshold**	**125**	**250**	**500**	**750**	**1,000**	**1,500**	**2,000**	**3,000**	**4,000**
1	Valid (%)				6			11	28	
	Average (dB HL)				94			85	85	
2	Valid (%)	72	100	100	100	100	72	100	17	83
	Average (dB HL)	70	80	82	89	98	96	96	99	96
3	Valid (%)		17	89	100	100	100	100	33	100
	Average (dB HL)		88	96	96	96	94	93	97	90
4	Valid (%)				11	6	6	11	28	89
	Average (dB HL)				101	104	97	98	98	96
5	Valid (%)				6					6
	Average (dB HL)				93					88
6	Valid (%)			28		33	11	6		17
	Average (dB HL)			99		100	100	102		98
7	Valid (%)			6	22	17		6		44
	Average (dB HL)			92	91	92		87		86
8	Valid (%)	100	100	100	78	100	100	100	100	100
	Average (dB HL)	55	61	86	96	85	86	92	95	82
9	Valid (%)							11	33	100
	Average (dB HL)							100	98	94
10	Valid (%)					6	6	17		61
	Average (dB HL)					94	87	85		86
11	Valid (%)		44	89	89	83	83	89	89	89
	Average (dB HL)		90	94	97	95	91	91	93	91
12	Valid (%)		6	6	28		22	6	89	100
	Average (dB HL)		85	92	90		86	85	81	80
13	Valid (%)				6					11
	Average (dB HL)				97					87
14	Valid (%)									11
	Average (dB HL)									84
15	Valid (%)		1				1			3
	Average (dB HL)		86				91			86

A validity score of 100% at a given frequency indicates that a successful threshold was derived during all 18 ECochG tests performed throughout the testing period. Validity scores vary considerably from person to person and from frequency to frequency. As expected in a group of CI recipients, hearing thresholds are high.

almost all cases since due to a lack of contextual information, making the test more challenging (35).

The relationship between AB phoneme scores and cochlear health was assessed using a series of correlations. Since ECochGs were, as anticipated, highly erratic, those thresholds were not included in the analyses. Furthermore, BKB scores were not correlated due to ceiling effects since most subjects performed well.

In order to assess whether subjects with the highest variability in their impedance measurements had worse speech perception compared with those with lower variation, overall impedance standard deviations per individual were correlated against AB phoneme scores. No statistically significant correlation was observed ($r = 0.138$, $n = 13$, $p = 0.653$).

To examine the relationship between potential cochlear dead regions and speech performance, four correlations between AB scores and mean eCAP thresholds for each electrode were performed. Weak correlations were observed in all cases except between AB scores and eCAPs derived from e5, where a moderate negative correlation was found. However, none of the four correlations between speech scores and e1 thresholds ($r = 0.092$, $n = 12$, $p = 0.776$), e5 thresholds ($r = -0.666$, $n = 8$, $p = 0.071$), e9 thresholds ($\tau b = -0.087$, $n = 9$, $p = 0.750$) or e13 thresholds ($\tau b = -0.132$, $n = 11$, $p = 0.580$) were found to be statistically significant. An additional correlation of the total number of successful eCAP thresholds vs. AB scores was also carried out but no statistically significant correlation was observed once again ($r = 0.352$, $n = 13$, $p = 0.238$).

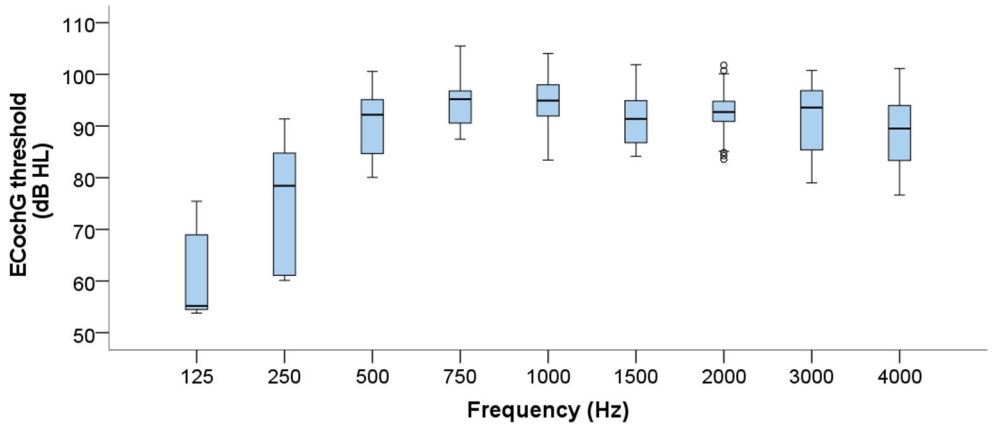

FIGURE 7
Boxplots displaying group level ECochG thresholds across the frequency range. Data from all 15 subjects are compiled, resulting in considerable differences in numbers of valid thresholds at each frequency.

TABLE 2 Mean speech test scores ($N = 13$).

Subject	BKB score (% correct)	AB score (% correct)
1	45.6	50.0
3	90.4	74.4
4	73.2	46.7
5	93.8	77.8
6	92.7	77.8
7	65.4	41.1
9	97.9	67.8
10	93.2	77.8
11	99.0	83.3
12	95.6	85.6
13	89.6	54.4
14	70.3	66.7
15	81.0	74.4

Subjects scored highly on the BKB sentence test, with 12 of 13 subjects attaining at least 70% correct. Results from the AB short word test were lower, but many participants still performed well.

PTA air conduction thresholds were derived from the implanted ear at the four key speech frequencies (500, 1,000, 2,000, and 4,000 Hz). From the 13 subjects tested, only 4 thresholds in total were successfully recorded, both at the two lower frequencies. Specifically, subject 6 had thresholds of 105 and 120 dB HL and subject 9 had thresholds of 75 and 85 dB HL, at 500 Hz and 1,000 Hz, respectively. In all other instances, no response was recorded at a maximum stimulation level of 115 dB HL at 500, 2,000, and 4,000 Hz and 120 dB HL at 1,000 Hz.

It was initially hypothesized that ECochGs would only be recorded in subjects with some degree of residual hearing, measured using PTA. However, a valid ECochG threshold was recorded at least once in every subject, with some participants demonstrating very high levels of ECochG threshold consistency but no PTA responses. Furthermore, ECochG results were not closely linked to residual hearing ability in the two individuals who did have PTA hearing thresholds. Specifically, subject 6 only showed valid ECochG thresholds at 500 and 1,000 Hz at approximately one third of the attempted measurements and subject 9 did not have any valid ECochG thresholds at the same frequencies over the entire testing period.

Discussion

To our knowledge, this is the first study to have CI recipients self-assess their CH without any clinician input on a daily basis over a 12-week period. The purpose of our work was 2 fold: (i) to evaluate the feasibility of using a CI to measure CH through participant self-assessment and (ii) to examine the pattern of electrode impedances, eCAPs and ECochGs over time. Not only were subjects very highly engaged with taking daily recordings, achieving excellent compliance results across all three measurements of interest, the results of the recordings themselves were as one would expect in the clinic, even with participants performing them at home, independently and unsupervised.

Electrode impedances were comparable with those collected from a considerably larger group of Advanced Bionics recipients in a recent study (6). In the vast majority of cases, impedances remained highly stable over time. Importantly, even when some degree of variation was observed, albeit minimal, values still fell well within the accepted normal clinical range (T Nauwelaers 2022, personal communication, 17 Oct). In the two instances (of excluded data) when values fell far beyond the normal range,

results were consistently high throughout the whole testing period. This suggests that factors relating to the CI itself, such as extracochlear electrode contacts, for example, triggered the high impedances as opposed to variation in the measurements themselves (6, 36).

Interestingly, we found that impedances recorded in the morning were higher than those performed in the evening. This may have been due to the fact that AM impedances were typically performed after a period of no electrical stimulation (i.e., overnight sleep without CI use), and previous studies have shown a reduction in impedance values following electrode stimulation, although this effect is typically observed in early days post-implantation (37, 38). It is plausible to assume impendences then steadily decreased throughout the day as a consequence of CI use, particularly since the difference itself was incredibly small (0.111 kΩ). Furthermore, consistent with previous studies (6, 39), we also found that impedances were the highest toward the base of the cochlea, at the site of surgery. This is likely due to increased osteogenesis, fibrous tissue and scarring at these cochlear regions (40).

eCAP measurements were also, in the vast majority of cases, stable over time, with every subject showing 100% measurement consistency at, at least one electrode. When eCAPs were recorded intermittently, this was typically associated with higher thresholds. It is plausible that in these instances, the maximum stimulation level and threshold were close together, resulting in erratic recordings and causing variation. A limitation of our study is that maximum stimulation levels were capped between 250 and 350 cu. Therefore, these higher thresholds might only have been reached on some occasions and not on others as a result of insufficient stimulation of the nerve (17, 18). It is likely that increasing the stimulation level in these cases would have resulted in more consistently successful thresholds being derived. However, due to participant comfort concerns and the self-assessment nature of the study, we opted not to further increase maximum eCAP stimulation levels beyond 350 cu, even when patients felt they could comfortably tolerate higher sound levels.

Just over half of all subjects recorded no eCAPs at all from particular electrodes, potentially suggesting poorer spiral ganglion coverage in corresponding regions of the cochlea (22, 23). Though the lack of eCAPs cannot guarantee the existence of dead regions, particularly since it is likely that higher stimulation levels, without the maximum limit of 350 cu, would have resulted in additional thresholds being revealed, it is still reassuring that all electrodes had consistently normal impedances. Our eCAP data suggest that daily eCAP measurements could, possibly, form one appropriate way of measuring the effectiveness of novel treatments for hearing loss. Specifically, if a therapy can be shown to reduce eCAP thresholds or enable eCAPs to be recorded from electrodes not previously possible, that could suggest the success of the therapy in increasing the population of local spiral ganglion neurons. However, an important limitation of our work is that that we only recorded from four electrodes across the array which significantly reduced the temporal resolution of our findings. Future work could implement the use of other methods that have been described to more intensively assess cochlear dead regions, such as panoramic eCAPs, for example (41, 42).

Surprisingly, although the participants were all profoundly deaf CI recipients with little-to-no expected residual hair cell function, a successful ECochG was measured at least once from at least one frequency in every individual. However, the thresholds were highly inconsistent, both between and within subjects, with only four participants displaying good levels of measurement consistency. As expected, significantly more successful recordings were made when thresholds were lower (i.e., better), with very few thresholds beyond 100 dB HL measured (though this was expected given the 115 dB HL stimulation level). Furthermore, since the ECochGs in this study were limited by their reliance on good acoustic tube and foam tip positioning, it is likely that poor placement by the subject would have impacted the recordings, which is another factor likely to have contributed to the variance. Interestingly, successful ECochGs were most likely to be recorded at 4,000 Hz, with approximately double the number of successful thresholds at this frequency compared to most other frequencies, though no behavioral thresholds were recorded at 4,000 Hz when subjects performed PTA. Although some studies have shown a strong correlation between ECochG thresholds and audiometric thresholds (11), we found no such relationship. In fact, we recorded many more ECochGs than audiometric thresholds, even though typically, ECochG signals are found at or above hearing thresholds (43). These contrasting findings highlight the unpredictable nature of the ECochG recording, particularly if it is measured by participants themselves as, unlike electrode impedances and eCAPs, the ECochG relies on an external acoustic stimulus.

We also investigated whether individuals with the highest variability in their impedance measurements, or ones with potential cochlear dead regions, differed in terms of their CI outcomes compared to subjects with lower impedance variation or those without absent eCAPs. However, we found no relationship between our CH measures and AB speech scores. This may be due to ceiling effects since the cohort were generally good CI performers and scored highly in the speech tests. This self-selection factor is a common limitation in this field since it tends to be those individuals who are doing well with their implants that come forward to participate in research. In addition, the variation observed in impedances across the group was only minimal and recordings fell within normal limits anyway (T Nauwelaers 2022, personal communication, 17 Oct). Perhaps if greater variation was observed with a higher number of very high or very low impedances, a stronger relationship with behavioral measures

may have been revealed. In addition, it is possible that our small sample did not have the power to reveal the extent of the relationship between CI outcomes and CH, if any, particularly since many of the eCAP correlations were run with only a handful of subjects as not every individual had an eCAP at every electrode (and behavioral speech data was not available for every participant).

To summarize, it is feasible for CI users to record cochlear heath data using their CIs, thus illustrating the power of using a CI to intensively assess CH. Exceptionally high participant compliance levels further indicate that subjects can themselves successfully monitor CH, even with an intensive data collection schedule of twice a day for 12 weeks. Electrode impedances and eCAPs, in particular, show good measurement consistency, making them worthy of further consideration and investigation when developing tools to objectively evaluate CH in early-phase trials of adjunctive cell-based therapies. Future work should investigate CH changes immediately following implantation in new CI recipients to assess early patterns post-implantation. Further studies involving a greater number of subjects with a greater degree of variation in CI outcomes and speech performance are required to determine the use of CH measures for assessing variation in CI outcomes.

Data availability statement

The raw data supporting the conclusions of this article will be made available by the authors, without undue reservation.

Ethics statement

The studies involving human participants were reviewed and approved by University of Nottingham Faculty of Medicine and Health Sciences Research Ethics Committee and the West Midlands - Black Country Research Ethics Committee. The patients/participants provided their written informed consent to participate in this study.

Author contributions

FM, AS, PB, TN, and DH were involved in the conception and design of the work. FM recruited participants and collected the data. Data analysis and interpretation was primarily conducted by FM, with guidance and advice offered by AS, PB, and DH. FM wrote the manuscript with technical input from PB. AS and DH commented on and reviewed the manuscript. All authors contributed to the article and approved the submitted version.

Funding

This work was joint funded by Rinri Therapeutics and a UKRI Innovation Scholars secondments: biomedical sciences award (awarded to FM, project number 70387). This paper presents independent research supported by the National Institute for Health Research (NIHR). The funders were not involved in the study design, collection, analysis, interpretation of data, the writing of this article, or the decision to submit it for publication.

Acknowledgments

The authors thank Advanced Bionics for kindly loaning the AIM devices for this study.

Conflict of interest

Author FM was seconded to Rinri Therapeutics Ltd as part of their Innovate UK award. Author PB was employed by Advanced Bionics GmbH.

The remaining authors declare that the research was conducted in the absence of any commercial or financial relationships that could be construed as a potential conflict of interest.

Publisher's note

Author disclaimer

The views expressed in this article are those of the author(s) and not necessarily those of the NHS, the NIHR, or the Department of Health and Social Care.

References

1. Wagner EL, Shin J-B. Mechanisms of hair cell damage and repair. *Trends Neurosci*. (2019) 42:414–24. doi: 10.1016/j.tins.2019.03.006

2. Contrera KJ, Betz J, Li LS, Blake CR, Sung YK, Choi JS, et al. Quality of life after intervention with a cochlear implant or hearing aid. *Laryngoscope*. (2016) 126:2110–5. doi: 10.1002/lary.25848

3. Geers AE, Sedey AL. Language and verbal reasoning skills in adolescents with 10 or more years of cochlear implant experience. *Ear Hear*. (2011) 32(1 Suppl.):39–48s. doi: 10.1097/AUD.0b013e3181fa41dc

4. Blebea CM, Ujvary LP, Necula V, Dindelegan MG, Perde-Schrepler M, Stamate MC, et al. Current concepts and future trends in increasing the benefits of cochlear implantation: a narrative review. *Medicina*. (2022) 58:747. doi: 10.3390/medicina58060747

5. Valenzuela CV, Lichtenhan JT, Lefler SM, Koka K, Buchman CA, Ortmann AJ. Intracochlear Electrocochleography and Speech Perception Scores in Cochlear Implant Recipients. Laryngoscope. (2021) 131:E2681-e8. doi: 10.1002/lary.29629

6. Caswell-Midwinter B, Doney EM, Arjmandi MK, Jahn KN, Herrmann BS, Arenberg JG. The relationship between impedance, programming and word recognition in a large clinical dataset of cochlear implant recipients. *Trends Hear*. (2022) 26:23312165211060983. doi: 10.1177/23312165211060983

7. Chen W, Jongkamonwiwat N, Abbas L, Eshtan SJ, Johnson SL, Kuhn S, et al. Restoration of auditory evoked responses by human ES-cell-derived otic progenitors. *Nature*. (2012) 490:278–82. doi: 10.1038/nature11415

8. Devarajan K, Staecker H, Detamore MS. A review of gene delivery and stem cell based therapies for regenerating inner ear hair cells. *J Funct Biomater*. (2011) 2:249–70. doi: 10.3390/jfb2030249

9. He S, Teagle HFB, Buchman CA. The electrically evoked compound action potential: from laboratory to clinic. *Front Neurosci*. (2017) 11:339. doi: 10.3389/fnins.2017.00339

10. Wilk M, Hessler R, Mugridge K, Jolly C, Fehr M, Lenarz T, et al. Impedance changes and fibrous tissue growth after cochlear implantation are correlated and can be reduced using a dexamethasone eluting electrode. *PLoS ONE*. (2016) 11:e0147552. doi: 10.1371/journal.pone.0147552

11. Koka K, Saoji AA, Litvak LM. Electrocochleography in cochlear implant recipients with residual hearing: comparison with audiometric thresholds. *Ear Hear*. (2017) 38:e161–7. doi: 10.1097/AUD.0000000000000385

12. Tykocinski M, Duan Y, Tabor B, Cowan RS. Chronic electrical stimulation of the auditory nerve using high surface area (HiQ) platinum electrodes. *Hear Res*. (2001) 159:53–68. doi: 10.1016/S0378-5955(01)00320-3

13. Hughes ML, Vander Werff KR, Brown CJ, Abbas PJ, Kelsay DMR, Teagle HFB, et al. A longitudinal study of electrode impedance, the electrically evoked compound action potential, and behavioral measures in nucleus 24 cochlear implant users. *Ear Hear*. (2001) 22:471–86. doi: 10.1097/00003446-200112000-00004

14. Dorman MF, Smith LM, Dankowski K, McCandless G, Parkin JL. Long-term measures of electrode impedance and auditory thresholds for the ineraid cochlear implant. *J Speech Lang Hear Res*. (1992) 35:1126–30. doi: 10.1044/jshr.3505.1126

15. Henkin Y, Kaplan-Neeman R, Muchnik C, Kronenberg J, Hildesheimer M. Changes over time in electrical stimulation levels and electrode impedance values in children using the Nucleus 24M cochlear implant. *Int J Pediatr Otorhinolaryngol*. (2003) 67:873–80. doi: 10.1016/S0165-5876(03)00131-9

16. Arnold L, Lindsey P, Hacking C, Boyle P. Neural response imaging (NRI) cochlear mapping: prospects for clinical application. *Cochlear Implants Int*. (2007) 8:173–88. doi: 10.1179/cim.2007.8.4.173

17. Shepherd RK, Hatsushika S, Clark GM. Electrical stimulation of the auditory nerve: the effect of electrode position on neural excitation. *Hear Res*. (1993) 66:108–20. doi: 10.1016/0378-5955(93)90265-3

18. Miller CA, Brown CJ, Abbas PJ, Chi SL. The clinical application of potentials evoked from the peripheral auditory system. *Hear Res*. (2008) 242:184–97. doi: 10.1016/j.heares.2008.04.005

19. Botros A, Psarros C. Neural response telemetry reconsidered: II. The influence of neural population on the ECAP recovery function and refractoriness. *Ear Hear*. (2010) 31:380–91. doi: 10.1097/AUD.0b013e3181cb41aa

20. Kim J-R, Tejani VD, Abbas PJ, Brown CJ. Intracochlear recordings of acoustically and electrically evoked potentials in Nucleus Hybrid L24 cochlear implant users and their relationship to speech perception. *Front Neurosci*. (2017) 11:216. doi: 10.3389/fnins.2017.00216

21. Pfingst BE, Zhou N, Colesa DJ, Watts MM, Strahl SB, Garadat SN, et al. Importance of cochlear health for implant function. *Hear Res*. (2015) 322:77–88. doi: 10.1016/j.heares.2014.09.009

22. Prado-Guitierrez P, Fewster LM, Heasman JM, McKay CM, Shepherd RK. Effect of interphase gap and pulse duration on electrically evoked potentials is correlated with auditory nerve survival. *Hear Res*. (2006) 215:47–55. doi: 10.1016/j.heares.2006.03.006

23. Ramekers D, Versnel H, Strahl SB, Smeets EM, Klis SF, Grolman W. Auditory-nerve responses to varied inter-phase gap and phase duration of the electric pulse stimulus as predictors for neuronal degeneration. *J Assoc Res Otolaryngol*. (2014) 15:187–202. doi: 10.1007/s10162-013-0440-x

24. NICE. *Cochlear implants for children and adults with severe to profound deafness: National Institute for Health and Care Excellence* (2019). Available online at: https://www.nice.org.uk/guidance/ta566/chapter/1-Recommendations (accessed May 19, 2022).

25. Bionics A. *AIM System*. Advanced Bionics (2022). Available online at: https://www.advancedbionics.com/us/en/home/professionals/aim-system.html (accessed May 13, 2022).

26. Zahnert T. The differential diagnosis of hearing loss. *Dtsch Arztebl Int*. (2011) 108:433–44. doi: 10.3238/arztebl.2011.0433

27. Campbell L, Kaicer A, Sly D, Iseli C, Wei B, Briggs R, et al. Intraoperative real-time cochlear response telemetry predicts hearing preservation in cochlear implantation. *Otol Neurotol*. (2016) 37:332–8. doi: 10.1097/MAO.0000000000000972

28. Buechner A, Bardt M, Haumann S, Geissler G, Salcher R, Lenarz T. Clinical experiences with intraoperative electrocochleography in cochlear implant recipients and its potential to reduce insertion trauma and improve postoperative hearing preservation. *PLoS ONE*. (2022) 17:e0266077. doi: 10.1371/journal.pone.0266077

29. BSA. Recommended Procedure Pure-tone air-conduction and bone-conduction threshold audiometry with and without masking. *Br Soc Audiol*. (2018):6–34. Available online at: https://www.thebsa.org.uk/wp-content/uploads/2018/11/OD104-32-Recommended-Procedure-Pure-Tone-Audiometry-August-2018-FINAL.pdf

30. Bench J, Kowal A, Bamford J. The BKB (Bamford-Kowal-Bench) sentence lists for partially-hearing children. *Br J Audiol*. (1979) 13:108–12. doi: 10.3109/03005367909078884

31. Boothroyd A. Statistical theory of the speech discrimination score. *J Acoust Soc Am*. (1968) 43:362–7. doi: 10.1121/1.1910787

32. Moore BCJ. Dead regions in the cochlea: conceptual foundations, diagnosis, and clinical applications. *Ear Hear*. (2004) 25:98–116. doi: 10.1097/01.AUD.0000120359.49711.D7

33. Zhang T, Dorman MF, Gifford R, Moore BCJ. Cochlear dead regions constrain the benefit of combining acoustic stimulation with electric stimulation. *Ear Hear*. (2014) 35:410–7. doi: 10.1097/AUD.0000000000000032

34. Baer T, Moore BCJ, Kluk K. Effects of low pass filtering on the intelligibility of speech in noise for people with and without dead regions at high frequencies. *J Acoust Soc Am*. (2002) 112:1133–44. doi: 10.1121/1.1498853

35. Vickers D, Eyles J, Brinton J, Glasberg B, Graham J. Conversion of scores between Bamford, Kowal and Bench (BKB) sentences and Arthur Boothroyd (AB) words in quiet for cochlear implant patients. *Cochlear Implants Int*. (2009) 10:142–9. doi: 10.1179/cim.2009.10.3.142

36. Goehring JL, Hughes ML, Baudhuin JL, Lusk RP. How well do cochlear implant intraoperative impedance measures predict postoperative electrode function? *Otol Neurotol*. (2013) 34:239–44. doi: 10.1097/MAO.0b013e31827c9d71

37. Masoud MZ, Pavaneh A, Hebetadin B, Muhammed K, Farzad TM. Alterations in electrode impedance values in response to electrode stimulation in the first mapping session of children using clarion cochlear implant. *J Int Adv Otol*. (2009) 5:361–364.

38. Molisz A, Zarowski A, Vermeiren A, Theunen T, De Coninck L, Siebert J, et al. Postimplantation changes of electrophysiological parameters in patients with cochlear implants. *Audiol Neurotol*. (2015) 20:222–8. doi: 10.1159/000377615

39. Sanderson AP, Rogers ETF, Verschuur CA, Newman TA. Exploiting routine clinical measures to inform strategies for better hearing performance in

cochlear implant users. *Front Neurosci*. (2018) 12:1048. doi: 10.3389/fnins.2018.01048

40. Fayad JN, Makarem AO, Linthicum FH, Jr. Histopathologic assessment of fibrosis and new bone formation in implanted human temporal bones using 3D reconstruction. *Otolaryngol Head Neck Surg*. (2009) 141:247–52. doi: 10.1016/j.otohns.2009.03.031

41. Cosentino S, DeVries L, Scheperle R, Bierer J, Carlyon R, Ieee, editors. Dual stage algorithm to identify channels with poor electrode-to-neuron interface in cochlear implant users. In: *41st IEEE International Conference on Acoustics, Speech and Signal Processing (ICASSP)*. Shanghai: PEOPLES R CHINA; New York, NY: IEEE; (2016). doi: 10.1109/ICASSP.2016.7471792

42. Garcia C, Goehring T, Cosentino S, Turner RE, Deeks JM, Brochier T, et al. The panoramic ECAP method: estimating patient-specific patterns of current spread and neural health in cochlear implant users. *Jaro*. (2021) 22:567–89. doi: 10.1007/s10162-021-00795-2

43. Dalbert A, Pfiffner F, Röösli C, Thoele K, Sim JH, Gerig R, et al. Extra- and intracochlear electrocochleography in cochlear implant recipients. *Audiol Neuro Otol*. (2015) 20:339–48. doi: 10.1159/000438742

frontiers | Frontiers in Neurology

TYPE Original Research
PUBLISHED 08 December 2022
DOI 10.3389/fneur.2022.1026695

OPEN ACCESS

EDITED BY
Stephen O'Leary,
The University of Melbourne, Australia

REVIEWED BY
Huizhan Liu,
Creighton University, United States
Lilian Downie,
Royal Children's Hospital, Australia

*CORRESPONDENCE
Lianhua Sun
sunlianhua@xinhuamed.com.cn
Jun Yang
yangjun@xinhuamed.com.cn

†These authors have contributed equally to this work

SPECIALTY SECTION
This article was submitted to Neuro-Otology, a section of the journal Frontiers in Neurology

RECEIVED 24 August 2022
ACCEPTED 14 November 2022
PUBLISHED 08 December 2022

CITATION
Sun L, Lin Z, Zhang J, Shen J, Wang X and Yang J (2022) Genetic etiological analysis of auditory neuropathy spectrum disorder by next-generation sequencing.
Front. Neurol. 13:1026695.
doi: 10.3389/fneur.2022.1026695

Genetic etiological analysis of auditory neuropathy spectrum disorder by next-generation sequencing

Lianhua Sun[1,2,3*†], Zhengyu Lin[1,2,3†], Jifang Zhang[1,2,3†], Jiali Shen[1,2,3], Xiaowen Wang[1,2,3] and Jun Yang[1,2,3*]

[1]Department of Otorhinolaryngology-Head and Neck Surgery, Xinhua Hospital, Shanghai Jiao Tong University School of Medicine, Shanghai, China, [2]Shanghai Jiao Tong University School of Medicine Ear Institute, Shanghai, China, [3]Shanghai Key Laboratory of Translational Medicine on Ear and Nose Diseases, Shanghai, China

Objective: Auditory neuropathy spectrum disease (ANSD) is caused by both environmental and genetic causes and is defined by a failure in peripheral auditory neural transmission but normal outer hair cells function. To date, 13 genes identified as potentially causing ANSD have been documented. To study the etiology of ANSD, we collected 9 probands with ANSD diagnosed in the clinic and performed targeted next-generation sequencing.

Methods: Nine probands have been identified as ANSD based on the results of the ABR tests and DPOAE/CMs. Genomic DNA extracted from their peripheral blood was examined by next-generation sequencing (NGS) for a gene panel to identify any potential causal variations. For candidate pathogenic genes, we performed co-segregation among all family members of the pedigrees. Subsequently, using a mini-gene assay, we examined the function of a novel splice site mutant of *OTOF*.

Results: We analyzed nine cases of patients with ANSD with normal CMs/DPOAE and abnormal ABR, discovered three novel mutants of the *OTOF* gene that are known to cause ANSD, and six cases of other gene mutations including *TBC1D24*, *LARS2*, *TIMM8A*, *MITF*, and *WFS1*.

Conclusion: Our results extend the mutation spectrum of the *OTOF* gene and indicate that the genetic etiology of ANSD may be related to gene mutations of *TBC1D24*, *LARS2*, *TIMM8A*, *MITF*, and *WFS1*.

KEYWORDS

auditory neuropathy spectrum disorder, targeted next-generation sequencing, gene mutation, etiological analysis, minigene assay

Introduction

Afferent nerve conduction problems combined with the proper operation of outer hair cells enduring otoacoustic emissions (OAE) and/or cochlear microphonics (CMs) are the hallmark symptoms of auditory neuropathy spectrum disease (ANSD) (1). The first case of ANSD was diagnosed by Starr et al. (2), who found that 10 individuals had

abnormal peripheral auditory neural transmission but normal outer hair cell function. The incidence of ANSD, on the other hand, is not fully clear, with studies reporting incidences ranging from <1% to almost 10% in patients with hearing impairment (3–6). The wide range of clinical characteristics in patients with ANSD in different studies (3) is reflected in the large variety of prevalence. Meanwhile, a variety of etiologies have been identified, including genetics, dysmaturity, cochlear nerve abnormalities, and prenatal infections such as measles, mumps, or cytomegalovirus—CMV. Prematurity, prenatal conditions, such as severe icterus and kernicterus, hypoxia induced by mechanical ventilation, septicemia, ototoxic medications, and meningitis were listed as postnatal causes, which might manifest symptoms later in life (3, 7, 8). Cochlear implantation is thought to be the best therapeutic option for patients with ANSD. Nevertheless, due to the widely diverse clinical treatment results, patients with ANSD who accepted cochlear implantation may experience faulty language and speech outcomes. Pre- or post-synaptic lesions or disorders of the central nervous system with hypoplasia of the auditory nerve may be relevant in this regard (9–15).

A total of 13 genes have been identified as causing ANSD thus far (16). Mutations of *OTOF*, *PJVK*, and *DIAPH3* are the most common hereditary causes of isolated ANSD (17), while *OTOF* mutations account for more than 18–41% of congenital individuals with ANSD in China (18, 19). To date, over 110 *OTOF* mutations have been identified (Human Gene Mutation Database).

In this study, we screened 9 cases of patients with ANSD who had normal results in distortion product otoacoustic emissions (DPOAE)/cochlear microphonic potentials (CM) but abnormal auditory brainstem responses (ABR); of which, we discovered 3 cases of *OTOF* gene mutation that were responsible for causing ANSD, and 6 cases of mutations in *TBC1D24*, *LARS2*, *TIMM8A*, *MITF*, and *WFS1* genes. Our research related to the etiological analysis of ANSD expanded the *OTOF* gene mutation spectrum and indicated the pathogenic role of *TBC1D24*, *LARS2*, *TIMM8A*, *MITF*, and *WFS1* genes in ANSD.

Methods

Subjects and clinical evaluations

Among 741 hearing-impaired patients undergoing genetic counseling, a total of 9 families were recruited in this study, from the department of otolaryngology-head and neck surgery of Xin Hua Hospital affiliated with Shanghai Jiao Tong University School of Medicine. Approvals were achieved by all individuals and their family members with informed consent prior to the study. Questionnaires were designed to collect the subjects' medical histories. Otological examinations were then conducted to evaluate the auditory conditions of the subjects, which included otoscopy, auditory brainstem response (ABR), pure-tone audiometric examination (PTA), cochlear microphonic potential (CM), and distortion product otoacoustic emission (DPOAE). Finally, we made the diagnosis of ANSD according to the abnormal results of ABR tests and the normal results of DPOAE/CM. This research was approved by the Ethics Committee of Xin Hua Hospital affiliated with Shanghai Jiao Tong University School of Medicine (No. XHEC-D-2021-047).

Next-generation sequencing

The genomic DNA of family members was extracted from peripheral blood leukocytes. The panel of 140 deafness-causative genes of the proband in family A diagnosed with ANSD was captured and sequenced by the Illumina sequencing platform and Hiseq X sequencer (Illumina, San Diego, CA, United States). The panel of 415 deafness-causative genes of 8 other probands diagnosed with ANSD was captured and sequenced by the Illumina sequencing platform and NextSeq 500 sequencer (Supplementary Table 1). Then, non-sense variants, frameshift, and splicing site were taken into further consideration with allele frequencies below 0.0005 for dominant inheritance and 0.005 for recessive inheritance in the 1,000 Genomes Project. Moreover, Mutation taster and SIFT software were then applied to evaluate the possible pathogenicity (20). Through targeted next-generation sequencing, potential causative variants could be detected, which were then confirmed by Sanger sequencing in each individual. Meanwhile, co-segregation analysis was also conducted for all family members if available. The three-dimensional structure of the mutation protein was built individually by SWISS-MODEL (https://swissmodel.expasy.org/) or visualized individually by Swiss-PdbViewer (http://spdbv.vital-it.ch/).

Mini-gene assay

Mini-gene assay was used to study whether the mutation near the splicing site of c.2406 + 2insT in *OTOF* affects the formation of mRNA by using vectors constructed *in vitro*. First of all, wild-type and mutant gene inserts were amplified from the genomic DNA of the proband and her mother in family B by nest PCR. Peripheral primers from forward to reverse and 5′- to 3′-, the same as below, of nest PCR were as follows: GTTGAAGTTCCCTGAAGCTCAGCCAGCTC and CCCTGGTCAGAGCTGCCCTG. Inner primers of nest PCR were as follows: CTCACTCCCCTGATCAACAG and GAAGAGCGTCTTGACCTTGGC. The inserts were cloned

TABLE 1 The gene mutations of the 9 families.

Gene	Mutation type	Nucleotide change (transcript version)	Amino acid change	InterAcmg	Mutationtaster	Pathogenic grade	SIFT (score)	Allele frequency in controls	Reference
Autosomal recessive									
OTOF	Stop coden	c.5308C > T (NM_194248)	p.Gln1770*	PVS1, PM2	Disease_causing_automatic (1)	Likely pathogenic	–	0/1,000	Novel
	Frameshift	c.4236del (NM_194248)	p.Glu1414Serfs*108	PVS1, PM2	–	Likely pathogenic	–	0/1,000	Novel
OTOF	Stop coden	c.4225A > T (NM_194248)	p.K1409*	PVS1, PM3_Strong, PM2	Disease_causing_automatic (1)	Pathogenic	–	0/1,000	PMID:23767834
	Splicing	c.2406 + 2_2406 + 3insT (NM_194248)	–	PVS1, PM2	–	Likely pathogenic	–	0/1,000	Novel
OTOF	Splicing	c.4961-3C > G (NM_194248)	–	PM3_Strong, PM2	–	Likely pathogenic	–	0/1,000	PMID:23767834
	Splicing	c.4091-1G > A (NM_194248)	–	PVS1,PM2	Disease_causing (1)	Likely pathogenic	–	0/1,000	Novel
TBC1D24	Missense	c.194G > A (NM_001199107)	p.R65H	PM2,PM5	Disease_causing (1)	Uncertain	Probably_damaging (0.997)	0/1,000	Novel
	Frameshift	c.1638delT (NM_001199107)	p.A547Pfs*21	PVS1_PM4,PM2	–	Uncertain	–	0/1,000	Novel
LARS2	Missense	c.764C > T (NM_015340)	p.A255V	PM2	Polymorphism (0.711)	Uncertain	Tolerated (0.119)	0/1,000	Novel
	Missense	c.1987C > T (NM_015340)	p.R663W	PM3_Strong,PM2,PP3	Disease_causing (1)	Likely pathogenic	Damaging (0)	0/1,000	PMID:28708303
Autosomal dominant									
TIMM8A	Frameshift	c.61_62insGGACCCGCAGTTGCAGC (NM_004085)	p.H21Rfs*11	PVS1,PM2	–	Likely pathogenic	–	0/1,000	Novel
MITF	Frameshift	c.733delA (NM_000248)	p.T245Pfs*3	PVS1,PM2	–	Likely pathogenic	–	0/1,000	Novel
WFS1	Missense	c.937C > T (NM_006005)	p.H313Y	PM3_Strong,PM2,PP3	Disease_causing (1)	Likely pathogenic	Tolerated (0.082)	0/1,000	PMID:16151413
WFS1	Missense	c.2029G > A (NM_006005)	p.A677T	PM3_Strong,PM1,PM2,PP3	Disease_causing (0.999)	Likely pathogenic	Tolerated (0.149)	0/1,000	PMID:26969326

* symbol indicates the stop codon; - symbol indicates no relevant information.

10.3389/fneur.2022.1026695

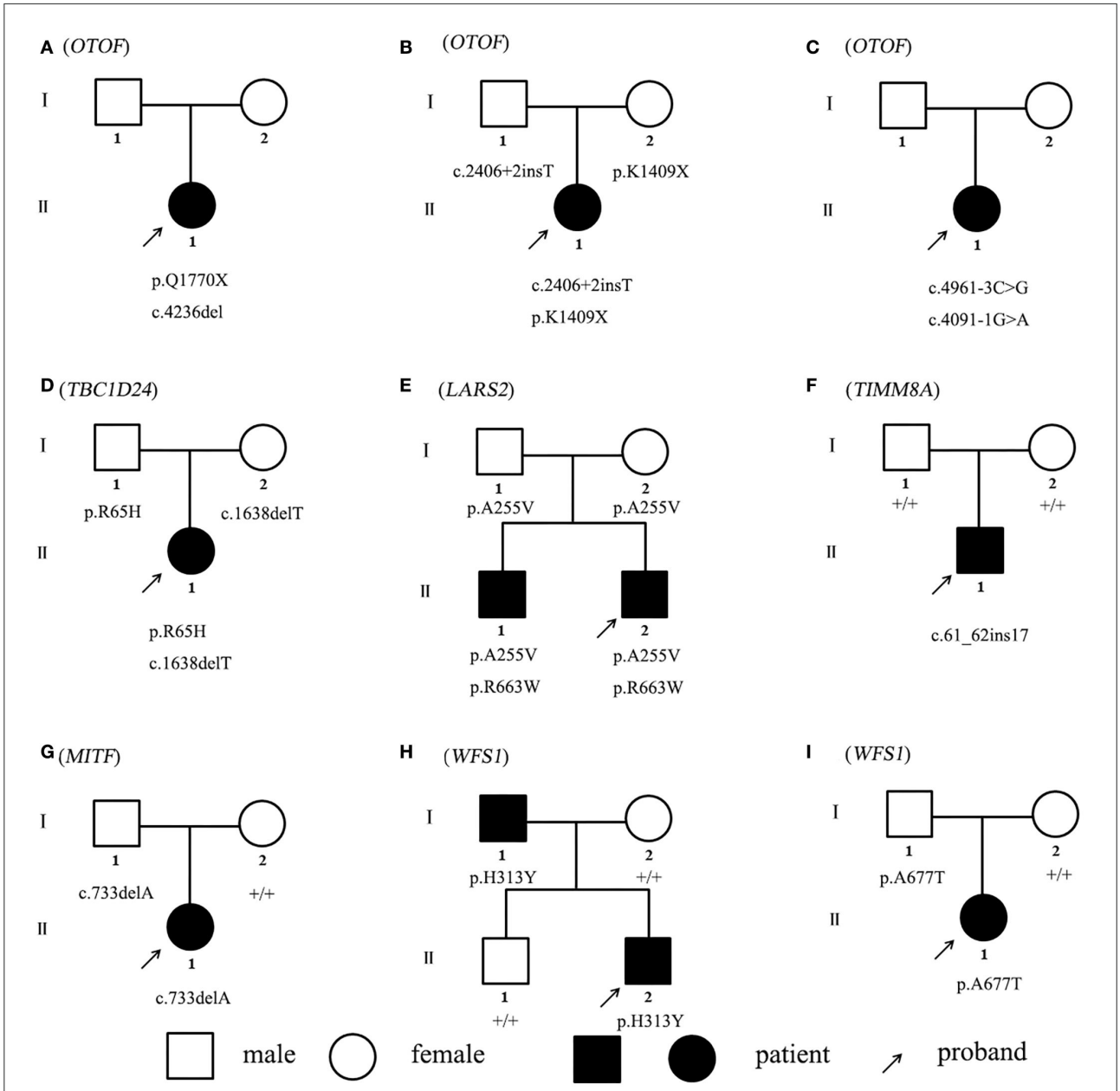

FIGURE 1
(A–I) Pedigrees of nine families. + represents the wild type after Sanger sequencing.

into the pcDNA3.1 and pEGFP-C1 vectors with multiple cloning sites. The mini-gene constructs were then transfected into HeLa and 293T cells separately using Lipofectamine^{TM} 3,000 transfection reagent (Thermo Fisher Scientific, Waltham, USA). Cells were harvested 48 h after transfection. In the end, the total RNA was extracted by Trizol (TaKaRa, Kyoto, Japan), reverse transcribed into cDNA by Hifair^{TM} reverse transcriptase (YEASEN, Shanghai, China), and the amplified products were analyzed by electrophoresis of agarose and Sanger sequencing, to confirm whether the mutant vector is spliced as wild type. The primers used to amplify the inserts cloned into pcDNA3.1 were as follows: AAACTTAAGCTTATGTGCCGCTTCCTCTCCCTCGCTG and TAGTGGATCCCTCGTCCGCCAGGAAGCGCA. The primers used to amplify the inserts cloned into pEGFP-C1 were as follows: GCTCAAGCTTCCTGCCGCTTCCTCTCCCTCGCTG and CCGCGGTACCCTCGTCCGCCAGGAAGCGCA.

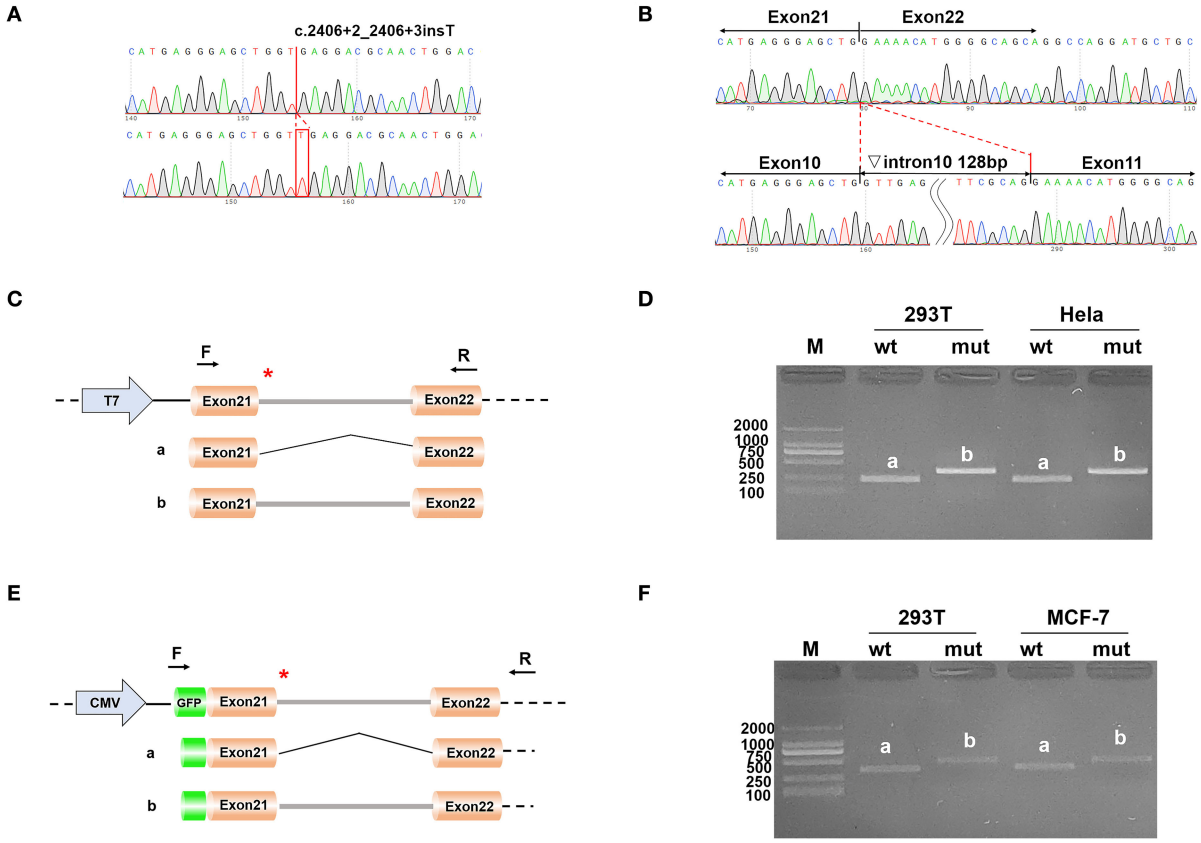

FIGURE 2
(A) The result of the selected clones by sequencing; **(B)** The result of final expressed products of cells by sequencing; **(C)** Construction strategy of pcDNA3.1 vectors; **(D)** Electrophoretic results of expression products of pcDNA3.1 vectors in cell lines; **(E)** Construction strategy of pEGFP-C1 vectors; and **(F)** Electrophoretic results of expression products of pEGFP-C1 vectors in cell lines.

Results

Clinical evaluations

Probands in the 9 Chinese families, including 5 girls and 4 boys, aged from 15 to 53 months were diagnosed with ANSD according to the abnormal results of ABR tests and normal results of DPOAE/CM. In addition to the audiological diagnosis of the probands, other members of the families need to be specifically described as follows. The father of the family G had normal hearing but excessive freckles all over his body. The father of the family H showed asymmetrical hearing loss with severe hearing loss in the right ear and mild hearing loss in the left ear in PTA testing. The proband of the family I was stunted and could not walk independently at 28 months old. His father showed normal hearing without other physical abnormalities. The parents of other families showed normal hearing without other physical abnormalities.

Genetic findings

Non-sense, frameshift, and splicing site variants with allele frequencies below 0.0005 for dominant inheritance and 0.005 for recessive inheritance were screened to detect potential causative variants by targeted NGS. Candidate causative variants are shown in Table 1. In the five recessive families, bi-allelic mutations identified in known deafness genes were confirmed by parental genotyping, including p.Q1770X + c.4263delC in *OTOF* (OMIM 603681) for Family A, c.2406 + 2insT + p.K1409X in *OTOF* (OMIM 603681) for Family B, c.4961-3C > G + c.4091-1G > A in *OTOF* (OMIM 603681) for Family C, p.R65H + c.1638delT in *TBC1D24* (OMIM 613577) for Family D, and p.A255V + p.R663W in *LARS2* (OMIM 604544) for Family E (Table 1). While in the four dominant families, we identified four dominant deafness-related heterozygous variants, c.61_62insGGACCCGCAGTTGCAGC in *TIMM8A* (OMIM 300356) for Family F, c.733delA in *MITF* (OMIM 156845) for Family G, p.H313Y in *WFS1* (OMIM 606201) for Family

H, and p.A677T in *WFS1* (OMIM 606201) for Family I, co-segregating with the hearing impairment (Figure 1). The co-segregation of the reported mutations was confirmed with the hearing phenotype in these family members by Sanger sequencing (Supplementary Table 2). Among them, there are 9 novel mutations that have not been reported previously in this study. According to ACMG guidelines, most of these mutations were classified as likely pathogenic, although there are three variations of uncertain significance, we suggest that they are important to study the etiology of the family, thus we have included them in the table (Table 1, Supplementary Figure).

Mini-gene assay of the splicing site

Two different strategies for constructing mini-genes were used (Figure 2). The wild type and mutant mini-genes were inserted into pcDNA3.1 and pEGFP-C1 vectors. A total of four recombinant vectors were transfected into different cell lines of 293T, Hela, and MCF-7. A total of eight samples were collected 48 h after transfection. The mini-gene construction strategy of pcDNA3.1-otof-wt/mut is to insert the complete fragment of exon21 (91 bp)—intron21 (127 bp)—exon22 (117 bp) of *OTOF* gene into pcDNA3.1 vector and observe whether there is abnormal splicing between exon21 and exon22 in c.2406 + 2 ins T *OTOF* mutant after transfection.

The results of RT-PCR indicated that the wild type had an electrophoretic band of the expected size (241 bp) in 293T and Hela cells, and the mutant was slightly larger than the wild type. Both wild type and mutant bands were sequenced. The sequencing results showed that the wild type was normal and its splicing mode was exon21–exon22; the mutant retained all intron21 of 128 bp, that is, the splicing mode of the mutant was exon21–intron21–exon22. We obtained the same results on the pEGFP-C1 vector, with 359 bp in the wild type and a larger electrophoretic band in the mutant (Figure 2).

Discussion

Auditory neuropathy spectrum disease is caused by defects in genes, which have been proven in previous studies in the recent two decades (3). Mutations in *OTOF* (OMIM 603681), which was the first identified gene of congenital ANSD, were the most common cause of these genetic defects (21). In previous studies, it has been elucidated that the *OTOF* gene located on chromosome 2p23.1 consists of 48 exons and encodes otoferlin, which is located in the basolateral region of the adult mammalian cochlea, and is mainly expressed in the inner hair cells, participates in the connection activities in afferent synapses. A reduction of synaptic vesicle exocytosis was observed at ribbon synapses with mutations of *OTOF* (22). Therefore, the auditory nerve function of patients with bi-allelic *OTOF* mutations could be assumed to be intact, and the site of the lesion is presumed to be presynaptic in the auditory neuron. Theoretically, good cochlear implant performance could be anticipated in patients with ANSD with *OTOF* gene mutations. This study expanded the mutation spectrum of the *OTOF* gene with four novel mutations of the *OTOF* gene identified.

The disorders associated with *TBC1D24* are characterized by some features which were described as distinct, recognized phenotypes originally, including deafness, epilepsy, intellectual disability, and osteodystrophy. The diagnosis of a *TBC1D24*-associated disorder is confirmed in an individual with bi-allelic *TBC1D24* pathogenic mutations, and the pattern of inheritance of *TBC1D24* mutation is autosomal recessive (23). *TBC1D24* is assumed to be a suitable candidate gene for ANSD for its involvement in the central nervous system and expression in the spiral ganglion (16). In this study, the family members denied that the patient had any symptoms other than deafness. Verification of future research is needed due to the two mutations of this study were classified as uncertain according to ACMG guidelines. Until now, our study is the first report of ANSD caused by *TBC1D24* mutations.

LARS2 variants are associated with disorders called Perrault syndrome (OMIM 615300) in most studies, characterized by premature ovarian failure and sensorineural hearing deafness (24). More recently, bi-allelic *LARS2* variants have been reported to lead to Perrault syndrome with neurological symptoms (25). In this study, the patients also showed symptoms of ANSD. In our study, the proband and his siblings were young boys and only showed hearing problems.

TIMM8A located in Xq22 encodes a small protein located in the mitochondrial intermembrane space associated with Deafness-dystonia-optic neuronopathy (DDON syndrome) also called Mohr–Tranebjaerg syndrome (MTS) (26). This was the first case of an 11-year-old Dutch boy with dystonia and deafness to report a *TIMM8A* mutation (27). Three patients with MTS with primary auditory neuropathy in China were the first to report *TIMM8A* variations (28). In this study, the patient developed auditory neuropathy symptoms, and the mutation was novel and *de novo*.

Heterozygous mutations in the *MITF* gene are strongly related to pigmentation disorders and deafness called Waardenburg Syndrome 2A (WS2A). Compound heterozygotes were recently elucidated in a novel syndrome involving coloboma, osteopetrosis, microphthalmia, macrocephaly, albinism, and deafness. Our previous studies have revealed that WS2A caused by *MITF* mutations is clinically related to excess freckles in Han Chinese deaf patients (29). To our knowledge, this is the first study reporting WS2A as a primary symptom of an ANSD.

WFS1 mutations lead to type 6/14/38 autosomal dominant non-syndromic deafness (DFNA) and Wolfram syndrome 1, an autosomal recessive neurodegenerative disease including deafness, optic nerve atrophy, and diabetes

insipidus (30). In this study, the inheritance pattern of Family H was autosomal dominant, while the proband exhibited symptoms of ANSD and the father exhibited symptoms of Wolfram syndrome 1 including deafness and optic nerve atrophy. The inheritance pattern of Family I was incomplete autosomal dominant, with the mutant father having no phenotype, while the mutant daughter exhibits an auditory neuropathy phenotype and developmental delay.

Conclusion

Our results from limited samples suggest that *OTOF* plays a leading role and *WFS1* plays a secondary role in the genetic etiology analysis of ANSD, which together constitute a complex genetic etiology of ANSD. Our results extend the mutation spectrum of the *OTOF* gene and indicate that the genetic etiology of ANSD may be related to gene mutations of *TBC1D24*, *LARS2*, *TIMM8A*, *MITF*, and *WFS1*.

Data availability statement

The datasets presented in this study can be found in online repositories. The name of the repository and accession number can be found below: National Center for Biotechnology Information (NCBI) BioProject, https://www.ncbi.nlm.nih.gov/bioproject/, PRJNA861021.

Ethics statement

The studies involving human participants were reviewed and approved by Ethics Committee of Xin Hua Hospital affiliated to Shanghai Jiao Tong University School of Medicine. Written informed consent to participate in this study was provided by the participants' legal guardian/next of kin.

Author contributions

LS wrote the article. ZL, JZ, JS, and XW collected the data. JY designed this study. All authors contributed to the article and approved the submitted version.

Funding

The study was supported by the National Natural Science Foundation of China with Grant/Award Number: 81873698.

Acknowledgments

We thank the family members for their cooperation in this work.

Conflict of interest

The authors declare that the research was conducted in the absence of any commercial or financial relationships that could be construed as a potential conflict of interest.

Publisher's note

Supplementary material

The Supplementary Material for this article can be found online at: https://www.frontiersin.org/articles/10.3389/fneur.2022.1026695/full#supplementary-material

References

1. Attias J, Greenstein T, Peled M, Ulanovski D, Wohlgelernter J, Raveh E. Auditory performance and electrical stimulation measures in cochlear implant recipients with auditory neuropathy compared with severe to profound sensorineural hearing loss. *Ear Hear.* (2017) 38:184–93. doi: 10.1097/AUD.0000000000000384

2. Starr A, Picton TW, Sininger Y, Hood LJ, Berlin CI. Auditory neuropathy. *Brain.* (1996) 119(Pt 3):741–53.

3. Moser T, Starr A. Auditory neuropathy-neural and synaptic mechanisms. *Nat Rev Neurol.* (2016) 12:135–49. doi: 10.1038/nrneurol.2016.10

4. Vignesh SS, Jaya V, Muraleedharan A. Prevalence and audiological characteristics of auditory neuropathy spectrum disorder in pediatric population: a retrospective study. *Indian J Otolaryngol Head Neck Surg.* (2016) 68:196–201. doi: 10.1007/s12070-014-0759-6

5. Boudewyns A, Declau F, van den Ende J, Hofkens A, Dirckx S, Van de Heyning P. Auditory neuropathy spectrum disorder (ANSD) in referrals from neonatal hearing screening at a well-baby clinic. *Eur J Pediatr.* (2016) 175:993–1000. doi: 10.1007/s00431-016-2735-5

6. Penido RC, Isaac ML. Prevalence of auditory neuropathy spectrum disorder in an auditory health care service. *Braz J Otorhinolaryngol.* (2013) 79:429–33. doi: 10.5935/1808-8694.20130077

7. Ehrmann-Müller D, Cebulla M, Rak K, Scheich M, Back D, Hagen R, et al. Evaluation and therapy outcome in children with auditory neuropathy spectrum disorder (ANSD). *Int J Pediatr Otorhinolaryngol.* (2019) 127:109681. doi: 10.1016/j.ijporl.2019.109681

8. Riggs WJ, Roche JP, Giardina CK, Harris MS, Bastian ZJ, Fontenot TE, et al. Intraoperative electrocochleographic characteristics of auditory neuropathy spectrum disorder in cochlear implant subjects. *Front Neurosci.* (2017) 11:416. doi: 10.3389/fnins.2017.00416

9. Santarelli R, Rossi R, Scimemi P, Cama E, Valentino ML, La Morgia C. OPA1-related auditory neuropathy: site of lesion and outcome of cochlear implantation. *Brain.* (2015) 138:563–76. doi: 10.1093/brain/awu378

10. Leigh J, Dettman S, Dowell R, Sarant J. Evidence: based approach for making cochlear implant recommendations for infants with residual hearing. *Ear Hear.* (2011) 32:313–22. doi: 10.1097/AUD.0b013e3182008b1c

11. Santarelli R, Starr A, Del Castillo I, Huang T, Scimemi P, Cama E, et al. Presynaptic and post-synaptic mechanisms underlying auditory neuropathy in patients with mutations in the OTOF or OPA 1 gene. *Audiol Med.* (2011) 9:59–66. doi: 10.3109/1651386X.2011.558764

12. Breneman AI, Gifford RH, Dejong MD. Cochlear implantation in children with auditory neuropathy spectrum disorder: long-term outcomes. *J Am Acad Audiol.* (2012) 23:5–17. doi: 10.3766/jaaa.23.1.2

13. Colletti L, Wilkinson EP, Colletti V. Auditory brainstem implantation after unsuccessful cochlear implantation of children with clinical diagnosis of cochlear nerve deficiency. *Ann Otol Rhinol Laryngol.* (2013) 122:605–12. doi: 10.1177/000348941312201002

14. Kutz JW, Lee KHIB, Booth TN, Sweeney MH, Roland PS. Cochlear implantation in children with cochlear nerve absence or deficiency. *Otol Neurotol.* (2011) 32:956–61. doi: 10.1097/MAO.0b013e31821f473b

15. Jeong SW, Kim LS. Auditory neuropathy spectrum disorder: predictive value of radiologic studies and electrophysiologic tests on cochlear implant outcomes and its radiologic classification. *Acta Otolaryngol.* (2013) 133:714–21. doi: 10.3109/00016489.2013.776176

16. Shearer AE, Hansen MR. Auditory synaptopathy, auditory neuropathy, and cochlear implantation. *Laryngoscope Investig Otolaryngol.* (2019) 4:429–40. doi: 10.1002/lio2.288

17. Del Castillo FJ, Del Castillo I. Genetics of isolated auditory neuropathies. *Front Biosci.* (2012) 17:1251–65. doi: 10.2741/3984

18. Chiu YH, Wu CC, Lu YC, Chen PJ, Lee WY, Liu AY, et al. Mutations in the OTOF gene in Taiwanese patients with auditory neuropathy. *Audiol Neurootol.* (2010) 15:364–74. doi: 10.1159/000293992

19. Zhang QJ, Han B, Lan L, Zong L, Shi W, Wang HY, et al. High frequency of OTOF mutations in Chinese infants with congenital auditory neuropathy spectrum disorder. *Clin Genet.* (2016) 90:238–46. doi: 10.1111/cge.12744

20. Sun L, Wang X, Hou S, Liang M, Yang J. Identification of MYO6 copy number variation associated with cochlear aplasia by targeted sequencing. *Int J Pediatr Otorhinolaryngol.* (2020) 128:109689. doi: 10.1016/j.ijporl.2019.109689

21. Lalayants MR, Mironovich OL, Bliznets EA, Markova TG, Polyakov AV, Tavartkiladze GA. OTOF-related auditory neuropathy spectrum disorder. *Vestn Otorinolaringol.* (2020) 85:21–5. doi: 10.17116/otorino20208502121

22. Roux I, Safieddine S, Nouvian R, Grati M, Simmler MC, Bahloul A, et al. Otoferlin, defective in a human deafness form, is essential for exocytosis at the auditory ribbon synapse. *Cell.* (2006) 127:277–89. doi: 10.1016/j.cell.2006.08.040

23. Balestrini S, Milh M, Castiglioni C, Lüthy K, Finelli MJ, Verstreken P, et al. TBC1D24 genotype-phenotype correlation: Epilepsies and other neurologic features. *Neurology.* (2016) 87:77–85. doi: 10.1212/WNL.0000000000002807

24. Demain LA, Urquhart JE, O'Sullivan J, Williams SG, Bhaskar SS, Jenkinson EM, et al. Expanding the genotypic spectrum of Perrault syndrome. *Clin Genet.* (2017) 91:302–12. doi: 10.1111/cge.12776

25. van der Knaap MS, Bugiani M, Mendes MI, Riley LG, Smith DEC, Rudinger-Thirion J, et al. Biallelic variants in LARS2 and KARS cause deafness and (ovario) leukodystrophy. *Neurology.* (2019) 92:e1225–37. doi: 10.1212/WNL.0000000000007098

26. Neighbors A, Moss T, Holloway L, Yu SH, Annese F, Skinner S, et al. Functional analysis of a novel mutation in the TIMM8A gene that causes deafness-dystonia-optic neuronopathy syndrome. *Mol Genet Genomic Med.* (2020) 8:e1121. doi: 10.1002/mgg3.1121

27. Tranebjaerg L, Hamel BCJ, Gabreels FJM, Renier WO, Van Ghelue M. A *de novo* missense mutation in a critical domain of the X-linked DDP gene causes the typical deafness-dystonia-optic atrophy syndrome. *Eur J Hum Genet.* (2000) 8:464–7. doi: 10.1038/sj.ejhg.5200483

28. Wang H, Wang L, Yang J, Yin L, Lan L, Li J, et al. Phenotype prediction of Mohr-Tranebjaerg syndrome (MTS) by genetic analysis and initial auditory neuropathy. *BMC Med Genet.* (2019) 20:11. doi: 10.1186/s12881-018-0741-3

29. Sun L, Li X, Shi J, Pang X, Hu Y, Wang X, et al. Molecular etiology and genotype-phenotype correlation of Chinese Han deaf patients with type I and type II Waardenburg syndrome. *Sci Rep.* (2016) 6:35498. doi: 10.1038/srep35498

30. Pallotta MT, Tascini G, Crispoldi R, Orabona C, Mondanelli G, Grohmann U, et al. Wolfram syndrome, a rare neurodegenerative disease: from pathogenesis to future treatment perspectives. *J Transl Med.* (2019) 17:238. doi: 10.1186/s12967-019-1993-1

frontiers | Frontiers in Neurology

TYPE Original Research
PUBLISHED 16 March 2023
DOI 10.3389/fneur.2023.1054105

OPEN ACCESS

EDITED BY
Stephen O'Leary,
The University of Melbourne, Australia

REVIEWED BY
Joseph Attias,
University of Haifa, Israel
Fan-Gang Zeng,
University of California, Irvine, United States

*CORRESPONDENCE
Hyo-Jeong Lee
✉ hyojlee@hallym.ac.kr

SPECIALTY SECTION
This article was submitted to Neuro-Otology, a section of the journal Frontiers in Neurology

RECEIVED 26 September 2022
ACCEPTED 27 February 2023
PUBLISHED 16 March 2023

CITATION
Han J-H, Lee J and Lee H-J (2023) The effect of noise on the cortical activity patterns of speech processing in adults with single-sided deafness. *Front. Neurol.* 14:1054105. doi: 10.3389/fneur.2023.1054105

The effect of noise on the cortical activity patterns of speech processing in adults with single-sided deafness

Ji-Hye Han[1,2], Jihyun Lee[1,2] and Hyo-Jeong Lee[1,2,3]*

[1]Laboratory of Brain and Cognitive Sciences for Convergence Medicine, Hallym University College of Medicine, Anyang, Republic of Korea, [2]Ear and Interaction Center, Doheun Institute for Digital Innovation in Medicine (D.I.D.I.M.), Hallym University Medical Center, Anyang, Republic of Korea, [3]Department of Otorhinolaryngology-Head and Neck Surgery, Hallym University College of Medicine, Chuncheon, Republic of Korea

The most common complaint in people with single-sided deafness (SSD) is difficulty in understanding speech in a noisy environment. Moreover, the neural mechanism of speech-in-noise (SiN) perception in SSD individuals is still poorly understood. In this study, we measured the cortical activity in SSD participants during a SiN task to compare with a speech-in-quiet (SiQ) task. Dipole source analysis revealed left hemispheric dominance in both left- and right-sided SSD group. Contrary to SiN listening, this hemispheric difference was not found during SiQ listening in either group. In addition, cortical activation in the right-sided SSD individuals was independent of the location of sound whereas activation sites in the left-sided SSD group were altered by the sound location. Examining the neural-behavioral relationship revealed that N1 activation is associated with the duration of deafness and the SiN perception ability of individuals with SSD. Our findings indicate that SiN listening is processed differently in the brains of left and right SSD individuals.

KEYWORDS

single-sided deafness (SSD), speech-in-noise processing, sound localization, hemispheric lateralization, auditory cortical activation

Introduction

One very common concern in individuals with single-sided deafness (SSD) is difficulty following a conversation in a noisy environment such as in classrooms and cocktail party situations. The difficulty arises due to limited accessibility to interaural cues, including the interaural time difference and the interaural level difference (1). Furthermore, this perceptual difficulty worsens with an increase in the duration or severity of hearing loss (2, 3). Nonetheless, conventional hearing-assistive devices, including bone-conduction and contralateral-routing-of-signals (CROS) hearing aids that aim to increase hearing thresholds in the auditory periphery, have shown very limited efficacy in overcoming listening difficulty (4, 5). These findings have led to the hypothesis that cortical elements such as the degree of cortical plasticity or the efficiency of neural transmission may significantly affect perceiving specific sounds in noise. Although concern over this phenomenon is widespread, there is a paucity of published studies in which researchers attempted to directly relate listening difficulty in noise to neural function in individuals with SSD.

Comprehending speech-in-noise (SiN) is a complex task involving both the auditory cortex and many other cortical regions, as evidenced by numerous neuroimaging studies (6–9). This could be because listening to and making sense of speech involves multiple steps of neural processing, including stimulus encoding, selective attention, and working memory. The multi-faceted neural processes involved in SiN perception assessed using various types of measurements such as behavioral tests (10), electrophysiology (11), and functional magnetic resonance imaging (fMRI) (12) have been applied to measure cortical processes during SiN listening. Evidence from previous studies indicates that sensory encoding in both peripheral and higher levels of cortical functioning contribute to SiN perception. For example, in listeners with normal hearing (NH), cortical alpha rhythms are related to digit-in-noise identification performance (13, 14) and those who had earlier subcortical responses reveal better SiN perception (15). These outcomes indicate that SiN listening stimulates different neural processing mechanisms from speech-in-quiet (SiQ) situations and the presence of noise alters the patterns of hemispheric lateralization in both the cortical and subcortical structures of the auditory system (16).

SiN perception is closely related to how an acoustic signal is transmitted along and transformed by the central auditory system. Given that introducing noise can disrupt signal encoding in the auditory system, noise that interferes with a signal is often referred to as a masker. Electroencephalography (EEG) has been applied to study effects of a masker on speech processing since it is sensitive to subtle neural changes and has excellent temporal resolution. Among the EEG components, it has been shown that the fidelity of N1/P2 is capable of predicting SiN performance in various populations, such as cochlear implant (CI) users and children with learning disorders (17–19). For instance, CI users revealed decreased N1 amplitude and delayed P2 latency in response to SiN listening, while the cortical responses are significantly associated with behavioral SiN measures (18). Neural responses in simulated unilateral CI users are temporally delayed for noise-vocoded speech tasks (20). Meanwhile, the patterns of hemispheric lateralization during SiN listening in individuals with SSD differ from those in NH people in that the alpha and theta neural activities are left-lateralized in the latter but greater toward the direction of the background noise in the former (21). Although the cortical processes in populations with hearing impairments during SiN listening have been investigated in recent years, only a few researchers have observed relationships between neural function and behavioral SiN performance in people with SSD. Hence, a more systematic approach to providing insight into the brain mechanism underlying SiN perception is needed.

Since spatial hearing is dependent on information based on the interaural acoustic difference and spectral cues, it is important for listening in a noisy environment as well. Moreover, unilateral hearing loss can incur deficits not only in behavioral sound localization but also in SiN perception (22, 23). Previously, we found that the cortical activity patterns evoked by the sound localization paradigm differ between left- and right-sided deafness (24). Indeed, the outcomes from previous studies suggest that sound-in-noise processing is different depending on the side of deafness. For instance, it has been reported that unlike right-sided deafness, left-sided deafness is accompanied by behavioral advantages for cognitively demanding sound localization and SiN tasks, which are likely related to higher brain functioning due to intact contralateral projection from the peripheral to the central auditory system (25). Vannson et al. (25) suggested an association between sound localization and cortical functional activity; they found that localization ability was better in participants with left-sided deafness than those with right-sided deafness and behavioral performance was related to stronger brain activation. The increased cortical activity in left-sided deafened people was assumed to be compensation for the loss of binaural hearing (26, 27). On the other hand, poorer localization performance was revealed by the right-sided deaf group, which was associated with larger activity ipsilateral to the hearing side. Moreover, prolonged reaction time to locate sound sources in the horizontal plane in right-sided deafened people offers more evidence for the functional difference with left-sided deafness, which can be interpreted as the consequence of the longer processing time needed to reach the right hemisphere in which auditory spatial cues are predominantly processed (24).

Apparent localization deficit based on auditory spatial perception after damaging areas in the auditory cortex in humans and animals, respectively, is distinctly different. In animal studies, the ability to locate sound sources on the opposite side to the damaged hemisphere is considerably decreased regardless of the ablated side (28). In contrast, damage to the right hemisphere in humans has a more pronounced effect on the ability to localize sound than damage to the left one. Zatorre and Penhune (29) suggested that damage to the right auditory cortex can disrupt spatial perception on both sides. Furthermore, it has been reported that patients with right hemisphere damage have significantly impaired sound localization from any location whereas those with left hemisphere damage are capable of locating sounds from the ipsilateral hemispace (29–31). Thus, it can be inferred that the auditory cortex in humans plays the role in supporting spatial processing and behavioral localization, which is in contrast to animals in which many aspects of sound localization can be accounted for by neural processing at the subcortical level. To determine whether unilaterally driven plasticity is different depending on the side of deafness, we compared the pattern of neural activity between left- and right-sided deafness at the cortex level in the present study.

In the current study, we measured cortical N1/P2 responses because these components are thought to be related to sensory encoding and cognitive processes, including SiN listening (32). An auditory cortical evoked response is known to be sensitive to the features of the stimulus, such as its intensity and frequency (33). Given that SiN perception relies on both accurate sensory encoding and successful cognitive processing, we expect that the N1/P2 responses are related to behavioral SiN ability in SSD people. In NH listeners, substantial changes in hemispheric lateralization for SiN tasks have been observed in that functional asymmetry shifts from the right to left hemisphere during adverse listening conditions (6). However, there is still uncertainty as to whether the rightward activation for SiN perception is consistently shown by persons with SSD. Since alteration of the functional lateralization following monaural hearing deprivation is different depending on the side of deafness (34–36), we anticipated that the SiN-induced changes in cortical activation and hemispheric laterality are distinct for left-sided and right-sided deafness. Furthermore, consistent with

10.3389/fneur.2023.1054105

TABLE 1 Clinical features of participants with single-sided deafness.

Participant	Deaf side	Age (year)	Gender	Duration of deafness (year)	Deafness onset (year)	Etiology	DE PTA threshold (dB HL)	NHE PTA thresholds (dB HL)
1	Rt	55	F	49	6	Unknown	118	10
2	Lt	76	M	7	69	ISSHL	118	11
3	Rt	64	F	6	58	ISSHL	117	13
4	Rt	58	M	3	55	Shock	83	6
5	Lt	45	M	37	8	ISSHL	87	17
6	Lt	50	F	11	39	Virus	86	6
7	Lt	42	F	34	8	Unknown	98	13
8	Rt	57	F	3	54	ISSHL	111	17
9	Rt	46	F	13	33	Cholesteatoma	79	12
10	Rt	42	M	24	18	Shock	97	5
11	Lt	51	F	10	41	Meniere's disease	110	20
12	Lt	26	F	26	1	Unknown	117.00	0.00
13	Lt	44	F	29	18	Unknown	95	12
14	Lt	23	F	22	5	ISSHL	75.00	5.00
15	Lt	43	M	1	43	ISSHL		7
16	Lt	19	M	19	1	Unknown	93.00	12.00
17	Rt	57	M	1	58	ISSHL	104	11
18	Rt	48	F	33	17	Unknown	117.00	6.00
19	Rt	54	M	3	51	Noise-induced	81	3
20	Rt	51	F	5	46	ISSHL	117	0.00

PTA, averaged thresholds of 250, 500, 1,000, 2,000, and 4,000 Hz. ISSHL (Idiopathic sudden sensorineural hearing loss); LSSD, left-sided single-sided deafness; RSSD, rightt-sided single-sided deafness; DE, deaf ear; NHE, normal hearing ear.

previous reports, we hypothesized that cortical activation is weaker and temporally prolonged as the duration of deafness becomes longer (24, 37).

Methods

Participants

Ten adults with right SSD (RSD; 6 female, mean age: 52.7 ± 6.2 years) and 10 with left SSD (LSD; 6 female, mean age: 41.9 ± 16.8 years) were recruited. All of the unilaterally deaf participants were right-handed and had profound hearing loss in one ear (average pure-tone audiometry threshold >90 dB HL) and NH (pure-tone thresholds <20 dB HL from 0.25 to 4 kHz, with evoked otoacoustic emissions) in the other ear. Neither of the unilaterally deaf groups had used a hearing aid before participating in this study. Eleven age- and gender-matched NH adults were recruited for comparison with the SSD groups (NH, 7 female, mean age: 52.2 ± 6.9 years). The NH group participants had normal pure-tone average thresholds in both ears and no neurological and cognitive issues. Informed consent was obtained from all participants prior to testing. All experimental protocols and methods were approved by the guidelines and regulations outlined in the Sacred Heart Hospital of Hallym University Institutional Review Board (IRB no. 2019-02-019) and were performed in accordance with the ethical standards laid down in the 1964 Declaration of Helsinki. A summary of the clinical data of participants with SSD is provided in Table 1.

Stimuli and procedure

Figure 1 shows an example of an acoustic sequence and the passive listening paradigm applied in this study. Natural /ba/–/pa/ speech stimuli with a noise masker at a signal to noise ratio (SNR) of +5 dB were used to evoke cortical responses. The noise masker was speech-shaped noise lasting 0.5 s created by applying the speech stimuli recorded from utterances by a male speaker and presented with speech stimuli simultaneously. The overall duration of each speech stimulus was 0.5 s, and the voice onset times were 30 and 100 ms for /ba/ and /pa/, respectively. The stimuli were presented through a StimTracker (Cedrus Corporation, CA, USA) system that allowed for EEG synchronization with the sound, and they were calibrated using a Brüel and Kjær (2260 Investigator, Nærum, Denmark) sound level meter set for frequency and slow time weighting with a ½ inch free-field microphone.

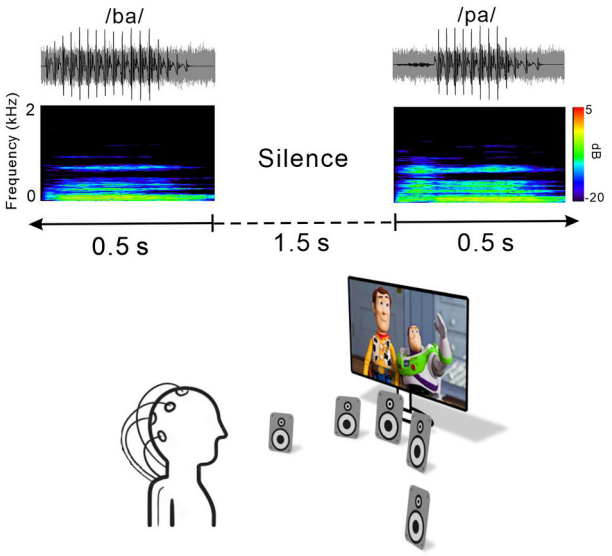

FIGURE 1
Speech stimulus and experimental listening conditions. Top, time waveforms of the CV syllable /ba/ and /pa/ with +5 dB speech-shaped masking noise. Middle, spectrogram of the acoustic stimuli. Each stimulus was embedded in 1.5 s of silence. Bottom, passive listening paradigm. During recording, subjects watched close-captioned movies of their choice.

For each electrophysiological test, speech stimuli /ba/ and /pa/ were presented through a loudspeaker horizontally located at each of five different azimuth angles (−60°, −15°, 0°, +15°, and +60°, where "+" indicates the right side while "–" indicates the left side) under both quiet and noise listening. The stimuli were randomly presented with an inter-stimulus interval from sound offset to onset fixed at 1.5 s. A total of 1,000 trials involving 100 trials each for the /ba/ and /pa/ sounds at the five different azimuth angles under quiet and noise listening conditions (ba/pa x five azimuth angles x quiet/noise conditions) were presented across two blocks. During recording, the subject was seated in a comfortable reclining chair and watched a silent closed-captioned movie of their choice while the stimuli were individually presented in the background through a loudspeaker horizontally located at each of the five different azimuth angles. The subject was instructed to ignore the sounds and not to move their head during the experiment. During the recording, the subject was alert and calm.

All of the speakers were located 1.2 m away from the subject at ear level and sounds were presented at 70 dB SPL (sound pressure level). Breaks were given upon request. The total recording time was ∼40 min.

Behavioral tests

All subjects including the SSD patients and NH controls participated in behavioral sound localization task. The sound localization was measured for speech sounds at the five different azimuth angles mentioned above. In each trial, speech stimuli were emanated from each speaker in a random order. For each of the presentation, participants indicate location where a sound was presented by pressing a corresponding button on the keyboard assigned a speaker number. For the task, stimuli were presented in 10 blocks of 1,000 trials (200 trials for each of the five different azimuth angles), with each lasting 4 min. Prior to undertaking the task, each participants completed 10 familiarization trials of the procedure. The sound localization task was conducted in a sound-attenuated booth. Speakers were 1.0 m from the subject's head. No feedback regarding the performance was given during the test. Only the sound localization test results for the behavioral performance are reported herein. Accuracy of sound localization task was calculated using the root-mean-square error (RMSE) and the mean absolute error (MAE). The RMSE was assessed using the root-mean square of the magnitudes of the differences between the azimuth of the sound location and the azimuth of the selected location across all trials. The MAE is the absolute error in degrees, divided by the total number of trials.

As a behavioral measure of speech perception, word-in-noise perception was measured by using the consonant perception test (CPT) (38). A total of 50 words were presented in a "C/V/C" (consonant/vowel/consonant) context with a female talker in speech-shaped noise at a SNR of 0 dB. The number of words correctly identified out of 50 was expressed as a percentage. Since the CPT is forced choice paradigm among 4 alternative choices, subjects were instructed to indicate which words were heard by choosing buttons *via* mouse click.

EEG recording

Electrophysiological data were collected by using a 64-channel actiCHamp Brain Products recording system (Brain Products GmbH, Inc., Munich, Germany). An electrode cap was placed on the scalp with electrodes positioned at equidistant locations (39, 40). The reference channel was positioned at the vertex while the ground electrode was located on the midline 50% of the distance to the nasion. Continuous data were digitized at 1,000 Hz and stored for offline analysis.

Data processing

Electrophysiological data were preprocessed by using Brain Vision Analyzer 2.0 (Brain Products GmbH, Inc., Munich, Germany). Data were band-pass-filtered (1–50 Hz) and down-sampled to 500 Hz. Visual inspection of the data included the removal of artifacts related to subject movements (exceeding 500 mV). Independent component analysis (ICA) (41) implemented in Brain Vision Analyzer was applied to remove artifacts related to eye blinking and movement, and cardiac activity. After ICA artifact reduction, the data were low-pass-filtered at 20 Hz and segmented from −200 to 1,000 ms with 0 ms at the onset of the stimulus and re-referenced to the average reference. Averages were obtained for each of the azimuth angles. Subsequent peak detection was performed by using the fronto-central electrodes for the N1/P2 components.

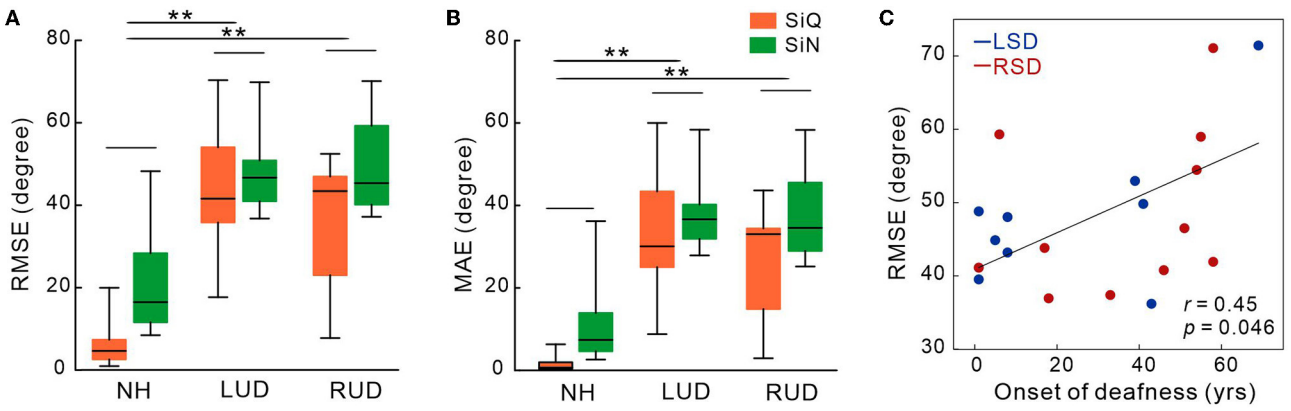

FIGURE 2
Mean root-mean-square error **(A)** and mean absolute error in degree **(B)** in subject groups with normal-hearing and with left- and right-sided deafness during the speech-in-quiet and speech-in-noise listening conditions. **(C)** The root-mean-square error correlations with the onset of deafness in SSD groups. Error bars: the standard error of the mean. RSD, right-sided single-sided deafness; LSD, left-sided single-sided deafness; NH, normal hearing; SiN, speech-in-noise; SiQ, speech-in-quiet; RMES, root-mean-square error; MAE, mean absolute error. $^{**}P < 0.01$.

Since we used an electrode cap with equidistant locations which use different electrode layout from the traditional 10–20 system, N1/P2 were measured from the averaged activities of three electrodes located at Cz in the international 10–20 system (40, 42).

Source analysis

Auditory evoked potential sources were computed by using BESA Research 7.0 (Brain Electrical Source Analysis, GmbH, Germany) as described previously (43). Dipole source analysis for N1 activity was performed on individual averaged waveforms and was implemented by using an average head model. To measure the dipole source activity for each subject, two symmetric regional dipole sources were seeded in the region of the auditory cortex (Talairch coordinates: ±49.5, −17, 9). In the next step, dipole fitting was executed in the mean area over a 20 ms window around the N1 peak on the global field power. A goodness of fit (GOF) was assessed for each subject over the 20 ms window. Data revealing an 80% or lower GOF were excluded from further analysis. As a result, 9 RSD, 9 LSD, and 11 NH subjects showed 80% or greater GOFs. During the analysis, the dipole sources were varied in location, orientation, and strength to fit tangential sources at the activation period maxima. The mean current over the 20 ms window centered on the peak of the tangential sources were assessed to conduct statistical analysis in each subject. In addition, BESA statistics 2.0 was performed for source space analysis. For the analysis, data files were created to compare between conditions (e.g., SiQ vs. SiN). The data files included information regarding source modeling in a 20 ms window in which maximal peaks were observed in the global field power. For the source modeling, sLORETA (standardized low resolution brain electromagnetic tomography) was conducted to evaluate source activation of individual subjects in the time range from 0 to 500 ms after stimulus onsets. The source activation differences in source space between SiQ and SiN conditions were assessed for each subject group using a paried *t*-test.

Statistical analysis

Repeated-measures analysis of variance (ANOVA) was performed for the behavioral data to examine the effects of noise (SiQ vs. SiN) and subject group (NH, RSD, and LSD) on the RMSE and MAE. The repeated-measures ANOVA was also conducted to assess the effects of azimuth angle, noise, and subject group on amplitudes and latencies of N1/P2 cortical potentials. For comparing brain activity during SiN and SiQ listening, we used the SiQ data presented in our previous study (24). Tukey's Honest Significant Difference (HSD) test was conducted for *post hoc* comparisons, while Pearson product-moment correlations were used to assess correlations between the behavioral/audiological data and the N1/P2 activities for the SSD groups. For the dipole source data, group differences in hemispheric laterality were calculated by using grand mean source waveforms. In addition, paired *t*-tests corrected for multiple comparisons and Monte-Carlo resampling techniques implemented in BESA Statistics 2.0 (44) examined differences in the strengths of the brain source spaces between the listening conditions. Clusters of voxels with *p*-values of <0.05 were considered significant, and the alpha criterion was manually set to 0.05 in BESA.

Results

Behavioral sound localization

Figures 2A, B show the mean RMSE and MAE for each subject groups. Repeated-measures ANOVA analyzing RMSE data revealed significant effects of noise [$F_{(1,27)} = 19.3$; $p < 0.0001$] and group [$F_{(1,27)} = 30.47$; $p < 0.0001$]. Tukey's HSD *post hoc* tests revealed the RMSE was larger (worse) in both LSD ($p = 0.001$) and RSD ($p = 0.001$) groups than in NH group. No difference in the RMSE was found between LSD and RSD groups. For noise effect, the RMSE was smaller for the SiQ than for the SiN condition ($p = 0.001$). Similar to the RMSE, significant group [$F_{(1,27)} = 29.9$; $p < 0.0001$] and noise [$F_{(1,27)} = 20.1$; $p = 0.0001$] effects were found

10.3389/fneur.2023.1054105

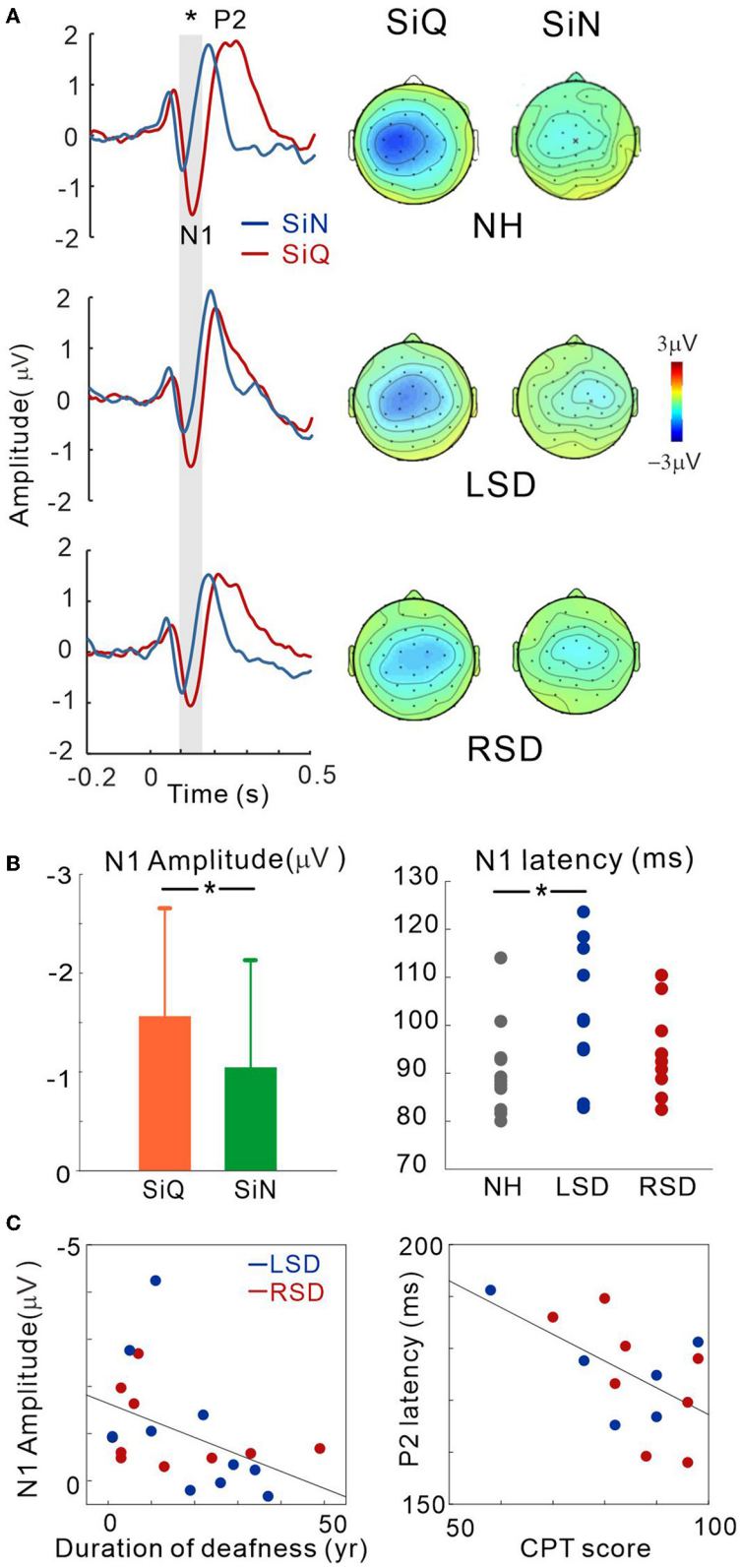

FIGURE 3
(A) Grand mean waveforms averaged stimuli emanated at azimuth angles of ±60° for the NH and ipsilateral to the hearing side for the SSD groups (+60° for the LSD; −60° for RSD) recorded *via* the frontal central (FC) electrodes for each subject group. Event-related potentials are shown for SiN (blue) and SiQ (red) listening. The gray highlighted area indicates the time window to measure the N1 response (80–150 ms). Topographical representation of the N1 response is presented for each subject group on the right side. **(B)** Listening condition (averaged across all groups) and group (averaged across all angles) comparisons for N1 amplitude and N1 latency, respectively. The error bars represent the standard error of the mean. *$P < 0.05$. **(C)** N1 amplitude correlations with the duration of deafness, and P2 latency correlation with word-in-noise perception scores measured using the CPT. RSD, right-sided single-sided deafness; LSD, left-sided single-sided deafness; NH, normal hearing; SiN, speech-in-noise; SiQ, speech-in-quiet.

for the MAE. *Post hoc* tests conducted for the group effect showed the MAE was larger in the SSD groups (both $p = 0.0001$) and SiN ($p = 0.0002$) compared to NH group and the SiQ condition, respectively. Figure 2C shows a correlation between the RMSE and age at the onset of deafness in SSD groups. The results indicate that the RMSE was greater as the age at the onset of deafness is older ($r = 0.45$, $p = 0.046$).

A subset of SSD subjects was able to complete the CPT tests, the results for which are shown in Figure 3C (the right panel). The average scores for CPT were 82.3 for left-sided deafness and 86.7 for right-sided deafness. The results of an independent samples *t*-test revealed no significant difference between the test scores ($p > 0.05$).

Cortical potentials

Figure 3A shows the grand mean waveforms for stimuli emanated at azimuth angles of ±60° for the NH and ipsilateral to the hearing side for the SSD groups (+60° for the LSD; −60° for RSD) under both SiN and SiQ conditions. The overall response was characterized by an N1 evocation at around 100 ms after stimulus onset followed by a P2 response. The magnitude of N1 was greater for SiQ than SiN listening whereas the P2 magnitudes were similar. Topographic examination of the N1 responses indicates that negativity was stronger for SiQ than SiN listening for all of the groups, while N1 activation in the NH group was lateralized toward the left hemisphere but more symmetrical over the brain in the SSD groups (Figure 3A).

Repeated-measures ANOVA was applied to examine the effect of sound location (−60°, −15°, 0°, +15°, +60° azimuth angles), type of stimulus (SiQ and SiN), and the group effect (NH, RSD, and LSD) on N1/P2 measures. Figure 3B shows the N1 amplitudes for the SiQ and SiN condition (averaged across all subjects) and N1 latencies for each subject groups (averaged across all angles). A significant effect of noise [$F_{(1,27)} = 5.7$; $p = 0.024$] was found for N1 amplitude. Tukey's HSD *post hoc* test results show that the N1 amplitudes for SiQ were larger than those for SiN ($p < 0.01$). In addition, a significant group × angle interaction [$F_{(8,108)} = 2.58$; $p = 0.012$] was revealed, and Tukey's HSD *post hoc* test results reveal that in the LSD group, the N1 amplitudes at azimuth angles of 0° ($p = 0.043$), +15° ($p = 0.034$), and +60° ($p = 0.007$) were smaller than those at −15°. In the RSD group, the N1 amplitudes at an azimuth angle of +60° were larger than those at −15° ($p = 0.037$) and +15° ($p = 0.034$). No significant interaction was found in NH group. For N1 latency, a significant effect of group [$F_{(2,28)} = 3.66$; $p = 0.038$] was found, and *post hoc* test results indicate that the N1 latencies for the LSD group were longer than those for the NH group ($p = 0.011$).

No significant differences were found for P2 amplitude. However, a significant effect of azimuth angle [$F_{(4,184)} = 4.5$; $p = 0.002$] was found for P2 latency. Tukey's HSD *post hoc* test results show that the P2 latencies at azimuth angles of −60° and +60° were longer than those at −15° ($p = 0.001$ for −60° and $p = 0.011$ for +60°), 0° ($p < 0.001$ for both), and +15° ($p = 0.009$ for −60° and $p = 0.017$ for +60°).

To assess whether N1/P2 responses to SiN stimuli are related to audiological factors or behavioral speech perception in SSD subjects, we examined the relationships between averaged N1/P2 measurements according to the duration of deafness and CPT scores. Since not all of the SSD subjects provided CPT scores, data from only 14 subjects (6 and 8 from the LSD and RSD groups, respectively) were used in the correlation analysis. Figure 3C shows that the averaged N1 amplitudes across all azimuth angles during the SiN task were inversely related to the duration of deafness in the SSD groups ($r = -0.45$, $p = 0.047$), suggesting that N1 decreases with a longer duration of deafness. In addition, the averaged P2 latencies were negatively correlated with CPT scores, indicating that P2 latency is shorter with better word-in-noise performance ($r = -0.57$, $p = 0.034$).

Dipole source analysis

This was conducted to examine the tangential source of N1 for SiN perception. To measure the SiN effect on N1 source activation, we also assessed the tangential components while SiQ listening and then compared them while SiN listening. Figure 4A shows N1 source activation averaged across all of the azimuth angles for the left and right hemispheres of the NH, LSD, and RSD groups. Repeated-measures ANOVA was conducted to measure the effects of noise, azimuth angle, and subject group on N1 dipole source amplitude and latency. For N1 source amplitude, a significant group/hemisphere interaction [$F_{(2,28)} = 8.25$; $p = 0.001$] was found. Tukey's *post hoc* analysis revealed that during SiN listening, N1 source activation in the LSD group was greater in the left hemisphere, which is contralateral to the hearing side ($p = 0.029$), while stronger ipsilateral activation (left hemisphere) was found in the RSD group ($p = 0.002$). No statistically significant difference between the hemispheres was found for SiQ listening, and no statistically significant asymmetrical dipole activation was found in the hemispheres of the NH group participants (both $p > 0.05$).

Figure 4B shows the *t*-test comparisons for the N1 source space to compare between the SiQ and SiN conditions for +60° and −60° azimuth angles in SSD groups. For this comparisons, we focused on −60° vs. +60° for the following reasons: (1) the findings in previous electrophysiological data suggest that N1 cortical activity is larger for stimuli containing more prominent spatial cues than for less spatially distinguishable stimuli (45); and (2) given that the −60° and 60° azimuth angles are closer to the hearing and deafened ears than the other angles, these conditions could better represent the effect of SSD on source activation. (3) cortical N1/P2 responses to ± 60° in SSD subjects were more delayed and larger compared to the smaller azimuth angles. For the LSD group, comparisons between SiQ and SiN listening revealed significant clusters ($p = 0.006$) with stronger activation in the frontal lobe (the left premotor and supplemotor areas) during SiN listening at an azimuth angle of −60° and in the temporal and occipital lobes at +60° ($p < 0.001$). Meanwhile, for the RSD group, significantly larger activation was found in the frontal area during SiN listening at azimuth angles of −60° ($p = 0.02$) and +60° ($p = 0.017$) (the left Broca area at −60° and the left dorsal anterior cingulate cortex at +60°).

Figure 4C depicts relationships between averaged N1 source latency and duration of deafness in subjects with SSD. Pearson

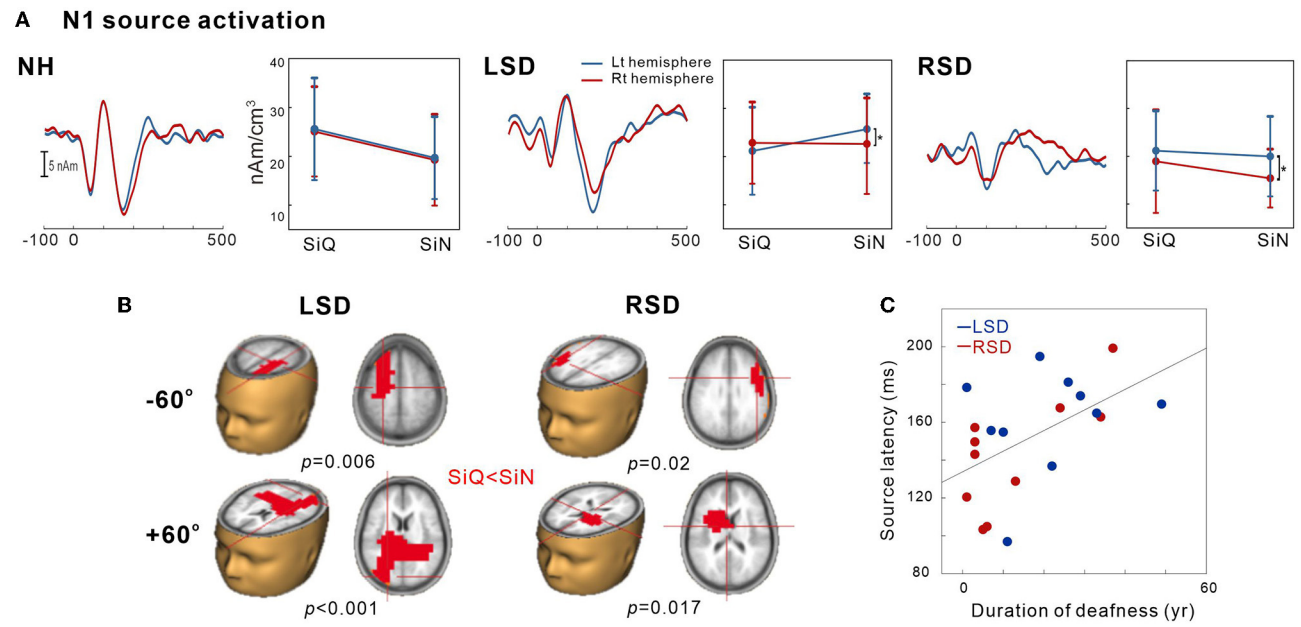

FIGURE 4
N1 source activation by the speech-in-quiet (SiQ) and speech-in-noise (SiN) stimuli. **(A)** The grand mean N1 dipole source waveforms for the left (blue) and the right hemispheres (red) for each subject group. The mean N1 source amplitudes for SiQ and SiN listening are presented for each group on the right side of the mean waveforms. The error bars represent the standard error of the mean. **(B)** Cluster data representing significant differences between the SiQ and SiN listening tasks in the brain source space. Red indicates that the SiN listening response was larger than for SiQ (a positive difference). Note that these clusters indicate which regions showed a significant difference while the crosshairs indicate a 3D point indicating the maximum difference in the comparison. **(C)** N1 source latency correlation with duration of deafness. RSD, right-sided single-sided deafness; LSD, left-sided single-sided deafness; NH, normal hearing.

product-moment correlation results revealed that N1 source latency to SiN stimuli was positively correlated to the duration of deafness ($r = 0.53$, $p = 0.017$), indicating more prolonged latencies with the longer duration of deafness.

Discussion

The aim of this study was to compare cortical responses during SiQ and SiN listening to characterize the cortical representation of SiN processing in persons with SSD. Given that the distinct patterns of brain activation depending on the side of deafness have been reported (24, 35, 46), we also compared the neural responses in LSD and RSD participants during SiN listening. We found that (1) the SiN is differently processed in the brains of left- and right-sided SSD in that the left-sided SSD revealed greater activity contralateral to the hearing side (left hemisphere), while the right-sided SSD showed the left hemispheric asymmetry. (2) the N1 modulation as a function of sound location was more evident in participants with left-sided deafness. In addition, (3) N1 activity and sound localization performance in SSD participants were associated with the deafness duration and the onset of deafness, respectively.

Analysis of N1 dipole source activity revealed that noise-degraded speech sounds incur differential effects on the hemispheric laterality depending on the side of deafness. For SiN listening, activity contralateral to the hearing side was greater with left-sided deafness but a contrastive pattern of lateralization in that stronger ipsilateral bias was revealed with right-sided deafness. Interestingly, no hemispheric laterality was found for SiQ listening in either SSD group. These results in dipole source activation enabled us to tease out the contributions of the hemispheres engaged in processing SiN stimuli and to confirm that the auditory system has active compensatory mechanisms mitigating degraded speech processing. In listeners with NH, contralateral activity is more predominant for left- than right-ear stimulation (47, 48). Nonetheless, in persons with SSD, the adaptation process of the left hemisphere could strengthen both the ipsilateral and contralateral pathways for processing degraded speech sounds. With right-sided deafness, stronger left-hemispheric activity has been attributed to functional plastic changes mainly occurring in the left hemisphere rather than the right one (49, 50). Strengthening the routes to the left hemisphere for SiN listening could be related to the left hemisphere playing a crucial role in speech and language function (51), which mainly contributes to the right-ear advantage for processing degraded speech sounds (16).

The results of a previous study examining alpha and theta rhythms in children with unilateral deafness and NH controls are inconsistent with our findings in that the neural activity in the NH group was lateralized to the left side during a quiet listening task whereas rightward asymmetry was found during a word-in-noise recognition task (21). However, this pattern of asymmetry decreased in children with unilateral hearing loss due to attenuated asymmetrical activation (21). Possible explanations for this discrepancy are (i) the type of noise used for evoking the response, (ii) the subjects' characteristics, and (iii) the listening conditions (passive vs. active). Given that for NH, increasing

the SNR decreases lateralization toward the right hemisphere (32), the low SNR used in our study would weaken hemispheric lateralization in NH listeners. In addition, most of the SSD participants in our study were adults who had acquired auditory deprivation later in life whereas children with congenital unilateral hearing loss were mainly recruited for the previous study by Cartocci et al. (21). It has been demonstrated that asymmetrical hearing loss occurring during early childhood compromises brain lateralization due to incomplete auditory development (52). In this regard, Burton et al. (49) proposed that congenital unilateral deafness can result in strengthening the contralateral pathway while acquired unilateral deafness can lead to over excitation of the ipsilateral pathway.

Interestingly, we found that cortical activation in right-sided deafness is independent of the direction of stimulation whereas left-sided deafness alters sites of activation according to the amount of spatial information. More specifically, in left-sided deafness, activation was found in the temporal and occipital lobes when sounds were presented from the side of the intact ear (an azimuth angle of $+60^{\circ}$), while the activation was greater in the frontal lobe for the stimuli presented on the deaf side (an azimuth angle of -60°). On the other hand, right-sided deafness produced strong activity in the frontal areas regardless of the side of stimulation (Figure 3B). The differential recruitment of the frontal and temporal regions for encoding spatial information could be closely related to the functional change brought about by cortical reorganization according to the side of deafness. The neural generators contributing to processing speech under adverse listening conditions are located in both the frontal and temporal lobes: the temporal lobe is thought to play a role in initial sound processing while the frontal cortex is more associated with the higher-order speech processing such as SiN listening (53). Indeed, the extensive frontal-temporal network including the anterior cingulate and the prefrontal cortex are preferentially activated for processing linguistic and spatial information (9, 54–56). However, in individuals with SSD, such functional organization of the cortex for SiN processing seems to be altered by deafness-driven plasticity. In particular, the activation of the frontal cortex observed in persons with SSD could reflect active adaptation processing in the cortex to enable higher cognitive resources to process degraded speech stimuli. Considering that individuals with right-sided deafness show the frontal lobe activation required to process sounds from both the deaf and hearing sides, right-sided deafness could require more effort for SiN processing than left-sided deafness in which the activation sites are allocated according to the side of stimulation. This interpretation is supported by a neuroimaging study showing that right-sided deafness is related to higher activation of the frontal cortical regions not seen in persons with left-sided deafness (57); the authors concluded that right-sided deafness enhances activation in the areas involved in the processing of degraded sounds. Our data corroborate this finding by explicating differential reorganization of the cortex according to the side of deafness for processing impoverished speech stimuli.

In addition to the different activation patterns between left- and right-side deafness, it is important to note that the roles of peripheral and central processing deficits in SiN perception differ between bilateral and unilateral deafness. Although both types of hearing loss induce changes in the central auditory system, peripheral loss is totally different. Bilateral hearing loss is accompanied by an elevation in the hearing threshold and a decrease in spectral processing but with access to bilateral cues in both the intensity and timing domains (58). On the other hand, hearing *via* the good ear in unilaterally deafened individuals can be as good as that of normal listeners for SiN perception when the speech and noise are presented to the good ear. In this sense, the loss of sound source localization is the main issue for SSD subjects in the case of a single talker whereas the loss of binaural processing reflects true SiN perception in the presence of multiple talkers.

Binaural processing is important for both sound localization and SiN perception because the neural processing for both tasks is closely related to each other (59). In the cocktail party situation, binaural hearing helps to lessen the masking of the target sounds by noise presented from other directions. Based on this effect, the binaural masking level difference (BMLD) improves sound detection when the phase of either the signal or the noise is inverted (60). In a free-field environment, a similar level of unmasking in humans (61) and animals (62) is obtained by spatially separating the signal and the masker. In an animal study, it has been found that the responses of the inferior colliculus (IC) neurons to BMLD stimuli are consistent with their ITD sensitivity to tone and noise (63). Furthermore, behavioral and functional changes with unilateral deprivation have been reported in animals with SSD. In particular, the outcomes of several single-neuron studies on the effect of unilateral deafness at the brainstem and cortex levels suggest an increase in the responsiveness of the IC and the primary auditory cortex neurons to acoustic stimulation on the side of the intact ear (64–66). For example, unilateral hearing loss in barn owls was accompanied by compensatory shifts in ITD sensitivity at the IC level (67). This may be related to weakening of the auditory pathways that convey input from the deprived ear in several brain areas, including the cochlear nucleus (68), the superior olive (69), and the IC (70). This outcome indicates that a change in the auditory pathway affects the capacity of the auditory system to adapt to unilateral deafness by becoming more dependent on the monaural spatial cues provided by the hearing ear.

At the neuroanatomical level, neurons in the IC change substantially following unilateral hearing loss because they need to be able to integrate various auditory spatial cues (71). In turn, it can be inferred that the IC is more susceptible to brain plasticity than other auditory pathway sites due to its functional characteristics (72). In animal studies, unilateral hearing loss weakened ipsilaterally mediated suppression in the IC ipsilateral to the deprived ear, albeit not at the level of the auditory cortex (73). In this respect, these results indicate that neuronal changes following unilateral deprivation are more apparent at the subcortical level rather than at the cortical level. Nonetheless, the neural basis for unilaterally deafened-induced plasticity at the IC level is not well characterized in humans, thereby suggesting the need for future work in this area.

Concerning the relative roles of peripheral and central processing deficits in SiN recognition by individuals with SSD, one important factor for SiN processing is the acoustic properties of the noise maker. The sensory aspects of SiN can be considered as how the acoustic signal is transduced by the ear and transmitted

and transformed along the central auditory system. External noise can cause disruption in signal encoding in the central auditory system, and for this reason, it is frequently referred to as a masker. Meanwhile, noise that interacts with a signal, leading to a degraded neural representation, is generally referred to as an "energetic masker." The term "energetic" comes from the level of interaction between the masker and the signal within the same critical bands at the same time. On the other hand, "informational masking" consists of a masker that is outside the critical bands so that both the target signal and the masker are audible. Energetic masking can produce interference within the peripheral auditory system whereas informational masking is often taxing on the cognitive resources required for selective attention (74). Given that the SiN performance of bilaterally or unilaterally deafened individuals according to the type of noise can vary, the effects of noise type and spatial cues on the performance have been extensively studied. In people with SSD, better performances were obtained with single-talker noise compared to using a multiple-talker distractor (75). In addition, SSD subjects perform poorly when speech and noise are presented from the same speaker due to a reduction in spatial cues (76). Meanwhile, listeners with bilateral hearing are more affected by multi-talker noise due to the loss of binaural hearing (3). Acoustically, multi-talker noise is dominated by energetic masking while single-talker noise contains both energetic and informational masking. Therefore, it can be inferred that single-talker noise with informational masking is more difficult for SSD individuals since it requires more attentional cognitive resources. Furthermore, this supports the notion that the cortical plasticity following monaural deprivation may not enhance some aspects of binaural hearing involving informational masking.

Under normal circumstances, N1/P2 cortical activities in response to acoustic noise decrease in amplitude and increase in latency (15, 32, 77). Similar to the observations for NH listeners, cortical N1 responses in persons with SSD were smaller during SiN compared to SiQ listening (36). However, our data reveal that in SSD individuals, the effect of degraded speech sounds on P2 response is much smaller than on N1 response. These results expand on previously reported findings by suggesting that noise-related changes can be mainly attributed to the N1 components. Our findings indicate that N1/P2 activities in persons with SSD undergo distinct changes with noise. It is known that N1 is significantly affected by the stimulus characteristics, such as frequency (78), intensity (79), and acoustic changes (40), whereas P2 is related to more higher-order cognitive processing, including perceptual experience (80) and auditory training (81, 82). When processing degraded speech sounds, N1 relies solely on the SNR without taking acoustic properties such as the absolute intensity of the signal into consideration (77, 83). This notion is supported by the findings from a previous study comparing responses to tone bursts with various levels of background noise in which substantial changes in the N1 amplitude as a function of noise were observed while no effect was evident for intensity changes (83). Contrary to N1 showing consistent changes with the noise masker, P2 noise-related changes are largely variable. Papesh et al. (84) reported that P2 is affected by interactions among stimulus variables including signal type, noise type, and experimental paradigm. Therefore, we assume that our experimental design is suitable for inducing changes in neural generators underlying the N1 rather than the P2 response.

Our results concerning the relationship between N1/P2 cortical activities and behavioral performance in SiN perception are in agreement with those from previous event-related potential studies (21, 24, 36). Notably, we found that sensor-level N1 amplitude and P2 latency are associated with the duration of deafness and word-in-noise ability, respectively. At the source level, N1 activity can be used to predict the duration of deafness and subjective speech perception in persons with SSD. In other words, the N1 response becomes progressively weaker with decreasing SiN perception and a longer duration of deafness. These results suggest that the brain mechanisms required for the neural processing of SiN stimuli are more difficult to induce in SSD individuals with longer duration of deafness. Given that a positive correlation between N1 activity and behavioral/perceptual SiN ability has been observed, successful SiN perception in persons with SSD could require more faithful neural encoding of degraded auditory input at the cortical level. However, the quality and amount of the brain plasticity in some SSD individuals (i.e., chronic SSD) is not sufficient to improve the neural activity for robust SiN perception (85, 86). In this case, higher-order cognitive controls such as attention and memory might efficiently improve SiN listening in SSD individuals (20). Taken together, our data leads us to infer that chronic unilaterally deafened people develop "SSD-specific" neural mechanisms to compensate for decreased ability to process SiN stimulus. Nevertheless, additional efforts to enhance cognitive controls such as auditory training could re-formulate the neural population required for SiN listening into a more "normal-like" pattern.

Data availability statement

The raw data supporting the conclusions of this article will be made available by the authors, without undue reservation.

Ethics statement

The studies involving human participants were reviewed and approved by Sacred Heart Hospital of Hallym University Institutional Review Board (IRB no. 2019-02-019). The patients/participants provided their written informed consent to participate in this study.

Author contributions

J-HH and JL collected the data and analyzed the data. J-HH, JL, and H-JL contributed to writing the manuscript. All authors contributed to the article and approved the submitted version.

Funding

This work was supported by the Basic Science Research Program through the National Research Foundation of

Korea (NRF) funded by the Ministry of Education (NRF-2022R1A2C1004862, NRF-2020R1I1A1A01070914, and NRF-2020R1A6A3A01099260) and by the Hallym University Research Fund and the Hallym University Medical Center Research Fund.

Conflict of interest

The authors declare that the research was conducted in the absence of any commercial or financial relationships that could be construed as a potential conflict of interest.

Publisher's note

References

1. Kumpik DP, King AJ, A. review of the effects of unilateral hearing loss on spatial hearing. *Hear Res.* (2019) 372:17–28. doi: 10.1016/j.heares.2018.08.003

2. Griffin AM, Poissant SF, Freyman RL. Speech-in-noise and quality-of-life measures in school-aged children with normal hearing and with unilateral hearing loss. *Ear Hear.* (2019) 40:139–48. doi: 10.1097/AUD.0000000000000667

3. Firszt J, Reeder R, Holden L. Unilateral hearing loss: understanding speech recognition and localization variability: implications for cochlear implant candidacy. *Ear Hear.* (2017) 38:159–73. doi: 10.1097/AUD.0000000000000380

4. Agterberg MJH, Snik AFM, Van de Goor RMG, Hol MKS, Van Opstal AJ. Sound-localization performance of patients with single-sided deafness is not improved when listening with a bone-conduction device. *Hear Res.* (2019) 372:62–8. doi: 10.1016/j.heares.2018.04.007

5. Siau D, Dhillon B, Andrews R, Green KMJ. Bone-anchored hearing aids and unilateral sensorineural hearing loss: Why do patients reject them? *J Laryngol Otol.* (2015) 129:321–5. doi: 10.1017/S0022215115000602

6. Shtyrov Y, Kujala T, Ilmoniemi RJ, Näätänen R. Noise affects speech-signal processing differently in the cerebral hemispheres. *Neuroreport.* (1999) 10:2189–92.

7. Anderson S, White-Schwoch T, Parbery-Clark A, Kraus N, A. dynamic auditory-cognitive system supports speech-in-noise perception in older adults. *Hear Res.* (2013) 300:18–32. doi: 10.1016/j.heares.2013.03.006

8. Obleser J, Wise RJS, Dresner MA, Scott SK. Functional integration across brain regions improves speech perception under adverse listening conditions. *J Neurosci.* (2007) 27:2283–9. doi: 10.1523/JNEUROSCI.4663-06.2007

9. Vaden KI, Teubner-Rhodes S, Ahlstrom JB, Dubno JR, Eckert MA. Cingulo-opercular activity affects incidental memory encoding for speech in noise. *Neuroimage.* (2017) 157:381–7. doi: 10.1016/j.neuroimage.2017.06.028

10. Dirks C, Nelson PB, Sladen DP, Oxenham AJ. Mechanisms of localization and speech perception with colocated and spatially separated noise and speech maskers under single-sided deafness with a cochlear implant. *Ear Hear.* (2019) 40:1293–306. doi: 10.1097/AUD.0000000000000708

11. Lewald J, Getzmann S. Electrophysiological correlates of cocktail-party listening. *Behav Brain Res.* (2015) 292:157–66. doi: 10.1016/j.bbr.2015.06.025

12. Golestani N, Hervais-Adelman A, Obleser J, Scott SK. Semantic vs. perceptual interactions in neural processing of speech-in-noise. *NeuroImage.* (2013) 79:52–61. doi: 10.1016/j.neuroimage.2013.04.049

13. Dimitrijevic A, Smith ML, Kadis DS, Moore DR. Cortical alpha oscillations predict speech intelligibility. *Front Hum Neurosci.* (2017) 11:88. doi: 10.3389/fnhum.2017.00088

14. Wöstmann M, Herrmann B, Maess B, Obleser J. Spatiotemporal dynamics of auditory attention synchronize with speech. *Proc Natl Acad Sci U S A.* (2016) 113:3873–8. doi: 10.1073/pnas.1523357113

15. Parbery-Clark A, Marmel F, Bair J, Kraus N. What subcortical-cortical relationships tell us about processing speech in noise. *Eur J Neurosci.* (2011) 33:549–57. doi: 10.1111/j.1460-9568.2010.07546.x

16. Bidelman GM, Bhagat SP. Right-ear advantage drives the link between olivocochlear efferent "antimasking" and speech-in-noise listening benefits. *Neuroreport.* (2015) 26:483–7. doi: 10.1097/WNR.0000000000000376

17. Wible B, Nicol T, Kraus N. Abnormal neural encoding of repeated speech stimuli in noise in children with learning problems. *Clin Neurophysiol.* (2002) 113:485–94. doi: 10.1016/S1388-2457(02)00017-2

18. Han JH, Lee J, Lee HJ. Noise-induced change of cortical temporal processing in cochlear implant users. *Clin Exp Otorhinolaryngol.* (2020) 13:241–8. doi: 10.21053/ceo.2019.01081

19. Fiedler L, Wöstmann M, Herbst SK, Obleser J. Late cortical tracking of ignored speech facilitates neural selectivity in acoustically challenging conditions. *Neuroimage.* (2019) 186:33–42. doi: 10.1016/j.neuroimage.2018.10.057

20. Kraus F, Tune S, Ruhe A, Obleser J, Wöstmann M. Unilateral acoustic degradation delays attentional separation of competing speech. *Trends Hear.* (2021) 25:3242. doi: 10.1177/23312165211013242

21. Cartocci G, Scorpecci A, Borghini G, Maglione AG, Inguscio BMS, Giannantonio S, et al. EEG rhythms lateralization patterns in children with unilateral hearing loss are different from the patterns of normal hearing controls during speech-in-noise listening. *Hear Res.* (2019) 42:1590–601. doi: 10.1016/j.heares.2019.04.011

22. Darwin CJ. Contributions of binaural information to the separation of different sound sources. *Int J Audiol.* (2006) 45:20–4. doi: 10.1080/14992020600782592

23. Shinn-Cunningham BG, Durlach NI, Held RM. Adapting to supernormal auditory localization cues. I. Bias and resolution. *J Acoust Soc Am.* (1998) 103:3656–66. doi: 10.1121/1.423088

24. Han J-H, Lee J, Lee H-J. Ear-specific hemispheric asymmetry in unilateral deafness revealed by auditory cortical activity. *Front Neurosci.* (2021) 15:698718. doi: 10.3389/fnins.2021.698718

25. Vannson N, Strelnikov K, James CJ, Deguine O, Barone P, Marx M. Evidence of a functional reorganization in the auditory dorsal stream following unilateral hearing loss. *Neuropsychologia.* (2020) 149:107683. doi: 10.1016/j.neuropsychologia.2020.107683

26. Kral A, Hubka P, Heid S, Tillein J. Single-sided deafness leads to unilateral aural preference within an early sensitive period. *Brain.* (2013) 136:180–93. doi: 10.1093/brain/aws305

27. Keating P, Rosenior-Patten O, Dahmen JC, Bell O, King AJ. Behavioral training promotes multiple adaptive processes following acute hearing loss. *Elife.* (2016) 5:e12264. doi: 10.7554/eLife.12264

28. Kavanagh G, Kelly J. Contribution of auditory cortex to sound localization by the ferret (Mustela putorius). *J Neurophysiol.* (1987) 57:1746–66.

29. Zatorre RJ, Penhune VB. Spatial localization after excision of human auditory cortex. *J Neurosci.* (2001) 21:6321–8. doi: 10.1523/JNEUROSCI.21-16-06321.2001

30. Clarke S, Bellmann A, Meuli RA, Assal G, Steck AJ. Auditory agnosia and auditory spatial deficits following left hemispheric lesions: evidence for distinct processing pathways. *Neuropsychologia.* (2000) 38:797–807. doi: 10.1016/S0028-3932(99)00141-4

31. Spierer L, Bellmann-Thiran A, Maeder P, Murray MM, Clarke S. Hemispheric competence for auditory spatial representation. *Brain.* (2009) 132:1953–66. doi: 10.1093/brain/awp127

32. Bidelman GM, Howell M. Functional changes in inter- and intra-hemispheric cortical processing underlying degraded speech perception. *Neuroimage.* (2016) 124:581–90. doi: 10.1016/j.neuroimage.2015.09.020

33. Näätänen R, Picton T. The N1 wave of the human electric and magnetic response to sound: a review and an analysis of the component structure. *Psychophysiology.* (1987) 24:375–425.

34. Ponton CW, Vasama JP, Tremblay K, Khosla D, Kwong B, Don M. Plasticity in the adult human central auditory system: evidence from late-onset profound unilateral deafness. *Hear Res.* (2001) 154:32–44. doi: 10.1016/S0378-5955(01)00214-3

35. Hanss J, Veuillet E, Adjout K, Besle J, Collet L, Thai-Van H. The effect of long-term unilateral deafness on the activation pattern in the auditory cortices of French-native speakers: Influence of deafness side. *BMC Neurosci.* (2009) 10:1–11. doi: 10.1186/1471-2202-10-23

36. Cañete OM, Purdy SC, Brown CRS, Neeff M, Thorne PR. Impact of unilateral hearing loss on behavioral and evoked potential measures of auditory function in adults. *J Am Acad Audiol.* (2019) 53:17096. doi: 10.3766/jaaa.17096

37. Kim J, Shim L, Bahng J, Lee H-J. Proficiency in using level cue for sound localization is related to the auditory cortical structure in patients with single-sided deafness. *Front Neurosci.* (2021) 15:1–11. doi: 10.3389/fnins.2021.749824

38. Ryu HD, Shim HY, Kim JS, A. study of the relation between korean consonant perception test (KCPT) and hearing thresholds as a function of frequencies. *Audiology.* (2011) 7:153–63. doi: 10.21848/audiol.2011.7.2.153

39. Debener S, Makeig S, Delorme A, Engel AK. What is novel in the novelty oddball paradigm? Functional significance of the novelty P3 event-related potential as revealed by independent component analysis. *Brain Res Cognit Brain Res.* (2005) 22:309–21. doi: 10.1016/j.cogbrainres.2004.09.006

40. Han JH, Dimitrijevic A. Acoustic change responses to amplitude modulation: a method to quantify cortical temporal processing and hemispheric asymmetry. *Front Neurosci.* (2015) 9:38. doi: 10.3389/fnins.2015.00038

41. Delorme A, Makeig S, EEGLAB. an open source toolbox for analysis of single-trial EEG dynamics including independent component analysis. *J Neurosci Methods.* (2004) 134:9–21. doi: 10.1016/j.jneumeth.2003.10.009

42. Han JH, Dimitrijevic A. Acoustic change responses to amplitude modulation in cochlear implant users: relationships to speech perception. *Front Neurosci.* (2020) 14:124. doi: 10.3389/fnins.2020.00124

43. Han J-H, Zhang F, Kadis DS, Houston LM, Samy RN, Smith ML, et al. Auditory cortical activity to different voice onset times in cochlear implant users. *Clin Neurophysiol Off J Int Feder Clin Neurophysiol.* (2016) 127:1603–17. doi: 10.1016/j.clinph.2015.10.049

44. Maris E, Oostenveld R. Nonparametric statistical testing of EEG- and MEG-data. *J Neurosci Methods.* (2007) 164:177–90. doi: 10.1016/j.jneumeth.2007.03.024

45. Palomäki KJ, Tiitinen H, Mäkinen V, May PJC, Alku P. Spatial processing in human auditory cortex: the effects of 3D, ITD, and ILD stimulation techniques. *Cognit Brain Res.* (2005) 24:364–79. doi: 10.1016/j.cogbrainres.2005.02.013

46. Khosla D, Ponton CW, Eggermont JJ, Kwong B, Don M, Vasama JP. Differential ear effects of profound unilateral deafness on the adult human central auditory system. *JARO J Assoc Res Otolaryngol.* (2003) 4:235–49. doi: 10.1007/s10162-002-3014-x

47. Hine J, Thornton R, Davis A, Debener S. Does long-term unilateral deafness change auditory evoked potential asymmetries? *Clin Neurophysiol.* (2008) 119:576–86. doi: 10.1016/j.clinph.2007.11.010

48. Vasama JP, Mäkelä JP. Auditory pathway plasticity in adult humans after unilateral idiopathic sudden sensorineural hearing loss. *Hear Res.* (1995) 87:132–40. doi: 10.1016/0378-5955(95)00086-J

49. Burton H, Firszt JB, Holden T, Agato A, Uchanski RM. Activation lateralization in human core, belt, and parabelt auditory fields with unilateral deafness compared to normal hearing. *Brain Res.* (2012) 1454:33–47. doi: 10.1016/j.brainres.2012.02.066

50. Van der Haegen L, Acke F, Vingerhoets G, Dhooge I, De Leenheer E, Cai Q, et al. Laterality and unilateral deafness: Patients with congenital right ear deafness do not develop atypical language dominance. *Neuropsychologia.* (2016) 93:482–92. doi: 10.1016/j.neuropsychologia.2015.10.032

51. Sininger YS, Cone-Wesson B. Asymmetric cochlear processing mimics hemispheric specialization. *Science.* (2004) 305:1581. doi: 10.1126/science.1100646

52. Gordon KA, Wong DDE, Papsin BC. Bilateral input protects the cortex from unilaterally-driven reorganization in children who are deaf. *Brain.* (2013) 136:1609–25. doi: 10.1093/brain/awt052

53. Rauschecker J, Scott S. Maps and streams in the auditory cortex: nonhuman primates illuminate human speech processing. *Nat Neurosci.* (2009) 12:1–7. doi: 10.1038/nn.2331

54. Tyler LK, Stamatakis EA, Post B, Randall B, Marslen-Wilson W. Temporal and frontal systems in speech comprehension: an fMRI study of past tense processing. *Neuropsychologia.* (2005) 43:1963–74. doi: 10.1016/j.neuropsychologia.2005.03.008

55. Bidelman GM, Myers MH. Frontal cortex selectively overrides auditory processing to bias perception for looming sonic motion. *Brain Res.* (2020) 1726:146507. doi: 10.1016/j.brainres.2019.146507

56. Binder J, Frost JA, Hammeke TA, Bellgowan PSF, Springer JA, Kaufman JN, et al. Human temporal lobe activation by speech and nonspeech sounds. *Cerebral Cortex.* (2000) 10:512–28. doi: 10.1093/cercor/10.5.512

57. Heggdal POL, Aarstad HJ, Brännström J, Vassbotn FS, Specht K. An fMRI-study on single-sided deafness: spectral-temporal properties and side of stimulation modulates hemispheric dominance. *NeuroImage Clin.* (2019) 24:101969. doi: 10.1016/j.nicl.2019.101969

58. Ahlstrom JB, Horwitz AR, Dubno JR. Spatial benefit of bilateral hearing aids. *Ear Hear.* (2009) 30:203–18. doi: 10.1097/AUD.0b013e31819769c1

59. Blauert J. *Binaural and Spatial Hearing in Real and Virtual Environments.* Mahwah: Lawrence Erlbaum Associates, Inc. (1997). p. 593–609

60. Licklider JCR. The influence of interaural phase relations upon the masking of speech by white noise. *J Acoust Soc Am.* (1948) 20:150–9.

61. Saberi K, Dostai L, Sadralodabai T, Bull V. Free-field release from masking. *J Acoust Soc Am.* (1991) 90:1355–70.

62. Hine JE, Martin RL, Moore DR. Free-field binaural unmasking in ferrets. *Behav Neurosci.* (1994) 108:196–205. doi: 10.1037/0735-7044.108.1.196

63. Jiang D, McAlpine D, Palmer AR. Detectability index measures of binaural masking level difference across populations of inferior colliculus neurons. *J Neurosci.* (1997) 17:9331–9. doi: 10.1523/JNEUROSCI.17-23-09331.1997

64. Kitzes LM, Semple MN. Single-unit responses in the inferior colliculus: Effects of neonatal unilateral cochlear ablation. *J Neurophysiol.* (1985) 53:1483–500. doi: 10.1152/jn.1985.53.6.1483

65. Moore DR, France S, Mcalpine D, Mossop JE, Versnel H. Plasticity of inferior colliculus and auditory cortex following unilateral deafening in adult ferrets. In: *Acoustical Signal Processing in the Central Auditory System.* New York, NY: Plenum Press (1997).

66. Reale RA, Brugge JF, Chan JCK. Maps of auditory cortex in cats reared after unilateral cochlear ablation in the neonatal period. *Dev Brain Res.* (1987) 34:281–90.

67. Gold JI, Knudsen EI, A. site of auditory experience-dependent plasticity in the neural representation of auditory space in the barn owl's inferior colliculus. *J Neurosci.* (2000) 20:3469–86. doi: 10.1523/JNEUROSCI.20-09-03469.2000

68. Moore DR, Kowalchuk NE. Auditory brainstem of the ferret : effects of unilateral cochlear lesions on cochlear nucleus volume and projections to the inferior colliculus. *J Comp Neurol.* (1988) 272:503–15.

69. Russell FA, Moore DR. Effects of unilateral cochlear removal on dendrites in the gerbil medial superior olivary nucleus. *Eur J Neurosci.* (1999) 11:1379–90.

70. Webster DB, State L, Orleans N. Auditory neuronal sizes after a unilateral conductive hearing loss. *Exp Neurol.* (1983) 140:130–40.

71. Chase SM, Young ED. Limited segregation of different types of sound localization information among classes of units in the inferior colliculus. *J Neurosci.* (2005) 25:7575–85. doi: 10.1523/JNEUROSCI.0915-05.2005

72. Yu X, Sanes DH, Aristizabal O, Wadghiri YZ, Turnbull DH. Large-scale reorganization of the tonotopic map in mouse auditory midbrain revealed by MRI. *Proc Natl Acad Sci.* (2007) 104:12193–8. doi: 10.1073/pnas.0700960104

73. Popescu MV, Polley DB. Monaural deprivation disrupts development of binaural selectivity in auditory midbrain and cortex. *Neuron.* (2010) 65:718–31. doi: 10.1016/j.neuron.2010.02.019

74. Mattys SL, Brooks J, Cooke M. Recognizing speech under a processing load: dissociating energetic from informational factors. *Cognit Psychol.* (2009) 59:203–43. doi: 10.1016/j.cogpsych.2009.04.001

75. May BL, Bowditch S, Liu Y, Eisen M, Niparko JK. Mitigation of informational aasking in individuals with single-sided deafness by intergraded bone conduction hearing loss. *Ear Hear.* (2014) 35:41–8. doi: 10.1097/AUD.0b013e31829d14e8

76. Rothpletz AM, Wightman FL, Kistler DJ. Informational masking and spatial hearing in listeners with and without unilateral hearing loss. *J Speech Lang Hear Res.* (2012) 55:511–31. doi: 10.1044/1092-4388(2011/10-0205)

77. Billings CJ, Bennett KO, Molis MR, Leek MR. Cortical encoding of signals in noise: effects of stimulus type and recording paradigm. *Ear Hear.* (2011) 32:53–60. doi: 10.1097/AUD.0b013e3181ec5c46

78. Dimitrijevic A, Michalewski HJ, Zeng FG, Pratt H, Starr A. Frequency changes in a continuous tone: auditory cortical potentials. *Clin Neurophysiol.* (2008) 119:2111–24. doi: 10.1016/j.clinph.2008.06.002

79. Dimitrijevic A, Lolli B, Michalewski HJ, Pratt H, Zeng FG, Starr A. Intensity changes in a continuous tone: auditory cortical potentials comparison with frequency changes. *Clin Neurophysiol.* (2009) 120:374–83. doi: 10.1016/j.clinph.2008.11.009

80. Ross B, Tremblay K. Stimulus experience modifies auditory neuromagnetic responses in young and older listeners. *Hear Res.* (2009) 248:48–59. doi: 10.1016/j.heares.2008.11.012

81. Tong Y, Melara RD, Rao A. P2 enhancement from auditory discrimination training is associated with improved reaction times. *Brain Res.* (2009) 1297:80–8. doi: 10.1016/j.brainres.2009.07.089

82. Tremblay K, Kraus N, McGee T, Ponton C, Otis AB. Central auditory plasticity: changes in the N1–P2 complex after speech-sound training. *Ear Hear.* (2001) 22:79–90. doi: 10.1097/00003446-200104000-00001

83. Billings CJ, Tremblay KL, Stecker GC, Tolin WM. Human evoked cortical activity to signal-to-noise ratio and absolute signal level. *Hear Res.* (2009) 254:15–24. doi: 10.1016/j.heares.2009.04.002

84. Papesh MA, Billings CJ, Baltzell LS. Background noise can enhance cortical auditory evoked potentials under certain conditions. *Clin Neurophysiol Off J Int Feder Clin Neurophysiol.* (2015) 126:1319–30. doi: 10.1016/j.clinph.2014.10.017

85. Lee HJ, Smieja D, Polonenko MJ, Cushing SL, Papsin BC, Gordon KA. Consistent and chronic cochlear implant use partially reverses cortical effects of single sided deafness in children. *Sci Rep.* (2020) 10:21526. doi: 10.1038/s41598-020-78371-6

86. Gordon K, Henkin Y, Kral A. Asymmetric hearing during development: the aural preference syndrome and treatment options. *Pediatrics.* (2015) 136:141–53. doi: 10.1542/peds.2014-3520

frontiers | Frontiers in Neurology

TYPE Original Research
PUBLISHED 14 April 2023
DOI 10.3389/fneur.2023.1158955

OPEN ACCESS

EDITED BY
Stefan Weder,
University Hospital of Bern,
Switzerland

REVIEWED BY
Jianyong Chen,
Shanghai Jiao Tong University,
China
Douglas Brungart,
Walter Reed National Military Medical Center,
United States

*CORRESPONDENCE
Chanan Shaul
✉ hananshaul@gmail.com

SPECIALTY SECTION
This article was submitted to
Neuro-Otology,
a section of the journal
Frontiers in Neurology

RECEIVED 04 February 2023
ACCEPTED 24 March 2023
PUBLISHED 14 April 2023

CITATION
Chen I, Eligal S, Menahem O, Salem R, Sichel J-Y, Perez R and Shaul C (2023) Time from sudden sensory neural hearing loss to treatment as a prognostic factor.
Front. Neurol. 14:1158955.
doi: 10.3389/fneur.2023.1158955

Time from sudden sensory neural hearing loss to treatment as a prognostic factor

Itay Chen, Shalom Eligal, Ori Menahem, Riki Salem, Jean-Yves Sichel, Ronen Perez and Chanan Shaul*

Department of Otolaryngology and Head and Neck Surgery, Shaare-Zedek Medical Center, Faculty of Medicine, Hebrew University of Jerusalem, Jerusalem, Israel

Introduction: The widely accepted treatment for sudden sensorineural hearing loss (SSNHL) is corticosteroid treatment (oral or intratympanic). The main goal of this work is to define the significance of the time between symptom onset and treatment initiation, as well as other prognostic factors, for hearing improvement.

Methods: This retrospective study included 666 patients treated for SSNHL. Demographic data, audiometry, treatment method, time since symptom onset, and associated symptoms were recorded for each patient. The patients were divided into five groups according to the treatment initiation time—half a week, one week, 2 weeks, 3 weeks, or 4 weeks and over—after symptom onset. The degree of improvement was assessed by comparing the audiometry at the beginning and the end of the treatment.

Results: The average period of hearing loss from symptom onset to treatment initiation was 10.8 days. Significant differences were found between the groups of half a week, one week, and 2 weeks and the groups of 3 weeks and 4 weeks and over (each separately, p <0.001). No difference was found between the half-week, one-week, and two-week groups, nor was there a difference between the three-week and four-week-and-over groups. A correlation was found between the treatment initiation time in days and the degree of improvement in hearing for both speech recognition threshold (SRT) and discrimination, R =0.26 p <0.001 and R =0.17 p <0.001, respectively. No correlation was found for gender, age of the patients, comorbidities, or associated symptoms.

Conclusion: The threshold for treatment initiation time is up to 2 weeks, after which the amplitude of hearing improvement decreases significantly. The other prognostic factors measured were not found to be statistically significant predictors.

KEYWORDS

hearing loss, corticosteorids, audiogram, intratymapnic injection, discrimination

1. Introduction

Sudden sensory neural hearing loss (SSNHL) is defined as sensory neural hearing loss that appears within 72 h and is manifested by a decrease of at least 30 decibels (dB) in three consecutive frequencies in audiometry (1). The annual incidence of SSNHL is 5–27 people per 100,000 (2), with a 32–65% chance of spontaneous recovery without treatment (3–6). Several

prognostic factors have been identified, including the patient's age, the degree of hearing loss (HL), and additional symptoms (e.g., tinnitus, vertigo) (6).

Oral treatment with corticosteroids (CTS) with varying periods and dosages is the recommended treatment nowadays. The latest guidelines of the American Academy of Otolaryngology (AAO) define treatment with oral CTS as an optional treatment with a moderate level of evidence (7). According to these guidelines, the recommended period of time for initiation of treatment with oral CTS is up to 14 days from symptom onset. Academia and the literature base this recommendation on laboratory evidence of an inflammatory cell death cascade in SSNHL; the CTS aims to stop this cascade, and the window of time is set to 14 days (7, 8).

It is natural to assume that these laboratory findings will have clinical consequences. However, there is no consensus in the literature as to whether there is a strong correlation between the time from symptom onset to initiation of treatment and hearing improvement. Fetterman et al. did not find a clear relationship between these two factors and therefore did not include treatment initiation time as a prognostic factor (9). In contrast, Cvorovic et al. found that initiating CTS treatment within 7 days of symptom onset has a better prognosis than initiating treatment later (10). Those studies looked for a correlation between the time from onset of HL to treatment initiation but did not directly compare patients who began treatment before and after 14 days. Furthermore, the AAO recommended that clinicians should offer intratympanic steroid therapy when patients have incomplete recovery from SSNHL, even two to 6 weeks after symptom onset (7).

So far, no comprehensive data have been published to evaluate the AAO guidelines and recommendations, particularly the precise onset of oral treatment (up to 14 days). The main objective of this paper is to determine the relationship between the time from symptom onset to initiation of CTS treatment and improvement in hearing among patients suffering from SSNHL. The secondary objectives are to investigate additional prognostic factors (e.g., smoking, ischemic heart disease) (IHD), diabetes mellitus (DM), hypertension (HTN), age, gender, the severity of HL, and accompanying symptoms (tinnitus, vertigo) and their degree of correlation with improvement under CTS treatment.

2. Materials and methods

A retrospective cohort study was conducted on patients admitted to the Department of Otolaryngology and Head–Neck Surgery at Shaare Zedek Medical Center, diagnosed with SSNHL, and hospitalized during 2012–2021. The institutional review board approved the study protocol with a waiver of informed consent.

The patients' general information was collected, including demographics, medical background (IHD, DM, HTN), medications, accompanying symptoms, and the time from symptom onset to initiation of treatment. At least two hearing tests were performed for each patient (before and at the end of the treatment). These tests measured pure tone audiometry (PTA), Speech Recognition Threshold (SRT), and discrimination.

The treatment protocol followed the AAO Head and Neck Surgery Guidelines; that is, with no contraindication to oral corticosteroids (OCS), all patients were treated with Prednisone 30 mg twice daily for 1 week, and if no sufficient improvement was seen (if there was still ≥10 dB sensorineural hearing loss in at least two frequencies) a salvage treatment with once-daily intratympanic dexamethasone injection was initiated for another week while tapering the OCS over 5 days (7).

Inclusion criteria were presentation with SSNHL; exclusion criteria were partial treatment, a different diagnosis from SSNHL (conductive HL, acoustic trauma, vestibular schwannoma, Meniere's disease), congenital HL, and failure to follow-up.

The final cohort of patients enrolled was divided into five groups according to the period of time from symptom onset to treatment initiation as follows: 1st group: up to half a week (1–3 days) from onset of HL; 2nd group: 4–7 days, 3rd group: 8–14 days, 4th group: 15–21 days, 5th group: 22 days and over.

2.1. Audiometry tests

Certified audiologists in our medical center performed audiometry. The tests were performed in soundproof booths using a Grason-Stadler (GSI-61/AudioStar Pro) audiometer (Minnesota, USA) with standard audiometric parameters. The audiometers were calibrated annually. Pure tone average (PTA) was calculated using 500, 1,000, and 2,000 Hz. Maximum speech discrimination score % (SD) and speech recognition thresholds (SRT) were included for analysis; SRT is the minimum hearing level at which an individual can recognize 50% of spondaic words. The maximum speech discrimination score was obtained at a level of 35 dB above the SRT, or at a softer level if the standard level exceeded the users' comfort level or maximum output of the audiometer. A list of 50 monosyllabic Hebrew words was presented mostly in the live voice condition, and the maximum score was determined as the percentage of words repeated correctly.

2.2. Data processing

The effectiveness of the treatment was measured by calculating the improvement in specific frequencies, SRT, and discrimination for each individual. The amplitude of HL was determined both absolutely by considering only the affected ear and relatively by comparing the HL of the affected ear to the healthy ear (given that the healthy ear was not damaged), as follows:

- Absolute: comparison between affected ear at the end of treatment (AFFend) and affected ear before treatment (AFFbef).
  The equation used for absolute SRT measurements:
  AFFend SRT - AFFbef SRT
- Relative: comparison between affected ear improvement and severity of HL. This was calculated by dividing the difference between AFFend and AFFbef by the relative HL (i.e., healthy ear minus AFFbef).
  The equation used for relative SRT measurements:

$$\frac{\text{AFFend SRT} - \text{AFFbef SRT}}{\text{Healthy SRT} - \text{AFFbef SRT}}$$

TABLE 1 Demographic information, including gender, comorbidities, and associated symptoms, as a function of time from symptom onset.

Weeks	0.5	1	2	3	4+	*p*
Number	202	177	159	61	67	
M/F	109/93	90/87	74/85	30/31	33/34	0.72
Age Mean ± SD (years)	48.5 ± 19	47.1 ± 20	51.9 ± 17	47.5 ± 17	47.4 ± 19	0.27
Smoking %	5	7	12	8	9	0.26
DM %	10	14	13	16	16	0.35
HTN %	24	23	19	21	27	0.77
IHD %	4	5	6	2	6	0.66
Tinnitus %	75	66	69	66	61	0.18
Vertigo %	35	36	30	30	19	0.12

The *p*-value represents the difference between half, one and 2 weeks vs. three and 4 weeks and over. M/F, male/female; DM, Diabetes Mellitus; HTN, Hypertension; IHD, Ischemic Heart Disease. *p*-value obtained from Kruskal-Wallis or ANOVA test as appropriate.

TABLE 2 Primary audiometry results according to treatment initiation time in weeks from symptom onset.

Weeks	0.5	1	2	3	4+	*p*
Number	202	177	159	61	67	
First test SRT dB	59.2 ± 35	62.2 ± 34	48.8 ± 32	38.9 ± 26	44.1 ± 28	**<0.001**
First test PTA dB	52.3 ± 30	52.4 ± 29	39 ± 25	37.5 ± 20	39.9 ± 23	**<0.001**
First test discrimination %	51.4 ± 43	50.7 ± 44	67.4 ± 39	76.6 ± 33	75 ± 33	**<0.001**
Healthy ear - affected ear. First test SRT dB	43.4 ± 33	44.5 ± 34	31.4 ± 27	25.3 ± 25	28.4 ± 25	**<0.001**
Healthy ear - affected ear. First test PTA dB	37.4 ± 28	37.7 ± 29	26.2 ± 18	26.9 ± 18	27.4 ± 20	**<0.001**
Healthy ear - affected ear discrimination %	45.2 ± 43	42.3 ± 43	26.5 ± 36	22.4 ± 33	21.6 ± 31	**<0.001**

Bold values: $p < 0.05$. Mean ± SD. The *p*-value (Kruskal-Wallis) represents the difference between half, one and 2 weeks vs. 3 and 4 weeks and over. SRT, Speech Recognition Threshold; dB, Decibels; PTA, Pure Tune Average.

2.3. Statistical analysis

All data were collected in spreadsheets using Microsoft Excel. The statistical analysis was performed using SPSS software (IBM® SPSS® Statistics, version 26, Chicago, IL, United States). The statistical comparison between the different groups (divided according to time from symptom onset to initiation of treatment) was made using the non-parametric Kruskal-Wallis test; in the case where a statistically significant difference was found among all groups, we used the Mann–Whitney test to compare any two different groups with Bonferroni correction for multiple tests.

All statistical tests were two-tailed. Statistical significance was defined as $p \leq 0.05$. The degree of correlation between the time from symptom onset to treatment initiation and other possible prognostic factors with the success of the treatment was tested using the Spearman correlation test, where statistical significance was defined as $p \leq 0.05$.

3. Results

During the period 2012–2021, 765 patients diagnosed with SSNHL were hospitalized at Shaare Zedek Medical Center. After reviewing the files, 99 patients were excluded from the initial cohort in accordance with the exclusion criteria.

The study's final cohort included 666 patients: 336 men and 330 women. Right ear SSNHL was present in 329 patients, while 324 patients presented with left ear SSNHL, and 13 patients presented with bilateral SSNHL. The demographic data, medical background, and accompanying SSNHL symptoms are presented in Table 1. No significant statistical difference was found among the five time groups for any of the above parameters.

The average period of HL from symptom onset to initiation of treatment was 10.8 days. Most patients presented within the first two weeks (538, 80%), while 61 patients (9%) presented more than 4 weeks after symptom onset (Table 1). Following 1 week of oral treatment, 283 patients showed no or only very mild improvement and continued for another week of intratympanic treatment.

The results of the first hearing test according to the different treatment groups are presented in Table 2. A statistically significant difference was found in both absolute and relative SRT, PTA, and speech discrimination between the different groups. Figure 1 shows hearing improvement in pure tone audiometry before and at the end of the treatment. No significant difference in improvement was found between the examined frequencies.

Hearing improvement at the end of the treatment according to the different treatment groups is presented in Table 3. After Bonferroni correction, statistically significant differences were found between the groups of half a week, one week, and 2 weeks, and the groups of 3 weeks and 4 weeks and over (each group independently) in SRT, PTA, and discrimination. No difference was found between half a week, one week, and 2 weeks. No difference was also found between the three-week group and the 4 weeks and above group (Table 3).

Table 4 presents the results of hearing improvement (in SRT) with respect to the severity of HL in the different treatment groups. The severity of HL was divided as follows: Mild HL (20–40 dB), Moderate and Moderate to Severe HL (40–70 dB), Severe HL (75–90 dB), and Profound HL (95–110 dB). According to the hearing loss severity, subgrouping analyses were made between time groups regarding gender, age, vascular risk factors (IHD, DM, HTN, smoking), and accompanying symptoms (tinnitus and vertigo). There was no statistical significance except for HTN in severe hearing loss, which also did not survive the Bonferroni correction (data not presented). Even after stratifying the results according to the severity of HL, the clear trend of significance is maintained between initiating treatment within 2 weeks of symptom onset and initiating treatment more than 2 weeks after symptom onset. A significant difference was found regarding relative SRT improvement between severity groups for all patients (Mild: 0.47 ± 0.5, Moderate: 0.45 ± 0.4, Severe: 0.54 ± 0.4, Profound: 0.29 ± 0.3, $p < 0.001$). After Bonferroni correction, statistically significant differences were found between Profound and each of the other three groups: Mild ($p < 0.001$), Moderate ($p = 0.02$), and Severe ($p = 0.001$). No difference was found between Mild, Moderate, and Severe (Figure 2).

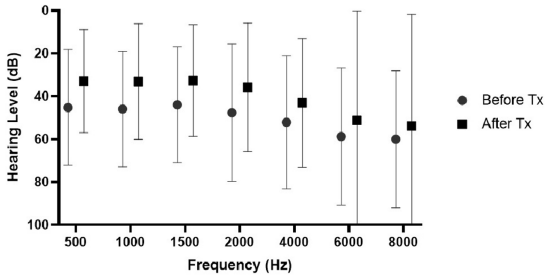

FIGURE 1
Hearing improvement following treatment according to the various frequencies of all 666 patients. Values represent mean and standard deviation.

A statistically significant correlation was found between treatment initiation in days (from symptom onset) and improvement in absolute and relative SRT and PTA indices ($R = 0.23$, $p < 0.001$, $R = 0.11$, $p < 0.019$, respectively).

No correlation was found between improvement in absolute and relative SRT indices and gender ($p = 0.2$ and $p = 0.18$, respectively) or age ($p = 0.32$ and $p = 0.22$, respectively). Furthermore, no correlation was found between vascular risk factors and improvement in absolute and relative SRT indices: DM ($p = 0.22$ and $p = 0.16$, respectively), IHD

TABLE 3 Hearing improvement indicators at the end of the treatment according to treatment initiation time in weeks from symptom onset.

Weeks	0.5	1	2	3	4+	*p*
Number	202	177	159	61	67	
SRT improvement dB	24.6 ± 23	23.4 ± 24	16.1 ± 17	5.8 ± 13	4.8 ± 7	**<0.001**
SRT relative improvement	0.53 ± 0.4	0.45 ± 0.4	0.41 ± 0.3	0.13 ± 0.5	0.2 ± 0.3	**<0.001**
PTA improvement dB	22.9 ± 24	19.8 ± 22	14.5 ± 13	5.5 ± 12	4.5 ± 8	**<0.001**
PTA relative improvement	0.52 ± 0.5	0.43 ± 0.5	0.4 ± 0.4	0.18 ± 0.4	0.24 ± 0.4	**<0.001**
Discrimination improvement %	30 ± 34	26 ± 33	18 ± 27	13 ± 18	7 ± 10	**<0.001**
Discrimination relative improvement	0.57 ± 0.4	0.52 ± 0.5	0.53 ± 0.4	0.51 ± 0.3	0.41 ± 0.5	0.3

Bold values: $p < 0.05$. Mean ± SD. The *p*-value (Kruskal-Wallis) represents the difference between half, one and 2 weeks vs. three and 4 weeks and over. SRT, Speech Recognition Threshold; dB, Decibels.

TABLE 4 Hearing improvement indicators at the end of the treatment according to treatment initiation time in weeks from symptom onset and hearing loss severity.

Hearing loss	Weeks	0.5	1	2	3	4+	*p*
Mild	Number	87	73	89	39	44	
	SRT improvement dB	10 ± 10	10 ± 10	8 ± 7	3 ± 8	5 ± 6	**<0.001**
	SRT relative improvement	0.63 ± 0.5	0.54 ± 0.2	0.49 ± 0.4	0.22 ± 0.6	0.29 ± 0.4	**<0.001**
Moderate	Number	46	35	37	15	12	
	SRT improvement dB	26 ± 18	19 ± 18	15 ± 13	9 ± 14	5 ± 8	**<0.001**
	SRT relative improvement	0.62 ± 0.3	0.43 ± 0.3	0.43 ± 0.3	0.25 ± 0.4	0.13 ± 0.2	**<0.001**
Severe	Number	24	21	9	2	6	
	SRT improvement dB	44 ± 25	35 ± 27	36 ± 15	20 ± 14	5 ± 6	**<0.001**
	SRT relative improvement	0.68 ± 0.3	0.54 ± 0.4	0.62 ± 0.2	0.31 ± 0.2	0.16 ± 0.2	**<0.001**
Profound	Number	42	43	20	4	4	
	SRT improvement dB	35 ± 26	34 ± 30	27 ± 30	5 ± 15	1 ± 0.25	**<0.001**
	SRT relative improvement	0.43 ± 0.3	0.4 ± 35	0.31 ± 0.3	0.5 ± 0.1	0.1 ± 0.3	**<0.001**

Bold values: $p < 0.05$. Mean ± SD. The *p*-value (Kruskal-Wallis) represents the difference between half, one, and 2 weeks vs. three and 4 weeks and over. SRT, Speech Recognition Threshold; dB, Decibels.

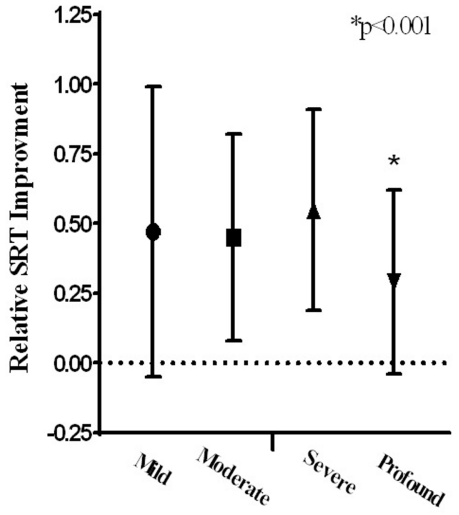

FIGURE 2
Relative SRT improvement according to hearing loss severity.

(p = 0.12 and p = 0.1, respectively), HTN (p = 0.81 and p = 0.62, respectively) and smoking (p = 0.61 and p = 0.45, respectively).

No correlation was found between improvement in absolute and relative SRT indices and the accompanying symptoms, tinnitus (p = 0.86 and p = 0.89, respectively) and vertigo (p = 0.85 and p = 0.43, respectively). Similarly, PTA and discrimination (absolute and relative) were not found to be in correlation with demographic parameters, vascular risk factors, or accompanying symptoms (data not presented).

In 65 patients, HL was in the high frequencies (above 30,000 Hz), with no loss of hearing in the lower and middle frequencies (Healthy SRT - AFFbef SRT = 0). The same trend of improvement described above was demonstrated; however, it was not significant due to the low numbers.

4. Discussion

In this study, we found an effect of the time from onset of SSNHL symptoms to treatment initiation on the amplitude of hearing improvement. A correlation of 20% was found between the time to treatment initiation and the degree of improvement in dB. Moreover, we found that the window of opportunity lasts up to 14 days, beyond which the effectiveness of the treatment decreases significantly. In addition, there is a clear, but not significant, trend of decreasing treatment efficacy from half a week to 2 weeks. Even after stratifying the results according to the severity of HL into four groups (mild, moderate, severe, and profound), the drop in treatment effectiveness after 2 weeks and the non-significant trend within the first two weeks are clearly maintained in each HL severity group. We found that tinnitus, vertigo, age, and patient medical background (IHD, DM, HTN) were not prognostic factors for hearing improvement.

This study is the first to examine the recommendations of the AAO, Head and Neck Surgery, published in 2012 and updated in 2019 (7, 11). For the first time, the recommendation to proceed to salvage treatment of intratympanic injection (ITI) with Dexamethasone after the failure of oral corticosteroid treatment (OCT) was examined. All patients included in this study were treated with Prednisone 60 mg daily for a week (except for patients whose blood sugar level and blood pressure were not balanced; in those cases, ITI was the initial treatment). In patients where a significant hearing improvement (baseline or close to baseline) was noticed at the end of the week with OCT treatment, another week of OCT tapper-down treatment was given. If no improvement was seen or slight improvement only, a laser myringotomy followed by ITI once daily with Dexamethasone was initiated for another week. The results of the hearing tests at the end of the treatment, whether they ended with OCT or ITI, were compared to the results of the first hearing test.

There is an inherent and significant difficulty involved in comparing the severity of HL and, consequently, the degree of improvement among different patients. In most cases, the patient's specific hearing threshold before the HL is unknown. Hence, the severity of HL and the consequent improvement cannot be determined. To overcome this problem, and assuming that in most patients, the hearing was symmetrical before the onset of unilateral HL (unless otherwise known), we used the results of the hearing test of the healthy ear as a reference for the condition of the diseased ear before the HL (10). We found a reference to this approach in the paper by Cvorovic et al., who used it the same way. It should be noted that the improvement in hearing is presented according to this method (relative) as well as in absolute terms (comparing before and after the affected ear).

Over the years, several retrospective studies have attempted to find prognostic factors for improvement concerning SSNHL. Among all the factors tested, the effect of the time from onset of HL to initiation of treatment was also tested. Fetterman et al. examined 184 patients treated with corticosteroids and found no correlation between time to initiation of treatment and improvement in hearing (9). In contrast, Byl et al., in a study published in 1977 that is considered a cornerstone in SSNHL research, found that for 26 patients treated with CTS, the treatment was effective if given up to 10 days after the onset of HL (3). Similarly, Change et al. found a worse prognostic factor among 146 patients starting treatment after the sixth day than among those starting treatment earlier (12). Xenellisand et al. also found a significant correlation between the time to initiation of treatment and improvement in hearing among 114 patients. Still, they did not specify the time point after which there was a substantial decrease in improvement (13). In a study on 541 patients, Cvorovic et al. found a significant difference in the degree of improvement in hearing if the treatment began more than 7 days after the onset of HL. The treatment given in this study was Prednisone 100 mg once a day for 7 days with no ITI treatment (10).

Despite accepted assumptions regarding the importance of the time to treatment initiation, more well-founded information is required to support this assumption. Moreover, there is a dispute as to what, if any, time period is relevant. In addition, the extent of the effect of the time to treatment initiation has never been examined with respect to the new recommendations, which include treatment with Prednisone 60 mg per day for 7 days and the addition of ITI treatment in case of a lack of improvement (11). In this study, for the first time, we found the precise time point (14 days) at which there is a significant drop in hearing gain following CTS treatment.

When examining the severity of hearing loss among the different time groups, it appears that patients who started treatment later

presented with milder hearing loss, both in SRT and in discrimination, compared to patients who began treatment earlier (Table 2). We can consider several explanations for this phenomenon. The degree of urgency to receive treatment may be lower for patients who suffer from milder HL since the HL is less noticeable. On the other hand, this trend may reflect a natural healing process over time, regardless of treatment. It can be assumed that patients who arrived after 2 weeks suffered initially from a more significant decrease in hearing that gradually improved over time. The average SRT results before treatment among the group that presented during the third week (group four: 61 patients) are similar to the results at the end of treatment for the groups that presented during the first week (groups one and two: 379 patients), 38.9 ± 26 and 36.7 ± 23, respectively. In other words, at the same time point since the onset of HL, the results were similar whether the patients received treatment or not. Therefore, we can conclude that the improvement of the early group is not a result of the CTS treatment but rather reflects the natural process of hearing improvement that took place in the group that presented later. A Cochrane review from 2013 concluded that the value of CTS in treating SSNHL remains unclear. The evidence obtained from randomized controlled trials presents contradictory outcomes, partly because the studies are based on an inadequate number of patients (14). These findings raise the question of whether CTS treatment helps at all.

No significant effects were found in the current study for any of the tested cardiovascular risk factors (CVRF): age, DM, IHD, HTN, and smoking. Previous studies have indicated that traditional cardiovascular risk factors such as HTN, DM, smoking, and IHD may contribute to SSNHL and have an impact on HL improvement (4, 10, 13, 15–18). However, these studies' weaknesses remain in their retrospective analysis, relatively small population sizes, and univariate analysis. Along the same line as our findings, Ullrich et al. and Ballesteros et al. found an identical frequency of CVRFs between controls and SSNHL patients (19, 20). Moreover, a meta-analysis recently published found that only hypercholesterolemia may be an independent risk factor for SSNHL but not other CVRF. They conclude that to clarify the relation between CVRFs and SSNHL, long-term, multi-center, and prospective studies are crucial but challenging (21). As with CVRF, the relationship between vertigo and tinnitus to severity and improvement in SSNHL is still controversial. An association between vertigo and poor auditory recovery prognosis has been observed (4, 12, 22, 23). Several theories have been described to explain this finding, including rupture of the labyrinthine membranes (24), the degree of biochemical alterations in the labyrinthine ionic composition (25), and the association with vestibular neuritis (26). However, as with our findings, in multivariate analysis, vertigo was not significantly associated with a worse hearing recovery prognosis (27). We believe that the strength of our study lies in the high number of patients included. Therefore, it further contributes to clarifying these doubtful questions.

This study has several limitations. First, it is a retrospective study and does not include a comparison with a control group. Of course, it is impossible to conduct such an analysis for ethical reasons since the accepted treatment worldwide is CTS, despite the absolute lack of evidence. In addition, among all patients presenting with SSNHL, there are many subgroups: HL at different frequencies, severity of HL, etc. Therefore, there is an inherent difficulty in including them all in one group. In this study, stratification was carried out as much as possible for these parameters. However, it is never possible to go down to the lowest resolution because this will create many groups with a small number of patients, affecting the statistical power of the analysis. Since this study's final cohort includes a large number of patients (666)—a larger sample than in all the studies carried out to date—we can assume that our results have critical statistical and clinical significance. Another limitation is the short-term follow-up since the last hearing test was conducted at the end of the treatment. However, this study aimed to compare treatment time groups at this time point, and we found significant differences. Moreover, most hearing improvements happened in the first few weeks (parallel to the end of treatment). No significant improvement or deterioration has been found in the long term, neither after several months nor after several years (28, 29).

5. Conclusion

The time from onset of HL to initiation of treatment is a prognostic factor with a correlation of *ca.* 20% with the degree of improvement in hearing. No significant trend was found within the first 14 days from the onset of HL. After 14 days, the effectiveness of the treatment drops dramatically. Age, accompanying symptoms (tinnitus, vertigo), smoking, and underlying diseases (IHD, DM, HTN) are not prognostic factors for hearing improvement and the success of CTS treatment.

Data availability statement

The raw data supporting the conclusions of this article will be made available by the authors, without undue reservation.

Author contributions

IC helped design the research, performed the research, analyzed the data, and took part in writing the manuscript. SE and OM performed the research and helped in data analysis. RS took a significant part in revising the paper. J-YS and RP helped in designing the study and writing of the manuscript. CS designed the study, analyzed the data, and drafted the paper. All authors contributed to the article and approved the submitted version.

Conflict of interest

The authors declare that the research was conducted in the absence of any commercial or financial relationships that could be construed as a potential conflict of interest.

Publisher's note

References

1. National Institute on Deafness and Other Communication Disorders. NIDCD Fact Sheet: Sudden Deafness In: . *Washington DUDoHaHS, editor. USA2018*

2. Alexander TH, Harris JP. Incidence of sudden sensorineural hearing loss. *Otol Neurotol*. (2013) 34:1586–9. doi: 10.1097/MAO.0000000000000222

3. Byl FM. Seventy-six cases of presumed sudden hearing loss occurring in 1973: prognosis and incidence. *Laryngoscope*. (1977) 87:817–25. doi: 10.1002/lary.5540870515

4. Byl FM. Sudden hearing loss: eight years' experience and suggested prognostic table. *Laryngoscope*. (1984) 94:647–61. doi: 10.1288/00005537-198405000-00014

5. Nosrati-Zarenoe R, Arlinger S, Hultcrantz E. Idiopathic sudden sensorineural hearing loss: results drawn from the Swedish national database. *Acta Otolaryngol*. (2007) 127:1168–75. doi: 10.1080/00016480701242477

6. Rauch SD. Clinical practice. Idiopathic sudden sensorineural hearing loss. *N Engl J Med*. (2008) 359:833–40. doi: 10.1056/NEJMcp0802129

7. Chandrasekhar SS, Tsai Do BS, Schwartz SR, Bontempo LJ, Faucett EA, Finestone SA, et al. Clinical practice guideline: sudden hearing loss (update). *Otolaryngol Head Neck Surg*. (2019) 161:S1–s45. doi: 10.1177/0194599819859885

8. McCall AA, Swan EE, Borenstein JT, Sewell WF, Kujawa SG, McKenna MJ. Drug delivery for treatment of inner ear disease: current state of knowledge. *Ear Hear*. (2010) 31:156–65. doi: 10.1097/AUD.0b013e3181c351f2

9. Fetterman BL, Saunders JE, Luxford WM. Prognosis and treatment of sudden sensorineural hearing loss. *Am J Otol* (1996); 17: 529–536

10. Cvorović L, Deric D, Probst R, Hegemann S. Prognostic model for predicting hearing recovery in idiopathic sudden sensorineural hearing loss. *Otol Neurotol*. (2008) 29:464–9. doi: 10.1097/MAO.0b013e31816fdcb4

11. Stachler RJ, Chandrasekhar SS, Archer SM, Rosenfeld RM, Schwartz SR, Barrs DM, et al. Clinical practice guideline: sudden hearing loss. *Otolaryngol Head Neck Surg*. (2012) 146:S1–S35. doi: 10.1177/0194599812436449

12. Chang NC, Ho KY, Kuo WR. Audiometric patterns and prognosis in sudden sensorineural hearing loss in southern Taiwan. *Otolaryngol Head Neck Surg*. (2005) 133:916–22. doi: 10.1016/j.otohns.2005.09.018

13. Xenellis J, Karapatsas I, Papadimitriou N, Nikolopoulos T, Maragoudakis P, Tzagkaroulakis M, et al. Idiopathic sudden sensorineural hearing loss: prognostic factors. *J Laryngol Otol*. (2006) 120:718–24. doi: 10.1017/S0022215106002362

14. Wei BP, Stathopoulos D, O'Leary S. Steroids for idiopathic sudden sensorineural hearing loss. *Cochrane Database Syst Rev*. (2013, 2013) :Cd003998. doi: 10.1002/14651858.CD003998.pub3

15. Chen I, Cohen O, Shaul C, Sichel JY, Perez R. Is it beneficial to treat patients presenting three weeks or longer after the onset of sudden sensorineural hearing loss? *J Int Adv Otol*. (2020) 16:323–7. doi: 10.5152/iao.2020.8489

16. Kang WS, Yang CJ, Shim M, Song CI, Kim TS, Lim HW, et al. Prognostic factors for recovery from sudden sensorineural hearing loss: a retrospective study. *J Audiol Otol*. (2017) 21:9–15. doi: 10.7874/jao.2017.21.1.9

17. Wen YH, Chen PR, Wu HP. Prognostic factors of profound idiopathic sudden sensorineural hearing loss. *Eur Arch Otorhinolaryngol*. (2014) 271:1423–9. doi: 10.1007/s00405-013-2593-y

18. Lin RJ, Krall R, Westerberg BD, Chadha NK, Chau JK. Systematic review and meta-analysis of the risk factors for sudden sensorineural hearing loss in adults. *Laryngoscope*. (2012) 122:624–35. doi: 10.1002/lary.22480

19. Ballesteros F, Alobid I, Tassies D, Reverter JC, Scharf RE, Guilemany JM, et al. Is there an overlap between sudden neurosensorial hearing loss and cardiovascular risk factors? *Audiol Neurootol*. (2009) 14:139–45. doi: 10.1159/000171475

20. Ullrich D, Aurbach G, Drobik C. A prospective study of hyperlipidemia as a pathogenic factor in sudden hearing loss. *Eur Arch Otorhinolaryngol*. (1992) 249:273–6. doi: 10.1007/BF00714491

21. Simões J, Vlaminck S, Seiça RMF, Acke F, Miguéis ACE. Cardiovascular risk and sudden sensorineural hearing loss: a systematic review and meta-analysis. *Laryngoscope*. (2023) 133:15–24. doi: 10.1002/lary.30141

22. Enache R, Sarafoleanu C. Prognostic factors in sudden hearing loss. *J Med Life*. (2008) 1:343–7.

23. Nakashima T, Yanagita N. Outcome of sudden deafness with and without vertigo. *Laryngoscope*. (1993) 103:1145–9. doi: 10.1288/00005537-199310000-00012

24. Simmons FB. Theory of membrane breaks in sudden hearing loss. *Arch Otolaryngol*. (1968) 88:41–8. doi: 10.1001/archotol.1968.00770010043009

25. Khetarpal U. Investigations into the cause of vertigo in sudden sensorineural hearing loss. *Otolaryngol Head Neck Surg*. (1991) 105:360–71. doi: 10.1177/019459989110500303

26. Rahko T, Karma P. New clinical finding in vestibular neuritis: high-frequency audiometry hearing loss in the affected ear. *Laryngoscope*. (1986) 96:198–9. doi: 10.1288/00005537-198602000-00013

27. Perez Ferreira Neto A, da Costa MR, Dore Saint Jean L, Ribeiro S, de Souza L, de Oliveira PN. Clinical profile of patients with unilateral sudden sensorineural hearing loss: correlation with hearing prognosis. *Otolaryngol Head Neck Surg*. (2021) 165:563–70. doi: 10.1177/0194599820986571

28. Pecorari G, Riva G, Naqe N, Bruno G, Nardo M, Albera R. Long-term audiometric outcomes in unilateral sudden sensorineural hearing loss without recurrence. *J Int Adv Otol*. (2019) 15:56–61. doi: 10.5152/iao.2019.6670

29. Psifidis AD, Psillas GK, Daniilidis J. Sudden sensorineural hearing loss: long-term follow-up results. *Otolaryngol Head Neck Surg*. (2006) 134:809–15. doi: 10.1016/j.otohns.2005.12.002

frontiers | Frontiers in Neurology

TYPE Original Research
PUBLISHED 27 April 2023
DOI 10.3389/fneur.2023.1090184

OPEN ACCESS

EDITED BY
Michael Strupp,
Ludwig Maximilian University of Munich, Germany

REVIEWED BY
Joseph Attias,
University of Haifa, Israel
Peter Thorne,
The University of Auckland, New Zealand

*CORRESPONDENCE
Fayez Bahmad Jr.
✉ fayezbjr@gmail.com

SPECIALTY SECTION
This article was submitted to Neuro-Otology, a section of the journal Frontiers in Neurology

RECEIVED 05 November 2022
ACCEPTED 30 March 2023
PUBLISHED 27 April 2023

CITATION
Caldas FF, Buzo BC, Masiero BS, Takeuti AA, Cardoso CC, Elias TGA and Bahmad F Jr. (2023) Novel cochlear implant assessment tool: Comparative analysis of children and adults. *Front. Neurol.* 14:1090184. doi: 10.3389/fneur.2023.1090184

Novel cochlear implant assessment tool: Comparative analysis of children and adults

Fernanda Ferreira Caldas[1,2], Byanka Cagnacci Buzo[3], Bruno Sanches Masiero[4], Alice Andrade Takeuti[1], Carolina Costa Cardoso[2], Thais Gomes Abrahão Elias[2] and Fayez Bahmad Jr.[1,2]*

[1]Department of the Faculty of Health Sciences, University of Brasilia, Brasília, Brazil, [2]Brasiliense Institute of Otorhinolaryngology, Brasília, Brazil, [3]Cochlear Latin America, São Paulo, Brazil, [4]Department of Communications, School of Electrical and Computer Engineering, University of Campinas, Campinas, Brazil

Objectives: To analyse the results of children and adults with cochlear implants (CIs) in pure tone audiometry (PTA) and speech perception tests. Tests were performed in two ways: using loudspeakers in the sound booth (SB) and with direct audio input (DAI) employing the *Cochlear Latin America BOX* (CLABOX).

Methods: Fifty individuals (33 adults and 17 children) participated in the study, including children aged between 8 and 13years; of these, 15 users had bilateral CIs, 35 had unilateral CIs, and all had severe to profound bilateral sensorineural hearing loss. All participants were evaluated in the SB with loudspeakers and the CLABOX with DAI. The following evaluations were conducted: PTA, speech recognition tests with the *hearing in noise test* (HINT).

Results: The results for PTA and HINT conducted in SB and with CLABOX presented no significant difference between children and adults.

Conclusion: The CLABOX tool presents a new possible method to evaluate PTA and speech recognition tests in adults and children, with results comparable to the conventional evaluation in the SB.

KEYWORDS

cochlear implant, speech perception, audiometry, adults, children

1. Introduction

Cochlear implants (CIs) are an effective and safe treatment that provides functional hearing and listening comprehension and aid in language acquisition in children. Implant placement surgery can be performed unilaterally or bilaterally, simultaneously or sequentially; to develop binaural skills, it is necessary to perform bilateral implant placement (1).

To maximize the rehabilitative benefits, including cochlear implants as part of the treatment plan, it's crucial to consider performing this surgery at a younger age. Research suggests that children who receive cochlear implants before the age of 3.5 years show a quicker development of the desired cortical morphology and latency in the cortical P1 wave response (2). Niparko (3) studied 188 implanted children. The group of children who received CIs at less than 18 months of age had significantly better comprehension and language results than children who underwent implantation between 18 and 36 months and those older than 36 months. Most children who

underwent implantation before 18 months had results parallel to their hearing peers; those who underwent implantation after 18 months of age had smaller increases in performance and greater variability in understanding and expression.

To evaluate and confirm the auditory abilities of cochlear implant users, traditional methods involve conducting pure tone audiometry (PTA) and speech recognition tests within a soundproof booth (SB) to assess skills such as speech detection and recognition. To perform these assessments accurately, the sound booth must have proper acoustic treatment to avoid wall reflections, approximating a free field condition, and minimal background noise to minimize external factors that could impact the test results (4, 5). It also requires high-quality loudspeakers.

An alternative to testing speech recognition in a SB is the direct audio input (DAI) assessment, which allows the input signal to bypass an external microphone, eliminating the oscillations of ambient noise and reverberation at the test site (6, 7).

Based on the need for new tools to assist audiologists in CI assessment and programming validation, the company *Cochlear Corporation* developed a portable box with a companion software called *Cochlear Latin America BOX* (CLABOX) to transmit the sound stimuli directly to the CI *via* DAI. In this study, we aimed to analyse PTA and speech perception tests results of children and adults using CIs performed in the SB and with the CLABOX with DAI.

2. Materials and methods

2.1. Ethics

The study was analysed and approved by the Research Ethics Committee of the Faculty of Health Sciences, University of Brasilia, under protocol 4327050. All participants and parents/guardians of the children consented to participate in the research. The study was carried out at a CI centre in the city of Brasilia, DF, Brazil.

2.2. Participants

Fifty individuals with CIs participated in the study (33 adults and 17 children). The children's ages ranged from 8 to 13 years, with a mean of 9.7 years (± 0.8 years). The adults' age ranged from 18 to 78 years, with a mean age of 32.3 years (± 5.8 years). 15 participants used bilateral CIs and 35 unilateral CIs; 38 had prelingual hearing loss, and 12 had postlingual hearing loss. Of these, all children were prelingual; of the adults, 12 were postlingual, and 21 were prelingual. All had at least 6 months of experience with CI use and were users of the *Cochlear Corporation* brand.

2.3. CLABOX with DAI assessment

To utilize the CLABOX with the DAI connector, it was necessary to install a driver for the audio interface Audiobox iOne-Presonus on the computer. The audio interface features a USB 2.0 connection, 24-bit resolution, and a frequency response of 20 Hz to 30 kHz, with 44.1, 48, 88.2, and 96 Hz sampling frequencies. The interface is connected to the cochlear implant through a stereo headphone output with an output impedance of 10 Ω.

The CLABOX calibration followed the same standards as the conventional audiometric calibration, according to ISO 8253 and the manufacturer's information. The software was written with MATLAB and has an accompanying graphical user interface (GUI) written with MATLAB's AppDesigner. The GUI had five tabs: one for the examiner to enter the individual's data, one for PTA, one for the Ling test, one for the speech recognition test, and one for the examiner to adjust high-level preferences. The software was compiled using MATLAB as a standalone application.

All participants used the same CP910 speech processor with identical settings. The audio cable accessory was in the "Only" option. Thus, the participant heard only the test stimuli directly from the software, with ambient sounds excluded (7, 8).

2.4. Evaluation in the SB with free field

A MADSEN audiometer, model Itera II, SB, REDUSOM brand, serial number 8020, was used. All tests were performed in free field condition, with the loudspeaker positioned at 0° azimuth and at a distance of one metre from the participant. Features like the adaptive directional microphone (SCAN mode) were deactivated.

2.5. Evaluation in the SB and CLABOX

To assess speech recognition, the Brazilian Portuguese version of the hearing in noise test (HINT) was applied (9–12). The software randomly selected the presentation of the sentence lists, and the examiner manually analysed the number of correct words in each sentence presented. Analysing the sentence in noise, a minimum of 75% correct answers was expected. The tests were always performed on separate ears under two conditions:

1. Fixed noise, with a signal-to-noise (S/N) ratio of +10 dB, 65 dB(A) of speech and 55 dB(A) of noise;
2. Adaptive noise, noise presented at 55 dB(A) with variable levels of 4 dB in the initial stage and 2 dB in the final stage, that is, 4 dB increments for the first four sentences and 2 dB increments for the rest.

To assess PTA, frequencies of 250, 500, 1,000, 2000, 3,000, 4,000 and 6,000 Hz were investigated in separate ears, with a pulsatile stimulus of 1.5 Hz in the free field. The four-tone average was also used (500, 1,000, 2,000 and 4,000 Hz).

2.6. Statistical analysis

This study used a significance level of 0.05 (5%) and 95% confidence intervals. Nonparametric statistical tests were used (Mann–Whitney test, Wilcoxon test, McNemar test, Kappa and Spearman correlation analysis). To complement statistical significance and determine effect sizes, Cohen's D (difference) was calculated, with values of 0.20 (small effect), 0.50 (medium effect), 0.80 (large effect) and 1.20 (very large effect). Only participants tested in the acoustic booth and with the CLABOX were analysed. This way, we obtained paired data, which were examined using the Wilcoxon test.

3. Results

The results of the comparison between children and adults in the SB, of the comparison of children and adults assessed by the CLABOX systems for speech recognition in the HINT, and data on tonal thresholds are presented in Tables 1, 2. These results present differences between children and adults and the evaluation between the two systems; however, they cannot be considered statistically significant (value of $p>0.05$). In the speech perception test with fixed noise (S/N + 10 dB) and in the SB ($p = 0.586$), children had 81.8% correct answers, and adults had 77.2% correct answers; with the CLABOX ($p = 0.784$), the result was 88.3% for both children and adults. In the HINT test with adaptive noise, in the SB ($p = 0.356$), the values of the S/N ratio were 2.80 dB (children) and 3.79 dB (adults), and with the CLABOX ($p = 0.769$), the results were 1.73 dB (children) and 2.38 dB (adults). In the PTA results, the four-tone average in the SB was 23.8 dB for children and 22.60 dB for adults, $p = 0.246$, while with the CLABOX, the four-tone average for children was 31.3 dB and 28.9 dB for adults, $p = 0.182$. The effect size (Cohen's d) was calculated to complement the statistical significance analysis. The values were small, and the maximum was 0.518, thus classified as medium. Thus, we confirm that the differences between these two groups of children and adults are small and not statistically significant.

Figures 1, 2 present the results for children and adult participants in box plot format, with the HINT in fixed noise (S/N + 10 dB) and adaptive noise (noise at 55 dB) in the SB and with the CLABOX. Figures 3, 4 show the PTA threshold data in the two systems when comparing children and adults. The figures with box plots represent the 25th and 75th percentiles (box boundaries) and medians (horizontal lines). The outliers are indicated with asterisks.

Table 3 shows an analysis of the ears of all participants who could not perform the speech perception test in fixed noise (R/S + 10 dB) using the CLABOX and SB. In the SB assessment, there were 30 participants with CI on the right ear (26.7% were children and 73.3% were adults) and 27 on the left (29.6% were children and 70.4% were adults). In the CLABOX assessment, there were 32 participants with CI on the right ear (31.3% were children and 68.8% were adults) and 28 ears on the left (32.1% were children and 67.9% were adults).

4. Discussion

The new CLABOX tool with the DAI connector allowed us to conduct practical evaluations compared to the SB's conventional evaluation. This would mainly be useful for centres that still do not have a way to evaluate and validate CI programming, as it is a small, light and easy-to-carry tool that can be used on a table.

Pure tone and speech perception tests were carried out on 50 participants (63 ears), including children and adults, and were performed only in the face-to-face condition. The evaluation with the DAI connection does not retain interference with background noise, room acoustics or reverberations, either in person or remotely (5, 6). The limitation of this study was that it was carried out in the first year of the coronavirus pandemic (COVID−19), which reduced the size of the sample.

Of the studies that used the connection by DAI and the SB in speech recognition tests (4, 6, 8, 13), only Goehring et al. (4) and Sevier et al. (8) collected data from adults and older children; however, the averages of the results were analysed together. This study presents speech recognition and PTA data from children and adults in separate groups.

In the evaluations between the CLABOX and SB tools, the results showed no significant differences in the PTA and speech perception tests in noise between the groups of children and adults. Sevier et al. (8) and de Graaff et al. (13) compared the results with the DAI connection in telepractice and SB using speech perception tests in silence and in noise and found similar results between the two forms of evaluation in silence; however, with the presence of noise, the modality with DAI presented better results.

The fact that children and adults have similar hearing performance can be explained by several factors, such as early implantation in children, effective use of the electronic device, and the active and effective participation of all families and/or guardians of these children in the hearing (re)habilitation

TABLE 1 Comparison of SB and CLABOX in the groups of children and adults in the speech perception test - HINT.

			Average	Median	Standard deviation	Q1	Q3	No	CI	*p*-value	Cohen's *d*
Fixed Noise	SB	Children	81.8%	80.3%	10.5%	77.3%	89.3%	15	5.3%	0.586	0.308
		Adult	77.2%	79.5%	17.5%	72.3%	91.8%	25	6.9%		
	CLABOX	Children	88.3%	90.0%	12.8%	85.0%	100%	15	6.5%	0.784	0.000
		Adult	88.3%	95.0%	14.1%	80.0%	100%	25	5.5%		
	Delta	Children	6.5%	4.8%	8.4%	3.6%	9.0%	15	4.2%	0.356	0.396
		Adult	11.1%	8.3%	13.5%	0.5%	21.7%	25	5.3%		
Adaptative Noise	SB	Children	2.80	2.60	3.68	1.08	4.08	15	1.86	0.394	0.279
		Adult	3.79	3.15	3.58	1.05	5.60	25	1.40		
	CLABOX	Children	1.73	1.37	3.68	−1.00	3.78	15	1.86	0.769	0.156
		Adult	2.38	2.13	4.56	−0.88	5.10	25	1.79		
	Delta	Children	−1.07	−1.44	2.62	−2.46	0.83	15	1.32	0.586	0.128
		Adult	−1.41	−2.35	2.72	−3.40	0.55	25	1.07		

TABLE 2 Comparison of SB and CLABOX in the groups of children and adults in the PTA.

			Average	Median	Standard deviation	Q1	Q3	No	CI	*p*-value	Cohen's *d*
250 Hz	SB	Children	32.0	35.0	8.2	25.0	40.0	23	3.4	0.358	0.235
		Adult	30.1	30.0	7.7	25.0	35.0	40	2.4		
	CLABOX	Children	33.9	30.0	7.8	30.0	37.5	23	3.2	0.173	0.448
		Adult	30.9	30.0	6.3	30.0	35.0	40	2.0		
	Delta	Children	1.96	5.00	8.36	−2.50	10.00	23	3.42	0.361	0.163
		Adult	0.75	0.00	7.03	−5.00	5.00	40	2.18		
500 Hz	SB	Children	25.0	25.0	5.8	25.0	25.0	23	2.4	0.908	0.086
		Adult	24.5	25.0	6.0	20.0	30.0	40	1.9		
	CLABOX	Children	34.8	35.0	9.2	27.5	42.5	23	3.8	0.135	0.509
		Adult	30.8	30.0	7.3	25.0	35.0	40	2.3		
	Delta	Children	9.78	10.00	8.98	5.00	15.00	23	3.67	0.071	0.451
		Adult	6.25	5.00	7.32	0.00	10.00	40	2.27		
1 kHz	SB	Children	25.7	25.0	4.8	25.0	25.0	23	2.0	0.059	0.518
		Adult	23.1	25.0	5.0	20.0	25.0	40	1.6		
	CLABOX	Children	33.0	30.0	8.6	30.0	37.5	23	3.5	0.094	0.499
		Adult	29.6	30.0	5.8	25.0	35.0	40	1.8		
	Delta	Children	7.39	10.00	10.10	5.00	12.50	23	4.13	0.461	0.108
		Adult	6.50	5.00	7.18	5.00	10.00	40	2.22		
2 kHz	SB	Children	22.2	20.0	4.2	20.0	25.0	23	1.7	0.456	0.180
		Adult	21.4	20.0	4.7	20.0	25.0	40	1.4		
	CLABOX	Children	29.3	30.0	6.4	25.0	32.5	23	2.6	0.818	0.123
		Adult	28.6	30.0	5.7	25.0	30.0	40	1.8		
	Delta	Children	7.17	5.00	7.95	2.50	12.50	23	3.25	0.994	0.010
		Adult	7.25	5.00	7.92	5.00	10.00	40	2.45		
3 kHz	SB	Children	22.0	20.0	4.7	20.0	25.0	23	1.9	0.760	0.088
		Adult	22.4	20.0	4.9	20.0	25.0	40	1.5		
	CLABOX	Children	29.8	30.0	7.1	25.0	35.0	23	2.9	0.232	0.359
		Adult	27.6	25.0	5.4	25.0	30.0	40	1.7		
	Delta	Children	7.83	5.00	9.27	2.50	12.50	23	3.79	0.399	0.344
		Adult	5.25	5.00	6.50	0.00	10.00	40	2.01		
4 kHz	SB	Children	22.2	20.0	5.0	20.0	25.0	23	2.0	0.406	0.162
		Adult	21.4	20.0	5.1	20.0	25.0	40	1.6		
	CLABOX	Children	28.0	25.0	4.9	25.0	30.0	23	2.0	0.196	0.328
		Adult	26.5	25.0	4.7	25.0	30.0	40	1.5		
	Delta	Children	5.87	5.00	5.96	5.00	10.00	23	2.44	0.823	0.130
		Adult	5.13	5.00	5.72	5.00	10.00	40	1.77		
6 kHz	SB	Children	20.9	20.0	6.0	17.5	25.0	23	2.4	0.333	0.161
		Adult	20.0	20.0	5.2	15.0	20.0	40	1.6		
	CLABOX	Children	25.0	25.0	7.7	25.0	25.0	23	3.1	0.874	0.020
		Adult	24.9	25.0	5.5	20.0	30.0	40	1.7		
	Delta	Children	4.13	5.00	6.85	0.00	7.50	23	2.80	0.471	0.123
		Adult	4.88	5.00	5.72	5.00	10.00	40	1.77		
Four-Tone average	SB	Children	23.8	22.5	3.9	21.3	23.8	23	1.6	0.246	0.300
		Adult	22.6	22.5	3.9	20.0	24.1	40	1.2		
	CLABOX	Children	31.3	30.0	6.8	26.9	35.6	23	2.8	0.182	0.436
		Adult	28.9	28.8	4.9	25.9	31.6	40	1.5		
	Delta	Children	7.55	7.50	7.35	3.13	11.25	23	3.00	0.382	0.202
		Adult	6.28	6.25	5.78	3.75	9.06	40	1.79		

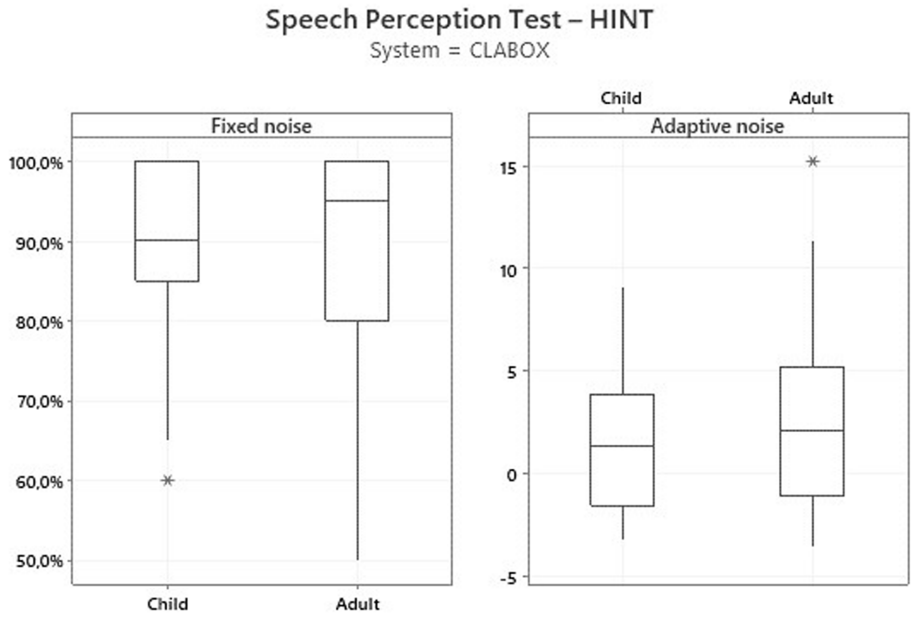

FIGURE 1
HINT with fixed noise (S/N+10dB) and adaptive noise at 55dB in the SB. The box plot represents the 25th and 75th percentiles (box boundaries) and the medians (horizontal line). Outliers are indicated with asterisks.

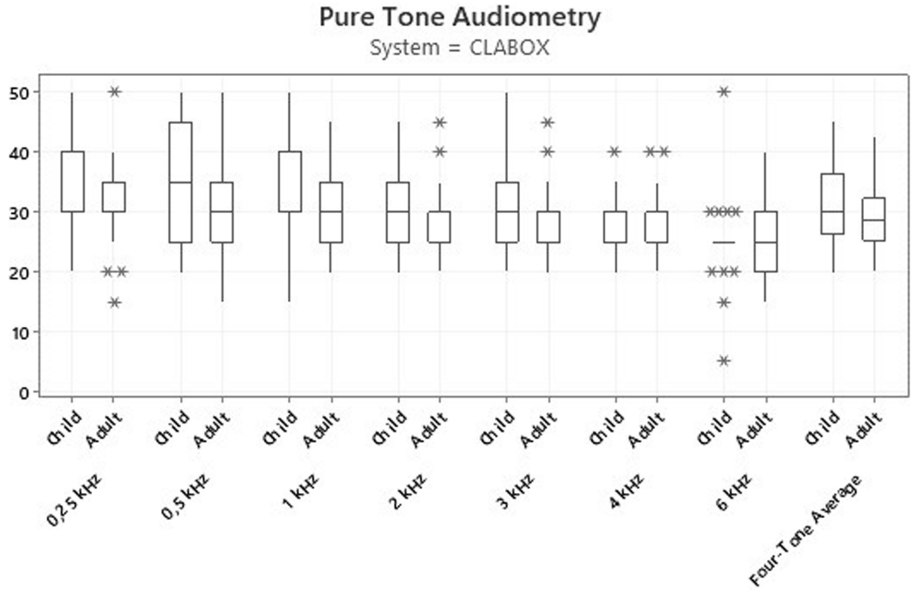

FIGURE 2
HINT with fixed noise (S/N+10dB) and adaptive noise at 55dB with the CLABOX. The box plot represents the 25th and 75th percentiles (box boundaries) and the medians (horizontal line). Outliers are indicated with asterisks.

process. The study by Sharma et al. (3) revealed that the central auditory system has greater plasticity in the first years of life; thus, children who undergo implantation in this period have improved cortical auditory development and the ability to respond to sounds months after implantation. Early intervention for hearing loss, centred on the family, takes place in partnership between families and professionals and is characterised by reciprocity, mutual trust, respect, honesty, shared tasks and open communication. Monitoring the evolution of listening and language skills is guided by the evolution of the child and the family (14).

In the study by Sbompato et al. (10), with normal-hearing children between 7 and 14 years of age, to assess speech perception, the results were worse in the HINT assessment when speech and noise were in the same position, that is, at 0° azimuth from the box, the S/N ratio was −3.20 dB. Novelli et al. (9) also evaluated normal-hearing children aged

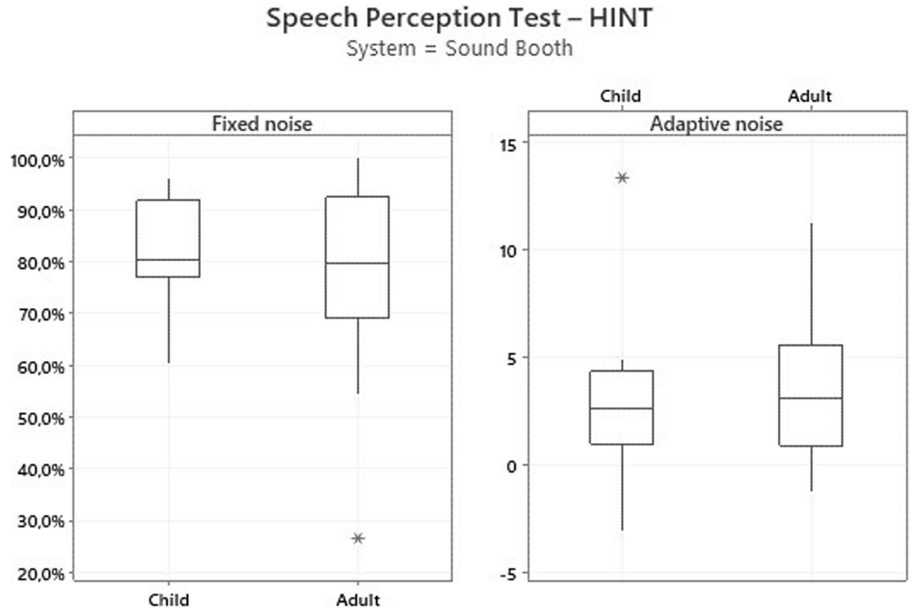

FIGURE 3
Thresholds for the PTA assessment in the SB. The results were not statistically significant at all frequencies evaluated. The box plot represents the 25th and 75th percentiles (box boundaries) and medians (horizontal lines). Outliers are indicated with asterisks.

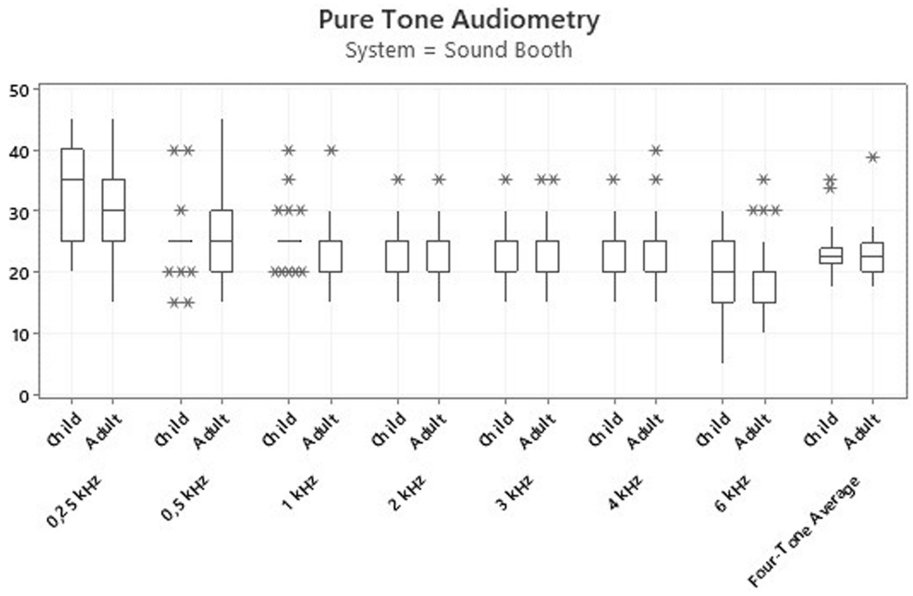

FIGURE 4
Thresholds for the PTA assessment with the CLABOX. The results were not statistically significant at all frequencies evaluated. The box plot represents the 25th and 75th percentiles (box boundaries) and medians (horizontal lines). Outliers are indicated with asterisks.

8 to 10 with the HINT and found an average S/N ratio with frontal noise of −2.61 dB. In this study, the tests were performed at 0° azimuth, with S/N ratio values of 2.80 dB for children and 3.79 dB for adults in the SB and 1.73 dB in children and 2.38 dB in children. Adults had the best results with the CLABOX; however, there was no significant difference. A difference between these studies occurred in the criterion of the percentage of correct answers in the sentences; in this study, the assertive results were selected with a more difficult percentage of 75% versus 50% in the other studies (9, 10). This shows that we established a more difficult criterion for the S/N ratio and in the difference between normal-hearing children and those with CIs (15).

Regarding the results in the adult group, in the standardisation of the HINT with 13 different languages, the test with the presence of noise in the frontal position was also more difficult than that in the other conditions, and the results were similar between the languages, with an average of −3.9 dB S/N (16). In this study, we had results with a positive S/N ratio in the speech-to-frontal noise tests in the adult population. In the study by Goff et al. (15), the HINT with adaptive

TABLE 3 Characterisation of participants by number of ears that were unable to perform the HINT.

		Fixed noise – SB		Fixed noise – CLABOX	
		Right ear	Left ear	Right ear	Left ear
Total		30	27	32	28
Children	N	8	8	10	9
	%	26.7%	29.6%	31.3%	32.1%
Adult	N	22	19	22	19
	%	73.3%	70.4%	68.8%	67.9%

noise had an average of 5.87 dB and a fixed average of 71.19%; thus, these data corroborated our results. In the SB, we found 81.8% on average for children, 77.2% for adults and 88.3% for children and adults using the CLABOX. Maurer et al. (17) evaluated the speech recognition of subjects with CIs and divided them into two groups according to the responses obtained: Group 1 had a good performance, indicated by speech recognition scores between 90 and 100%, and Group 2 had poor performance with scores between 0 and 85% (17).

The studies that compared speech recognition between the tests with DAI and SB's connection were conducted in silence and in noise (4, 6, 8, 13). In this study, we also evaluated speech recognition in noise and included the assessment of PTA; the results revealed no significant difference between the groups of children and adults. The SB had a four-tone average of 23.8 dB for children and 22.60 dB for adults, while WITH the CLABOX we observed 31.3 dB for children and 28.9 dB for adults.

The HINT measures the sentence recognition threshold, which is defined with the presentation in silence or in noise (S/N) for a listener to recognize the sentences; however, when the test is performed with CI users, some listeners may be unable to repeat the entire sentence, even in a silent condition (18, 19). Thus, some participants were not able to perform the HINT. In the SB, we had 30 ears on the right side, 27 ears on the left side, 32 ears on the right side and 28 ears on the left side. This fact can be justified by the difficulty in speech discrimination and recognition and not by the form of evaluation between the connection by DAI and the SB. This analysis may help one reach the conclusion that the CLABOX is a new assessment tool for speech recognition in individuals with CIs, both adults and children. The CLABOX tool may also be a possible option for use in countries that are starting or expanding CI indications due to its practicality of evaluation and cost-effectiveness.

In conclusion, the CLABOX tool proved to be a new assessment possibility in PTA and speech recognition tests, for adults and children, compared to the conventional assessment in the SB.

Data availability statement

The original contributions presented in the study are included in the article/supplementary material, further inquiries can be directed to the corresponding author.

Ethics statement

The studies involving human participants were reviewed and approved by Ethics Committee of the Faculty of Health Sciences, University of Brasilia. Written informed consent to participate in this study was provided by the participants' legal guardian/next of kin.

Author contributions

FC conceived and planned the experiments and wrote the manuscript with support from AT, CC, and TE. BB and BM were responsible for developing the CLABOX tool. FB supervised and reviewed the manuscript. All authors contributed to the article and approved the submitted version.

Conflict of interest

BB was employed by company Cochlear Latin America.

The remaining authors declare that the research was conducted in the absence of any commercial or financial relationships that could be construed as a potential conflict of interest.

Publisher's note

All claims expressed in this article are solely those of the authors and do not necessarily represent those of their affiliated organizations, or those of the publisher, the editors and the reviewers. Any product that may be evaluated in this article, or claim that may be made by its manufacturer, is not guaranteed or endorsed by the publisher.

References

1. Ramos-Macías A, Deive-Maggiolo L, Artiles-Cabrera O, González-Aguado R, Borkoski-Barreiro SA, Masgoret-Palau E, et al. Bilateral cochlear implants in children: acquisition of binaural hearing. *Acta Otorrinolaringol Esp*. (2013) 64:31–6. doi: 10.1016/j.otorri.2012.06.011

2. Sharma A, Dorman MF, Kral A. The influence of a sensitive period on central auditory development in children with unilateral and bilateral cochlear implants. *Hear Res*. (2005) 203:134–43. doi: 10.1016/j.heares.2004.12.010

3. Niparko JK, Tobey EA, Thal DJ, Eisenberg LS, Wang NY, Quittner AL, et al. CDaCI investigative team. Spoken language development in children following cochlear implantation. *JAMA*. (2010) 303:1498–506. doi: 10.1001/jama.2010.451

4. Goehring JL, Hughes ML, Baudhuin JL, Valente DL, McCreery RW, Diaz GR, et al. The effect of technology and testing environment on speech perception using telehealth with cochlear implant recipients. *J Speech Lang Hear Res*. (2012) 55:1373–86. doi: 10.1044/1092-4388(2012/11-0358)

5. Hughes ML, Goehring JL, Baudhuin JL, Diaz GR, Sanford T, Harpster R, et al. Use of telehealth for research and clinical measures in cochlear implant recipients: a validation study. *J Speech Lang Hear Res*. (2012) 55:1112–27. doi: 10.1044/1092-4388(2011/11-0237)

6. de Graaff F, Huysmans E, Qazi OU, Vanpoucke FJ, Merkus P, Goverts ST, et al. The development of remote speech recognition tests for adult Cochlear implant users: the effect of presentation mode of the noise and a reliable method to deliver sound in home environments. *Audiol Neurootol*. (2016) 21:48–54. doi: 10.1159/000448355

7. Chen C, Stein AL, Hughes ML, Morris HR, Litvak LM, Zeitler DM. Testing speech perception with Cochlear implants through digital audio streaming in a virtual sound booth: a feasibility study. *J Am Acad Audiol*. (2021) 32:219–28. doi: 10.1055/s-0041-1722990

8. Sevier JD, Choi S, Hughes ML. Use of direct-connect for remote speech-perception testing in Cochlear implants. *Ear Hear*. (2019) 40:1162–73. doi: 10.1097/aud.0000000000000693

9. Novelli CL, Carvalho NG, Colella-Santos MF. Hearing in noise test, HINT-Brazil, in normal-hearing children. *Braz J Otorhinolaryngol*. (2018) 84:360–7. doi: 10.1016/j.bjorl.2017.04.006

10. Sbompato AF, Corteletti LC, Moret Ade L, Jacob RT. Hearing in noise test Brazil: standardization for young adults with normal hearing. *Braz J Otorhinolaryngol*. (2015) 81:384–8. doi: 10.1016/j.bjorl.2014.07.018

11. Bevilacqua MC, Banhara MR, Da Costa EA, Vignoly AB, Alvarenga KF. The Brazilian Portuguese hearing in noise test. *Int J Audiol*. (2008) 47:364–5. doi: 10.1080/14992020701870205

12. Melo RD, Menezes DC, Pacífico FA, Advíncula KP, Griz SM. Brazilian Portuguese hearing in noise test (HINT): different interpretation criteria for individuals' responses. *Codas*. (2017) 29:e20160082. Portuguese, English. doi: 10.1590/2317-1782/20172016082

13. de Graaff F, Huysmans E, Merkus P, Theo Goverts S, Smits C. Assessment of speech recognition abilities in quiet and in noise: a comparison between self-administered home testing and testing in the clinic for adult cochlear implant users. *Int J Audiol*. (2018) 57:872–80. doi: 10.1080/14992027.2018.1506168

14. Moeller MP, Carr G, Seaver L, Stredler-Brown A, Holzinger D. Best practices in family-centered early intervention for children who are deaf or hard of hearing: an international consensus statement. *J Deaf Stud Deaf Educ*. (2013) 18:429–45. doi: 10.1093/deafed/ent034

15. Goffi-Gomez MVS, Muniz L, Wiemes G, Onuki LC, Calonga L, Osterne FJ, et al. Contribution of noise reduction pre-processing and microphone directionality strategies in the speech recognition in noise in adult cochlear implant users. *Eur Arch Otorhinolaryngol*. (2021) 278:2823–8. doi: 10.1007/s00405-020-06372-2

16. Soli SD, Wong LL. Assessment of speech intelligibility in noise with the hearing in noise test. *Int J Audiol*. (2008) 47:356–61. doi: 10.1080/14992020801895136

17. Maurer J, Collet L, Pelster H, Truy E, Gall??go S. Auditory late cortical response and speech recognition in Digisonic cochlear implant users. *Laryngoscope*. (2002) 112:2220–4. doi: 10.1097/00005537-200212000-00017

18. Govaerts PJ, Vaerenberg B, De Ceulaer G, Daemers K, De Beukelaer C, Schauwers K. Development of a software tool using deterministic logic for the optimization of cochlear implant processor programming. *Otol Neurotol*. (2010) 31:908–18. doi: 10.1097/mao.0b013e3181dd160b

19. Nilsson M, Soli SD, Sullivan JA. Development of the hearing in noise test for the measurement of speech reception thresholds in quiet and in noise. *J Acoust Soc Am*. (1994) 95:1085–99. doi: 10.1121/1.408469

frontiers | Frontiers in Neurology

TYPE Original Research
PUBLISHED 23 May 2023
DOI 10.3389/fneur.2023.1183116

OPEN ACCESS

EDITED BY
Ulrich Hoppe,
University of Erlangen Nuremberg, Germany

REVIEWED BY
Daniel John Brown,
Curtin University, Australia
Artur Lorens,
Institute of Physiology and Pathology of Hearing (IFPS), Poland

*CORRESPONDENCE
Wilhelm Wimmer
✉ wilhelm.wimmer@unibe.ch

RECEIVED 09 March 2023
ACCEPTED 25 April 2023
PUBLISHED 23 May 2023

CITATION
Schraivogel S, Aebischer P, Weder S, Caversaccio M and Wimmer W (2023) Cochlear implant electrode impedance subcomponents as biomarker for residual hearing. *Front. Neurol.* 14:1183116. doi: 10.3389/fneur.2023.1183116

Cochlear implant electrode impedance subcomponents as biomarker for residual hearing

Stephan Schraivogel[1,2], Philipp Aebischer[1,2], Stefan Weder[2], Marco Caversaccio[1,2] and Wilhelm Wimmer[2,3]*

[1]Hearing Research Laboratory, ARTORG Center for Biomedical Engineering Research, University of Bern, Bern, Switzerland, [2]Department of ENT—Head and Neck Surgery, Inselspital, Bern University Hospital, University of Bern, Bern, Switzerland, [3]Department of Otorhinolaryngology, TUM School of Medicine, Klinikum Rechts der Isar, Technical University of Munich, Munich, Germany

Introduction and objectives: Maintaining the structural integrity of the cochlea and preserving residual hearing is crucial for patients, especially for those for whom electric acoustic stimulation is intended. Impedances could reflect trauma due to electrode array insertion and therefore could serve as a biomarker for residual hearing. The aim of this study is to evaluate the association between residual hearing and estimated impedance subcomponents in a known collective from an exploratory study.

Methods: A total of 42 patients with lateral wall electrode arrays from the same manufacturer were included in the study. For each patient, we used data from audiological measurements to compute residual hearing, impedance telemetry recordings to estimate near and far-field impedances using an approximation model, and computed tomography scans to extract anatomical information about the cochlea. We assessed the association between residual hearing and impedance subcomponent data using linear mixed-effects models.

Results: The progression of impedance subcomponents showed that far-field impedance was stable over time compared to near-field impedance. Low-frequency residual hearing demonstrated the progressive nature of hearing loss, with 48% of patients showing full or partial hearing preservation after 6 months of follow-up. Analysis revealed a statistically significant negative effect of near-field impedance on residual hearing (−3.81 dB HL per kΩ; $p < 0.001$). No significant effect of far-field impedance was found.

Conclusion: Our findings suggest that near-field impedance offers higher specificity for residual hearing monitoring, while far-field impedance was not significantly associated with residual hearing. These results highlight the potential of impedance subcomponents as objective biomarkers for outcome monitoring in cochlear implantation.

KEYWORDS

hearing preservation monitoring, cochlear trauma, electrode-tissue interface, follow-up, objective measure

1. Introduction

With more than 1 million implanted devices worldwide, the cochlear implant (CI) is the most successful treatment for patients suffering from partial to complete deafness (1). CI candidacy has been relaxed to include patients with residual acoustic hearing. For these patients in particular, preservation of residual hearing and structural integrity of the

cochlea during and after CI surgery are important goals to improve hearing outcomes (2–4). However, a considerable number of patients lose their residual hearing either during or after cochlear implantation [mean hearing preservation after 1 month: 82%, 6 months: 76%, and 12 months or more: 69%; (5)]. Intraoperative loss of residual hearing is associated with intracochlear trauma (6, 7) caused by the insertion of the electrode array. Postoperative hearing loss is related to fibrous tissue and new bone formation in the cochlea (8, 9). Another reason for postoperative hearing loss could be inflammatory/foreign body response to the platinum-iridium electrodes and the surrounding silicon carrier (10, 11).

Reliable biomarkers are needed for continuous monitoring and adaptation to changes in residual hearing, especially for electric acoustic CI recipients (12). Impedance telemetry allows measuring electrical impedances and has been performed since the first CIs (13). Impedances are in focus for several purposes, including insertion outcome monitoring [e.g., insights into the cochlear microenvironment around CI electrode contacts (14), fibrous tissue growth (15, 16), or inner ear pathologies (17)], electrode position monitoring within the cochlea (18–21), or continuous monitoring of electrode contact integrity with remote apps (22).

In an exploratory study, we demonstrated the association between clinical impedances and residual hearing (23). The term clinical impedance encompasses a mixed quantity that can be divided into contributions from the electrode-electrolyte interface and nearby bulk resistance (near-field impedance) and electrical resistance through biological tissue from the stimulating electrode to the ground electrode on the implant body (far-field impedance) (21, 24). Based on these findings, we hypothesize that impedance subcomponents could yield more specific data to monitor hearing performance in the follow-up after cochlear implantation. Therefore, the aim of this study is to evaluate the association between residual hearing and impedance subcomponents of a previously published approximation model (21) in a known collective from a previous study (23).

2. Methods

2.1. Study design

We performed a refined retrospective analysis of residual hearing and impedance subcomponent data from the same cases as previously reported in Wimmer et al. (23). The study was approved by our local institutional review board (ID 2019-01578). The study included patients who met the following criteria: (a) underwent cochlear implantation at our center between January 2009 and June 2021, (b) having an electrode array from MED-EL (Innsbruck, Austria), (c) having a low-frequency residual hearing (i.e., between 0.125 and 1 kHz) of at least 5 dB HL, and (d) having a postoperative follow-up of at least two pure tone audiograms and corresponding impedance telemetry recordings within a minimum of 6 months.

2.2. Residual hearing data

According to the standard clinical procedure, we used a clinical audiometer along with insert earphones or a headphone to measure pure tone air conduction hearing thresholds in dB hearing level (HL) at seven frequencies (0.125, 0.25, 0.5, 1, 2, 4, and 8 kHz). All audiological measurements were performed in an acoustic chamber. We calculated residual hearing as the absolute difference between the maximum detectable hearing levels by the audiometer (i.e., 90 dB HL at 0.125 kHz, 110 dB HL at 0.25 kHz, and 120 dB HL for the remaining frequencies) and the measured hearing thresholds at the corresponding frequency. Low-frequency Pure tone average (PTA) was computed as the mean of residual hearing at frequencies between 0.125 and 1 kHz.

2.3. Impedance telemetry data

Impedance telemetry data were recorded using the standard clinical protocol of the manufacturer's telemetry software (MAESTRO, MED-EL, Austria) and were recorded in the same sessions as pure tone audiometry. In addition, to analyze the by-case progression of impedances over time, we retrieved all available impedance telemetry data from the day of implantation up to a maximum follow-up time of 100 months. The clinical electrode impedance can be subdivided into two components: near-field and far-field impedance. The near-field impedance is associated with the local cochlear microenvironment around the stimulating electrode. The far-field impedance provides information about the electrical return path through biological tissue from the stimulating electrode to the ground electrode on the implant body (24). We estimated the far-field impedance, also called tissue resistance, using bivariate spline extrapolation of the impedance telemetry recordings as established in previous work (20, 21). Subsequently, near-field impedance was defined as the difference between clinical impedance and far-field impedance. We excluded data from extracochlear electrodes that were identified from computed tomography (CT) scans (18 electrodes from six cases, see demographics, Supplementary Table 1). In addition, we excluded samples of a single electrode from further analysis if an open circuit was detected by the manufacturer's telemetry software (at 30 electrodes from eight cases).

2.4. Computed tomography data

We used the open-source software 3D slicer (25) to measure the cochlear base length and width (26, 27) in the preoperative CT scans and calculated the cochlear duct length without the hook region length [i.e., starting at an angular insertion depth of 0° (28–30)]:

$$CDL(0^\circ) = 1.71 \times (1.18\, A_{OC} + 2.69\, B_{OC} - \sqrt{0.72\, A_{OC}\, B_{OC}}) + 0.18, \quad (1)$$

where A_{OC} and B_{OC} are the cochlear base length and width subtracted by 1 mm, respectively.

2.5. Statistical analysis

We used a linear mixed-effects model to assess the relationship between near and far-field impedances and residual hearing. For each case, repeated measurements were taken on different

days after cochlear implantation. To account for the dependence of observations, we used a case-level random intercepts model, which allows the intercept to vary per case, i.e., for each case a unique effect is added to the overall intercept. Random slopes of impedance subcomponents allowed different by-case slopes for the independent variables.

First, we created a model with residual hearing (in dB HL) as the dependent variable and impedance subcomponents (in kΩ) as the independent variables. In addition, the follow-up time (in months), the implanted side (left vs. right), the gender (female vs. male), the electrode array type (FLEX24, FLEX28, FLEXSoft, or Standard), the cochlear duct length (in mm), and age (in years) were included as fixed effects. We added interaction terms between the impedance subcomponents and follow-up time, as impedance changes are associated with follow-up time (23). We assumed correlations between random slopes for near-field and far-field impedances [i.e., random effects were specified as *(near-field impedance + far-field impedance | case-level)*]. We compared the model depending on impedance subcomponents to a second model depending on the total clinical impedance and the same fixed effects as in the first model.

The models were compared in terms of the Akaike information criterion (AIC) and the Bayesian information criterion (BIC), the amount of explained variance of the dependent variable by the independent variables (using the coefficient of determination R^2), and the amount of explained variance due to grouping [using the Intraclass correlation coefficient (ICC)]. The statistical analysis was performed in the RStudio environment (31) using the lme4 package (32).

3. Results

3.1. Demographics and word recognition

We considered a total of 704 recordings in our center's database between January 2009 and June 2021. Of these, 42 patients met the inclusion criteria. The patients' age ranged from 10 to 80 years (median age 57 years). Of the 24 female and 18 male patients, there were 21 left and right-sided implantations, respectively. With 26 cases, the majority were implanted with a FLEX28 electrode array. Partially inserted electrode arrays were present in six cases (1 case each with 1 and 2 extracochlear electrodes, three cases with 3, and 1 case with 6). After activation for 6 months, the median word recognition score was 100% (interquartile range [90, 100]%) for the German Freiburg numbers test and 58% (interquartile range [40, 73]%) for the German Freiburg monosyllabic word test (see Supplementary Table 1).

3.2. Impedance subcomponents progression over time

We analyzed impedance subcomponents progression based on 635 recordings with a mean follow-up time of 24 months (ranging from 21 to 99 months). Mean far-field impedances were more stable over time compared to mean near-field impedances (case-level standard deviations of ∼0.1–0.7 kΩ and 1–2.4 kΩ, respectively; Figure 1). After the date of implantation, near-field impedances increased strongly until the first activation session (first month) and stabilized after ∼6–12 months. These dynamics were most pronounced at the most apical electrode and decreased toward the round window until electrode 10 (see Supplementary Figure 1).

Far-field impedances did not show these dynamics. For the two most basal electrodes, near-field impedances increased over time starting 3 months after implantation. In contrast, far-field impedances at the two most basal electrodes already began to increase between the date of implantation and activation (first month). In general, mean levels of far-field impedances were higher at the apical than at the basal electrodes. Eight cases showed patterns of impedance deviation that were not seen in the other cases (Figure 1). We observed a long-term increase in impedances (cases 34, 41), single events of impedance spikes (case 13), and fluctuating impedances (cases 20, 24, 28, 33, 40).

3.3. Residual hearing progression over time

The progression of residual hearing and impedances (i.e., clinical impedance, near-field impedance, and far-field impedance) over time shows, for most of the 42 cases, a negative correlation between the two variables (see Supplementary Figures 2–4). Preoperative residual hearing from the 42 cases was in the range of 9–65 dB HL with a mean of 37 dB HL. Over time, 12 cases (29%) completely lost their residual hearing after a mean follow-up time of 25 months (ranging from 7 to 49 months). Residual hearing was still present in the remaining 30 cases (71%) at the last audiological assessment in our dataset (mean follow-up time of 35 months, ranging from 1 to 98 months). Hearing preservation after 6 months, according to (33), is shown in Supplementary Table 1.

3.4. Association of residual hearing and impedance subcomponents

We included a total of 152 audiological measurements and the same number of concurrent telemetry recordings from the 42 cases in the linear mixed-effects models for residual hearing. Near-field impedance had a statistically significant negative effect on residual hearing (−3.81 dB HL per kΩ, $p < 0.001$; Table 1). Postoperative follow-up time was also associated with a significant negative effect on residual hearing (−0.29 dB HL per month; $p < 0.001$). The FLEX28, FLEXSoft, and Standard electrode arrays were associated with significantly lower preoperative residual hearing than the FLEX24 electrode array (−20.46 dB HL, $p < 0.001$; −23.73 dB HL, $p = 0.004$; −33.11 dB HL, $p = 0.01$, respectively). The interaction of time with both near-field and far-field impedances showed an association with residual hearing (0.06 and −0.28 dB HL, respectively; $p < 0.001$ for both). No significant effects of far-field impedance, side, gender, age at implantation, or cochlear duct length were found.

Figure 2 shows, for each case, the fitted random intercepts and slopes between residual hearing and near-field impedance. The resulting slopes (i.e., the effect of an increase in near-field

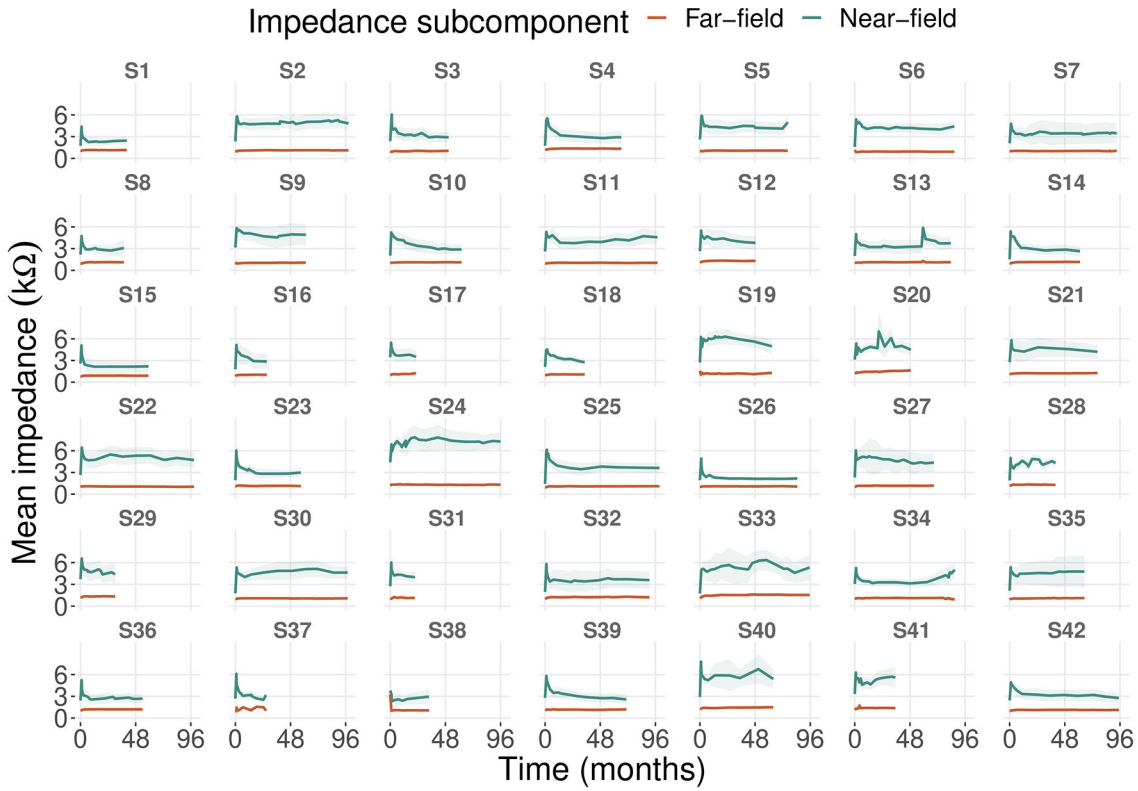

FIGURE 1
Progression of mean near-field and far-field impedances of 42 cases including all electrodes. The shaded area represents the 95% confidence interval of the mean.

impedance by 1 kΩ on residual hearing in dB HL) were negative for all cases except 8, 14, and 32.

The linear mixed-effects model depending on clinical impedance resulted in the same significant effects on residual hearing as the near and far-field model (see Supplementary Table 3). Clinical impedance was associated with a statistically significant negative effect on residual hearing (−3.8 dB HL per kΩ; p <0.001). The comparison of the two linear mixed-effects models resulted in lower AIC and BIC indices of the near and far-field model compared to the clinical impedance model (see Supplementary Table 2). In addition, the conditional R^2 of the near and far-field model was 2% higher (R^2 = 87%), while the marginal R^2 (i.e., explained variance by the fixed effects only) was the same for both models. The ICC of the near and far-field model was 3% higher compared to the clinical impedance model (ICC = 76%).

4. Discussion

4.1. Impedance subcomponents progression over time

Near-field impedances increased strongly until the first month after implantation (Figure 1), which was also observed for clinical impedances (17, 23, 34). This might be due to intracochlear inflammatory reactions or wound healing (22, 23, 35). Intracochlear trauma and fibrous tissue formation are most prominent in the basal turn (36–38). We observed this in the long-term increase of near-field impedances, especially at the two most basal electrodes (see Supplementary Figure 1). More apically located electrodes are associated with higher far-field impedances (21). On average, we found higher far-field impedances near the apex than in the basal turn (see Supplementary Figure 1).

We propose to assign the unusual patterns of near-field impedances (i.e., deviating from the initial rise in near-field impedance to CI activation and subsequent stabilization) to three groups (Figure 1). The long-term increase of near-field impedances in the first group might be due to fibrous tissue growth in the hook region (9, 36), reducing electrical conductivity near most basal electrodes. Single near-field impedance spikes or fluctuating near-field impedances in the second and third groups could be related to clinical events such as hearing loss, tinnitus, or vertigo (17). However, we found no such events in the medical records of these cases.

4.2. Residual hearing progression over time

Slopes of residual hearing progression over time were negative in all cases except for case 18 (see Supplementary Figure 2). Seventy-one percent of cases in our dataset had remaining residual hearing at the last audiological assessment. Our findings

TABLE 1 Linear mixed-effects model summary table for residual hearing (in dB HL) depending on near-field and far-field impedance including all electrodes.

	Coefficient	95% CI	*p*-value
Intercept	64.12	[−0.95; 129.9]	0.08
Time (months)	−0.29	[−0.43; −0.16]	<0.001
Near-field impedance (kΩ)	−3.81	[−4.57; −3.05]	<0.001
Far-field impedance (kΩ)	1.67	[−2.55; 5.92]	0.44
$Side_R$	−1.24	[−8.34; 5.87]	0.75
$Gender_M$	−1.14	[−8.37; 6.13]	0.77
Age at implantation (years)	0.18	[−0.03; 0.4]	0.12
Cochlear duct length (mm)	−0.54	[−2.4; 1.29]	0.6
$Electrode\ array_{FLEX28}$	−20.46	[−28.54; −12.41]	<0.001
$Electrode\ array_{FLEXSoft}$	−23.73	[−37.67; −9.78]	0.004
$Electrode\ array_{Standard}$	−33.11	[−55.63; −10.59]	0.01
Interaction of time with near-field impedance	0.06	[0.05; 0.07]	<0.001
Interaction of time with far-field impedance	−0.28	[−0.39; −0.16]	<0.001
Num. obs.	1,747		
Num. groups: Cases	42		

R, right; M, male; CI, confidence interval.

are comparable to Snels et al. (5), who found mean hearing preservation after 12 months or more of ∼70%. However, in the presented cases with remaining residual hearing, the mean follow-up was considerably higher (35 months).

4.3. Association of residual hearing and impedance subcomponents

Near-field impedance showed a strong association with residual hearing (−3.81 dB HL per kΩ, Table 1). In line with our findings, Tejani et al. (39) found elevated access resistance R_a in cases with loss of residual hearing, while the polarization impedance Z_p remained stable. In our study, near-field impedance consists of the polarization impedance Z_p and the bulk resistance R_b (R_b is part of the access resistance R_a). This contrasts with Leblans et al. (16), who defined near and far-field impedances as subcomponents of the access resistance R_a. Near-field impedance had approximately the same effect on residual hearing as clinical impedance. This is because the far-field impedance remained relatively stable over time, and most impedance fluctuations were due to the near-field impedance. The model depending on impedance subcomponents was better than the model depending on clinical impedance because the former explained more variance in residual hearing (conditional R^2 = 87%). Because the improvement in explaining variance is small (2%), the subcomponent model does not provide substantially better performance on group level. However, the model can explicitly demonstrate the isolated contributions to long-term variation of the near- and far-field components and serve as a basis for further investigation. In this context, we consider near-field impedance to be most clinically relevant. In addition, individual long-term variations in far-field impedances can be isolated that could otherwise have affected the accuracy of the model.

We included electrode array type and cochlear duct length as fixed effects in the model. We observed a preference for shorter electrode arrays to preserve a comparatively high preoperative residual hearing (see Supplementary Figure 5). The active stimulation range (i.e., the array's length from the middle of the first to the middle of the last electrode) is shortest for FLEX24 (20.9 mm), followed by FLEX28 (23.1 mm) and FLEXSoft, Standard (26.4 mm). However, the sample size in our dataset was not evenly distributed among the different electrode array types (26 × FLEX28, 12 × FLEX24, 3 × FLEXSoft, and 1 × Standard). The distribution of preoperative residual hearing was wider for the FLEX28 electrode array than for the other. A longer cochlea does not appear to have influenced the choice of electrode array type in our dataset (see Supplementary Figure 6). Therefore, we kept electrode array type and cochlear duct length as fixed effects.

For the model, we did not include pure tone frequency as a fixed effect. Therefore, we created a separate model for residual hearing with pure tone frequency (categorical, in kHz) as an additional fixed effect (i.e., modeling residual hearing at distinct frequencies instead of low-frequency PTA). The model resulted in the same significant effects on residual hearing, except for the FLEXSoft electrode array (see Supplementary Table 4). The effect of near-field impedance on residual hearing was approximately 1 dB HL smaller than in the model with low-frequency PTA as the dependent variable. As expected, pure tone frequency had a significant effect on residual hearing. This was expected because residual hearing varies with position in the cochlea and is best preserved over time in the apical region (40). Preoperative residual hearing was highest at 0.25 kHz and not at the lowest frequency of 0.125 kHz.

In contrast to Wimmer et al. (23), we did not divide the electrodes into subgroups for our analysis of residual hearing and impedance telemetry data. While the low-frequency range from 0.125 to 1 kHz corresponds to the most apical electrodes [insertion depth of ∼360–720°, (41)], Wimmer et al. (23) found that the most significant effect on residual hearing is observed in the impedance data of the most basal electrodes. Fibrous tissue and new bone formation in the cochlea resulting from electrode array insertion could reduce basilar membrane compliance not only near the round window (8) but also at multiple locations along the entire auditory pathway from the oval window to the apex. Based on this, we decided to include data from all electrodes in our analysis.

During model checks, we observed collinearities between independent variables. High Variance inflation factors (VIFs) were present for the near-field impedance (VIF = 1.03, tolerance = 0.98) and the interaction between follow-up time and far-field impedance (VIF = 46.86, tolerance = 0.02). As VIF might be inflated in the presence of interaction terms (42), we checked multicollinearity among independent variables without interaction terms. This resulted in only a low correlation among independent variables.

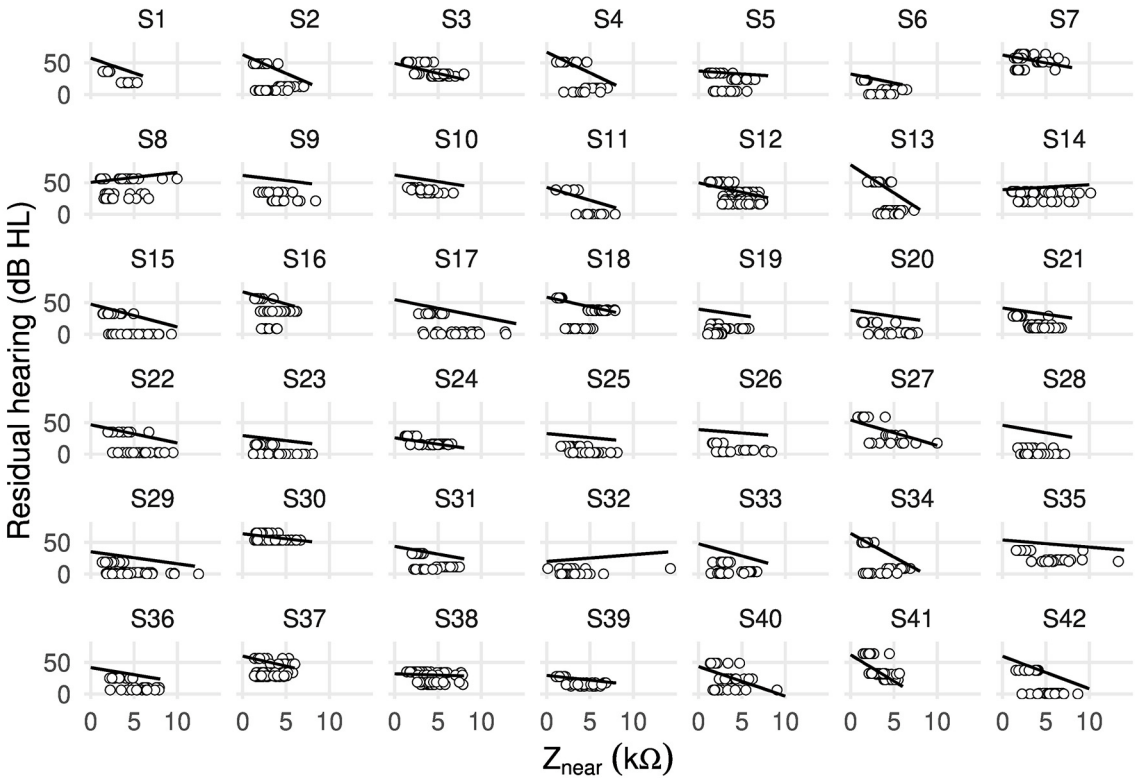

FIGURE 2
Scatter plot showing random intercepts and random slopes as estimated by the linear mixed-effects model between residual hearing (in dB HL) and near-field impedance Z_{near} (in kΩ) including all electrodes of 42 cases.

4.4. Study limitations and outlook

We could not measure near and far-field impedances directly but estimated them from the recorded impedance matrix using an approximation model (21). Estimated impedance subcomponents could therefore have included contributions from the complementary subcomponent and vice versa. Ultimately, this could have introduced modeling errors for residual hearing using impedance subcomponents. Advanced measurement techniques (43) could overcome this limitation and measure directly the polarization impedance (as part of the near-field impedance) and access resistance (which includes the far-field impedance). Our analysis was based on only 152 audiological measurements from 42 cases. Future studies need to verify our results in a larger dataset.

This study did not investigate the influence of electrode insertion depth on residual hearing. As electrode location is a potential biomarker for intracochlear trauma and hearing preservation (3), this could improve the prediction accuracy for residual hearing.

5. Conclusion

In this study, we showed that near-field impedance is strongly associated with postoperative residual hearing. This supports our hypothesis that impedance subcomponents provide a more specific analysis of the cochlear microenvironment and hearing performance compared with conventional impedance telemetry. As far-field impedance was not associated with changes in residual hearing, we concluded that residual hearing is primarily influenced by the local cochlear microenvironment around the electrode contacts. To further improve modeling accuracy for residual hearing, future studies will need to use advanced measurement techniques for direct measurement of impedance subcomponents.

Data availability statement

The original contributions presented in the study are included in the article/Supplementary material, further inquiries can be directed to the corresponding author.

Ethics statement

The studies involving human participants were reviewed and approved by Kantonale Ethikkommission Bern Universität Bern (ID 2019-01578). Written informed consent to participate in this study was provided by the participants' legal guardian/next of kin.

Author contributions

SS: methodology, software, formal analysis, visualization, and writing—original draft. PA: methodology and writing—review and editing. SW: data curation and writing—review and editing. MC: resources and writing—review and editing. WW: conceptualization, methodology, formal analysis, writing—review

and editing, project administration, and funding acquisition. All authors contributed to the article and approved the submitted version.

Funding

This study was funded by the ENT Department, Bern University Hospital. Open-access funding provided by University of Bern.

Conflict of interest

The authors declare that the research was conducted in the absence of any commercial or financial relationships that could be construed as a potential conflict of interest.

Publisher's note

Supplementary material

The Supplementary Material for this article can be found online at: https://www.frontiersin.org/articles/10.3389/fneur.2023.1183116/full#supplementary-material

References

1. Zeng FG. Celebrating the one millionth cochlear implant. *JASA Express Lett.* (2022) 2:077201. doi: 10.1121/10.0012825

2. Gstoettner W, Kiefer J, Baumgartner WD, Pok S, Peters S, Adunka O. Hearing preservation in cochlear implantation for electric acoustic stimulation. *Acta Otolaryngol.* (2004) 124:348–52. doi: 10.1080/00016480410016432

3. James C, Albegger K, Battmer R, Burdo S, Deggouj N, Deguine O, et al. Preservation of residual hearing with cochlear implantation: how and why. *Acta Oto-laryngol.* (2005) 125:481–91. doi: 10.1080/00016480510026197

4. Helbig S, Adel Y, Rader T, Stöver T, Baumann U. Long-term hearing preservation outcomes after cochlear implantation for electric-acoustic stimulation. *Otol Neurotol.* (2016) 37:e353–9. doi: 10.1097/MAO.0000000000001066

5. Snels C, IntHout J, Mylanus E, Huinck W, Dhooge I. Hearing preservation in cochlear implant surgery: a meta-analysis. *Otol Neurotol.* (2019) 40:145–53. doi: 10.1097/MAO.0000000000002083

6. Giardina CK, Brown KD, Adunka OF, Buchman CA, Hutson KA, Pillsbury HC, et al. Intracochlear electrocochleography: response patterns during cochlear implantation and hearing preservation. *Ear Hear.* (2019) 40:833. doi: 10.1097/AUD.0000000000000659

7. Starovoyt A, Pyka G, Putzeys T, Balcaen T, Wouters J, Kerckhofs G, et al. Human cochlear microstructures at risk of electrode insertion trauma, elucidated in 3D with contrast-enhanced microCT. *Sci Rep.* (2023) 13:2191. doi: 10.1038/s41598-023-29401-6

8. Quesnel AM, Nakajima HH, Rosowski JJ, Hansen MR, Gantz BJ, Nadol JB Jr. Delayed loss of hearing after hearing preservation cochlear implantation: human temporal bone pathology and implications for etiology. *Hear Res.* (2016) 333:225–34. doi: 10.1016/j.heares.2015.08.018

9. Nadol JB Jr, O'Malley JT, Burgess BJ, Galler D. Cellular immunologic responses to cochlear implantation in the human. *Hear Res.* (2014) 318:11–7. doi: 10.1016/j.heares.2014.09.007

10. Seyyedi M, Nadol JB Jr. Intracochlear inflammatory response to cochlear implant electrodes in humans. *Otol Neurotol.* (2014) 35:1545–51. doi: 10.1097/MAO.0000000000000540

11. Foggia MJ, Quevedo RV, Hansen MR. Intracochlear fibrosis and the foreign body response to cochlear implant biomaterials. *Laryngosc Invest Otolaryngol.* (2019) 4:678–83. doi: 10.1002/lio2.329

12. Sprinzl GM, Schoerg P, Edlinger SH, Magele A. Long-term hearing preservation in electric acoustic cochlear implant candidates. *Otol Neurotol.* (2020) 41:750–7. doi: 10.1097/MAO.0000000000002627

13. Mens LH. Advances in cochlear implant telemetry: evoked neural responses, electrical field imaging, and technical integrity. *Trends Amplif.* (2007) 11:143–59. doi: 10.1177/1084713807304362

14. Tykocinski M, Cohen LT, Cowan RS. Measurement and analysis of access resistance and polarization impedance in cochlear implant recipients. *Otol Neurotol.* (2005) 26:948–56. doi: 10.1097/01.mao.0000185056.99888.f3

15. Wilk M, Hessler R, Mugridge K, Jolly C, Fehr M, Lenarz T, et al. Impedance changes and fibrous tissue growth after cochlear implantation are correlated and can be reduced using a dexamethasone eluting electrode. *PLoS ONE.* (2016) 11:e0147552. doi: 10.1371/journal.pone.0147552

16. Leblans M, Sismono F, Vanpoucke F, van Dinther J, Lerut B, Kuhweide R, et al. Novel impedance measures as biomarker for intracochlear fibrosis. *Hear Res.* (2022) 2022:108563. doi: 10.1016/j.heares.2022.108563

17. Shaul C, Bester CW, Weder S, Choi J, Eastwood H, Padmavathi K, et al. Electrical impedance as a biomarker for inner ear pathology following lateral wall and peri-modiolar cochlear implantation. *Otol Neurotol.* (2019) 40:e518–26. doi: 10.1097/MAO.0000000000002227

18. Giardina CK, Krause ES, Koka K, Fitzpatrick DC. Impedance measures during *in vitro* cochlear implantation predict array positioning. *IEEE Trans Biomed Eng.* (2017) 65:327–35. doi: 10.1109/TBME.2017.2764881

19. Hoppe U, Brademann G, Stöver T, de Miguel AR, Cowan R, Manrique M, et al. Evaluation of a transimpedance matrix algorithm to detect anomalous cochlear implant electrode position. *Audiol Neurotol.* (2022) 27:347–55. doi: 10.1159/000523784

20. Schraivogel S, Aebischer P, Wagner F, Weder S, Mantokoudis G, Caversaccio M, et al. Postoperative impedance-based estimation of cochlear implant electrode insertion depth. *Ear Hear.* (2023). doi: 10.1097/AUD.0000000000001379. [Epub ahead of print].

21. Aebischer P, Meyer S, Caversaccio M, Wimmer W. Intraoperative impedance-based estimation of cochlear implant electrode array insertion depth. *IEEE Trans Biomed Eng.* (2020) 68:545–55. doi: 10.1109/TBME.2020.3006934

22. Parre no M, Di Lella FA, Fernandez F, Boccio CM, Ausili SA. Toward self-measures in cochlear implants: Daily and "Homemade" impedance assessment. *Front Digit Health.* (2020) 2:582562. doi: 10.3389/fdgth.2020.582562

23. Wimmer W, Sclabas L, Caversaccio MD, Weder S. cochlear implant electrode impedance as potential biomarker for residual hearing. *Front Neurol.* (2022) 13:886171. doi: 10.3389/fneur.2022.886171

24. Vanpoucke FJ, Zarowski AJ, Peeters SA. Identification of the impedance model of an implanted cochlear prosthesis from intracochlear potential measurements. *IEEE Trans Biomed Eng.* (2004) 51:2174–83. doi: 10.1109/TBME.2004.836518

25. Fedorov A, Beichel R, Kalpathy-Cramer J, Finet J, Fillion-Robin JC, Pujol S, et al. 3D Slicer as an image computing platform for the Quantitative Imaging Network. *Magn Reson Imaging.* (2012) 30:1323–41. doi: 10.1016/j.mri.2012.05.001

26. Anschuetz L, Weder S, Mantokoudis G, Kompis M, Caversaccio M, Wimmer W. Cochlear implant insertion depth prediction: a temporal bone accuracy study. *Otol Neurotol.* (2018) 39:e996–1001. doi: 10.1097/MAO.0000000000002034

27. Rathgeb C, Dematté M, Yacoub A, Anschuetz L, Wagner F, Mantokoudis G, et al. Clinical applicability of a preoperative angular insertion depth prediction method for cochlear implantation. *Otol Neurotol.* (2019) 40:1011–7. doi: 10.1097/MAO.0000000000002304

28. Alexiades G, Dhanasingh A, Jolly C. Method to estimate the complete and two-turn cochlear duct length. *Otol Neurotol.* (2015) 36:904–7. doi: 10.1097/MAO.0000000000000620

29. Schurzig D, Timm ME, Batsoulis C, Salcher R, Sieber D, Jolly C, et al. A novel method for clinical cochlear duct length estimation toward patient-specific cochlear implant selection. *OTO Open*. (2018) 2:2473974X18800238. doi: 10.1177/2473974X18800238

30. Alshalan A, Abdelsamad Y, Assiri M, Alsanosi A. Cochlear implantation: the variation in cochlear height. *Ear Nose Throat J*. (2022) 1–7. doi: 10.1177/01455613221134860

31. RStudio Team. *RStudio: Integrated Development Environment for R*. Boston, MA: RStudio Team (2022). Available online at: http://www.rstudio.com/

32. Bates D, Mächler M, Bolker B, Walker S. Fitting linear mixed-effects models using lme4. *J Stat Softw*. (2015) 67:1–48. doi: 10.18637/jss.v067.i01

33. Skarzynski H, Van de Heyning P, Agrawal S, Arauz S, Atlas M, Baumgartner W, et al. Towards a consensus on a hearing preservation classification system. *Acta Oto-Laryngol*. (2013) 133(Suppl. 564):3–13. doi: 10.3109/00016489.2013.869059

34. Busby P, Plant K, Whitford L. Electrode impedance in adults and children using the Nucleus 24 cochlear implant system. *Cochlear Implants Int*. (2002) 3:87–103. doi: 10.1179/cim.2002.3.2.87

35. Alhabib SF, Abdelsamad Y, Yousef M, Alzhrani F, Hagr A. Effect of early activation of cochlear implant on electrode impedance in pediatric population. *Int J Pediatr Otorhinolaryngol*. (2021) 140:110543. doi: 10.1016/j.ijporl.2020.110543

36. Geerardyn A, Zhu M, Wu P, O'Malley J, Nadol J Jr, Liberman MC, et al. Three-dimensional quantification of fibrosis and ossification after cochlear implantation via virtual re-sectioning: Potential implications for residual hearing. *Hear Res*. (2023) 428:108681. doi: 10.1016/j.heares.2022.108681

37. Aebischer P, Mantokoudis G, Weder S, Anschuetz L, Caversaccio M, Wimmer W. *In-Vitro* study of speed and alignment angle in cochlear implant electrode array insertions. *IEEE Trans Biomed Eng*. (2021) 69:129–37. doi: 10.1109/TBME.2021.3088232

38. Rahman MT, Chari D, Ishiyama G, Lopez I, Quesnel AM, Ishiyama A, et al. Cochlear implants: causes, effects and mitigation strategies for the foreign body response and inflammation. *Hear Res*. (2022) 2022:108536. doi: 10.1016/j.heares.2022.108536

39. Tejani VD, Yang H, Kim JS, Hernandez H, Oleson JJ, Hansen MR, et al. Access and polarization electrode impedance changes in electric-acoustic stimulation cochlear implant users with delayed loss of acoustic hearing. *J Assoc Res Otolaryngol*. (2022) 23:95–118. doi: 10.1007/s10162-021-00809-z

40. Hough K, Verschuur CA, Cunningham C, Newman TA. Macrophages in the cochlea; an immunological link between risk factors and progressive hearing loss. *Glia*. (2022) 70:219–38. doi: 10.1002/glia.24095

41. Li H, Helpard L, Ekeroot J, Rohani SA, Zhu N, Rask-Andersen H, et al. Three-dimensional tonotopic mapping of the human cochlea based on synchrotron radiation phase-contrast imaging. *Sci Rep*. (2021) 11:4437. doi: 10.1038/s41598-021-83225-w

42. Francoeur RB. Could sequential residual centering resolve low sensitivity in moderated regression? Simulations and cancer symptom clusters. *Open J Stat*. (2013) 2013:36A004. doi: 10.4236/ojs.2013.36A004

43. Di Lella FA, Parre no M, Fernandez F, Boccio CM, Ausili SA. Measuring the electrical status of the bionic ear. Re-thinking the impedance in cochlear implants. *Front Bioeng Biotechnol*. (2020) 8:568690. doi: 10.3389/fbioe.2020.568690

frontiers | Frontiers in Neurology

TYPE Original Research
PUBLISHED 07 July 2023
DOI 10.3389/fneur.2023.1104574

OPEN ACCESS

EDITED BY
Stephen O'Leary,
The University of Melbourne, Australia

REVIEWED BY
Charles Liberman,
Harvard University, United States
Huib Versnel,
University Medical Center Utrecht, Netherlands

*CORRESPONDENCE
Douglas C. Fitzpatrick
✉ dcf@med.unc.edu

RECEIVED 21 November 2022
ACCEPTED 19 June 2023
PUBLISHED 07 July 2023

CITATION
Haggerty RA, Hutson KA, Riggs WJ, Brown KD, Pillsbury DC, Adunka OF, Buchman CA and Fitzpatrick DC (2023) Assessment of cochlear synaptopathy by electrocochleography to low frequencies in a preclinical model and human subjects.
Front. Neurol. 14:1104574.
doi: 10.3389/fneur.2023.1104574

Assessment of cochlear synaptopathy by electrocochleography to low frequencies in a preclinical model and human subjects

Raymond A. Haggerty[1], Kendall A. Hutson[1], William J. Riggs[2], Kevin D. Brown[1,3], Harold C. Pillsbury[1,3], Oliver F. Adunka[2], Craig A. Buchman[4] and Douglas C. Fitzpatrick[1]*

[1]Department of Otolaryngology, University of North Carolina at Chapel Hill, Chapel Hill, NC, United States, [2]Department of Otolaryngology, The Ohio State University, Columbus, OH, United States, [3]University of North Carolina School of Medicine, Chapel Hill, NC, United States, [4]Department of Otolaryngology, Washington University in St. Louis, St. Louis, MO, United States

Cochlear synaptopathy is the loss of synapses between the inner hair cells and the auditory nerve despite survival of sensory hair cells. The findings of extensive cochlear synaptopathy in animals after moderate noise exposures challenged the long-held view that hair cells are the cochlear elements most sensitive to insults that lead to hearing loss. However, cochlear synaptopathy has been difficult to identify in humans. We applied novel algorithms to determine hair cell and neural contributions to electrocochleographic (ECochG) recordings from the round window of animal and human subjects. Gerbils with normal hearing provided training and test sets for a deep learning algorithm to detect the presence of neural responses to low frequency sounds, and an analytic model was used to quantify the proportion of neural and hair cell contributions to the ECochG response. The capacity to detect cochlear synaptopathy was validated in normal hearing and noise-exposed animals by using neurotoxins to reduce or eliminate the neural contributions. When the analytical methods were applied to human surgical subjects with access to the round window, the neural contribution resembled the partial cochlear synaptopathy present after neurotoxin application in animals. This result demonstrates the presence of viable hair cells not connected to auditory nerve fibers in human subjects with substantial hearing loss and indicates that efforts to regenerate nerve fibers may find a ready cochlear substrate for innervation and resumption of function.

KEYWORDS

electrocochleography, auditory nerve, hair cells, cochlear microphonic, deep learning

Introduction

Recent animal studies have shown that synapses between the inner hair cells and the auditory nerve, rather than hair cells themselves, are the elements most sensitive to destruction by moderate noise exposure (1–4). Using noise exposures that produced only temporary threshold shifts and no loss of hair cells, up to half of the synapses can be lost, despite thresholds for distortion product otoacoustic emissions, auditory brainstem responses, and compound

action potentials returning to normal. The explanation is that excitotoxic effects of over-stimulation is greatest in fibers with low spontaneous rates that have high thresholds, while the high-spontaneous rate fibers that have low-thresholds remained intact (5–7).

Since determination of audiometric thresholds are the primary basis for detecting human hearing loss, and thresholds would be unchanged if the fibers with the lowest thresholds remain intact, the clinical implications of a large but undetected loss of auditory nerve fibers are obvious. Consequently, a substantial effort has been mounted to determine if cochlear synaptopathy is present in humans and if it leads to 'hidden hearing loss,' i.e., deficits such as decreased ability for hearing in noisy backgrounds that are not detectable by a change in the audiogram. In general, this effort has shown that cochlear synaptopathy in humans occurs anatomically primarily as a function of age (8–10), but has not conclusively shown a functional correlate [reviewed by (11)]. One approach has been to test different audiometrically-normal populations that are expected to have higher or lower levels of noise exposure (12, 13), or that report greater lifetime noise exposures (14–16). In general, these studies have found no performance decrements with greater noise exposure on a variety of primarily speech in noise perception tests that, theoretically, should be affected by cochlear synaptopathy. Objective tests, including amplitude and latency of waves I and V (13, 17, 18), middle ear muscle reflex (19, 20), the summating potential (SP), or SP to compound action potential (CAP) ratio in electrocochleography (ECochG) (19, 21), and envelope and frequency following responses (22) have also yielded mixed results, with some showing important suggestive evidence of increased cochlear synaptopathy in groups with greater noise exposure.

More recent animal work (7, 23–25) as well as older studies (26, 27) suggest that the loss of synapses may be partially reversible, and that the excitotoxic effects may include low spontaneous rate fibers as well (28). Recovery of synaptic function could explain why the effects of cochlear synaptopathy in noise-exposed but relatively young human subjects have been difficult to show. However, in older subjects with permanent threshold increases the effects of cochlear synaptopathy may be present. Anatomical studies of immunolabeled synapses and fiber counts in the osseous spiral lamina on human temporal bones suggest that synaptopathy is present and increases with age (8–10). Another finding consistent with cochlear synaptopathy under a condition of substantial hearing loss is a high correlation reported between ECochG amplitude and speech perception outcomes in adults with cochlear implants (CIs, $r = 0.69$) (29–31). Because the relationship between preoperative audiometric thresholds and postoperative speech perception outcomes is weak (32–34), the ECochG measurement must be capturing information about the health of spiral ganglion cells available for electrical stimulation that is different from the audiogram. The explanation offered by Fontenot et al. (29) is that hair cell activity recorded from ECochG is disconnected from nerve fibers, i.e., cochlear synaptopathy is present. In this view, hair cell activity acts as a metric of 'cochlear health,' in that hair cells within a functional organ of Corti can help support spiral ganglion cells and thus lead to better speech perception outcomes.

To test this view, we created cochlear synaptopathy in gerbils using neurotoxins and characterized the ECochG for neural and hair cells in normal hearing gerbils and in gerbils with a high frequency noise exposure intended to mimic the sloping pattern of hearing loss found in many adult CI subjects. The sloping pattern consists of little or no sensitivity to high frequencies (greater than about 1,500 Hz) and variable hearing to low frequencies, including some with minimal or moderate hearing loss (35). The responses to the gerbils before and after neurotoxins were then compared to ECochG recordings from human CI subjects and others where the round window (RW) was available during surgery. We report that the human groups displayed proportions of hair cell and neural activity in their ECochG recordings to low frequencies similar to the recordings of animals treated with neurotoxins to produce cochlear synaptopathy.

Materials and methods

Animal and human subjects

Protocols for the use of gerbils, *Meriones unguiculatus*, were approved by the Institutional Animal Care and Use Committee (IACUC) at the University of North Carolina at Chapel Hill, following the standards of the National Institutes of Health and Committee on Care and Use of Laboratory Animals.

Data from human subjects was obtained intraoperatively with approval of the Institutional Review Boards at the University of North Carolina at Chapel Hill and the Ohio State University. Informed consent was obtained from all adult participants. Parental consent was obtained for pediatric subjects and patient assent was obtained from children between 7 and 18 years. Inclusion criteria for ECochG were that potential subjects were scheduled to receive a CI after the medical and audiological evaluation had established candidacy or were undergoing a surgery where the RW was accessible. Potential candidates were excluded from the study if they were not fluent in English, were undergoing revision surgery, or presented with severe inner ear malformations. The subject pool was therefore a mix of subjects of all ages typically seen at large centers for otologic or neurologic surgeries.

Experimental design

ECochG principles

The ECochG response contains contributions from hair cells and the auditory nerve that mix in complex ways as stimulus frequency and intensity are varied. A main component from hair cells is the cochlear microphonic (CM), so-called because it faithfully mirrors the input waveform to the point that a listener can understand what was said when listening to the ECochG recording (36, 37). To low frequencies, the CM is mixed with the auditory nerve neurophonic (ANN), a neural component that also follows the stimulus waveform due to phase-locking in auditory nerve fibers (38, 39). Thus, to low frequencies the CM and ANN are mixed in ECochG.

A description of some of the biophysical elements that produce the CM and ANN are shown in Figure 1. The CM (Figure 1A) is produced by currents flowing through stereocilia as mechanosensitive transduction channels open and close with basilar membrane movement. When the sound level is low, the stereocilia are in the linear part of their operating range (Figure 1A1) and the CM produced to a tonal input (bottom row) is essentially sinusoidal. As the sound level increases (Figure 1A2), output saturation is reached, but not

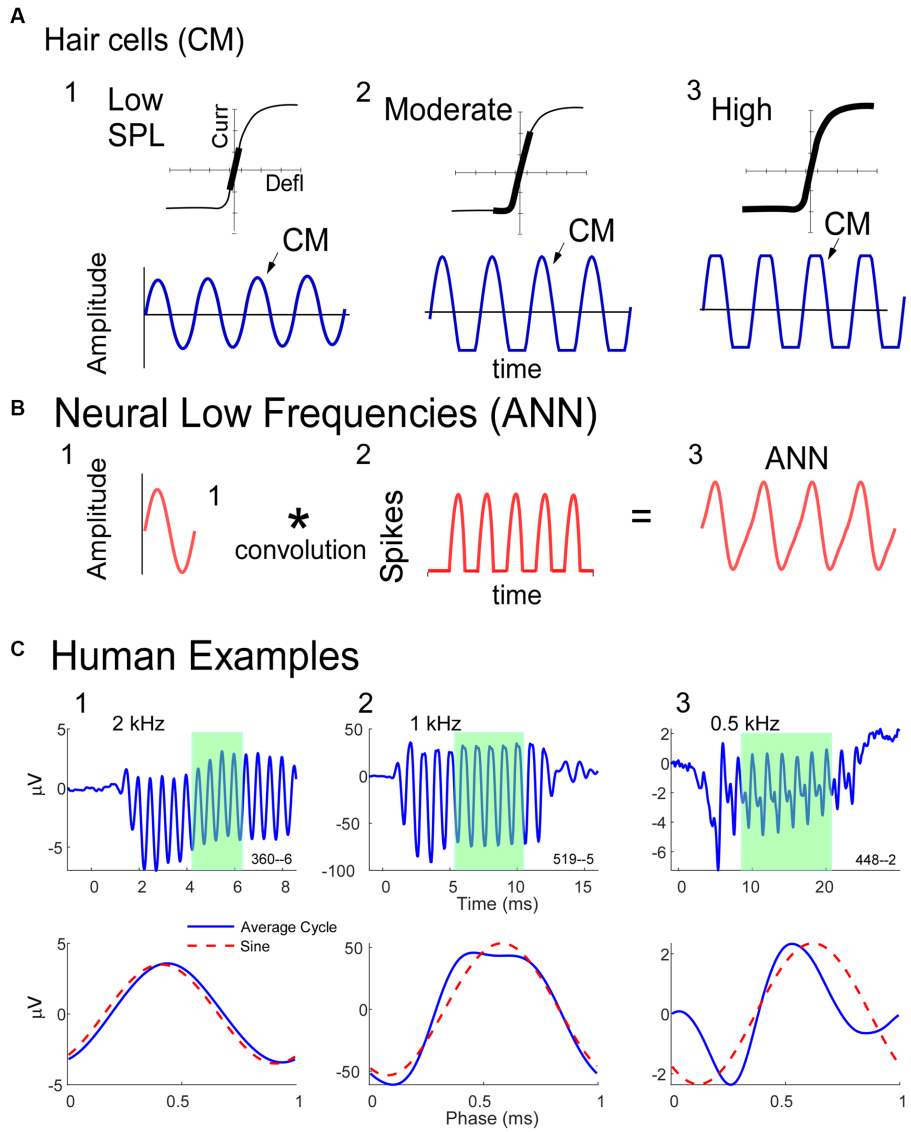

FIGURE 1
Schematic model of some of the biophysics of hair cell and neural sources for the ECochG potentials. **(A)** The CM is produced by the opening and closing of channels in the stereocilia of hair cells. To low intensities (left) the response is within the linear part of the operating range (top) and the CM produced is sinusoidal at the stimulus frequency (bottom). With increased intensity there will be asymmetric saturation (middle) to the degree the operating point is offset from the middle. To high intensities symmetric saturation will occur (right). **(B)** The ANN is produced by the phase-locked firing of auditory nerve fibers to low frequency sounds (<~1.5 kHz in gerbils and humans). It can be modeled as the convolution of a unit potential, or shape of the action potential as it appears at the RW, with the distribution of action potentials across all fibers that produce the ensemble response. **(C)** ECochG to 90 dB nHL tone bursts from three human CI subjects. The top row is the time waveform to condensation phase and the bottom is the 'average cycle,' or average of the cycles during the steady-state response (from shaded regions in top row). 1. In this case the average cycle shows little distortion to a 4 kHz tone burst, consistent with its being above the phase-locking range for the ANN and in the linear region of the CM (as in **A**, left). 2. In this case the response to a 1 kHz tone burst shows asymmetric saturation (as in **A**, middle). 3. Responses to a low frequency (0.5 kHz) tone burst. Here there is extensive distortion in the average cycle but not of a type that can be produced by hair cells, so is due instead to the ANN.

symmetrically. Typically, more channels are closed than open at rest, producing saturation first in the hyperpolarizing direction of stereociliary movement. The asymmetry in the saturation is greater for inner than for outer hair cells (40). At high levels (Figure 1A3) saturation is to both directions, but the asymmetry remains. Thus, the shapes of the ECochG response produced by the CM will either be sinusoidal (Figure 1A1), asymmetrically saturated (Figure 1A2), or with a symmetrically saturated component as well (Figure 1A3).

The ANN is produced by the summed, synchronous activity of nerve action potentials as they phase-lock to the stimulus fine structure. Based on the extensive literature describing the CAP, which is the summed, synchronous activity of auditory nerve fibers to stimulus onsets (41–44), the ANN (Figure 1B) can be described as a unit potential (Figure 1B1), or shape of an action potential as it appears at the RW, convolved with the distribution of action potentials coming in a cyclic fashion from individual auditory nerve fibers (Figure 1B2). Because the spike rate cannot go below zero, the auditory nerve output is a rectified version of the stimulus input. The shape of the unit potential resembles an action potential with positive and negative components, so when convolved with the PST

histogram the ANN (Figure 1B3) has positive and negative components.

Examples of how ECochG responses follow these principles in humans CI subjects are shown in Figure 1C. For each of three cases, the top row shows the ECochG time waveform to condensation phase stimulation, and the bottom row shows an "average cycle," or average of each cycle in the steady-state response (shaded regions in top row). The average cycle is equivalent to a period histogram, a common representation of the cycle PST in Figure 1B2. It will be our primary unit of analysis for this report. For case 1, there was no ANN since the frequency (4 kHz) was above the phase-locking range, and the average cycle was sinusoidal (as in Figure 1A1). For Case 2, the average cycle (to 1 kHz) had a shape characteristic of asymmetrical saturation, as in Figure 1A2. Case 3 (right) shows the response to a low frequency (0.5 kHz) tone burst. Here, the average cycle does not match one of the possible shapes for the CM (Figure 1A), so the presence of an ANN is indicated.

The average cycle as the unit of analysis for detecting and measuring the CM and ANN

As we will describe in the next sections, we have developed methods for detecting the presence of the ANN and estimating its magnitude, along with that of the CM, using the average cycles as the main unit of analysis. Previous methods to identify the ANN have been primarily spectral (46–48) or used masking (49–52). Spectral methods rely on the 2nd harmonic in the summed responses to the two phases, under the assumption that the rectified responses to opposite stimulus phases will interleave to form what has recently been called the 'Auditory Nerve Overlapping Waveform" (48, 53). At low and moderate intensities, the second harmonic is predominantly neural, so the ANOW is expected to be proportional to the ANN. However, the ANN is periodic with the stimulus frequency, so most of its energy is in the 1st harmonic, where it overlaps spectrally with the CM. In addition, at moderate and high intensities some of the second harmonic can be from asymmetric saturation of the CM, so the size of the second harmonic does not provide a quantitative estimate of the ANN. The other approach is masking, under the assumption that neural responses will adapt while HC responses will not. Masking can demonstrate the presence of the ANN but the proportion that is masked is dependent on the time and frequency relationships between masker and probe. In addition, obtaining a reliable data set using masking is not feasible while monitoring ECochG during a CI surgery or clinic visit.

The approach we have used is to estimate the CM and ANN using a model where the average cycle is the input and then equations developed from Figure 1 are used to estimate the amounts of CM and ANN that produce the best fit (45). Here we are augmenting this model with a deep learning algorithm (DLA) to first identify cases with or without ANN. The purpose of the DLA is to correct an issue with the analytic model, which estimates at least a small ANN even to high frequencies above the phase-locking range. This result is because the CM-only responses can deviate slightly from the expected shapes (45). The DLA makes no assumptions about expected shapes.

Acoustic stimulation and recording

The acoustic stimulation and recordings of cochlear responses in both gerbils and humans were performed using a Bio-logic Navigator Pro (Natus Medical Inc., San Carlos, CA) as described previously (29, 45, 54, 55). The speaker was an Etymotic, ER-3B. The recording electrode was a stainless-steel probe of the type used for facial nerve monitoring during CI surgeries (Neurosign 3,602-00-TE, Magstim Co., Wales, UK), placed at the round window in both gerbil and humans. For human subjects, surface electrodes over the contralateral mastoid and on the forehead, and for gerbils, needle electrodes in the neck muscles and tail, served as the inverting and reference electrode, respectively. Gain was 1,000x for gerbils and 50,000x for humans. In some cases, for both gerbils and humans the sound tube was crimped which removed the responses, indicating that they were not contaminated by electrical artifact.

Stimuli were tone bursts alternating in condensation and rarefaction phases, with 100 (gerbil) or 250 (human) repetitions to each phase. Tone burst frequencies were 250, 500, 750, 1,000, 2000 and 4,000 Hz. Calibration was performed using a ¼" microphone and measuring amplifier (Bruel & Kjaer, Naerum, Denmark) and a 2 cm brass chamber for humans, and using a probe tube in the closed field in the ear canal of gerbils. High-pass filter settings for the recordings was 10 Hz in humans and 1 Hz in gerbils, and low-pass settings were 5,000 Hz (250–1,000 Hz tone frequencies), 10,000 Hz (for 2000 Hz) or 15,000 Hz (for 4,000 Hz tone frequency).

Gerbil and human data sets

We present ECochG data from RW recordings in gerbil and human subjects with different hearing conditions (Table 1). For gerbils entering the recording part of the study, the auditory status was either normal-hearing (NH) or high-frequency-noise-induced hearing loss (HF-NIHL). Animals were classified as NH if untreated by noise or pharmacological agents prior to the experiment, and if ECochG signal magnitudes and thresholds were within the "normal" range for NH animals observed in this and previous experiments (45, 56). At 4 kHz, for example, CM magnitudes to 90 dB SPL were > 40 dB SPL and thresholds <10 dB SPL in all animals. In the HF-NIHL animals, the cut-off frequency of the 122 dB SPL noise was 4 kHz, which corresponds to approximately halfway along the characteristic frequency regions of the gerbil cochlea (57). In previous studies we showed that both outer and inner hair cells were removed in basal parts of the cochlea in response to the intense noise exposure used (58, 59). For both types of hair cells the transition from few or no hair cells to complete preservation was sharp and showed little variability as a percentage of distance from the apex of the basilar membrane compared to the total length, across animals (OHCs = 49.8 ± 4.50% and IHCs = 58.9 ± 4.46%,

TABLE 1 Data sets.

Species	Hearing condition	Cases
Gerbil	NH[1]	54
Gerbil	NH (post KA)[1]	20
Gerbil	HF-NIHL[2]	10
Gerbil	HF-NIHL (post KA)[2]	7
Human	CI[3]	166
Human	Non-CI[3]	42

[1]Normal hearing.
[2]High-frequency noise induced hearing loss.
[3]Cochlear implant.

$n = 19$, errors are standard deviation). The more basal transition zone for IHCs showed a greater resistance to the noise, and there were often some IHCs preserved in the hook region of the cochlea as well. A few cases in the previous studies showed less or no hair cell loss, and, similarly, some cases here had CM thresholds that overlapped with normal hearing animals and were excluded. All of the HF-NIHL animals used here had CM thresholds to 4 kHz and higher that were > 50 dB SPL compared to an average of 0 dB SPL for the NH animals. The HF-NIHL condition was intended to mimic that of CI many subjects, where residual hearing, if present, is typically restricted to the apical half of the cochlea (frequencies <1.5 kHz in humans, <4 kHz in gerbils). Both gerbil groups (NH and HF-NIL) were also studied after the neurotoxin kainic acid (KA) was applied to produce cochlear synaptopathy. The KA was 60 mM in artificial perilymph consisting of (in mM): 127.5 NaCl, 3.5 KCl, 25 NaHCO3, 1.3 CaCl2, 1.2 MgCl2, 0.75 NaH2PO4, and 11 glucose, and pH adjusted to 7.3 with HCl (60), heated to 37 degrees C. It was placed at the RW for 1 h. With this protocol the loss of auditory nerve response is nearly total for the basal cochlea, but less so for the apical, due to the cochlea's diffusion characteristics [see an anatomical image of the effects of KA in Figure 4 of Pappa et al. (56)]. Some of the NH animals here are the same as from the Pappa et al. study, and the same criterion for inclusion after KA was used. This criterion was that an increase in CM threshold between pre and post KA responses to 4 kHz, which is above the phase-locking range where the ongoing response is purely CM, i.e., from hair cells and thus not expected to be affected by the KA, had to be within 3 dB. This criterion resulted in exclusion of three animals.

The human subjects comprised surgical patients where the RW was accessible intraoperatively and included both CI and non-CI subjects. The CI subjects spanned all age groups. The non-CI subjects were undergoing surgery for a vestibular schwannoma or for Ménière's disease, except for one subject who had a tumor removed from the jugular foramen allowing access to the RW.

Deep learning algorithm

Since responses to low frequencies in an NH animal should always contain an ANN, while those to high frequency should not, these represent an ideal training set for a DLA to recognize its presence or absence in an average cycle. The input to the DLA (Figure 2A) was a tensor of the average cycles defined by condensation, rarefaction, difference, and alternating waveforms, using the responses to phase-alternating stimuli. These average cycles were normalized for amplitude and for 0 starting phase. The DLA was an implementation of Bidirectional Long Short-Term Memory (BiLSTM) layers, which are a specific subtype of recurrent neural networks that are frequently used on sequence data because they have an increased memory for events that are distant from each other (61). The bidirectional nature of the BiLSTM provides information about dependencies from both the forward and backward direction at every point. Finally, a dense layer with a sigmoid activation function was used to encode each of the ECochGs as either 'ANN present' or 'ANN absent.'

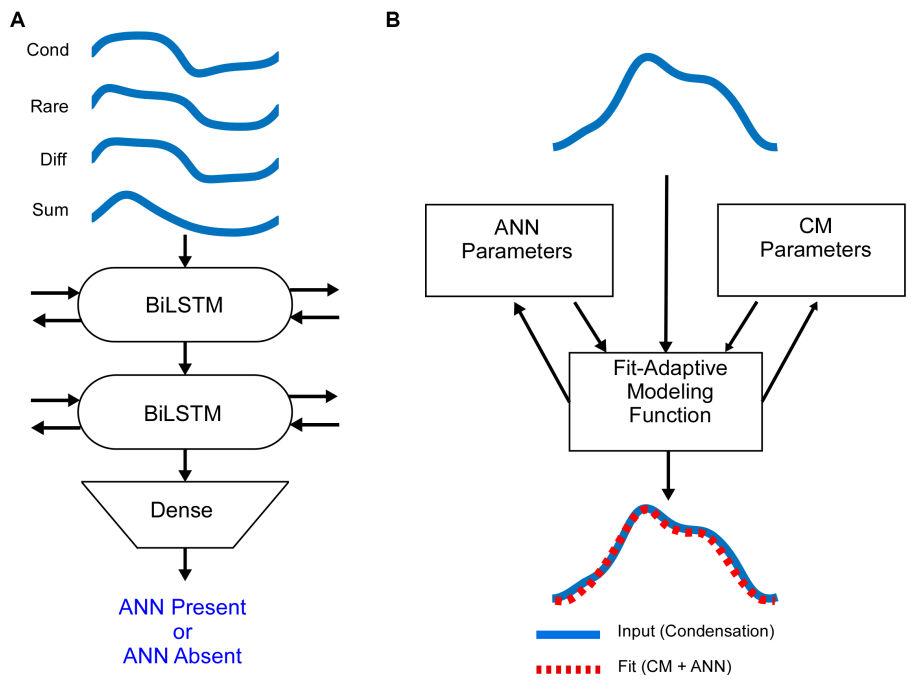

FIGURE 2
Mathematical models **(A)**. The average cycle for condensation, rarefaction, difference and alternating curves, normalized to amplitude and shifted to start at zero phase, were used as the input to the DLA. The network consisted of two layers of Bidirectional Long Short Term Memory (BiLSTM) nodes, followed by a dense node (see text and Material and Methods for further descriptions). The output was either ANN-present or ANN-absent. The training data was from NH animals, where low frequencies are ANN-present and high frequencies are ANN-absent. **(B)** Schematic of the biophysically based model used to determine the amount of CM and ANN. The input to the model is the average cycle to condensation phase stimuli. It is then modeled by a fit-adaptive function which updates ANN and CM parameters (see text) to produce an output which best matches the input [from (45)].

The DLA was implemented in Python using the Keras library with TensorFlow as a backend. The architecture of the network was an input layer, followed by two BiLSTM layers with 50 recurrent units each, and finally a dense layer with a sigmoid activation function. The DLA was compiled with parameters to search for the best accuracy using a binary-crossentropy loss function with the adam optimizer.

The DLA weights were trained on the training set for 500 epochs, after which the increase in epoch accuracy and epoch loss leveled off and were validated on the test set. The final weights were saved so that they could be loaded and used for future classification tasks.

Because only the shapes of the cycles, and not amplitude or phase, are considered, the results from the neural network are generalizable for different experimental data sets. Each of the gerbil and human data sets were collected with the same recording and stimulation equipment and parameters.

Analytic model and ANN proportion

Once an ECochG is labeled as ANN Present or Absent, we use a fit-adaptive function to model the contributions of the ANN and CM based on a depiction of the biophysical properties that produce each in Figure 1, as shown in Figure 2B (45). Briefly, the model mathematically describes the shapes of the CM and ANN and convolves them to create an average cycle of the ECochG, which it compares to the known signal and adjusts parameters until the error is minimized. Differences from the previous study were that the average cycles were interpolated to 100 points using a spline instead of linear interpolation, and several different starting parameters were run to help avoid local minima. Parameters for the CM were amplitude, phase, and differential saturation of the peak and trough, and for the ANN were amplitude and a 'spread of excitation' parameter that allowed the cycle histogram to increase in width to account for summation across fibers with varying phase. The model optimized these parameters and reported the values for the CM and ANN that produced the best fit. From these values, the proportion of ANN was simply $ANN\ proportion = \frac{ANN}{CM + ANN}$, where CM and ANN are their respective amplitudes in μV.

Results

The complex shape of average cycle is caused by the ANN

In gerbils, it can be demonstrated that a complex shape of an average cycle, not expected from the CM alone (Figure 1) is caused by the ANN. In Figure 3, examples are shown before and after KA was applied to the round window. To a high-frequency tone burst in an NH animal (Figure 3A, 3 kHz), the average cycle had a sinusoidal shape to a moderate intensity (50 dB SPL, left), while to a high intensity (90 dB, right) it was asymmetrically saturated. Both shapes are characteristic of the CM-only waveform, and the KA had little effect. In contrast, to a low-frequency stimulus (Figure 3B), the shape prior to the KA was not consistent with a CM-only response, while after KA the average cycle was sinusoidal to the moderate intensity and was saturated to the high intensity. The effect of KA at the high intensity was subtle (arrow), but the small deviation in the pre-KA shape was a consistent feature not seen in cases that did not have an ANN. In Figure 3C there is a further example of a low-frequency response, but this time in an HF-NIHL animal. Here, two features stand out: the pre-KA curves are particularly distorted to both low and high intensities, and the effect of the neurotoxin appears to be incomplete. The high degree of pre-KA distortion for HF-NIHL animals compared to NH animals was a characteristic result further considered below. A partial effect of the KA was common to both gerbil groups and is presumably because of incomplete diffusion to the apex, so some ANN remains. This effect is minimized in NH animals at high sound levels, where the largest part of the response is from the base of the cochlea where the removal of the neural elements with KA is more complete.

Performance of the DLA model

The model was trained and tested on 1764 average cycles from the 54 NH animals, including 641 to low frequencies (0.25–0.75 kHz) and 1,123 to high frequencies (2–6 kHz). The expectation is that in NH animals the responses to low frequencies within the phase-locking range (<2000 Hz) will all contain an ANN, while none of the frequencies above that range will. Thus, these represent "true known" responses.

The data was split 70/30 into training and test sets. The model weights were trained for 500 epochs, after which the increase in epoch accuracy and epoch loss leveled off. With this distribution, the model had a sensitivity for correct detection of an ANN of 99.1%, and a specificity for correct rejection of an ANN of 98.0% (Figure 4A).

When considered on a frequency-by-frequency basis, the proportion of average cycles identified by the DLA as having ANN was >95% for 0.25 to 0.75 kHz, which then dropped to <5% for frequencies of 1.5 kHz and higher (Figure 4B). The proportion at 1 kHz was about 75%. The overall phase-locking to 1 kHz may be reduced because it is near the cut-off frequency for both gerbils and humans, but a reduction in the ANN may also be because the width of a unit potential begins to exceed the width of a cycle of phase-locking (47). Consequently, 1 kHz was not used in the analyses of ANN proportion.

Analytical model results

In the NH animals, to low-frequency tones (250, 500, and 750 Hz), the ANN proportion decreased as the CM increased (Figure 4C, left). The color scale shows this relative increase in the CM compared to the ANN to be largely a function of intensity. The relatively few that were excluded by the DLA are shown below the line rather than at zero with some jitter added for clarity. To high-frequency tone bursts (≥2000 Hz), most average cycles were reported by the DLA to have no ANN (Figure 4C, right).

There are more parameters than equations in the analytic model, so the fits do not necessarily represent unique solutions to the parameters. We used multiple starting points to avoid local minima but fits at some distance from the correct values can occur from parameter optimization. A check that the model was estimating reasonable values was to compare its output to that of an independent method of analyzing an average cycle which did not make

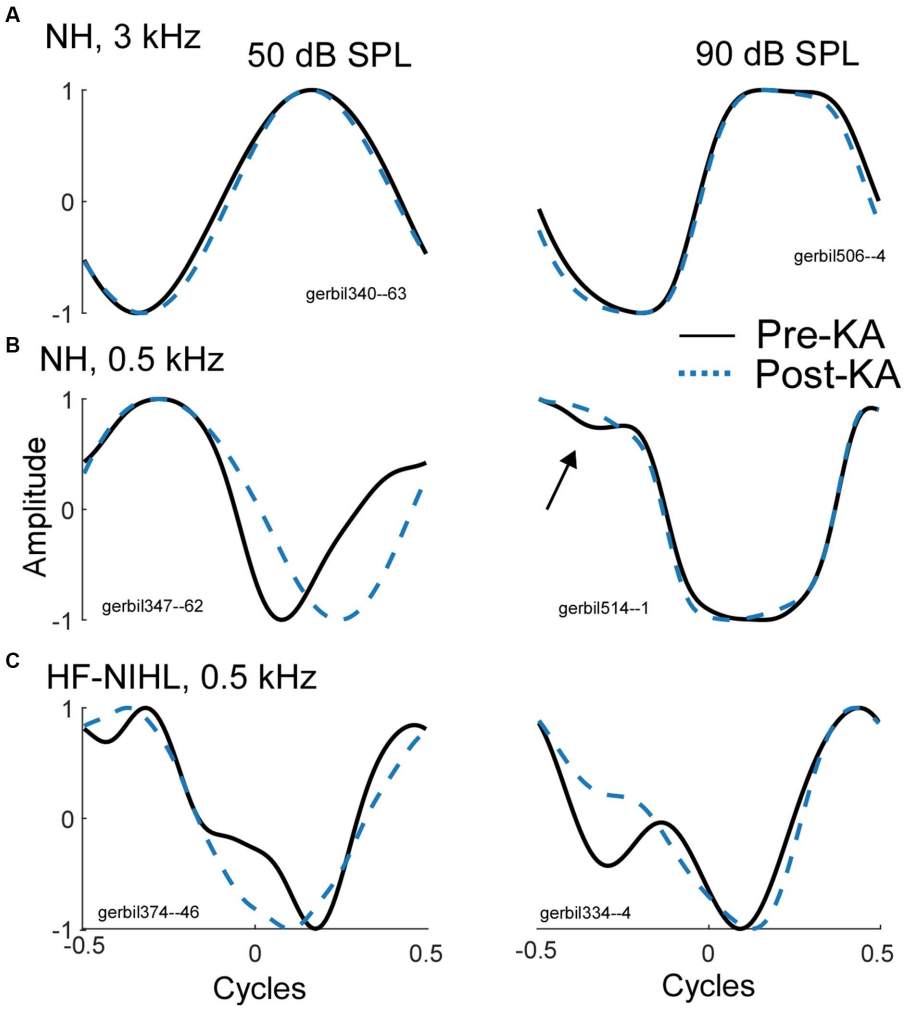

FIGURE 3
Effects of the neurotoxin KA to produce cochlear synaptopathy. **(A)** After application of KA, the responses to a high frequency (3 kHz), whether sinusoidal (left) or saturated (right) did not change, indicating no ANN. **(B)** To low frequencies (500 Hz) in NH animals the curves became simpler and consistent with that expected for CM-only. **(C)** To low frequencies from HF-NIHL animals also simplified after the KA, but pre-KA were even more distorted than in the NH cases, and the effect of KA appeared to be only partial, as was also common to low frequencies in some cases for NH animals.

assumptions about the shapes that make up the CM and ANN. For each low-frequency average cycle, we performed a cross-correlation with all the average cycles to high frequencies and measured the root-mean square value of the residuals in the case with the closest fit. The idea was that the smaller the residuals, or the closer a match to a CM-only case, the less ANN would be present. We found that this metric correlated well ($r = 0.883$) with the ANN proportion (Figure 4D), suggesting that the analytic model, which provides values the ANN and CM, scales with actual rather than far distant values.

Effects of neurotoxins and noise exposure on the ANN proportion in gerbils

As would be expected, post-KA, NH animals (Figure 5A) had a large increase in the numbers of responses to low frequency (<1,000 Hz) judged by the DLA to have no ANN (24.8% compared to 2.0% in NH animals from Figure 5A). Similarly, the ANN proportion was in general smaller, indicating less ANN relative to the CM than before the KA (mean = 0.33 ± 0.176 for the Pre-KA vs. 0.21 ± 0.13 for the Post-KA). However, since most cases still had some ANN the action of the neurotoxin was often only partial. Finally, the effect of intensity was decreased, with most cases showing a small ANN proportion even to low intensities. A quantification of this decrease in the effect of intensity is the slope of the best fit regression line through all of the data, which was 0.52/dB for the Pre-KA NH condition and 0.27/dB for the Post-KA condition.

For the HF-NIHL animals, prior to the KA the DLA again showed that almost all responses to low frequencies had an ANN (Figure 5B). The removal of hair cells from the basal half of the cochlea did reduce the CM, as expected. However, the HF-NIHL animals showed an *increased* proportion of ANN, especially to higher intensities, compared to the NH distributions in Figure 5C, which will later be better quantified. After KA (Figure 5C) the DLA again found more responses without an ANN, and the ANN proportion decreased, indicating partial to complete synaptopathy in most cases.

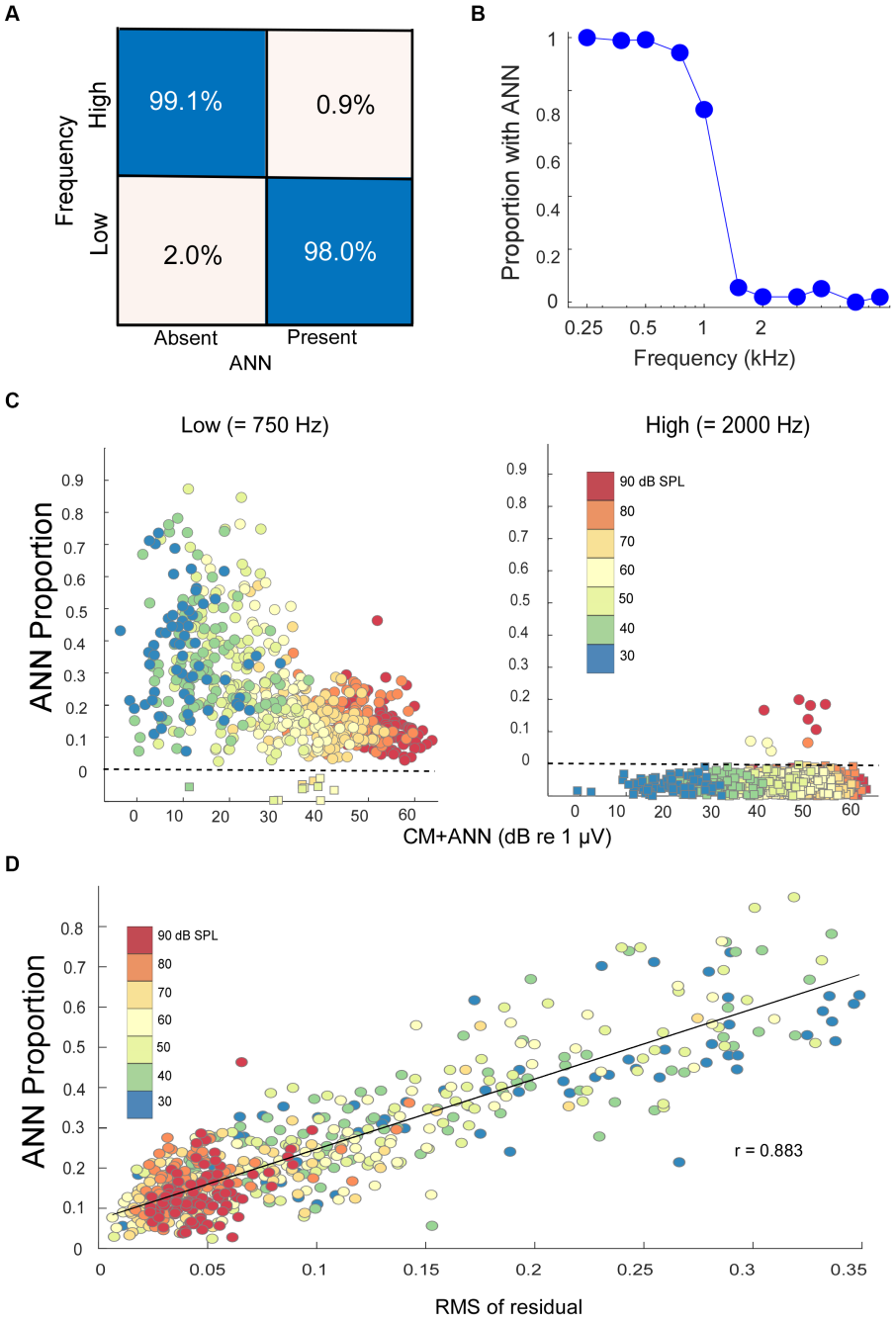

FIGURE 4
Modeling results. **(A)** Confusion matrix of the results with NH animals, confirmed with an independent test set, indicating the DLA was able to correctly identify and reject the presence of ANN at a high rate. **(B)** Percentage of the cases where an ANN was detected from the DLA as a function of stimulus frequency in NH animals. **(C)** The ANN proportion as a function of the size of the CM + ANN, both reported by the model, for NH gerbils to low and high frequencies. For cases with no ANN according to the DLA, the model was run without the ANN component. Each symbol is the ANN proportion to a frequency/intensity combination, so there are many points for each gerbil. The square symbols below the dotted line had no ANN according to the DLA, and were plotted at 0 with jitter added to make the points more visible. **(D)** Comparison of the ANN proportion with an independent method of estimating relative size of the ANN. The metric is the root mean square value of residuals in a regression of each low frequency average cycle with its best fit among the high frequency cases. The high correlation (r = 0.883) indicates the CM and ANN are reported from the analytic model in reasonable proportions.

The growth of the CM (as computed from the model) is linear over the intensity range of 30–90 dB SPL, while for the HF-NIHL animals it saturates at a moderate intensity. The early saturation in HF-NIHL animals (Figure 5D) is because the spread of excitation toward the base of the cochlea as the intensity is raised is limited by the loss of hair cells. In contrast, the ANN (Figure 5E) in the NH animals grows at a comparatively slower rate, and the difference between NH and HF-NIHL animals is much smaller. The result is that the difference between the CM and ANN (Figure 5F) grows with intensity in the NH animals but does not in the HF-NIHL animals.

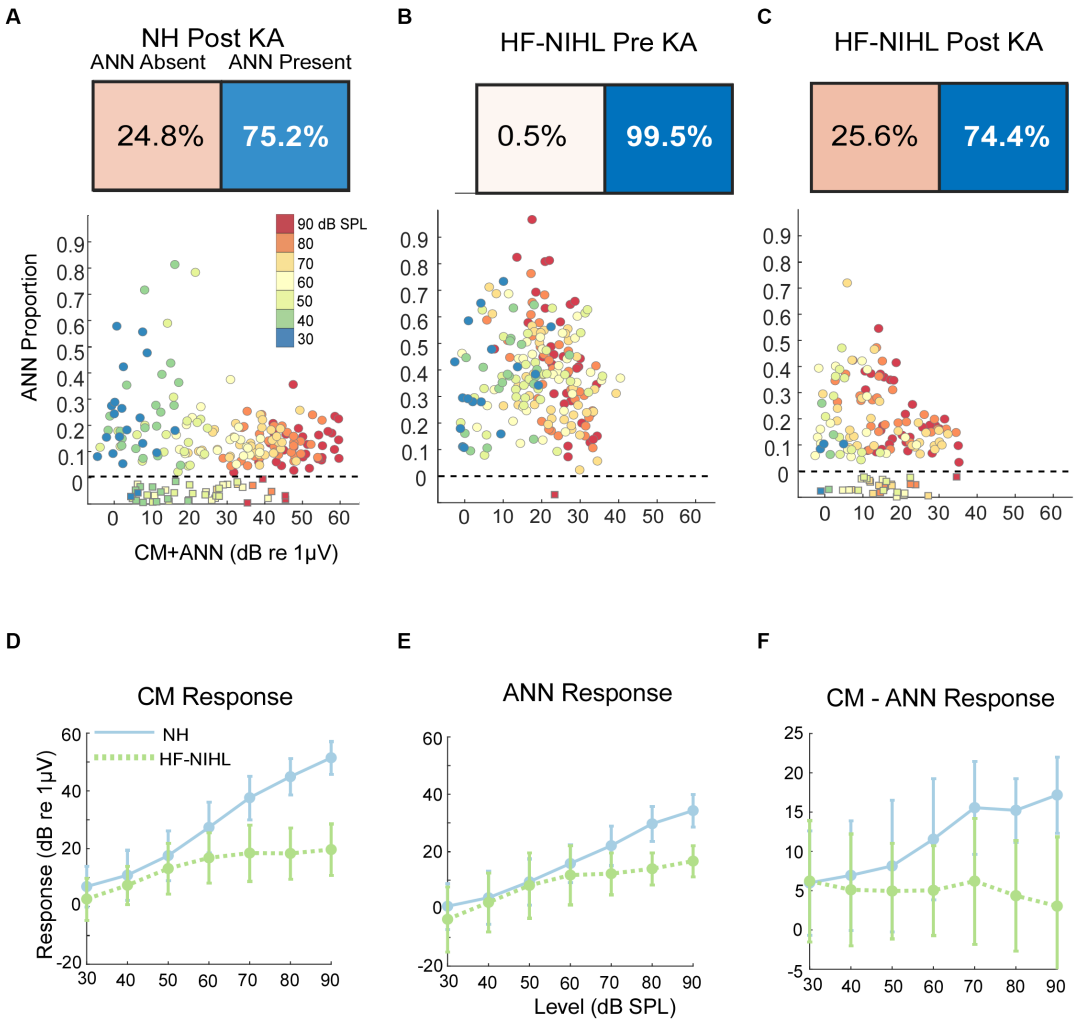

FIGURE 5
Results in gerbils. **(A)** Effects of the neurotoxin KA on low-frequency average cycles. There is a higher proportion of ANN-absent cases and less ANN overall than prior to KA (compare with **B**). **(B)** Results to low frequencies from HF-NIHL cases. The CM is reduced, but the proportion of ANN is high. **(C)** Results from HF-NIHL cases after KA. There is an increase in ANN-absent cases and in the ANN proportion of most cases. **(D)** Comparison of the CM in NH and HF-NIHL animals (pre-KA). The CM saturates in the HF-NIHL animals, due to limited spread of excitation because the basal cochlea is non-functional. **(E)** Comparison of the ANN. The effect in the HF-NIHL animals is similar but smaller than with the CM. **(F)** Difference between the CM and ANN. This difference grew in the NH animals due to spread of excitation but not in the HF-NIHL animals, where it was blocked. Error bars represent standard deviations.

Results in humans

Our human data sets were CI subjects and others where the round window was available during surgery. A metric used to characterize the overall responses from each subject is the 'Total Response (TR),' which is a summed measure of the output of the cochlea to a range of frequencies (29, 31, 62, 63) (see Materials and Methods). Specifically, the TR is calculated from the sum of the response magnitudes to each frequency, with the response at each frequency measured as the sums of significant peaks to the stimulus frequency and 2nd and 3rd first harmonics. The frequencies used were 0.25, 0.5, 0.75, 1, 2, and 4 kHz. The TRs for the CI subjects (Figure 6A) covered a wide range independent of age. For the youngest children many of the cases with large TR were auditory neuropathy spectrum disorder (ANSD) subjects, which is a condition characterized by loss or desynchrony of auditory nerve firing with preservation of cochlear function, and so may be related to cochlear synaptopathy. The TRs for non-CI subjects (Figure 6B), were on average larger than for the CI subjects, but interestingly the cases with the highest values were similar for each data set. Even the one subject with audiometric thresholds within the normal range had a level only near the maximum of the other groups, not above them.

To low frequencies (0.25, 0.5, and 0.75 kHz), the DLA reported that CI and non-CI (Figures 6C,D) subjects both had a large fraction (28.9 and 26.7%, respectively) with no detectable ANN. Of the remainder there was a wide distribution, including some with evidence of a strong ANN (e.g., >25% of the combined responses).

Human groups are most similar to gerbil groups exposed to KA

A comparison of the distributions of ANN proportion across the six groups is shown in Figure 7A. These distributions encompass

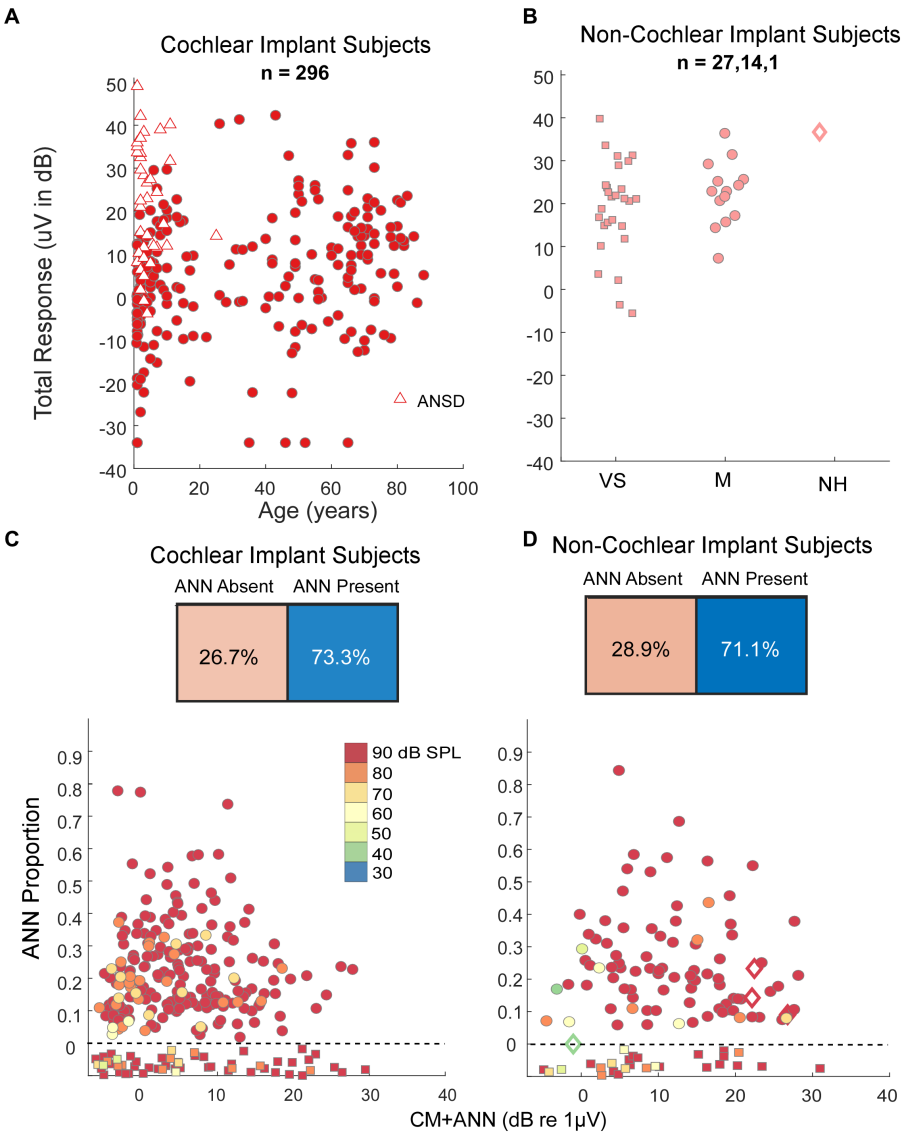

FIGURE 6
Results in human subjects. **(A)** Distribution of 'Total Response' (TR, a measure of the responses summed across frequencies, see text) in CI subjects. There is a wide range of responses independent of age, with the largest TR often seen in children with auditory neuropathy spectrum disorder (ANSD). **(B)** TR in non-CI subjects as a function of age. The largest TR in each group, including the case with no auditory-related syndrome and thresholds in the normal range, were similar to the largest in CI subjects. VS, vestibular schwannoma. M, Meniere's, NH, Normal Hearing. **(C)** Output of the DLA and distribution of ANN proportion in CI subjects. There were many cases judged by the DLA to have no ANN, but otherwise there was a wide range of ANN present. **(D)** Output of the DLA and distribution of ANN proportion in non-CI subjects. Similar to the CI subjects, there were many cases judged by the DLA to have no ANN, but otherwise there was a wide range of ANN present.

different frequencies and intensities for each animal and human subject. The results of multiple comparisons, based on standard errors corrected for multiple comparisons (Figure 7B, alpha = 0.083), were that the pre-KA, HF-NIHL gerbils showed the largest proportion of ANN and was distinct from the other data sets. The gerbils with the next highest proportion of ANN were the pre-KA NH animals, and the ANN proportion was significantly greater than for any of the remaining groups. The distributions in both of the post-KA animal groups were not significantly different from each other or from the two human groups. Recall that the noise exposure for the HF-NIHL animals was intended to mimic that of subjects, particularly CI subjects, with high frequency hearing loss. Thus, if hair cell loss was the main cause of hearing dysfunction leading to cochlear implantation, the human CI subjects should have most closely resembled the pre-KA, HF-NIHL animals. Instead, their distribution, and the distribution of non-CI subjects, was most like that of the gerbil groups after application of neurotoxin that produced a complete or partial synaptopathy, which implies synaptopathy is present in the human subjects as well.

ECochG thresholds are often better than behavioral in CI subjects

A behavioral threshold is typically based on activity in one or a few sensory receptors that result in only a few action potentials (64,

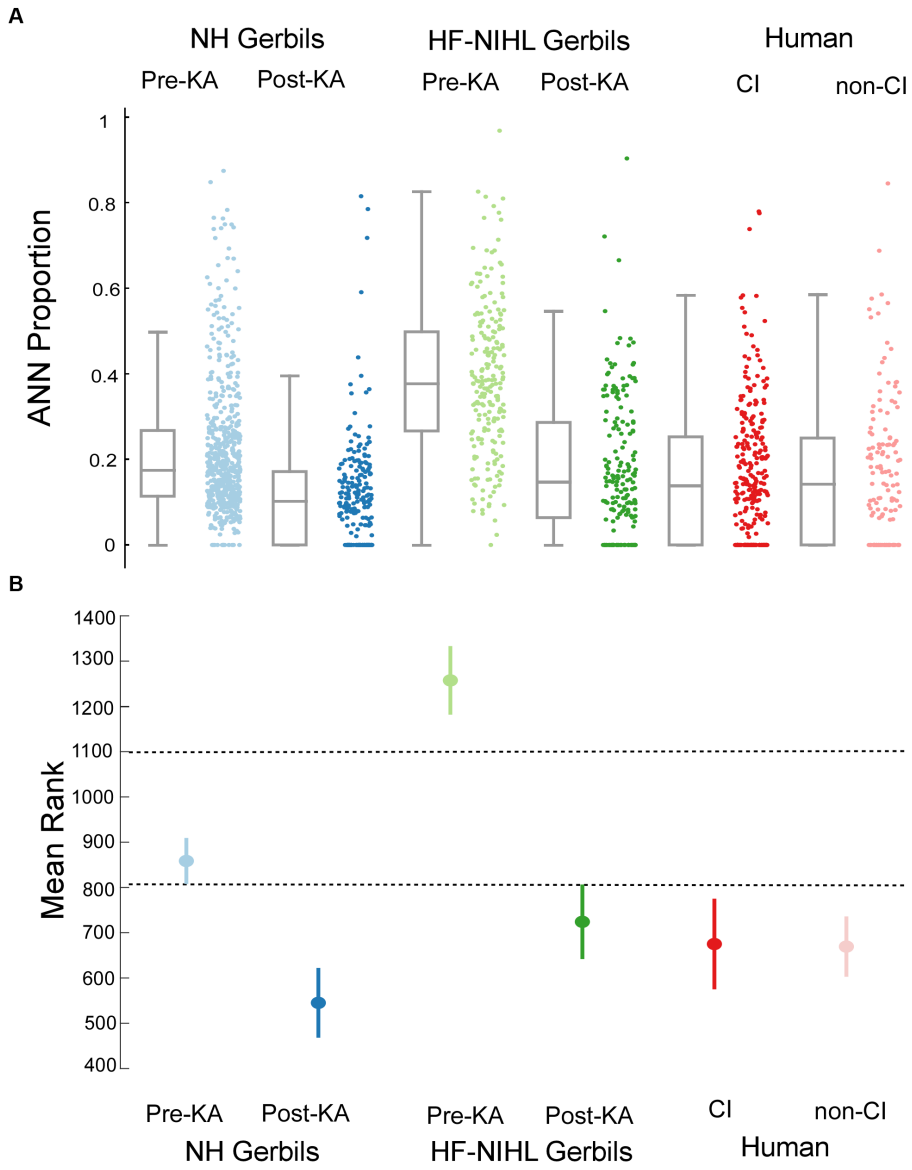

FIGURE 7
Comparisons across the gerbil and human data sets. **(A)** Scatter plots show the distributions of ANN proportion, and the box plots show median, semi-interquartile ranges, and whiskers that include 1.5 times the inter-quartile range. **(B)** Means and standard errors with correction for multiple comparisons (alpha = 0.083).

65). In contrast, generation of an evoked potential requires the summed, synchronous activity of numerous responding elements. Therefore, a behavioral threshold is expected to be more sensitive than an evoked potential. However, in CI subjects the ECochG threshold, recorded perioperatively, was often more sensitive than the pre-operative audiometric thresholds. An example is shown in Figures 8A,B, where the subject had severe hearing loss to low frequencies (250 and 500 Hz) and profound hearing loss to higher frequencies (Figure 8A, blue). However, the ECochG responses to both 500 Hz and 2 kHz were large (Figure 8B) such that the estimated threshold from the ECochG was only in the range of mild hearing loss to all frequencies (Figure 9, red). Time for data collection in the operating room is limited, so for frequencies other than 500 Hz we collected responses only to 90 dB nHL. To estimate threshold, we used a linear interpolation where a 1 dB reduction in stimulus level produced a 1 dB reduction in response, and threshold was taken as a response level of 0.02 μV (−34 dB re 1 μV), which is the threshold sensitivity for a response to achieve significance under good recording conditions (see Methods for significance criteria). When time permitted, we performed a level series to 500 Hz in 10 dB steps to better estimate actual thresholds, interpolated between the last significant response and the first non-significant response. When compared to the thresholds calculated from 90 dB nHL responses they were similar (Figure 8C) and the differences were typically in the direction where actual thresholds were better than calculated from the 90 dB nHL response (below the line of equivalence). This result was because large responses tended to be saturated, so that reductions in level did not produce corresponding drops in responses for the first 10 to 20 dB. Errors in this direction would cause the actual sensitivity of ECochG thresholds to be underestimated.

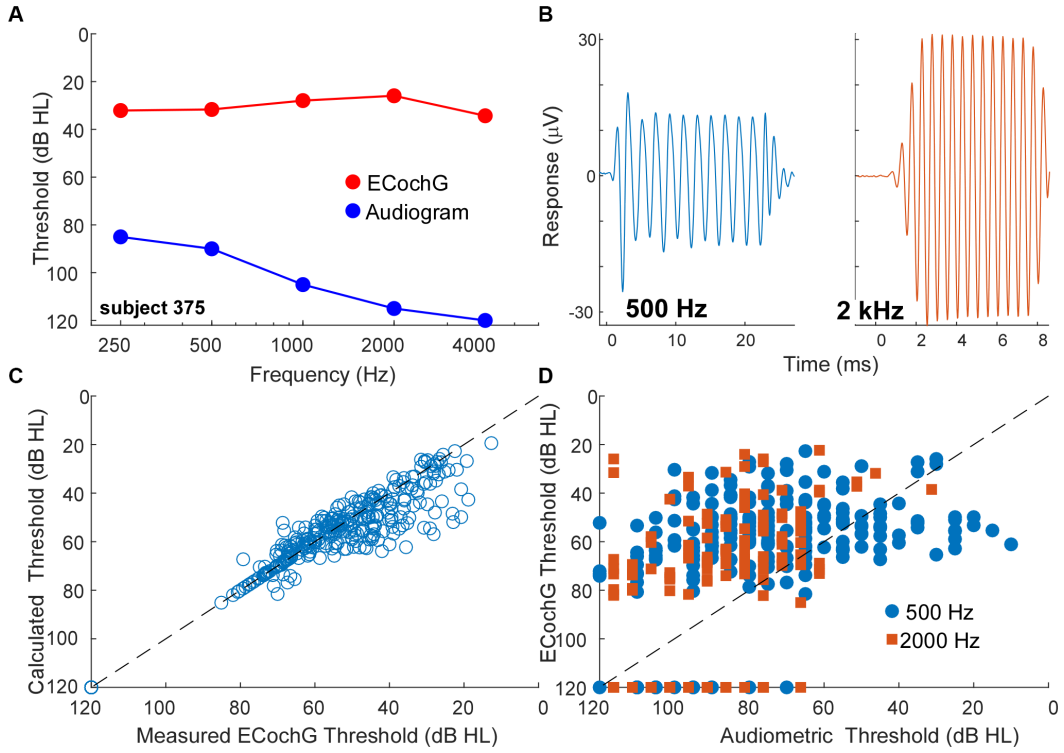

FIGURE 8
ECochG thresholds are more sensitive than behavioral thresholds. **(A)** An example of ECochG threshold vs. behavioral. Despite having severe to profound hearing loss as shown by the audiogram, the ECochG is only in the range of mild hearing loss. **(B)** ECochG responses to 500 and 2000 Hz at 90 dB nHL. **(C)** Calculated ECochG Thresholds perform better than Audiometric Thresholds for both 500 and 2000 Hz. **(D)** Calculated thresholds are mostly similar to measured thresholds. Any deviations were typically in the direction where actual thresholds were better than calculated thresholds.

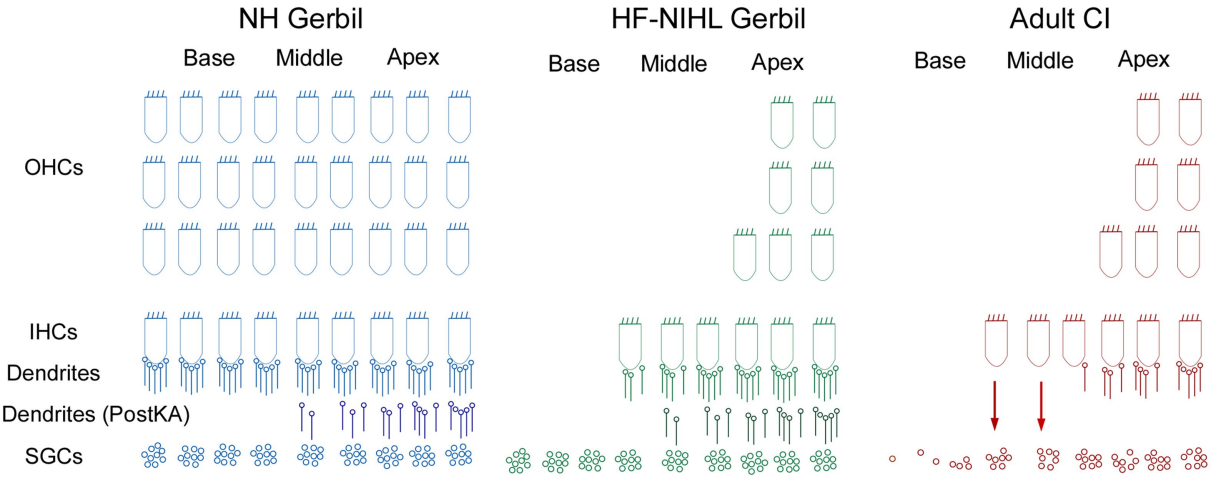

FIGURE 9
Schematic of the cochlear hearing postulated for each of the models used in this study. In NH gerbils, OHC, IHCs, and connections of ICs to spiral ganglion cells (SGCs) are present. In the Post KA condition, the dendrites between the IHCs are SGCs are severed in the basal cochlea but partially preserved in the apex. In HF-HIHL gerbils, the outer hair cells are removed to a greater extent than the inners, and in the Pre KA condition there is a normal complement of connected dendrites resulting in the increased overall proportion of ANN compared to NH animals. Post KA there is typically complete disconnection of dendrites from IHCs in the basal cochlea but only partial in the apical parts. The SGCs remain were the dendrites have been removed but are not visible in the recordings. In the adult CI subjects, the progressive hearing loss results in extensive hair cell loss in the basal cochlea, but at the transition zone to relatively preserved hearing there are groups of presumably primarily IHCs that are still present but with severed connections to the SGSs. The presence of hair cells and a functional organ of Corti may allow for continued production of trophic substances (arrows) that support SGC survival. The distribution of remaining neural connections with IHCs more closely resembled the Post KA than the Pre KA condition.

A trend for better evoked potential activity than behavioral was present overall, as shown for 500 and 2000 Hz in Figure 8D. Here, points above the line of equivalence indicate better ECochG than audiometric threshold. Considering all frequencies from 250 Hz to

4 kHz, a two-way ANOVA showed a main effect of frequency, in that higher frequencies showed less sensitivity for both behavioral and ECochG thresholds ($F = 58.5$, df = 4, $p < 0.0001$), and a main effect of measurement type, with ECochG showing significantly better sensitivity than behavior ($F = 25.8$, df = 1, $p < 0.0001$). The interaction between frequency and response type was significant ($F = 4.8$, df = 4, $p = 0.0008$), because the effect of frequency was smaller with ECochG, i.e., ECochG thresholds showed less of an increase to higher frequencies than did the audiometric thresholds.

Discussion

Using data from normal-hearing gerbils as a training set, a DLA was used to identify waveforms that contained a neural component, the ANN, in ECochG responses to low-frequency sounds. In waveforms judged to have an ANN present, an analytic model estimated its proportion in the overall response. The models developed were then applied to ECochG data from both gerbil and human subjects. The gerbil groups included NH and HF-NIHL animals, with the HF-NIHL group intended to mimic the primarily low-frequency hearing condition of many CI subjects. Both gerbil groups were also tested after a neurotoxin was placed on the RW membrane to induce cochlear synaptopathy. The human subjects were surgical cases where the RW was accessible, which included CI subjects, subjects with Meniere's disease undergoing a labyrinthectomy, and cases with a vestibular schwannoma that was being resected. The human groups had ANN proportions similar to those of gerbils after the neurotoxin, indicating the presence of cochlear synaptopathy in the human groups. In addition, thresholds to ECochG in the human subjects were generally more sensitive than those in the audiogram, a further indication that the recordings were from hair cells disconnected from auditory nerve fibers.

The deep learning algorithm to identify the presence or absence of the ANN

The average cycles are sequential data, so a logical choice of neural network architecture was a Recurrent Neural Network (RNN), which is designed to utilize sequential information. Past information is stored in state vectors, which are considered at each point, so dependencies on past information can be used. Bidirectional RNNs consider dependencies on both past and future information (66). Note that the DLA created makes no assumptions about the underlying biophysics and, because of the choice of training set, did not require any expert curation of features. The training set was from NH gerbils where all responses to low frequency sounds contain an ANN, but none of the responses to high frequency sounds do, since they are above the phase-locking range detectable with ECochG (47, 55, 67). The input was average cycles, normalized in amplitude and starting phase, so that the algorithm operates only on variations in shape. By using responses across multiple frequencies and intensities within each range, the samples included a wide spectrum of waveform shapes that exemplify ANN-present or ANN-absent responses. The shapers were different enough that the DLA had both a high sensitivity and specificity (>95% for both).

The analytic model to estimate the proportion of the ANN and CM

The analytic model provides a quantitative estimate of the sizes of the CM and ANN in a given response. Other methods, whether spectral, masking, or our correlation-fitting analysis (Figure 4D), are proportional to the size of the ANN but are not similarly quantitative. The good fit between the ANN proportion and the correlation-fitting analysis of ANN strength (Figure 4D) indicates that the parameters used are sufficiently constrained to a reasonable range to account for CM and ANN magnitudes. However, the model is over-determined, so that the solutions are not unique. We therefore consider the quantitative values to be reasonably accurate in the aggregate but with a range of uncertainty in particular cases.

The theoretical basis of the model (Figure 1) does not include all the relevant parameters that can lead to complex shapes of the average cycle. In particular, additional modeling (not shown here) indicates that complex shapes for the CM can be created if responses from different parts of the cochlea with different phases both have some amount of saturation. However, the experiments with neurotoxins suggest that the main source of complex average cycles is neural in the form of the ANN, because most complex average cycles resolve to those described in Figure 1A as typical for a predominance of CM over ANN. Furthermore, complex shapes with responses to high frequencies are rare. However, the current model includes only a subset of the biophysics underlying the shapes of average cycles and that future versions could include more parameters.

The model showed an *increase* in the proportion of ANN compared to CM in the HF-NIHL versus NH animals' response to low frequencies. The intense noise used (122 dB for 4 h) produced an almost complete loss of OHCs and IHCs to frequencies above the cut-off of 4 kHz (58, 59). An explanation for the increase in proportional ANN may relate to the loss of spread of excitation to the basal cochlea, which in the normal hearing case will dominate the responses. That is, as the intensity increases the responses recruited from the basal cochlea occur in-phase due to the speed of the traveling wave through the basal cochlea (68, 69). In contrast, when the responses are coming from the apical cochlea some have different phases due to the slowing of the traveling wave near the characteristic frequency region. Thus, the CM response will grow more slowly with intensity due to interference. In contrast, the neural response will spread but the action potentials will not cancel as sine waves do. In addition to phase issues, the neural potential that produces the ANN is also likely to reach saturation prior to the CM. Above threshold, the rate at which low spontaneous rate fiber comes out of the relatively refractory period, which governs the overall rate of skipped cycles, is not dependent on intensity, so the rate saturates at a moderate intensity (70). Viewed another way, because of phase-locking the maximum rate that a fiber can contribute is dependent as much on the frequency as the intensity, because the maximum rate is less than one spike per cycle (except in the case of peak-splitting to the lowest frequencies).

Cochlear synaptopathy in animal studies

Cochlear synaptopathy, using noise exposure and anatomical verification, has been identified in several species including mice,

guinea pigs, and macaques (1, 4, 71). Its hallmark is loss of synapses and neural activity in the face of preserved hair cells and auditory thresholds. The ability to preserve auditory thresholds is due to selective preservation of low-threshold, high-spontaneous rate fibers (5, 6). In studies using CBA/CaJ mice, the loss of synapses was found to be irreversible (1), and the possibility of permanent loss of synapses combined with preserved audiometric thresholds led to concerns of significant "hidden hearing loss" in humans (72). Recently, it has been shown that in other strains of mice and in guinea pigs the loss of synapses is not permanent (23–25). However, these studies also show that in animals with some degree of permanent hearing loss, there is a continued synaptopathy, suggesting cochlear self-repair mechanisms may not be stable through a lifetime.

Cochlear synaptopathy in human subjects

Human temporal bone studies show a greater preservation of hair cells than neural structures in aging subjects and those with greater hearing loss (8–10). To test for a physiological correlate, we compared gerbil and human subject groups based on RW recordings, where cochlear physiology can be explored with a high signal-to-noise ratio. The shapes of the average cycles were similar between gerbil and human subjects and reflect the same biophysical principles that underly each (e.g., Figures 1, 3). This similarity allows for comparisons between humans and experimentally manipulated gerbils. There are, of course, major differences between the species. One is the size of the response at the RW, with human responses about an order of magnitude smaller than gerbils (maximums of tens rather than hundreds of microvolts). Smaller responses in humans are likely to be due to the increased size of the cochlea, where responses at the RW must travel through larger spaces than in small animals. Response magnitudes with intracochlear recordings during CI insertion in humans, where the electrode can be close to the source generators, can reach hundreds of microvolts [e.g., (73–75)].

Interestingly, the largest responses were the same between the CI and non-CI subjects, despite the greater degree of hearing loss expected in CI subjects. The largest responses of both CI and non-CI subjects were similar to the single human case with normal hearing. Many of the CI cases with the largest responses were children with ANSD (Figure 6A), a condition related to cochlear synaptopathy where neural or inner hair cell dysfunction is present, but cochlear responses can be relatively normal (76, 77). In a previous study in children receiving CIs, ANSD cases could have a substantial ANN, similar to a control group of non-ANSD children receiving CIs (78). What was different was a very large CM and negative-polarity SP to high frequencies in ANSD compared to non-ANSD children, which was typically not accompanied by a CAP. The explanation for the large negative SP is the loss of neural and/or inner hair contributions to the SP which have a positive polarity (56, 79).

In addition to a distribution of ANN proportion comparable to animals treated with neurotoxins, another indication of cochlear synaptopathy is the overlapping thresholds between ECochG and behavior in CI subjects. In many cases the threshold for ECochG responses were lower (better) than the audiometric thresholds, which is not the expected direction for an evoked potential compared to behavior. Previous studies have also shown thresholds for ECochG to be better than for audiometry in some cases (80–82). An important issue is calibration, since in our study and most others the ECochG and audiometric thresholds are measured at different times and with different equipment. However, one study (82) measured ECochG through the implant in the clinic and audiometric thresholds at the same session with the same equipment, and this study also reported many ECochG thresholds to be better than behavioral. A better threshold for an evoked potential is not expected because a behavioral threshold can be obtained from very few active fibers (64, 65), while an evoked potential is determined by the summed, synchronous activity of many responding elements. Thus, hair cell function that is better than behavioral sensitivity is an indication of cochlear synaptopathy in CI subjects.

Finally, it has been shown in adult subjects and children implanted at greater than 6 years of age that larger ECochG magnitudes are associated with better speech perception outcomes with electrical hearing (29). These results contrast with preoperative tone audiometric thresholds, which are not predictive of speech perception outcomes with the implants (32, 34, 83). The explanation proposed is that some of the ECochG responses are from hair cells disconnected from auditory nerve fibers, i.e., cochlear synaptopathy, and that the presence or absence of functional hair cells indicates overall 'cochlear health.' This cochlear health is then indirectly related to the functional status of the auditory nerve available for electrical stimulation. Illustrations of the expected hearing conditions studied here are shown in Figure 9. In NH animals, all of the elements of OHC, IHCs, and connections of ICs to spiral ganglion cells (SGCs) are present. In the Post KA condition, the connections between the IHCs are SGCs are severed in the basal cochlea but partially preserved in the apex due to diffusion characteristics. In the HF-NIHL animals, the OHCs are removed to a greater extent than the inner (58), and in the Pre KA condition a nearly normal complement of dendrites exist to the remaining hair cells, resulting in the increased overall proportion of ANN compared to NH animals. As with NH animals, the KA then causes a similar variable but typically partial removal of the neural input. The SGCs remain viable for the 1-month interval between exposure and ECochG but are not visible to the ECochG. In the adult CI subjects, the progressive hearing loss results in extensive hair cell loss in the basal cochlea, but at the transition to relatively preserved hearing there are groups of primarily IHCs that are still present but with severed connections to the SGCs. These hair cells are visible to ECochG but not the audiogram. In addition to the hair cells themselves, the organ of Corti, endolymphatic potential, tectorial membrane and other features that support hair cell transduction must also be functional and can provide trophic substances (arrows) such as growth factors and neurotrophins that support SGC survival (84, 85). In the absence of this support, a greater proportion of SGCs are removed and the information provided by electrical stimulation is reduced. Although the hair cell distribution in the CI subjects and HF-NIHL animals are similar, the remaining connected neural portion more closely resembles the Post KA than the Pre KA condition.

There is currently a major effort underway to investigate the use of ECochG as a real-time monitor of cochlear health during CI surgery to detect and possibly lessen cochlear trauma during implantation and thereby improve hearing preservation and speech perception outcomes [reviewed by (86)]. The presence of cochlear synaptopathy in these subject effects the interpretation of the ECochG

recordings. Current methods focus primarily on the responses to a single frequency, typically 500 Hz, delivered at high intensity (>100 dB SPL), to monitor changes from the apical electrode as the insertion progresses (75, 86–88). To a 500 Hz stimulus at high intensity, the recordings are primarily, although not exclusively, the CM, which because of cochlear synaptopathy will not be directly reflective of acoustic hearing. While changes in these responses can be a useful indicator of trauma that is worthwhile to avoid because it can lead to worsening of subsequent effects, such as foreign body response and fibrosis, such changes are unlikely to directly reflect the degree of hearing preservation to be expected. Thus, an additional fruitful focus as a monitor for trauma in hearing preservation cases could be the ANN, which is more directly related to neural preservation.

In cases where the RW recording was available during labyrinthectomy or during an acoustic tumor removal, the distribution of TR in these subjects was on average higher than for CI subjects, but the maxima were similar. These subjects often have a hearing loss due to endolymphatic hydrops, compression of the auditory nerve, or effects on blood supply to the cochlea (89–91). Still, the hearing loss is generally less than in CI subjects. However, like the CI subjects, the distribution of ANN-present and ANN-absent subjects was similar to gerbils with partial loss of synapses from neurotoxin applied to the RW, indicating a degree of cochlear synaptopathy in these subjects as well.

Limitations and future directions

The human data revealed many cases where an ANN was not detected by the DLA, yet in some of these cases hearing, especially in non-CI subjects, was present. Consequently, it appears that an ANN can exist without detection by current ECochG. In these cases, basal hair cells may be present and dominate the responses, while surviving neural responses from the apex, or from within the core of the auditory nerve, are too small to be detected. This pattern would also be an indication of cochlear synaptopathy in the more basally located hair cells.

The potential benefit of a condition with functional, surviving hair cells is in the realm of neural regeneration. If regeneration is required to reintroduce hair cells and a functional organ of Corti, the prospect is daunting. However, if only a reconnection between nerves and still-existing hair cells is needed, the problem is more straightforward, and promising trends in this direction are being seen. Along with the anatomical studies that reached a similar conclusion (10), our physiological study indicates cochlear synaptopathy is likely to be relatively common, including those with substantial hearing loss, so that regenerative therapies targeting neural regrowth have a strong prospect of finding a ready substrate for reinnervation.

Conclusion

Cochlear synaptopathy is loss of synapses while hair cells are intact. Though largely accepted to happen in animals, evidence in humans is still limited. We used a combination of deep learning and mathematical modeling to analyze the contributions of the ANN and CM in ECochG. We showed that human subjects-both with and without cochlear implants-are not significantly different from gerbils who have been treated with neurotoxin, indicating some degree of cochlear synaptopathy in these subjects.

Data availability statement

The raw data supporting the conclusions of this article will be made available by the authors, without undue reservation.

Ethics statement

The studies involving human participants were reviewed and approved by Institutional Review Boards at the University of North Carolina at Chapel Hill and the Ohio State University. Written informed consent to participate in this study was provided by the participants or legal guardian if less than 18 years old and child's assent if > 7 years old. The animal study was reviewed and approved by Institutional Animal Care and Use Committee (IACUC) at the University of North Carolina at Chapel Hill.

Author contributions

RH and DF: conceptualization, software, formal analysis, data curation, writing – original draft, and visualization. RH, KH, WR, KB, HP, OA, and CB: methodology. KH, DF, WR, KB, HP, OA, and CB: investigation. WR, KH, KB, HP, OA, and CB: writing – review and editing. DF: supervision, project administration, and funding acquisition. All authors contributed to the article and approved the submitted version.

Funding

This work was supported by the Office of the Assistant Secretary of Defense for Health Affairs through the Hearing Restoration Research Program under Award No. W81XWH-19-1-0609. The opinions, interpretations, conclusions, and recommendations are those of the authors and are not necessarily endorsed by the Department of Defense.

Acknowledgments

We thank Stephen Pulver for expert technical assistance and John Grose for helpful comments on an earlier draft of the manuscript.

Conflict of interest

DF, OA, CB, HP, and KB have consulting arrangements and research projects with MED-EL, Cochlear Corp, and/or Advanced Bionics. CB also consults for Envoy Medical and IotaMotion. OA and CB have an equity interest in Advanced Cochlear Diagnostics.

The remaining authors declare that the research was conducted in the absence of any commercial or financial relationships that could be construed as a potential conflict of interest.

Publisher's note

References

1. Kujawa SG, Liberman MC. Adding insult to injury: cochlear nerve degeneration after "temporary" noise-induced hearing loss. *J Neurosci*. (2009) 29:14077–85. doi: 10.1523/JNEUROSCI.2845-09.2009

2. Kujawa SG, Liberman MC. Synaptopathy in the noise-exposed and aging cochlea: primary neural degeneration in acquired sensorineural hearing loss. *Hear Res*. (2015) 330:191–9. doi: 10.1016/j.heares.2015.02.009

3. Liberman MC, Kujawa SG. Cochlear synaptopathy in acquired sensorineural hearing loss: manifestations and mechanisms. *Hear Res*. (2017) 349:138–47. doi: 10.1016/j.heares.2017.01.003

4. Lin HW, Furman AC, Kujawa SG, Liberman MC. Primary neural degeneration in the Guinea pig cochlea after reversible noise-induced threshold shift. *J Assoc Res Otolaryngol*. (2011) 12:605–16. doi: 10.1007/s10162-011-0277-0

5. Bourien J, Tang Y, Batrel C, Huet A, Lenoir M, Ladrech S, et al. Contribution of auditory nerve fibers to compound action potential of the auditory nerve. *J Neurophysiol*. (2014) 112:1025–39. doi: 10.1152/jn.00738.2013

6. Furman AC, Kujawa SG, Liberman MC. Noise-induced cochlear neuropathy is selective for fibers with low spontaneous rates. *J Neurophysiol*. (2013) 110:577–86. doi: 10.1152/jn.00164.2013

7. Hickman TT, Hashimoto K, Liberman LD, Liberman MC. Cochlear synaptic degeneration and regeneration after noise: effects of age and neuronal subgroup. *Front Cell Neurosci*. (2021) 15:684706. doi: 10.3389/fncel.2021.684706

8. Makary CA, Shin J, Kujawa SG, Liberman MC, Merchant SN. Age-related primary Cochlear neuronal degeneration in human temporal bones. *J Assoc Res Otolaryngol*. (2011) 12:711–7. doi: 10.1007/s10162-011-0283-2

9. Viana LM, O'Malley JT, Burgess BJ, Jones DD, Oliveira CA, Santos F, et al. Cochlear neuropathy in human presbycusis: confocal analysis of hidden hearing loss in post-mortem tissue. *Hear Res*. (2015) 327:78–88. doi: 10.1016/j.heares.2015.04.014

10. Wu PZ, Liberman LD, Bennett K, de Gruttola V, O'Malley JT, Liberman MC. Primary neural degeneration in the human cochlea: evidence for hidden hearing loss in the aging ear. *Neuroscience*. (2019) 407:8–20. doi: 10.1016/j.neuroscience.2018.07.053

11. Bramhall N, Beach EF, Epp B, Le Prell CG, Lopez-Poveda EA, Plack CJ, et al. The search for noise-induced cochlear synaptopathy in humans: Mission impossible? *Hear Res*. (2019) 377:88–103. doi: 10.1016/j.heares.2019.02.016

12. Fulbright ANC, Le Prell CG, Griffiths SK, Lobarinas E. Effects of recreational noise on threshold and Suprathreshold measures of auditory function. *Semin Hear*. (2017) 38:298–318. doi: 10.1055/s-0037-1606325

13. Grose JH, Buss E, Hall JW 3rd. Loud music exposure and Cochlear Synaptopathy in young adults: isolated auditory brainstem response effects but no perceptual consequences. *Trends Hear*. (2017) 21:233121651773741. doi: 10.1177/2331216517737417

14. Guest H, Munro KJ, Prendergast G, Millman RE, Plack CJ. Impaired speech perception in noise with a normal audiogram: no evidence for cochlear synaptopathy and no relation to lifetime noise exposure. *Hear Res*. (2018) 364:142–51. doi: 10.1016/j.heares.2018.03.008

15. Prendergast G, Millman RE, Guest H, Munro KJ, Kluk K, Dewey RS, et al. Effects of noise exposure on young adults with normal audiograms II: behavioral measures. *Hear Res*. (2017) 356:74–86. doi: 10.1016/j.heares.2017.10.007

16. Yeend I, Beach EF, Sharma M, Dillon H. The effects of noise exposure and musical training on suprathreshold auditory processing and speech perception in noise. *Hear Res*. (2017) 353:224–36. doi: 10.1016/j.heares.2017.07.006

17. Bramhall NF, Konrad-Martin D, McMillan GP, Griest SE. Auditory brainstem response altered in humans with noise exposure despite normal outer hair cell function. *Ear Hear*. (2017) 38:e1–e12. doi: 10.1097/AUD.0000000000000370

18. Mehraei G, Hickox AE, Bharadwaj HM, Goldberg H, Verhulst S, Liberman MC, et al. Auditory brainstem response latency in noise as a marker of cochlear synaptopathy. *J Neurosci*. (2016) 36:3755–64. doi: 10.1523/JNEUROSCI.4460-15.2016

19. Grant KJ, Mepani AM, Wu P, Hancock KE, de Gruttola V, Liberman MC, et al. Electrophysiological markers of cochlear function correlate with hearing-in-noise performance among audiometrically normal subjects. *J Neurophysiol*. (2020) 124:418–31. doi: 10.1152/jn.00016.2020

20. Mepani AM, Kirk SA, Hancock KE, Bennett K, de Gruttola V, Liberman MC, et al. Middle ear muscle reflex and word recognition in "Normal-hearing" adults: evidence for cochlear synaptopathy? *Ear Hear*. (2020) 41:25–38. doi: 10.1097/AUD.0000000000000804

21. Liberman MC, Epstein MJ, Cleveland SS, Wang H, Maison SF. Toward a differential diagnosis of hidden hearing loss in humans. *PLoS One*. (2016) 11:e0162726. doi: 10.1371/journal.pone.0162726

22. Bharadwaj HM, Masud S, Mehraei G, Verhulst S, Shinn-Cunningham BG. Individual differences reveal correlates of hidden hearing deficits. *J Neurosci*. (2015) 35:2161–72. doi: 10.1523/JNEUROSCI.3915-14.2015

23. Hickman TT, Hashimoto K, Liberman LD, Liberman MC. Synaptic migration and reorganization after noise exposure suggests regeneration in a mature mammalian cochlea. *Sci Rep*. (2020) 10:19945. doi: 10.1038/s41598-020-76553-w

24. Shi L, Liu L, He T, Guo X, Yu Z, Yin S, et al. Ribbon synapse plasticity in the cochleae of Guinea pigs after noise-induced silent damage. *PLoS One*. (2013) 8:e81566. doi: 10.1371/journal.pone.0081566

25. Wang J, Yin S, Chen H, Shi L. Noise-induced Cochlear Synaptopathy and ribbon synapse regeneration: repair process and therapeutic target. *Adv Exp Med Biol*. (2019) 1130:37–57. doi: 10.1007/978-981-13-6123-4_3

26. Puel JL, Ruel J, Gervais d'Aldin C, Pujol R. Excitotoxicity and repair of cochlear synapses after noise-trauma induced hearing loss. *Neuroreport*. (1998) 9:2109–14. doi: 10.1097/00001756-199806220-00037

27. Pujol R, Puel JL. Excitotoxicity, synaptic repair, and functional recovery in the mammalian cochlea: a review of recent findings. *Ann N Y Acad Sci*. (1999) 884:249–54. doi: 10.1111/j.1749-6632.1999.tb08646.x

28. Suthakar K, Liberman MC. Auditory-nerve responses in mice with noise-induced cochlear synaptopathy. *J Neurophysiol*. (2021) 126:2027–38. doi: 10.1152/jn.00342.2021

29. Fontenot TE, Giardina CK, Dillon MT, Rooth MA, Teagle HF, Park LR, et al. Residual cochlear function in adults and children receiving cochlear implants: correlations with speech perception outcomes. *Ear Hear*. (2019) 40:577–91. doi: 10.1097/AUD.0000000000000630

30. McClellan JH, Formeister EJ, Merwin WH 3rd, Dillon MT, Calloway N, Iseli C, et al. Round window electrocochleography and speech perception outcomes in adult cochlear implant subjects: comparison with audiometric and biographical information. *Otol Neurotol*. (2014) 35:e245–52. doi: 10.1097/MAO.0000000000000557

31. Walia A, Shew MA, Kallogjeri D, Wick CC, Durakovic N, Lefler SM, et al. Electrocochleography and cognition are important predictors of speech perception outcomes in noise for cochlear implant recipients. *Sci Rep*. (2022) 12:3083. doi: 10.1038/s41598-022-07175-7

32. Gifford RH, Dorman MF, Shallop JK, Sydlowski SA. Evidence for the expansion of adult cochlear implant candidacy. *Ear Hear*. (2010) 31:186–94. doi: 10.1097/AUD.0b013e3181c6b831

33. Holden LK, Firszt JB, Reeder RM, Uchanski RM, Dwyer NY, Holden TA. Factors affecting outcomes in cochlear implant recipients implanted with a perimodiolar electrode array located in Scala tympani. *Otol Neurotol*. (2016) 37:1662–8. doi: 10.1097/MAO.0000000000001241

34. Lazard DS, Vincent C, Venail F, van de Heyning P, Truy E, Sterkers O, et al. Pre-, per-and postoperative factors affecting performance of postlinguistically deaf adults using cochlear implants: a new conceptual model over time. *PLoS One*. (2012) 7:e48739. doi: 10.1371/journal.pone.0048739

35. Carlson ML. Cochlear implantation in adults. *N Engl J Med*. (2020) 382:1531–42. doi: 10.1056/NEJMra1904407

36. Riggs WJ, Hiss MM, Skidmore J, Varadarajan VV, Mattingly JK, Moberly AC, et al. Utilizing Electrocochleography as a microphone for fully implantable Cochlear implants. *Sci Rep*. (2020) 10:3714. doi: 10.1038/s41598-020-60694-z

37. Wever EG, Bray C. Action currents in the auditory nerve in response to acoustic stimulation. *Proc Nat Acad Sci U S A*. (1930) 16:344–50. doi: 10.1073/pnas.16.5.344

38. Henry KR. Auditory nerve neurophonic recorded from the round window of the Mongolian gerbil. *Hear Res*. (1995) 90:176–84. doi: 10.1016/0378-5955(95)00162-6

39. Snyder RL, Schreiner CE. The auditory neurophonic: basic properties. *Hear Res*. (1984) 15:261–80. doi: 10.1016/0378-5955(84)90033-9

40. Russell IJ. Cochlear receptor potentials In: AI Basbaum, A Kaneko, GM Shepherd and G Westheimer, editors. *The senses, a comprehensive reference*. San Diego: Elsevier (2008). 319–58.

41. Chertoff ME. Analytic treatment of the compound action potential: estimating the summed post-stimulus time histogram and unit response. *J Acoust Soc Am*. (2004) 116:3022–30. doi: 10.1121/1.1791911

42. Goldstein MH, Kiang NYS. Synchrony of neural activity in electric responses evoked by transient acoustic stimuli. *J Acoust Soc Am*. (1958) 30:107–14. doi: 10.1121/1.1909497

43. Kiang NYS, Moxon EC, Kahn AR. The relationship of gross potentials recorded from cochlea to single unit activity in the auditory nerve In: RJ Ruben, C Elberling and

G Salomon, editors. *Electrocochleography*. Baltimore: University Park Press (1976). 95–115.

44. Versnel H, Prijs VF, Schoonhoven R. Round-window recorded potential of single-fibre discharge (unit response) in normal and noise-damaged cochleas. *Hear Res*. (1992) 59:157–70. doi: 10.1016/0378-5955(92)90112-Z

45. Fontenot TE, Giardina CK, Fitzpatrick DC. A model-based approach for separating the cochlear microphonic from the auditory nerve neurophonic in the ongoing response using Electrocochleography. *Front Neurosci*. (2017) 11:592. doi: 10.3389/fnins.2017.00592

46. Kim JR, Tejani VD, Abbas PJ, Brown CJ. Intracochlear recordings of acoustically and electrically evoked potentials in nucleus hybrid L24 Cochlear implant users and their relationship to speech perception. *Front Neurosci*. (2017) 11:216. doi: 10.3389/fnins.2017.00216

47. Lichtenhan JT, Cooper NP, Guinan JJ Jr. A new auditory threshold estimation technique for low frequencies: proof of concept. *Ear Hear*. (2013) 34:42–51. doi: 10.1097/AUD.0b013e31825f9bd3

48. Lichtenhan JT, Hartsock JJ, Gill RM, Guinan JJ Jr, Salt AN. The auditory nerve overlapped waveform (ANOW) originates in the Cochlear apex. *J Assoc Res Otolaryngol*. (2014) 15:395–411. doi: 10.1007/s10162-014-0447-y

49. Snyder RL, Schreiner CE. Forward masking of the auditory nerve neurophonic (ANN) and the frequency following response (FFR). *Hear Res*. (1985) 20:45–62. doi: 10.1016/0378-5955(85)90058-9

50. Snyder RL, Schreiner CE. Auditory neurophonic responses to amplitude-modulated tones: transfer functions and forward masking. *Hear Res*. (1987) 31:79–91. doi: 10.1016/0378-5955(87)90215-2

51. Verschooten E, Robles L, Joris PX. Assessment of the limits of neural phase-locking using mass potentials. *J Neurosci*. (2015) 35:2255–68. doi: 10.1523/JNEUROSCI.2979-14.2015

52. Verschooten E, Shamma S, Oxenham AJ, Moore BCJ, Joris PX, Heinz MG, et al. The upper frequency limit for the use of phase locking to code temporal fine structure in humans: a compilation of viewpoints. *Hear Res*. (2019) 377:109–21. doi: 10.1016/j.heares.2019.03.011

53. Lee C, Valenzuela CV, Goodman SS, Kallogjeri D, Buchman CA, Lichtenhan JT. Early detection of Endolymphatic Hydrops using the auditory nerve overlapped waveform (ANOW). *Neuroscience*. (2020) 425:251–66. doi: 10.1016/j.neuroscience.2019.11.004

54. Choudhury B, Fitzpatrick DC, Buchman CA, Wei BP, Dillon MT, He S, et al. Intraoperative round window recordings to acoustic stimuli from cochlear implant patients. *Otol Neurotol*. (2012) 33:1507–15. doi: 10.1097/MAO.0b013e31826dbc80

55. Forgues M, Koehn HA, Dunnon AK, Pulver SH, Buchman CA, Adunka OFet al. Distinguishing hair cell from neural potentials recorded at the round window. *J Neurophysiol*. (2014) 111:580–93. doi: 10.1152/jn.00446.2013

56. Pappa AK, Hutson KA, Scott WC, Wilson JD, Fox KE, Masood MM, et al. Hair cell and neural contributions to the cochlear summating potential. *J Neurophysiol*. (2019) 121:2163–80. doi: 10.1152/jn.00006.2019

57. Muller M. The cochlear place-frequency map of the adult and developing Mongolian gerbil. *Hear Res*. (1996) 94:148–56. doi: 10.1016/0378-5955(95)00230-8

58. Choudhury B, Adunka OFDemason CE, Ahmad FI, Buchman CA, Fitzpatrick DC. Detection of intracochlear damage with cochlear implantation in a gerbil model of hearing loss. *Otol Neurotol*. (2011) 32:1370–8. doi: 10.1097/MAO.0b013e31822f09f2

59. Suberman TA, Campbell AP, Adunka OFBuchman CA, Roche JP, Fitzpatrick DC. A gerbil model of sloping sensorineural hearing loss. *Otol Neurotol*. (2011) 32:544–52. doi: 10.1097/MAO.0b013e31821343f5

60. Mikulec AA, Plontke SK, Hartsock JJ, Salt AN. Entry of substances into perilymph through the bone of the otic capsule after intratympanic applications in guinea pigs: implications for local drug delivery in humans. *Otol Neurotol*. (2009) 30:131–8. doi: 10.1097/MAO.0b013e318191bff8

61. Reimers N, Gurevych I (2017) *Optimal hyperparameters for deep LSTM-networks for sequence labeling tasks*. arXiv preprint arXiv:1707.06799.

62. Canfarotta MW, O'Connell BP, Giardina CK, Buss E, Brown KD, Dillon MT, et al. Relationship between electrocochleography, angular insertion depth, and Cochlear implant speech perception outcomes. *Ear Hear*. (2020) 42:941–8. doi: 10.1097/AUD.0000000000000985

63. Walia A, Shew MA, Lee DS, Lefler SM, Kallogjeri D, Wick CC, et al. Promontory Electrocochleography recordings to predict speech-perception performance in Cochlear implant recipients. *Otol Neurotol*. (2022) 43:915–23. doi: 10.1097/MAO.0000000000003628

64. Barlow HB, Levick WR, Yoon M. Responses to single quanta of light in retinal ganglion cells of the cat. *Vision Res Suppl*. (1971) 11:87–101. doi: 10.1016/0042-6989(71)90033-2

65. Bialek W. Physical limits to sensation and perception. *Annu Rev Biophys Biophys Chem*. (1987) 16:455–78. doi: 10.1146/annurev.bb.16.060187.002323

66. Schuster M, Paliwal KK. Bidirectional recurrent neural networks. *Ieee T Signal Proces*. (1997) 45:2673–81. doi: 10.1109/78.650093

67. He W, Porsov E, Kemp D, Nuttall AL, Ren T. The group delay and suppression pattern of the cochlear microphonic potential recorded at the round window. *PLoS One*. (2012) 7:e34356. doi: 10.1371/journal.pone.0034356

68. Robles L, Ruggero MA. Mechanics of the mammalian cochlea. *Physiol Rev*. (2001) 81:1305–52. doi: 10.1152/physrev.2001.81.3.1305

69. van der Heijden M, Versteegh CP. Energy flux in the cochlea: evidence against power amplification of the traveling wave. *J Assoc Res Otolaryngol*. (2015) 16:581–97. doi: 10.1007/s10162-015-0529-5

70. Parham K, Zhao H-B, Kim DO. Responses of auditory nerve fibers of the unanesthetized decerebrate cat to click pairs as simulated echoes. *J Neurophysiol*. (1996) 76:17–29. doi: 10.1152/jn.1996.76.1.17

71. Valero MD, Burton JA, Hauser SN, Hackett TA, Ramachandran R, Liberman MC. Noise-induced cochlear synaptopathy in rhesus monkeys (*Macaca mulatta*). *Hear Res*. (2017) 353:213–23. doi: 10.1016/j.heares.2017.07.003

72. Schaette R, McAlpine D. Tinnitus with a normal audiogram: physiological evidence for hidden hearing loss and computational model. *J Neurosci*. (2011) 31:13452–7. doi: 10.1523/JNEUROSCI.2156-11.2011

73. Bester CW, Campbell L, Dragovic A, Collins A, O'Leary SJ. Characterizing Electrocochleography in Cochlear implant recipients with residual low-frequency hearing. *Front Neurosci*. (2017) 11:141. doi: 10.3389/fnins.2017.00141

74. Calloway NH, Fitzpatrick DC, Campbell AP, Iseli C, Pulver S, Buchman CA, et al. Intracochlear electrocochleography during cochlear implantation. *Otol Neurotol*. (2014) 35:1451–7. doi: 10.1097/MAO.0000000000000451

75. Harris MS, Riggs WJ, Giardina CK, O'Connell BP, Holder JT, Dwyer RT, et al. Patterns seen during electrode insertion using Intracochlear Electrocochleography obtained directly through a Cochlear implant. *Otol Neurotol*. (2017) 38:1415–20. doi: 10.1097/MAO.0000000000001559

76. Gibson WP, Sanli H. Auditory neuropathy: an update. *Ear Hear*. (2007) 28:102S–6S. doi: 10.1097/AUD.0b013e3180315392

77. Starr A, Picton TW, Sininger Y, Hood LJ, Berlin CI. Auditory neuropathy. *Brain*. (1996) 119:741–53. doi: 10.1093/brain/119.3.741

78. Riggs WJ, Roche JP, Giardina CK, Harris MS, Bastian ZJ, Fontenot TE, et al. Intraoperative electrocochleographic characteristics of auditory neuropathy spectrum disorder in cochlear implant subjects. *Front Neurosci*. (2017) 11:416. doi: 10.3389/fnins.2017.00416

79. Lutz BT, Hutson KA, Trecca EMC, Hamby M, Fitzpatrick DC. Neural contributions to the cochlear summating potential: spiking and dendritic components. *J Assoc Res Otolaryngol*. (2022) 23:351–63. doi: 10.1007/s10162-022-00842-6

80. Abbas PJ, Tejani VD, Scheperle RA, Brown CJ. Using neural response telemetry to monitor physiological responses to acoustic stimulation in hybrid cochlear implant users. *Ear Hear*. (2017) 38:409–25. doi: 10.1097/AUD.0000000000000400

81. Coulthurst S, Nachman AJ, Murray MT, Koka K, Saoji AA. Comparison of pure-tone thresholds and Cochlear microphonics thresholds in pediatric Cochlear implant patients. *Ear Hear*. (2020) 41:1320–6. doi: 10.1097/AUD.0000000000000870

82. Koka K, Saoji AA, Litvak LM. Electrocochleography in Cochlear implant recipients with residual hearing: comparison with audiometric thresholds. *Ear Hear*. (2016) 38:e161–7.

83. Holden LK, Finley CC, Firszt JB, Holden TA, Brenner C, Potts LG, et al. Factors affecting open-set word recognition in adults with cochlear implants. *Ear Hear*. (2013) 34:342–60. doi: 10.1097/AUD.0b013e3182741aa7

84. Green SH, Bailey E, Wang Q, Davis RL. The Trk A, B, C's of neurotrophins in the cochlea. *Anat Rec (Hoboken)*. (2012) 295:1877–95. doi: 10.1002/ar.22587

85. Suzuki J, Corfas G, Liberman MC. Round-window delivery of neurotrophin 3 regenerates cochlear synapses after acoustic overexposure. *Sci Rep*. (2016) 6:24907. doi: 10.1038/srep24907

86. Trecca EMC, Riggs WJ, Mattingly JK, Hiss MM, Cassano MAdunka OF. Electrocochleography and Cochlear implantation: a systematic review. *Otol Neurotol*. (2020) 41:864–78. doi: 10.1097/MAO.0000000000002694

87. Dalbert A, Rohner P, Roosli C, Veraguth D, Huber A, Pfiffner F. Correlation between electrocochleographic changes during surgery and hearing outcome in cochlear implant recipients: a case report and systematic review of the literature. *Otol Neurotol*. (2020) 41:318–26. doi: 10.1097/MAO.0000000000002506

88. O'Leary S, Briggs R, Gerard JM, Iseli C, Wei BPC, Tari S, et al. Intraoperative observational real-time Electrocochleography as a predictor of hearing loss after Cochlear implantation: 3 and 12 month outcomes. *Otol Neurotol*. (2020) 41:1222–9. doi: 10.1097/MAO.0000000000002773

89. Knox GW, McPherson A. Meniere's disease: differential diagnosis and treatment. *Am Fam Physician*. (1997) 55:1193–84.

90. Roosli C, Linthicum FH Jr, Cureoglu S, Merchant SN. Dysfunction of the cochlea contributing to hearing loss in acoustic neuromas: an underappreciated entity. *Otol Neurotol*. (2012) 33:473–80. doi: 10.1097/MAO.0b013e318248ee02

91. Samii M, Matthies C. Management of 1000 vestibular schwannomas (acoustic neuromas): hearing function in 1000 tumor resections. *Neurosurgery*. (1997) 40:248–62. doi: 10.1097/00006123-199702000-00005

frontiers | Frontiers in Neurology

TYPE Original Research
PUBLISHED 13 July 2023
DOI 10.3389/fneur.2023.1221443

OPEN ACCESS

EDITED BY
Stefan Weder,
University Hospital of Bern, Switzerland

REVIEWED BY
Christo William Bester,
The University of Melbourne, Australia
Christoph Dinh,
Massachusetts General Hospital and Harvard Medical School, United States

*CORRESPONDENCE
Hidehiko Okamoto
✉ okamoto@iuhw.ac.jp

RECEIVED 12 May 2023
ACCEPTED 27 June 2023
PUBLISHED 13 July 2023

CITATION
Kadowaki S, Morimoto T, Pijanowska M, Mori S and Okamoto H (2023) 80 Hz auditory steady state responses (ASSR) elicited by silent gaps embedded within a broadband noise.
Front. Neurol. 14:1221443.
doi: 10.3389/fneur.2023.1221443

80 Hz auditory steady state responses (ASSR) elicited by silent gaps embedded within a broadband noise

Seiichi Kadowaki[1], Takashi Morimoto[2], Marta Pijanowska[3,4], Shuji Mori[5] and Hidehiko Okamoto[1]*

[1]Department of Physiology, International University of Health and Welfare Graduate School of Medicine, Narita, Japan, [2]Department of Audiological Engineering, RION Co., Ltd., Tokyo, Japan, [3]Office of Medical Education, International University of Health and Welfare School of Medicine, Narita, Japan, [4]Graduate School of Humanities and Sociology, University of Tokyo, Tokyo, Japan, [5]Department of Informatics, Graduate School of Information Science and Electrical Engineering, Kyusyu University, Fukuoka, Japan

Introduction: Although auditory temporal processing plays an important role in speech comprehension, it cannot be measured by pure tone audiometry. Auditory temporal resolution is often assessed by behavioral gaps-in-noise test. To evaluate whether auditory temporal resolution could be objectively assessed, we measured the auditory steady state response (ASSR) elicited by silent gaps embedded within broadband noises at 80 Hz.

Methods: We prepared six sound types as test stimuli. One was a continuous broadband noise without a silent interval as a control stimulus and the others were broadband noises with 80 Hz silent intervals of 0.4, 0.8, 1.6, 3.1, and 6.3 ms.

Results: Significant ASSRs were recorded only when the gap length was longer than the behavioral thresholds and the ASSR amplitude increased as the gap length increased.

Conclusion: Eighty Hertz gap-evoked ASSR appears to reflect the neural activity related to the auditory gap processing and may be used as an objective measure of auditory temporal resolution in humans.

KEYWORDS

auditory steady state response (ASSR), electroencephalography (EEG), gap, human, temporal processing, speech

1. Introduction

Time is a very important variable in hearing because all sounds vary in frequency and amplitude over time. Complex natural sound signals such as speech and music can be decomposed into slowly varying "envelope" and rapidly oscillating "fine structure." Out of the two, envelope plays a more important role in speech comprehension (1). Auditory temporal resolution is the ability to detect temporal changes of sound stimuli and to correctly recognize the envelope of sound signals. The temporal resolution of the auditory system is often assessed by the gap detection test. This test uses sound stimuli with silent gaps to estimate the minimum perceivable gap length (2, 3). It should be noted that this method requires the participant to take an action in response to the sound signal whenever they perceived the gap. As such, this method is not objective since the participant's personality, varying levels of concentration and dexterity necessary for the physical action of pressing the button may affect the results to some extent. Therefore, many studies currently aim to find objective measures of the temporal resolution using neuroimaging techniques.

Previous studies have shown that gaps embedded in continuous tones elicit various types of event related potentials. In an experiment by Uther et al. (4), continuous 2,000 Hz pure tones inserted with silent gaps of 3, 5, and 7 ms evoked mismatch negativity (MMN) and the MMN amplitude was proportional to the gap length. Electrophysiological studies have shown that the main sources of MMN are located close to the primary and secondary auditory cortex (5). Furthermore, Werner et al. (6) found that the behavioral gap detection threshold is similar to the neurophysiological gap detection threshold which was estimated by the sensitivity of the V wave of the auditory brainstem response elicited by silent gaps embedded within a broadband noise. The neural generator of V wave is thought to be the inferior colliculus (7). It remains elusive whether it is the cortex or the brainstem that plays a more important role in auditory gap detection.

In our previous study (8), we have obtained clear 40 Hz auditory steady state responses (ASSRs) elicited by the silent gaps of 3.125, 6.25, and 12.5 ms embedded within a broadband noise. The ASSR is one of the objective hearing tests used in clinical practice. Its neural sources and sensitivity depend on the modulation frequency. The 40 Hz ASSR appears to originate in the region spanning from the primary auditory cortex (9). It is considered to have a higher signal-to-noise ratio while the subject is awake (10). On the other hand, the 80 Hz ASSR appears to originate primarily from subcortical sources (11), and sleep has little effect on the response (12).

In the previous study, we demonstrated that gaps embedded within a broadband noise elicited clear 40 Hz ASSR; however, there has been no report that investigated the ASSR elicited by gap stimulus presented at the 80 Hz rate and compared the gap-evoked ASSR and the behavioral gap detection thresholds. The 80 Hz ASSR has the advantage of being an objective measure used in clinical practice because it can be measured reliably even during sleep (13). In this study, we conducted an experiment to verify whether the ASSR can be elicited by 80 Hz silent gaps of different lengths that are below and above the behavioral threshold. The results would contribute to developing a non-invasive objective measure of auditory temporal resolution in humans.

2. Methods

2.1. Participants

Twenty-one students (10 males) were recruited at the International University of Health and Welfare for this experiment. Their ages ranged from 18 to 31 (median 20). Eighteen participants were right-handed and three were left-handed, and all had normal hearing and no neurological or psychiatric disorders. They were fully informed about the study and gave written informed consent for their participation. The present study was approved by the Ethics Committee of the International University of Health and Welfare, School of Medicine and conformed to The Code of the World Medical Association (Declaration of Helsinki).

2.2. Stimuli and experimental design for electroencephalography recording

Six types of white noise of 1 min duration were used as sound stimuli (sampling rate: 48,000 Hz). One type was a white noise without a silent interval as a control stimulus (GAP_0), and the others were white noises with 80 Hz silent intervals of 0.396 (GAP_0.4), 0.792 (GAP_0.8), 1.563 (GAP_1.6), 3.125 (GAP_3.1), and 6.25 ms (GAP_6.3; Figure 1 and Supplementary Audios 1–6). The stimuli were randomly played for 30 min, resulting in 5 min of each GAP condition (1 min × 5 times × 6 noise types). All auditory stimuli were designed in the MATLAB environment (The MathWorks Inc., MA, USA). Participants were presented with stimuli at an intensity of 70 dBA SPL via ER-3A insert earphones (Etymotic Research Inc., IL, USA). Figure 2 displays the amplitude spectra of the sound stimuli measured at the earpiece by using Ear Simulator TYPE 4157 (Bruel & Kjaer Sound & Vibration Measurement A/S, Denmark). EEG recordings were performed with participants seated comfortably in a silent electromagnetically shielded room. They were instructed to watch a silent movie with captions during experiments.

2.3. Behavioral data

The detection threshold of 80 Hz gap inserted sound stimuli and single gap inserted stimuli were measured in all participants. An adaptive, three-alternative forced-choice, two-down, one-up procedure was used to track the 70.7% correct rate for gap detection threshold (GDT) determination as described in detail in the previous studies (14, 15). The threshold for the length of detectable gap was tested at an intensity of 70 dBA SPL via ER-3A insert earphones, same as in the ASSR measurements. The duration of the white noise (sampling rate: 48,000 Hz) was set to 500 ms. In the detection threshold condition for a single gap inserted stimulus, each test sound contains only one silent gap in the middle, whereas in the detection threshold condition for an 80 Hz gap inserted sound stimulus, each test sound contains 40 silent gaps because the gaps are embedded at 80 Hz. The inter-stimulus interval between two successive test sounds was 500 ms. The gap length started from 7 ms. The step size was set to 1 ms in the first four reversals and 0.5 ms thereafter. The measurements were continued for 12 reversals, and the threshold was estimated as the mean of the values for the last eight reversals. Thresholds were measured twice, and the mean of the two measurements was used as the detection threshold.

2.4. Data acquisition and analysis

Sound stimuli were presented via Multi Trigger System Ver.2 (MTS0410, Medical Try System, Co., Ltd., Japan), which simultaneously sent triggers to Neurofax EEG1200 (Nihon Koden, Co., Ltd., Japan). We used six types of triggers (GAP_0, GAP_0.4, GAP_0.8, GAP_1.6, GAP_3.1, and GAP_6.3) and, apart from the control condition (GAP_0), the triggers were synchronized with the gap offset (or the onset of the noise segment). The EEG signals were recorded using a Neurofax EEG1200 system at a sampling

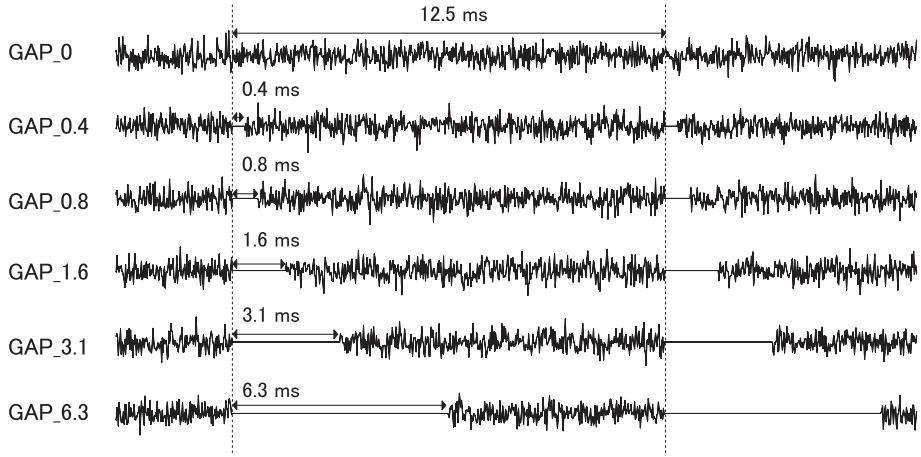

FIGURE 1
Stimulus conditions. Exemplary sound waveforms of test sound stimuli with silent intervals of 0 ms (GAP_0), 0.396 ms (GAP_0.4), 0.792 ms (GAP_0.8), 1.563 ms (GAP_1.6), 3.125 ms (GAP_3.1), and 6.25 ms (GAP_6.3) are depicted from top to bottom.

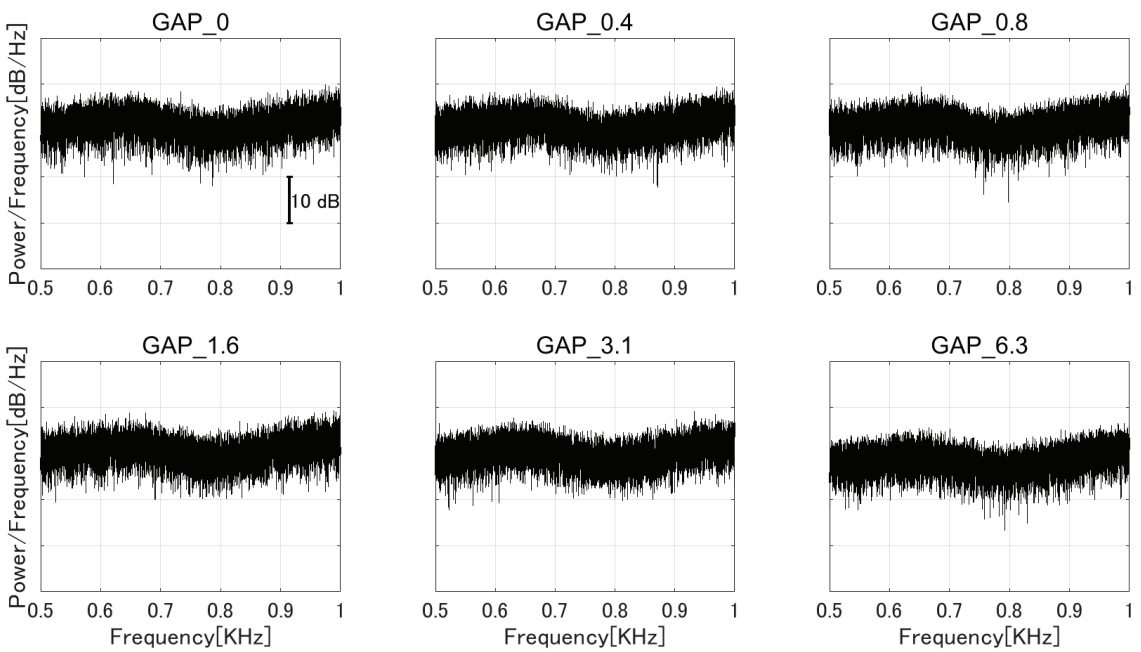

FIGURE 2
The amplitude spectra of the sound stimuli measured at the earpiece by using an ear simulator [GAP_0 **(top left)**, GAP_0.4 **(top center)**, GAP_0.8 **(top right)**, GAP_1.6 **(bottom left)**, GAP_3.1 **(bottom center)**, and GAP_6.3 **(bottom right)**].

rate of 1,000 Hz. The recording electrodes (Ag/AgCl) were located at Cz according to the international 10–20 system. The averaged signal of two electrodes placed on both mastoids was used as a reference electrode and the ground electrode was located around the forehead midpoint. Electrode impedance was maintained below 15 kΩ. Recorded EEG data were exported as ASCII files and were analyzed offline using Matlab R2020a and EEGLAB (16).

For EEG waveforms, a fast Fourier transform (FFT) was computed in each condition and amplitude spectra were extracted after removing the power line fluctuations at 50 Hz using the Clean-Line plugin for EEGLAB. In order to obtain ASSR, an epoching procedure was applied to the EEG signals. While the 80 Hz cycle necessitates the triggers to be placed at 12.5 ms intervals, this was difficult due to 1,000 Hz sampling rate. This problem was resolved by placing a marker every 25 ms in a 40 Hz cycle and calculating two cycles as one epoch. One minute sound stimulus contained 2,400 epochs, and for each GAP condition, the sound stimulus was presented 5 times, resulting in 12,000 epochs. A total of 60,000 epochs were labeled in all GAP conditions of each participant. EEG waveforms were bandpass filtered (70–90 Hz) offline and epochs of 0–24 ms (25 sampling points) from the markers were separately averaged after artifact rejection (set to a

threshold of ± 20 μV) for each GAP condition (GAP_0, GAP_0.4, GAP_0.8, GAP_1.6, GAP_3.1, and GAP_6.3) for each participant. The obtained ASSR waveforms were fitted into the 80 Hz sinusoidal curves and the amplitudes were used for the statistical analysis.

Next, we calculated component synchrony measure (CSM) (17) and estimated GDT from the CSM obtained at Cz. The acquired EEG was filtered by a bandpass filter with cutoff frequencies of 79 and 81 Hz. Then the filtered EEG was divided into 600 epochs of 500 ms length and grouped into 10 groups, each containing 60 epochs. We obtained ten averaged waveforms based on those 60 epochs and the CSM is calculated using the following formula:

$$CSM\,(m) = \left(\frac{1}{10}\sum_{k=1}^{10}\sin\psi_k\,[m]\right)^2 + \left(\frac{1}{10}\sum_{k=1}^{10}\cos\psi_k\,[m]\right)^2$$

Where, ψ denotes phase of ten averaged waveforms ($k = 1, 2, 3, \ldots 10$) and m denotes frequency. CSM value varies from 0 to 1. The value is equal to 1 if the phases of epochs are the same and approaches 0 when the phases change randomly. The criterion for the presence of response is set at $M + 3SD$ (= 0.385), where M denotes the mean of CSM value for non-response and SD denotes standard deviation. The obtained CSM functions as silent interval lengths were approximated by a sigmoid function, and the silent interval length whose obtained sigmoid function exceeded 0.385 was defined as GDT estimated from the CSM values.

2.5. Statistical analysis

In order to minimize the inter-individual differences, the ASSR amplitudes were normalized with respect to the mean ASSR amplitude averaged across all GAP conditions (GAP_0, GAP_0.4, GAP_0.8, GAP_1.6, GAP_3.1, and GAP_6.3) for each participant. Thereafter, the normalized ASSR amplitudes were evaluated by means of a one-way analysis of variance (ANOVA) using gap length (Gap_0, GAP_0.4, GAP_0.8, GAP_1.6, GAP_3.1, and GAP_6.3) as a factor and multiple-comparisons were analyzed using the Tukey's honestly significant difference test.

The CSMs calculated from EEG were similarly evaluated by means of a one-way ANOVA using gap length (Gap_0, GAP_0.4, GAP_0.8, GAP_1.6, GAP_3.1, and GAP_6.3) as a factor and multiple-comparisons were analyzed using the Tukey's honestly significant difference test.

The relationships between GDT estimated from the CSM values, single gap behavioral GDT, and 80 Hz gap behavioral GDT were evaluated based on correlation analysis.

3. Results

After the measurements were obtained from all participants, the collected data were analyzed. The average of the behavioral data of single gap GDT was 2.76 and the 95% confidence interval obtained by boot-strap resampling tests (iteration = 100,000) was 2.60–2.92. The average of the behavioral 80 Hz gap GDT was 0.994 and the 95% confidence interval obtained by boot-strap resampling tests (iteration = 100,000) was 0.902–1.101. For the EEG analysis, the mean rejection rate of the obtained epochs was 6.6%. Figure 3 shows grand averaged FFT waveforms under each condition. No clear response at 80 Hz was observed under GAP_0, GAP_0.4, and GAP_0.8 conditions in contrast to GAP_1.6, GAP_3.1, and GAP_6.3 conditions, where prominent responses at 80 Hz were observed. Figure 4 shows grand averaged EEG waveforms under each condition. Similar to the FFT results, no significant ASSR was evoked in the GAP_0, GAP_0.4, and GAP_0.8 conditions. In the GAP_1.6, GAP_3.1, and GAP_6.3 conditions, clear EEG was evoked and the amplitude increased as the gap length increased.

Figure 5 shows the mean normalized ASSR amplitude in each GAP condition together with the corresponding 95% confidence intervals obtained by boot-strap resampling tests (iteration = 100 000). A one-way ANOVA applied to the normalized ASSR amplitude revealed a significant main effect for gap length [$F_{(5, 120)} = 299.66$, $p < 0.0001$]. As shown in Table 1, the *post-hoc* multi-comparison revealed significant differences between GAP_0 and GAP_3.1 ($p < 0.0001$), GAP_0 and GAP_6.25 ($p < 0.0001$), GAP_0.4 and GAP_1.6 ($p = 0.048$), GAP_0.4 and GAP_3.1 ($p < 0.0001$), GAP_0.4 and GAP_6.25 ($p < 0.0001$), GAP_0.8 and GAP_3.1 ($p < 0.0001$), GAP_0.8 and GAP_6.25 ($p < 0.0001$), GAP_1.6 and GAP_3.1 ($p < 0.0001$), GAP_1.6 and GAP_6.25 ($p < 0.0001$), and GAP_3.1 and GAP_6.25 ($p < 0.0001$). The ASSR amplitudes gradually increased with an increase in the gap duration.

Figure 6 shows the mean CSMs calculated from EEG in each GAP condition together with the corresponding 95% confidence intervals obtained by boot-strap resampling tests (iteration = 100 000). For the results in GAP_1.6, GAP_3.1, and GAP_6.25, the mean CSM gradually increased as GAP length increased. A one-way ANOVA applied to the CSM revealed a significant main effect for gap length [$F_{(5, 120)} = 41.33$, $p < 0.0001$]. As shown in Table 1, the *post-hoc* multiple comparison revealed significant differences between GAP_0 and GAP_1.6 ($p = 0.011$), GAP_0 and GAP_3.1 ($p < 0.0001$), GAP_0 and GAP_6.25 ($p < 0.0001$), GAP_0.4 and GAP_3.1 ($p < 0.0001$), GAP_0.4 and GAP_6.25 ($p < 0.0001$), GAP_0.8 and GAP_3.1 ($p < 0.0001$), GAP_0.8 and GAP_6.25 ($p < 0.0001$), GAP_1.6 and GAP_3.1 ($p = 0.011$), GAP_1.6 and GAP_6.25 ($p < 0.0001$), and GAP_3.1 and GAP_6.25 ($p < 0.0001$).

There was no significant correlation between GDT estimated from the CSM values and single gap behavioral GDT ($r = 0.1566$, $p = 0.4978$), between GDT estimated from the CSM values and 80 Hz gap behavioral GDT ($r = 0.1699$, $p = 0.4617$), nor between the behavioral single gap GDT and the behavioral 80 Hz gap GDT ($r = 0.3994$, $p = 0.0728$).

4. Discussion

The results of the present study demonstrated that 80 Hz ASSR can be elicited by silent gaps embedded within a broadband noise in people with normal hearing. Significant ASSRs were elicited only by test sound stimuli with silent intervals longer than 1 ms, which was the gap detection threshold derived from behavioral data. The ASSRs elicited by GAP_0.4 and GAP_0.8, which were below the behavioral threshold, were similar to those elicited in the GAP_0 condition, in which a continuous broadband noise was used as a sound stimulus. These results suggest that

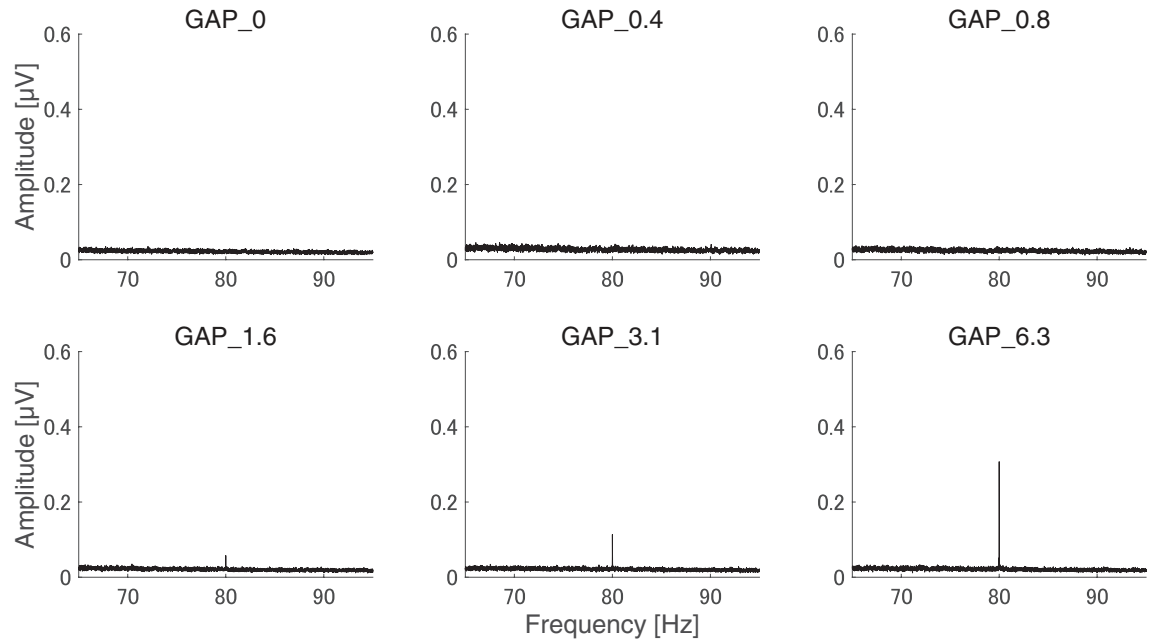

FIGURE 3
Group means of the electroencephalography (EEG) amplitude spectra. Grand averaged ($N = 21$) EEG amplitude spectra corresponding to GAP_0 **(top left)**, GAP_0.4 **(top center)**, GAP_0.8 **(top right)**, GAP_1.6 **(bottom left)**, GAP_3.1 **(bottom center)**, and GAP_6.3 **(bottom right)** are displayed. Clear induced brain responses are visible at 80 Hz in the GAP_1.6, GAP_3.1, and GAP_6.3 conditions.

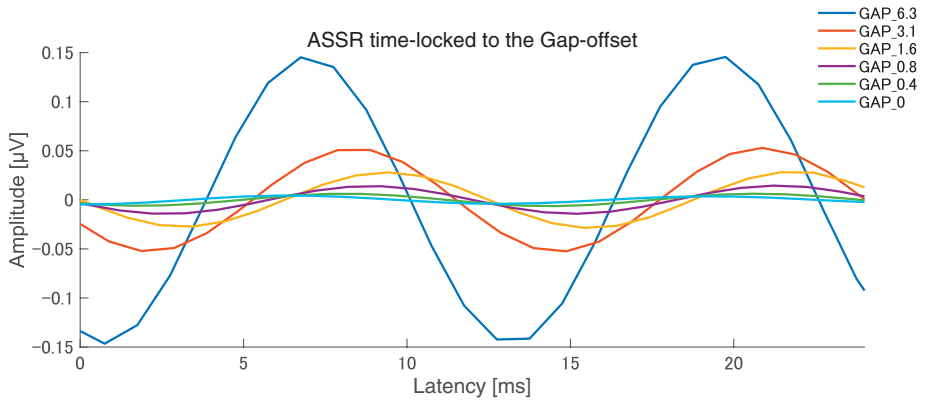

FIGURE 4
Grand averaged auditory steady state responses (ASSRs) elicited by 80 Hz silent gaps. The graph displays the grand-averaged waveforms of participants ($N = 21$). Blue, red, yellow, purple, green, light blue color lines represent GAP_6.3, GAP_3.1, GAP_1.6, GAP_0.8, GAP_0.4, and GAP_0 conditions, respectively (see legends in the right upper corner).

significant ASSRs were elicited only when the length of the silent gaps exceeded the behavioral threshold. This implies that auditory temporal resolution may be objectively measured using the 80 Hz gap-evoked ASSR.

It is known that stimuli differing in modulation frequencies elicit ASSR originating in different brain areas. Previous studies compared cortical and subcortical neural activity with 40 and 80 Hz amplitude modulated sound stimulations. Herdman et al. (11) measured the ASSR elicited by amplitude modulated tones with three modulation frequencies, 12, 39, and 88 Hz. They estimated the neural sources using multi dipole model, revealing that 88 and 39 Hz amplitude modulated tones mainly elicited subcortical and cortical neural activity, respectively. Additionally, Farahani et al. (18) measured the ASSR elicited by amplitude modulated white noise with the modulation frequencies of 3.91, 19.53, 40.04, and 80.08 Hz and estimated the neural source using a minimum-norm imaging technique. They reached the same conclusions as Herdman et al.—subcortical activity dominant at 80 Hz and cortical activity dominant at 40 Hz. Following these results, it has been widely accepted that the 80 Hz ASSR is elicited mainly in the subcortical regions.

Regarding the neural center for auditory temporal processing enabling auditory gap detection, previous studies have suggested that auditory cortex rather than brainstem plays a key role

(19–22). Ison et al. (19) measured gap detection thresholds in rats by acoustic startle reflex using a white noise with silent gaps. KCl injections caused cortical disruptions in rats, inducing prolonged gap detection thresholds, whereas the disruption of auditory brainstem had little effect on gap detection. The results suggested that cortex plays a major role in auditory temporal processing. Syka et al. (21) also demonstrated that neural activity related to auditory temporal processing was delayed after surgical removal of the rat auditory cortex. Similarly, human studies on patients with damage to cerebral hemispheres reported impaired auditory temporal processing regarding the auditory stimuli presented to the ear contralateral to the damaged hemisphere. Jafari et al. (23) performed Gaps-In-Noise test (GIN test, a form of gap detection test) in patients with right hemisphere infarction, patients with left hemisphere infarction and normal subjects. All participants had normal pure tone audiograms; however, the results indicated that auditory temporal processing was impaired when the GIN test was performed on the ear contralateral to the infarction site. Lavasani et al. (24) found that the GDT became longer in patients with temporal epilepsy with normal pure tone audiograms, indicating that auditory temporal processing was impaired in those people. Moreover, research done by Bamiou et al. (25) suggested that insula plays an important role in auditory temporal processing, since patients with insular hemispheric infarction showed prolonged GDT.

In the present study, we used gap sounds that are thought to be processed in the auditory cortex, yet we obtained clear 80 Hz ASSR which are mostly associated with the brainstem. The results obtained could be interpreted as follows. First, while

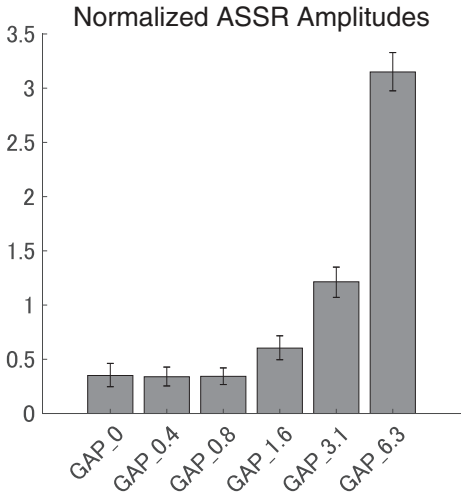

FIGURE 5
Group means of the normalized auditory steady state response (ASSR) amplitudes. Group means ($N = 21$) of the normalized ASSR amplitudes elicited by silent gaps of 0 ms (GAP_0), 0.396 ms (GAP_0.4), 0.792 ms (GAP_0.8), 1.563 ms (GAP_1.6), 3.125 ms (GAP_3.1), and 6.25 ms (GAP_6.3) embedded within broadband noises. The error bars denote 95% confidence intervals.

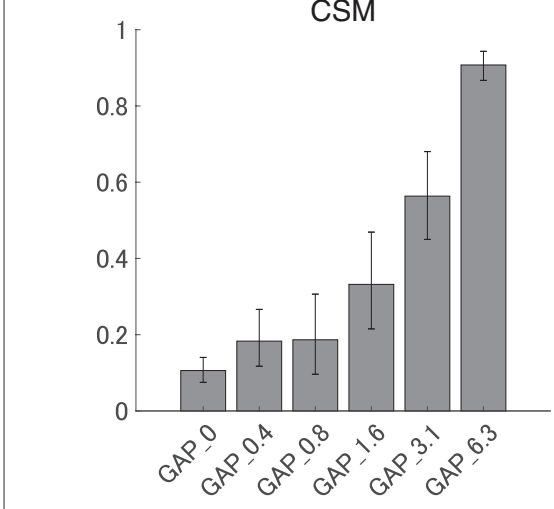

FIGURE 6
Group means of the component synchrony measure (CSM) of auditory steady-state response (ASSR). Group means ($N = 21$) of the CSM elicited by silent gaps of 0 ms (GAP_0), 0.396 ms (GAP_0.4), 0.792 ms (GAP_0.8), 1.563 ms (GAP_1.6), 3.125 ms (GAP_3.1), and 6.25 ms (GAP_6.3) embedded within broadband noises. The error bars denote 95% confidence intervals.

TABLE 1 *p*-values of *post-hoc* multi comparisons between GAP conditions using Tukey's multiple comparison test.

	GAP length	0	0.4	0.8	1.6	3.1
Normalized amplitude	0.4	1	–	–	–	–
	0.8	1	1	–	–	–
	1.6	0.069	0.048	0.054	–	–
	3.1	<0.0001	<0.0001	<0.0001	<0.0001	–
	6.3	<0.0001	<0.0001	<0.0001	<0.0001	<0.0001
CSM	0.4	0.840	–	–	–	–
	0.8	0.807	1	–	–	–
	1.6	0.011	0.0232	0.262	–	–
	3.1	<0.0001	<0.0001	<0.0001	<0.0001	–
	6.3	<0.0001	<0.0001	<0.0001	<0.0001	<0.0001

the 80 Hz ASSR is generally believed to originate primarily from the brainstem, the signal appears to be contaminated with the neural activity in the auditory cortex (18, 26). Therefore, the results obtained in the present study might reflect a portion of 80 Hz ASSR derived from the auditory cortex. Alternatively, the present results could imply that the auditory temporal processing involved in the gap detection occurs at least partially in the brainstem. Galambos et al. (10) first reported that the ASSR amplitude became maximal at the modulation rate of 40 Hz. The 40 Hz ASSR was found to become smaller with sleep, sedation, and anesthesia (27). On the other hand, a higher modulation frequency (70–110 Hz) provided a stable ASSR even during sleep or under sedation (13, 28). The ASSRs elicited by 80 Hz amplitude modulated tones are clinically used as an objective audiometry and are often measured during sleep since the signal-to-noise ratio of 80 Hz ASSR improves during sleep (29). In the present study, the participants were awake during the EEG recording; however, the 80 Hz gap-evoked ASSR may become more prominent during sleep. Eighty hertz ASSR recording during sleep would be especially useful for infants and children who could not stay still during the EEG recording.

Interestingly, the detection threshold of 80 Hz gap inserted sound stimuli was significantly shorter than the normal single gap GDT. While the single gap GDT (mean: 2.76 ms) in the present study was similar to those obtained in the previous studies (30, 31), the regular insertion of gaps at 80 Hz appears to shorten the GDT. Bacon et al. (32) measured detection thresholds of sinusoidal amplitude modulation on a broadband noise and found that normal hearing participants could detect up to 1,024 Hz modulation frequency. The results indicated that the participants could detect the envelope fluctuations of about 1 ms. Moreover, Ross and Pantev (33) measured behavioral GDT and the auditory evoked fields elicited by gaps embedded within 500 Hz tones with 40 Hz amplitude modulation. Normally, the gap detection of pure tones with frequencies between 400 and 1,000 Hz was estimated to be between 6 and 8 ms (34); however, Ross and Pantev's (33) results showed that the detection threshold for the gap embedded within the 40 Hz AM tone was 3 ms and the gap duration of 3 ms elicited significant auditory evoked fields. Similar to the above results, the present study also demonstrated that the detection thresholds for gaps embedded within sounds with repetitive envelope fluctuations became shorter than those embedded within continuous sounds with no repetitive fluctuation (35). One might argue that the insertion of periodic gaps added spectral components corresponding to the stimulation rate (80 Hz) and its harmonics, and consequently the participants might have detected the corresponding spectral components. In the present study, we used white noise segments longer than and equal to the half (6.25 ms) of one 80 Hz cycle and thus the 80 Hz gap inserted sound stimuli had spectral components similar to the control white noise as shown in Figure 2. Another possibility is that the participants might have detected the spectral splatter caused by the steep onset and offset sound envelopes of the gap. However, we used white noise as sound stimuli and the onset and offset of white noise did not give a spectral cue since the spectral splatter was masked by the white noise. Therefore, it is less likely that the participants in the present study detected the spectral changes of test sound stimuli instead of temporal ones.

We found no significant relationship between the GDT estimated from the CSM and the behavioral GDT. All the participants in the present study were young adults and had normal hearing. This could explain why there was little variance in the behavioral GDTs among the participants. Moreover, alertness and motivation of the participants appears to have a stronger impact on the behavioral results than the inter-individual difference. It is necessary to conduct similar studies on people with suspected deterioration of auditory temporal resolution, such as auditory neuropathy patients (36, 37) and the elderly (38).

Recent studies focused their attention on people who have normal pure tone audiogram but struggle to listen to speech signals especially in noisy environments (39, 40). This symptom may derive from impaired temporal processing in the auditory system (41). It remains elusive whether speech perception is significantly correlated with the within-channel gap detection threshold (42). According to Tyler et al. (43) and Snell et al. (44) who used noise bursts as stimulus sounds, GDT and speech perception under noise are significantly correlated, while Strouse et al. (45) and Snell et al. (46) found no significant correlation. Although most of those results were obtained in cross-sectional studies, a longitudinal study by Babkoff and Fostick (38) showed a significant relationship between temporal processing and speech perception even after corrections for auditory level and cognitive ability.

Therefore, the gap-evoked ASSR obtained in the present study may reflect the auditory temporal processing and speech comprehension ability. Many ailments thought to be related to impaired auditory temporal processing, such as hidden hearing loss, auditory processing disorder, and other listening difficulties, are currently diagnosed mainly on the basis of the patients' subjective symptoms. The gap-evoked ASSR can be introduced as an objective diagnostic measure for such cases. Moreover, objective measure of auditory temporal processing can be used as a screening test for children with language and speech developmental delays, allowing early detection and early therapeutic intervention for them. Additionally, in cases of elderly patients with communication problems, measurement of gap-evoked ASSR could potentially help discriminate between patients suffering from dementia and those with impaired auditory temporal processing.

5. Conclusions

Significant ASSRs and CSMs were elicited only by test stimuli with gap lengths above the behavioral threshold. The test stimuli with gap lengths below the behavioral threshold elicited ASSRs similar to those elicited by the continuous broadband noise. Eighty Hertz gap-evoked ASSR may provide insights into the neural mechanisms of auditory temporal processing and may be applied to objectively and non-invasively measure auditory temporal resolution in humans.

Data availability statement

The raw data supporting the conclusions of this article will be made available by the authors, without undue reservation.

Ethics statement

The studies involving human participants were reviewed and approved by Ethics Committee of the International University of Health and Welfare, School of Medicine. The patients/participants provided their written informed consent to participate in this study.

Author contributions

HO conceived and designed research. SK, TM, and HO performed the experiments. SK and HO analyzed the data. SK, TM, MP, SM, and HO interpreted the results of experiments. SK prepared the figures and drafted the manuscript. All authors edited and revised the manuscript and approved the final version of the manuscript.

Funding

This research was supported by the Japan Society for the Promotion of Science (JSPS) KAKENHI Grant Numbers JP18K09327 and JP23H00990.

Acknowledgments

We are grateful to the participants for their diligent cooperation.

Conflict of interest

TM was employed by RION Co., Ltd.

The remaining authors declare that the research was conducted in the absence of any commercial or financial relationships that could be construed as a potential conflict of interest.

Publisher's note

Supplementary material

The Supplementary Material for this article can be found online at: https://www.frontiersin.org/articles/10.3389/fneur.2023.1221443/full#supplementary-material

SUPPLEMENTARY AUDIO 1
An exemplary sound file of GAP_0.

SUPPLEMENTARY AUDIO 2
An exemplary sound file of GAP_0.4.

SUPPLEMENTARY AUDIO 3
An exemplary sound file of GAP_0.8.

SUPPLEMENTARY AUDIO 4
An exemplary sound file of GAP_1.6.

SUPPLEMENTARY AUDIO 5
An exemplary sound file of GAP_3.1.

SUPPLEMENTARY AUDIO 6
An exemplary sound file of GAP_6.3.

References

1. Shannon R V., Zeng FG, Kamath V, Wygonski J, Ekelid M. Speech recognition with primarily temporal cues. *Science.* (1995) 270:303–4. doi: 10.1126/SCIENCE.270.5234.303

2. Giannela Samelli A, Schochat E. The gaps-in-noise test: gap detection thresholds in normal-hearing young adults. *Int J Audiol.* (2008) 47:238–45. doi: 10.1080/14992020801908244

3. Musiek FE, Shinn JB, Jirsa R, Bamiou DE, Baran JA, Zaida E. GIN (Gaps-In-Noise) test performance in subjects with confirmed central auditory nervous system involvement. *Ear Hear.* (2005) 26:608–18. doi: 10.1097/01.aud.0000188069.80699.41

4. Uther M, Jansen DHJ, Huotilainen M, Ilmoniemi RJ, Näätänen R. Mismatch negativity indexes auditory temporal resolution: evidence from event-related potential (ERP) and event-related field (ERF) recordings. *Cogn Brain Res.* (2003) 17:685–91. doi: 10.1016/S0926-6410(03)00194-0

5. Näätänen R, Paavilainen P, Rinne T, Alho K. The mismatch negativity (MMN) in basic research of central auditory processing: a review. *Clin Neurophysiol.* (2007) 118:2544–90. doi: 10.1016/J.CLINPH.2007.04.026

6. Werner LA, Folsom RC, Mancl LR, Syapin CL. Human auditory brainstem response to temporal gaps in noise. *J Speech Lang Hear Res.* (2001) 44:737–50. doi: 10.1044/1092-4388(2001/058)

7. Parkkonen L, Fujiki N, Mäkelä JP. Sources of auditory brainstem responses revisited: contribution by magnetoencephalography. *Hum Brain Mapp.* (2009) 30:1772–82. doi: 10.1002/HBM.20788

8. Kadowaki S, Morimoto T, Okamoto H. Auditory steady state responses elicited by silent gaps embedded within a broadband noise. *BMC Neurosci.* (2022) 23:27. doi: 10.1186/s12868-022-00712-0

9. Gutschalk A, Mase R, Roth R, Ille N, Rupp A, Hähnel S, et al. Deconvolution of 40 Hz steady-state fields reveals two overlapping source activities of the human auditory cortex. *Clin Neurophysiol.* (1999) 110:856–68. doi: 10.1016/S1388-2457(99)00019-X

10. Galambos R, Makeig S, Talmachoff PJ. A 40-Hz auditory potential recorded from the human scalp. *Proc Natl Acad Sci USA.* (1981) 78:2643–7. doi: 10.1073/pnas.78.4.2643

11. Herdman AT, Lins O, van Roon P, Stapells DR, Scherg M, Picton TW. Intracerebral sources of human auditory steady-state responses. *Brain Topogr.* (2002) 15:69–86. doi: 10.1023/A:1021470822922

12. Picton TW, John MS, Dimitrijevic A, Purcell D. Human auditory steady-state responses: respuestas auditivas de estado estable en humanos. *Int J Audiol.* (2009) 42:177–219. doi: 10.3109/14992020309101316

13. Aoyagi M, Watanabe T, Ito T, Abe Y. Reliability and frequency specificity of auditory steady-state response detected by phase spectral analysis. *J Acoust Soc Am.* (2007) 122:EL58. doi: 10.1121/1.2761888

14. Levitt H. Transformed up-down methods in psychoacoustics. *J Acoust Soc Am.* (1971) 49:467–77. doi: 10.1121/1.1912375

15. Zeng FG, Kong YY, Michalewski HJ, Starr A. Perceptual consequences of disrupted auditory nerve activity. *J Neurophysiol.* (2005) 93:3050–63. doi: 10.1152/JN.00985.2004/ASSET/IMAGES/LARGE/Z9K0050545510014.JPEG

16. Delorme A, Makeig S. EEGLAB: an open source toolbox for analysis of single-trial EEG dynamics including independent component analysis. *J Neurosci Methods.* (2004) 134:9–21. doi: 10.1016/j.jneumeth.2003.10.009

17. Aoyagi M. Auditory steady-state response (ASSR). *Audiol Jpn.* (2006) 49:135–45. doi: 10.4295/AUDIOLOGY.49.135

18. Farahani ED, Wouters J, van Wieringen A. Brain mapping of auditory steady-state responses: a broad view of cortical and subcortical sources. *Hum Brain Mapp.* (2021) 42:780–96. doi: 10.1002/HBM.25262

19. Ison JR, O'Connor K, Bowen GP, Bocirnea A. Temporal resolution of gaps in noise by the rat is lost with functional decortication. *Behav Neurosci.* (1991) 105:33–40. doi: 10.1037/0735-7044.105.1.33

20. Weible AP, Moore AK, Liu C, Deblander L, Wu H, Kentros C, et al. perceptual gap detection is mediated by gap termination responses in auditory cortex. *Curr Biol.* (2014) 24:1447–55. doi: 10.1016/J.CUB.2014.05.031

21. Syka J, Rybalko N, Mazelová J, Druga R. Gap detection threshold in the rat before and after auditory cortex ablation. *Hear Res.* (2002) 172:151–9. doi: 10.1016/S0378-5955(02)00578-6

22. Threlkeld SW, Penley SC, Rosen GD, Fitch RH. Detection of silent gaps in white noise following cortical deactivation in rats. *Neuroreport.* (2008) 19:893–8. doi: 10.1097/WNR.0b013e3283013d7e

23. Jafari Z, Esmaili M, Delbari A, Mehrpour M, Mohajerani MH. Auditory temporal processing deficits in chronic stroke: a comparison of brain damage lateralization effect. *J Stroke Cerebrovasc Dis.* (2016) 25:1403–10. doi: 10.1016/J.JSTROKECEREBROVASDIS.2016.02.030

24. Lavasani AN, Mohammadkhani G, Motamedi M, Karimi LJ, Jalaei S, Shojaei FS, et al. Auditory temporal processing in patients with temporal lobe epilepsy. *Epilepsy Behav.* (2016) 60:81–5. doi: 10.1016/J.YEBEH.2016.04.017

25. Bamiou DE, Musiek FE, Stow I, Stevens J, Cipolotti L, Brown MM, et al. Auditory temporal processing deficits in patients with insular stroke. *Neurology.* (2006) 67:614–9. doi: 10.1212/01.WNL.0000230197.40410.DB

26. Tsuchimoto R, Kanba S, Hirano S, Oribe N, Ueno T, Hirano Y, et al. Reduced high and low frequency gamma synchronization in patients with chronic schizophrenia. *Schizophr Res.* (2011) 133:99–105. doi: 10.1016/J.SCHRES.2011.07.020

27. Picton TW, Vajsar J, Rodriguez R, Campbell KB. Reliability estimates for steady-state evoked potentials. *Electroencephalogr Clin Neurophysiol.* (1987) 68:119–31. doi: 10.1016/0168-5597(87)90039-6

28. Rance G, Rickards FW, Cohen LT, De Vidi S, Clark GM. The automated prediction of hearing thresholds in sleeping subjects using auditory steady-state evoked potentials. *Ear Hear.* (1995) 16:499–507. doi: 10.1097/00003446-199510000-00006

29. Levi EC, Folsom RC, Dobie RA. Amplitude-modulation following response (AMFR): effects of modulation rate, carrier frequency, age, and state. *Hear Res.* (1993) 68:42–52. doi: 10.1016/0378-5955(93)90063-7

30. Green DM, Forrest TG. Temporal gaps in noise and sinusoids. *J Acoust Soc Am.* (1998) 86:961. doi: 10.1121/1.398731

31. He N-J, Horwitz AR, Dubno JR, Mills JH. Psychometric functions for gap detection in noise measured from young and aged subjects. *J Acoust Soc Am.* (1999) 106:966. doi: 10.1121/1.427109

32. Bacon SP, Viemeister NF. Temporal modulation transfer functions in normal-hearing and hearing-impaired listeners. *Int J Audiol.* (1985) 24:117–34. doi: 10.3109/00206098509081545

33. Ross B, Pantev C. Auditory steady-state responses reveal amplitude modulation gap detection thresholds. *J Acoust Soc Am.* (2004) 115:2193. doi: 10.1121/1.1694996

34. Moore BCJ, Peters RW, Glasberg BR. Detection of temporal gaps in sinusoids: effects of frequency and level. *J Acoust Soc Am.* (1993) 93:1563. doi: 10.1121/1.406815

35. Plack CJ. *The Sense of Hearing*. London: Routledge. (2018). p. 338. doi: 10.4324/9781315208145

36. Kumar Narne V, Alain C, Hospital B. Temporal processing and speech perception in noise by listeners with auditory neuropathy. *PLoS ONE.* (2013) 8:e55995. doi: 10.1371/JOURNAL.PONE.0055995

37. Narne VK, Vanaja CS. Perception of speech with envelope enhancement in individuals with auditory neuropathy and simulated loss of temporal modulation processing. *Int J Audiol.* (2009) 48:700–7. doi: 10.1080/14992020902931574

38. Babkoff H, Fostick L. Age-related changes in auditory processing and speech perception: cross-sectional and longitudinal analyses. *Eur J Ageing.* (2017) 14:269–81. doi: 10.1007/S10433-017-0410-Y/METRICS

39. Moore DR, Ferguson MA, Edmondson-Jones AM, Ratib S, Riley A. Nature of auditory processing disorder in children. *Pediatrics.* (2010) 126:e382–90. doi: 10.1542/PEDS.2009-2826

40. Sharma M, Purdy SC, Kelly AS. Comorbidity of auditory processing, language, and reading disorders. *J Speech Lang Hear Res.* (2009) 52:706–22. doi: 10.1044/1092-4388(2008/07-0226)

41. Phillips DP, Comeau M, Andrus JN. Auditory temporal gap detection in children with and without auditory processing disorder. *J Am Acad Audiol.* (2010) 21:404–8. doi: 10.3766/jaaa.21.6.5

42. Grose JH, III JWH, Buss E, Hatch D. Gap detection for similar and dissimilar gap markers. *J Acoust Soc Am.* (2001) 109:1587. doi: 10.1121/1.1354983

43. Tyler RS, Summerfield Q, Wood EJ, Fernandes MA. Psychoacoustic and phonetic temporal processing in normal and hearing-impaired listenersa). *J Acoust Soc Am.* (1982) 72:740–52. doi: 10.1121/1.388254

44. Snell KB, Mapes FM, Hickman ED, Frisina DR. Word recognition in competing babble and the effects of age, temporal processing, and absolute sensitivity. *J Acoust Soc Am.* (2002) 112:720–7. doi: 10.1121/1.1487841

45. Strouse A, Ashmead DH, Ohde RN, Grantham DW. Temporal processing in the aging auditory system. *J Acoust Soc Am.* (1998) 104:2385–99. doi: 10.1121/1.423748

46. Snell KB, Frisina DR. Relationships among age-related differences in gap detection and word recognition. *J Acoust Soc Am.* (2000) 107:1615–26. doi: 10.1121/1.428446

frontiers | Frontiers in Neurology

TYPE Original Research
PUBLISHED 08 August 2023
DOI 10.3389/fneur.2023.1181539

OPEN ACCESS

EDITED BY
Brian John McKinnon,
University of Texas Medical Branch at Galveston, United States

REVIEWED BY
Chunfu Dai,
Fudan University, China
Aarno Dietz,
Kuopio University Hospital, Finland

*CORRESPONDENCE
Stefan Weder
✉ stefan.weder@insel.ch

RECEIVED 07 March 2023
ACCEPTED 26 June 2023
PUBLISHED 08 August 2023

CITATION
Schuerch K, Wimmer W, Rummel C, Caversaccio MD and Weder S (2023) Objective evaluation of intracochlear electrocochleography: repeatability, thresholds, and tonotopic patterns.
Front. Neurol. 14:1181539.
doi: 10.3389/fneur.2023.1181539

Objective evaluation of intracochlear electrocochleography: repeatability, thresholds, and tonotopic patterns

Klaus Schuerch[1,2], Wilhelm Wimmer[3], Christian Rummel[4], Marco Domenico Caversaccio[1,2] and Stefan Weder[1,2]*

[1]Department of ENT, Head and Neck Surgery, Inselspital, Bern University Hospital, University of Bern, Bern, Switzerland, [2]Hearing Research Laboratory, ARTORG Center for Biomedical Engineering Research, University of Bern, Bern, Switzerland, [3]Department of Otorhinolaryngology, TUM School of Medicine, Klinikum Rechts der Isar, Technical University of Munich, Munich, Germany, [4]Support Center for Advanced Neuroimaging (SCAN), University Institute for Diagnostic and Interventional Neuroradiology, Inselspital, Bern University Hospital, University of Bern, Bern, Switzerland

Introduction: Intracochlear electrocochleography (ECochG) is increasingly being used to measure residual inner ear function in cochlear implant (CI) recipients. ECochG signals reflect the state of the inner ear and can be measured during implantation and post-operatively. The aim of our study was to apply an objective deep learning (DL)-based algorithm to assess the reproducibility of longitudinally recorded ECochG signals, compare them with audiometric hearing thresholds, and identify signal patterns and tonotopic behavior.

Methods: We used a previously published objective DL-based algorithm to evaluate post-operative intracochlear ECochG signals collected from 21 ears. The same measurement protocol was repeated three times over 3 months. Additionally, we measured the pure-tone thresholds and subjective loudness estimates for correlation with the objectively detected ECochG signals. Recordings were made on at least four electrodes at three intensity levels. We extracted the electrode positions from computed tomography (CT) scans and used this information to evaluate the tonotopic characteristics of the ECochG responses.

Results: The objectively detected ECochG signals exhibited substantial repeatability over a 3-month period (bias-adjusted kappa, 0.68; accuracy 83.8%). Additionally, we observed a moderate-to-strong dependence of the ECochG thresholds on audiometric and subjective hearing levels. Using radiographically determined tonotopic measurement positions, we observed a tendency for tonotopic allocation with a large variance. Furthermore, maximum ECochG amplitudes exhibited a substantial basal shift. Regarding maximal amplitude patterns, most subjects exhibited a flat pattern with amplitudes evenly distributed over the electrode carrier. At higher stimulation frequencies, we observed a shift in the maximum amplitudes toward the basal turn of the cochlea.

Conclusions: We successfully implemented an objective DL-based algorithm for evaluating post-operative intracochlear ECochG recordings. We can only evaluate and compare ECochG recordings systematically and independently from experts with an objective analysis. Our results help to identify signal patterns and create a

better understanding of the inner ear function with the electrode in place. In the next step, the algorithm can be applied to intra-operative measurements.

KEYWORDS

ECochG, deep learning, electrophysiology, cochlear implants, hearing loss, signal processing, electric acoustic stimulation, hearing preservation

1. Introduction

Electrocochleography (ECochG) is increasingly being used to measure residual inner ear function in cochlear implant (CI) recipients. This facilitates the direct recording of signals from the implant electrode array either during or at any time after implant surgery. Using the ECochG signals, we can map and monitor the inner ear tonotopic and temporary function. ECochG is an umbrella term for four different inner ear potentials (i.e., cochlear microphonic CM, auditory neurophonic ANN, compound action potential CAP, and summating potential SP) (1–3). The CM/DIF response is the most common in the analysis of inner ear function because it is the most reliable and robust cochlear signal (4). It was calculated by subtracting the responses to the condensation (CON) and rarefaction (RAR) polarity stimuli.

The signal characteristics of the ECochG measurements provide different insights into the cochlear function. Several publications have reported that abrupt drops in the CM/DIF amplitudes during cochlear implantation may be associated with traumatic inner ear events (5–8). In a post-operative setting, CM/DIF signals exhibited a strong correlation with audiometric hearing thresholds (9, 10). Furthermore, the CM/DIF amplitudes varied across the electrode carrier, depending on the recording site. In contrast to the assumption that the amplitude peaks at the tonotopic position for a given acoustic stimulus (11–17), different amplitude patterns along the cochlear duct have been described (i.e., basal and flat amplitude patterns) (11, 12, 14).

Until now, the diagnostic gold standard for analyzing ECochG signals has been expert visual inspection. However, this approach entails several limitations. Visual interpretation depends on experts and requires experience in the field. Hence, reproducibility is limited, longitudinal data can only be assessed to a limited extent, and different studies may reach different results, hampering direct comparisons. Moreover, if the signal-to-noise ratio (SNR) is poor, recordings are often not included in the analysis, leading to selection and reporting biases. In conclusion, a deeper and more systematic understanding of the signal behavior is needed before ECochG recordings can be used and interpreted in clinical routine. Therefore, new analytical approaches are required for this purpose.

In our previous study, we proposed machine-learning models that objectively identified CM/DIF signals (18). The Hotelling's T^2 Test and Deep Learning (DL) approach yielded high accuracies. The proposed objectification methods make observations transparent because the analysis is always performed in the same manner. Furthermore, no data were neglected owing to a poor SNR avoiding a selection bias. Therefore, the objective analysis method facilitates the study and comparison of the longitudinal data and ECochG patterns.

The aim of the current study was to apply our objective algorithm and evaluate the repeatability and patterns of the intracochlear ECochG measurements. We tested three hypotheses: (i) longitudinal ECochG measurements remain stable with unchanged residual inner ear function (repeatability); (ii) ECochG thresholds correlate with hearing thresholds; and (iii) for different frequencies, CM/DIF amplitudes show their maxima at different intracochlear locations according to their tonotopic organization.

2. Methods

This prospective cohort study was conducted in accordance with the Declaration of Helsinki and approved by the local institutional review board (KEK-BE 2019-01578). Written informed consent was obtained from the individuals for the publication of any potentially identifiable data included in this article.

2.1. Data acquisition

We included 20 adults in our study (n = 21 ears; 12 females, eight males; mean age, 60.0 years; SD = 16.5 years, range, 25–82 years). All subjects received an implant from the same manufacturer (MED-EL, Innsbruck, Austria) at least 6 months prior to the study participation. This period is important to avoid rapid post-operative changes in the inner ear function, which occur predominantly within the first months after implantation (19).

In total, we conducted three measurement sessions, as shown in Figure 1: (i) the first session was at least 6 months after implantation, (ii) the second session was 2–48 h after the first measurement, and (iii) the third session was 2–4 months after the second measurement. To obtain residual hearing, a pure-tone audiogram was performed at the beginning of sessions (i) and (iii) using a calibrated setup in a certified acoustic chamber (Interacoustics, Middlefart, Denmark). The subjects' audiograms are shown in the Supplementary material. According to Rasetshwane et al. (20), the subjects categorized the loudness of the acoustic ECochG stimuli into seven categories (not audible, very soft, soft, medium, loud, very loud, and too loud). The evaluated dataset is available at Schuerch et al. (21).

During the ECochG recordings, we used pure-tone stimuli at 250 Hz, 500 Hz, 750 Hz, 1 kHz, 1.5 kHz, and 2 kHz using the research Maestro software (version 8.03 AS and 9.03 AS, MED-EL, Innsbruck, Austria) (22). As a minimum requirement, we recorded the ECochG potentials at four electrodes (1, 4, 7, and 10) and three intensity levels (supra-threshold: 5 dB below the

discomfort level, near-threshold: 10 dB above the pure-tone hearing threshold of the measured frequency, and sub-threshold: 10 dB below the pure-tone hearing threshold of the measured frequency). Additional adjacent intensity levels and electrodes were measured when the time permitted and when the subject agreed. For each electrode, the intensity level, frequency, and 100 epochs of each polarity (CON/RAR) were measured, digitized at 120 kHz, and stored separately.

In all but one subject (ID PO8), a routinely performed post-operative computed tomography (CT) scan of the temporal bone was available, from which we calculated the intracochlear electrode positions and their corresponding theoretical tonotopic frequencies using Otoplan software (version 3, CASCINATION, Bern, Switzerland). For the subject ID PO8, we used the average insertion depths obtained from 57 subjects using Flex28 electrodes (23).

2.2. Data analysis

2.2.1. Preprocessing

To test our three hypotheses, we focused on the CM/DIF signal. We preprocessed the ECochG data as described in Schuerch et al. (18). We used the following steps: (i) removal of stitching artifacts; (ii) application of a Gaussian-weighted averaging method to remove uncorrelated epochs (24, 25); (iii) calculation of the CM/DIF signal by subtracting the CON and RAR recordings (1, 3); and (iv) application of a bandpass filter (100 Hz/5 kHz) (4). The signal-to-noise ratio (SNR) was calculated using the plus-minus averaging method (26). We obtained the SNR for each polarity separately and averaged both values to obtain the final SNR.

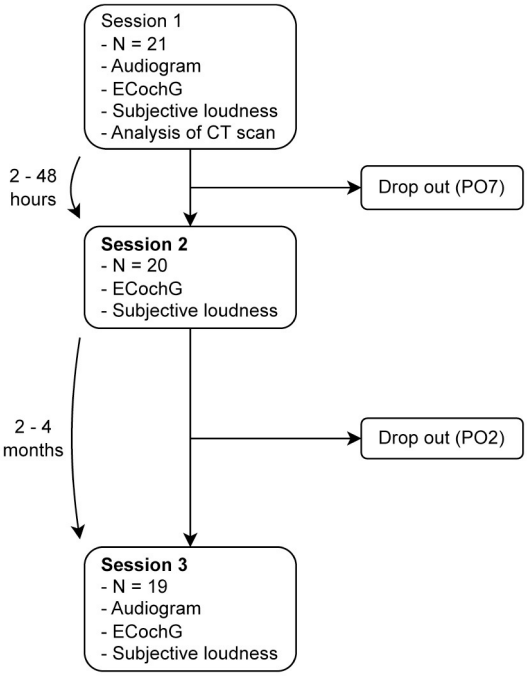

FIGURE 1
We performed three measurement sessions: (i) at least 6 months after implantation, (ii) within 2–48 h after the first measurement, and (iii) 2–4 months after the second measurement. Two subjects did not complete all the three sessions; one of them suffered from a complete hearing loss, so that no intracochlear signals could be measured, and the other withdrew from the study for personal reasons. PO, subject ID.

2.2.2. Objectification

We used our previously described DL algorithm to classify the CM/DIF signals into "response present" and "response absent" subgroups (18). Using these categories, we tested three hypotheses: (i) repeatability, (ii) correlation with hearing thresholds, and (iii) frequency-specific amplitude maxima with respect to the tonotopic position.

2.2.3. Repeatability

We analyzed the repeatability of the CM/DIF signals using prevalence-adjusted and bias-adjusted kappa (PABAK), which considers the prevalence and chance of agreement (27–29). Because PABAK and Cohen kappa were designed to compare only two variables (in our data: sessions), we computed them for all possible combinations (sessions: 1 and 2, 1 and 3, and 2 and 3). Finally, the kappa values across all three sessions were averaged to obtain the overall kappa value as proposed in (30). We evaluated the kappa values for three different intensity categories: (i) sub-threshold (intensity < 0 dB), (ii) near-threshold (25 dB $>$ intensity ≥ 0 dB), and (iii) supra-threshold (intensity ≥ 25 dB). The interpretation of the kappa values was based on that of Landis and Koch et al. (31). The kappa values were calculated using epiR (v. 2.0.52), R (v. 4.1.2), rpy2 (v. 3.5.4), and Python (v. 3.9.7) (32, 33). We tested whether the sessions matched by using McNemar's test and the Python Statsmodels module (v. 0.13.2) (34).

2.2.4. Threshold analysis

We compared the objectively detected CM/DIF thresholds with the objective audiometry and subjective thresholds. First, we identified the relative stimulus intensities (ECochG stimulus-audiometric threshold) that produced objectively detected responses and non-responses, respectively. Second, for each stimulus type and subject, we determined the lowest relative stimulus intensity that still elicited an objective response. These values were compared to the pure-tone threshold and individual loudness perception. The objective responses elicited by higher acoustic intensities were neglected in this part of the analysis.

2.2.5. Tonotopy and pattern analysis

For the tonotopic and pattern analysis, we used the measurement session with the most recordings for each subject. First, the CM/DIF amplitudes were normalized. A weighted mean was then calculated separately for all

10.3389/fneur.2023.1181539

TABLE 1 Demographics of the 21 ears examined.

Subj. ID	Gender	Age (years)	Side	Etiology	Electrode array	Insertion angle (°)	ToM (month)	PTA (dB HL)
PO0	F	51–60	R	Progressive HL	Flex28	561	10	68.8
PO1	M	71–80	R	Progressive HL	Flex28	526	17	110.0
PO2	M	71–80	L	Progressive HL	Flex24	419	46	66.3
PO3	M	71–80	L	Congenital genetic	Flex28	524	9	85.0
PO4	F	21–30	R	Congenital genetic	Flex28	550	20	101.3
PO5	F	61–70	R	Progressive HL	Flex28	578	28	92.5
PO6	F	71–80	R	Meniere's disease	Flex28	536	78	90.0
PO7	M	81–90	L	Progressive HL	Flex28	547	75	113.8
PO8	F	21–30	R	Congenital genetic	Flex28	530	57	85.0
PO9	F	41–50	R	Progressive HL	Flex28	555	22	83.8
PO10	F	51–60	R	Progressive HL	Flex24	456	13	97.5
PO11	F	71–80	L	Progressive HL	Flex28	350	70	100.0
PO12	M	41–50	R	Meningitis	Flex28	564	11	81.3
PO13	F	61–70	L	Progressive HL	Flex28	526	22	93.8
PO14	F	51–60	R	Congenital genetic	Flex24	531	174	95.0
PO15	M	41–50	L	Meningitis	Flex28	538	6	75.0
PO16	M	61–70	R	Meniere's disease	Flex28	632	7	106.3
PO17	M	51–60	R	Sudden HL	Flex28	493	11	91.3
PO18	M	71–80	R	Progressive HL	Flex28	461	70	96.3
PO19	F	61–70	R	Progressive HL	Flex24	466	131	91.3
PO20	F	31–40	L	Progressive HL	Flex24	402	6	39.0
Mean		59.5				511.6	42.0	88.7

Pure-tone average (PTA) values in dB hearing level were calculated as the mean of the hearing thresholds at 125, 250, 500, and 1,000 Hz. Subj., subject; ToM, time of measurement in months after implantation; HL, hearing loss.

stimulation frequencies to assess the tonotopic distribution of the signal amplitudes. The weighted mean was calculated as follows:

$$\overline{X} = \frac{\sum_{i=1}^{n} w_i x_i}{\sum_{i=1}^{n} w_i}$$

where $\overline{X}$ is the weighted mean, n is the number of signals, w is the normalized amplitude, and x is the tonotopic position of the signal.

Finally, we checked for the presence of intracochlear CM/DIF patterns (that is, apical response, basal response, medial response, and flat response) similar to the previous findings by Bester et al. (11, 12). We integrated the frequency allocations from Li et al. (35) and divided them into the following tonotopic regions: apical (20–500 Hz), medial (500–4,000 Hz), and basal (4,000–20,677 Hz). We defined our patterns based on these frequency regions. We assigned a pattern of the maximum CM/DIF amplitude in one of the regions, which exceeded the median of all other recording locations by 30% or more for a given stimulus (11). We defined the "flat" pattern as in Bester et al. when multiple or no significant peaks from two or more tonotopic regions occurred (11).

3. Results

Table 1 lists the demographic characteristics of the subjects. The subjects most commonly had progressive hearing loss with a mean low frequency pure tone average (PTA at 125 Hz, 250 Hz, 500 Hz, and 1 kHz) of 88.7 dB HL (range: 39.0–113.8 dB HL). The subjects received either a Flex24 or Flex28 electrode with a mean insertion depth of 509° (range: 350° to 632°).

CM/DIF responses were detected in all subjects except for one who dropped out after the first session. Overall, the CM/DIF responses were detected in 27.5% of the signals (sub-threshold, near-threshold, and supra-threshold) and in 37.8% of the signals with acoustic stimulation above the hearing level (near-threshold and supra-threshold). The CM/DIF amplitudes ranged from 4.56 μV_{pp} to 74.46 μV_{pp}. The sample recordings of CM/DIF, ANN/SUM, CON, RAR, and their individual Fast Fourier Transform (FFT) power spectra are shown in the Supplementary material (subject PO8).

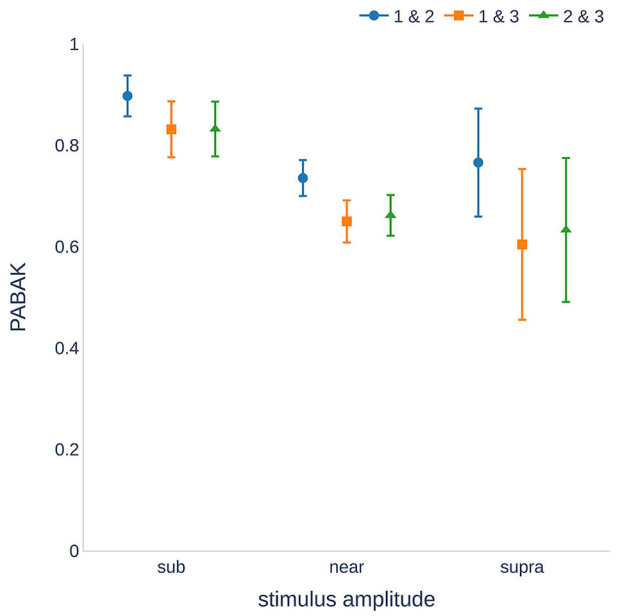

FIGURE 2
Reproducibility of the measurements ranged from substantial to almost perfect (29). The sub-threshold stimuli showed higher reproducibility than the near and supra-threshold stimulation. Higher variance was found for supra-threshold stimulation because fewer recordings were available. PABAK, prevalence-adjusted and bias-adjusted kappa; dB, decibel.

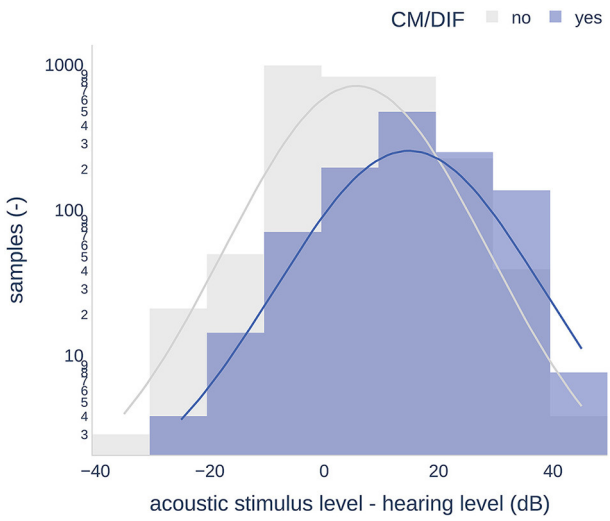

FIGURE 3
Histogram of objectively analyzed CM/DIF responses including all stimulation frequencies and intensity levels. Acoustic stimulus level-hearing level indicates the intensity of the stimulation relative to the individual's hearing threshold.

3.1. Repeatability

Our data showed substantial reproducibility across the three measurement sessions, as indicated by an average PABAK of 0.68 (Cohen's kappa coefficient of 0.61 and an accuracy of 84.1%). Figure 2 shows the PABAK values for combinations of the three recording sessions and three intensity levels (calculated as the difference between the stimulus level and individual hearing threshold).

The highest PABAK values were observed in the sub-threshold group. There was a wider confidence interval for the supra-threshold group because of the smaller number of recordings (stimulation of 25 dB above the hearing threshold was not possible for all individuals and frequencies). It should also be noted that the PABAK values for sessions 1 and 2 were consistently higher than those of the other session combinations. A further analysis of the sensitivity and specificity revealed that sessions 1 and 2 were not significantly different ($p = 0.499$, McNemar's test), whereas sessions 1 and 3, and 2 and 3 were significantly different ($p = 0.009$ and $p < 0.001$, respectively). Detailed information on the calculation of the kappa values can be found in the Supplementary material.

3.2. Thresholds

The mean PTAs were 88.7 dB HL (SD = 22.4) and 89.1 dB HL (SD = 20.9) for the first and third sessions, respectively. There were no significant differences between the two sessions (one-tailed paired-samples t-test, p = 0.096). Higher stimulation amplitudes generally resulted in a higher number of ECochG responses. Figure 3 shows a histogram of the CM/DIF recordings based on the relative stimulation level. It shows a considerable overlap between the distribution of the recordings with (blue shaded area) and without (gray shaded area) an objectively detected response. Both distributions showed a bell-shaped distribution, with large variances (range of ECochG response present: −30 to 48 dB, range of ECochG not present: −40 to 48 dB). The mean relative stimulation level for the recordings with a detected response was 14.1 dB (SD = 11.4), which was significantly higher than the mean relative stimulation level for the recordings without a detected response (3.5 dB, SD = 11.1, $p < 0.001$, one-tailed paired-samples t-test).

Figure 4 and Table 2 compare the individual ECochG thresholds with audiometric thresholds. We examined the frequency dependence of the CM/DIF and audiometric thresholds (Figure 4A) using linear regression models, which yielded r^2 values between 0.50 and 0.76 ($p < 0.001$), indicating a moderate dependence between the two. Analyzing the same data in terms of subjects' perceived loudness (Figure 4B), we found r^2 values between 0.64 and 0.95 ($p < 0.001$). The linear model fits the data best for very soft and soft perceptions.

3.3. Tonotopy and patterns

Owing to the variable size of the cochlea in our study cohort, the insertion depth of the electrode varied considerably (ranging from 350° to 632°, see Table 1). Figure 5 shows the variance of the tonotopic positions of all the 12 electrodes. According to our cochlear frequency subdivision (i.e., apical, medial, and

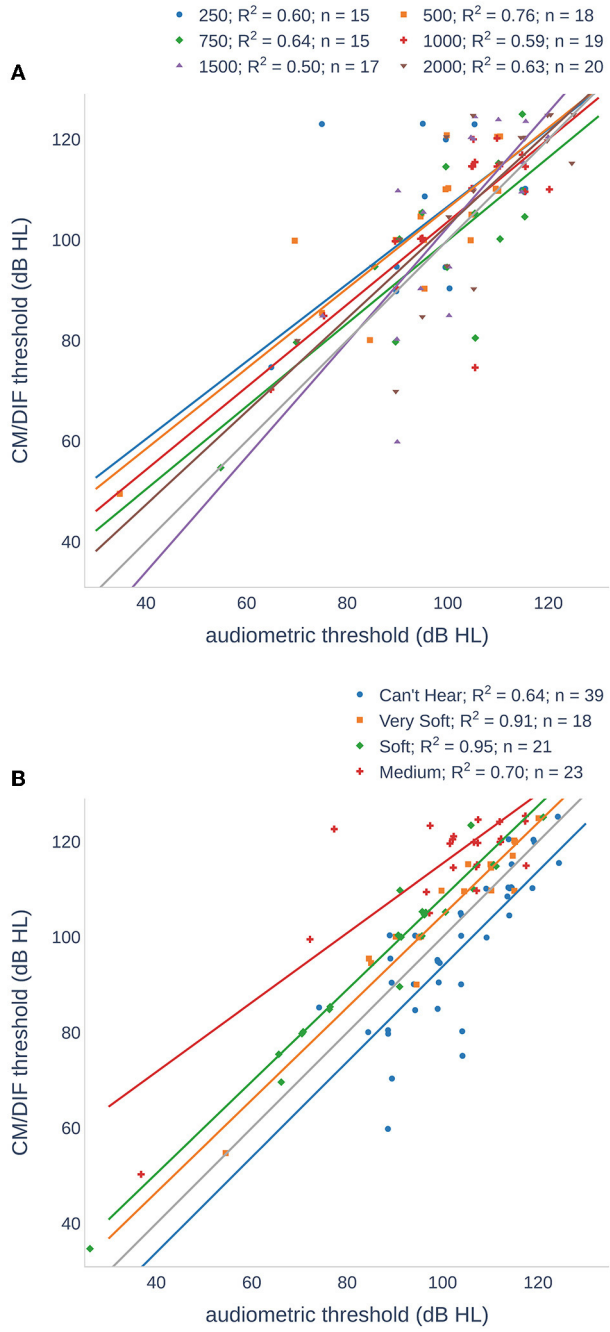

FIGURE 4
Scatter plots of CM/DIF thresholds as a function of audiometric thresholds for all subjects. **(A)** The CM/DIF thresholds were grouped according to their stimulus frequency. **(B)** The CM/DIF thresholds were grouped into four categories according to their subjective loudness: (i) can not hear (blue), (ii) very soft (orange), (iii) soft (green), and (iv) medium (red). The solid lines show the linear regression in both plots.

basal parts of the cochlea), not all electrodes reached the apical region (n = 6).

Regarding the intracochlear amplitude distributions, Figure 7 shows the normalized amplitude as a function of the tonotopic and stimulus frequencies. We found a predominance of flat patterns, occurring in 44 cases, followed by medial and basal, each occurring in 27 and 26 cases, respectively. The least common pattern was apical, occurring in only one case. Otherwise, all stimulation frequencies were observed for all the other patterns. However, the basal pattern was more pronounced at frequencies >500 Hz. Additionally, for each subject, we examined whether there was a change in the amplitude pattern as a function of the stimulation frequency. Figure 8 shows the patterns observed for each subject for each stimulus frequency, respectively. For example, subject PO8 showed the same CM/DIF response pattern for all stimulation frequencies (i.e., basal pattern; amplitude maxima for all frequencies occurred in the basal part of the cochlea). In contrast, subject PO16 showed a more dynamic pattern with the amplitude maxima changing from medial (250–1,000 Hz) to flat (1,500 Hz) to apical (2,000 Hz).

4. Discussion

In this study, we used an objective DL-based algorithm to evaluate intracochlear, post-operative ECochG signals recorded three times over a period of ∼3 months. The use of an objective algorithm has several advantages, for instance, the data are analyzed independently of experts and always in the same manner. Regardless of the SNR, all the data were included in the analysis, which prevented selection and reporting bias. Finally, our algorithm is open-access, which makes the analysis transparent (18). Therefore, we were able to study and compare cross-sectional and longitudinal ECochG data systematically in the first place. In our analysis, we used the following three research questions: Are the recordings longitudinally reproducible?; is there a correlation with the pure-tone threshold?; and can we detect patterns for stimuli of different frequencies?

4.1. Repeatability

Our results showed substantial repeatability of the CM/DIF responses over the three measurement sessions (PABAK 0.68, accuracy of 83.8%) (31). This result is comparable to other neurophysiological findings, such as waving the V responses in the auditory brainstem measurements (36, 37). Analysis of the combination of two sessions showed a higher PABAK value for sessions 1 and 2 (0.74) than for sessions 1 and 3 (0.65) and 2 and 3 (0.66). This could also be shown statistically, where there was only a significant difference between sessions 1 and 3, and sessions 2 and 3, but not between sessions 1 and 2. A possible explanation for this finding is the altered measurement conditions, such as a change in the eartip placement, which could reduce the presented intensity level of the acoustic stimulus (38). However, a random effect without a clear pattern was expected in this case. Therefore, we suspect that we were detecting a discrete longitudinal change in the inner ear function although the hearing thresholds were unchanged between sessions 1 and 3. It is well-known that pure-tone audiometry cannot detect small changes in hearing and is prone to variability (39). Additionally, other studies have shown that the inner ear function of CI users declines over the years (19, 40). This decline may be caused by the natural course of

TABLE 2 Mean and SD of the difference between audiometric and CM/DIF threshold.

	CM/DIF vs. audiometric threshold (dB HL), our data		CM/DIF vs. audiometric threshold (dB HL), Koka et al. (10)		CM/DIF vs. audiometric threshold (dB nHL), Haumann et al. (9)	
Group	Mean	SD	Mean	SD	Mean	SD
250 Hz	−8.5	15	−6	8	−12.0	17.5
500 Hz	−7.6	9.0	−6	8	5.9	11.8
750 Hz	−0.3	10.7	−4	9		
1 kHz	−3.3	9.7	0.3	9	23.0	11.4
1.5 kHz	−2.8	13.0	3	8		
2 kHz	−2.5	10.0	2	9		
Can't hear	6.2	9.0				
Very soft	−4.6	4.6				
Soft	−8.7	4.4				
Medium	−15.7	9.6				

SD, standard deviation.

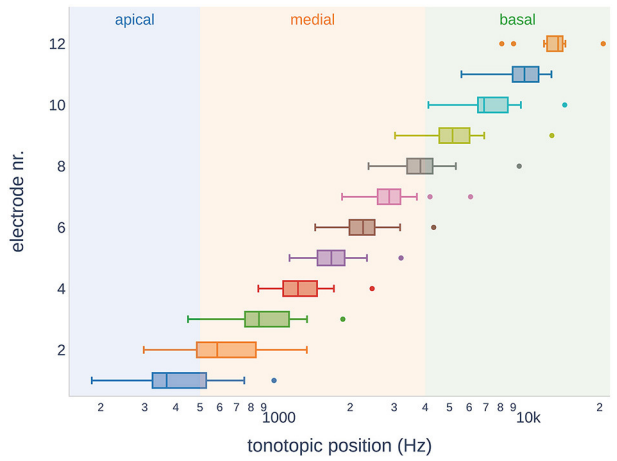

FIGURE 5
Tonotopic positions of the electrodes in the study subjects. Across the subjects, some electrodes showed overlap in the tonotopic region. It should be noted that not all electrode arrays reached the apical region of the cochlea.

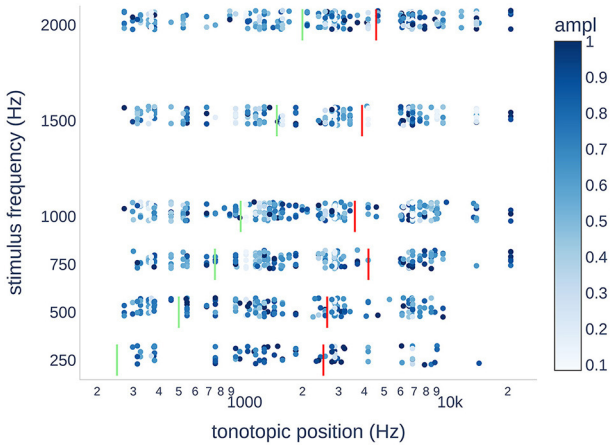

FIGURE 6
Scatter plot of the normalized CM/DIF response amplitudes for each stimulus frequency. The expected tonotopic position is shown in green. The weighted mean tonotopic position found is shown in red. In terms of the tonotopic position, there was a large variance in the objectively present ECochG responses. Generally, the tonotopic position was found to be higher than the stimulation frequency by up to an order of magnitude. Outliers at 20,677 Hz were all from PO19.

the inner ear disease or by slowly progressive cochlear fibrosis as part of the immune response to the electrode array (41). However, the assumption that ECochG can reliably detect discrete inner ear changes should be confirmed in follow-up studies.

Figure 6 shows the normalized CM/DIF amplitudes for all subjects and stimulus frequencies. The weighted mean of the CM/DIF responses (represented by red bars) was substantially higher than the expected tonotopic position (represented by green bars). Furthermore, we observed signals in all the tonotopic regions for each stimulus, with a large variance in the data points. We found a moderate relationship between the stimulus frequency and weighted means of the CM/DIF responses (r^2 = 0.70, p = 0.039). The mean tonotopic positions for the 250 and 500 Hz stimuli were located in the medial cochlear region, whereas the mean tonotopic positions for the higher frequency stimuli were located in the medial and basal regions.

In our results, PABAK values were the highest for the sub-threshold stimulation and the lowest for the near-threshold stimulation. This is not surprising because small variations can lead to a CM/DIF response being detected (or not) by the algorithm. It should be noted that the supra-threshold group contained fewer values because not all subjects had a hearing threshold that allowed >25 dB stimulation at all

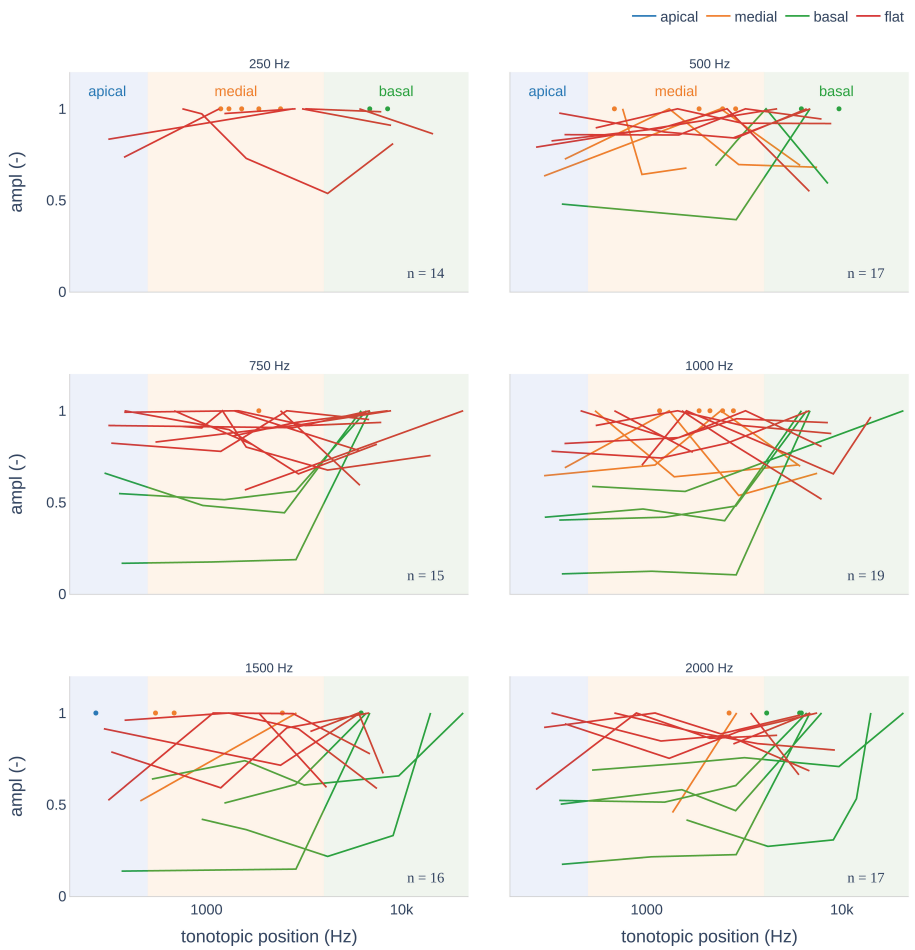

FIGURE 7
CM/DIF pattern distributions recorded from pure-tone stimuli. Depending on the cochlear frequency regions, we distinguished between an apical, medial, and basal peak. If the ECochG amplitudes were approximately the same over the entire electrode array, this was referred to as a flat pattern.

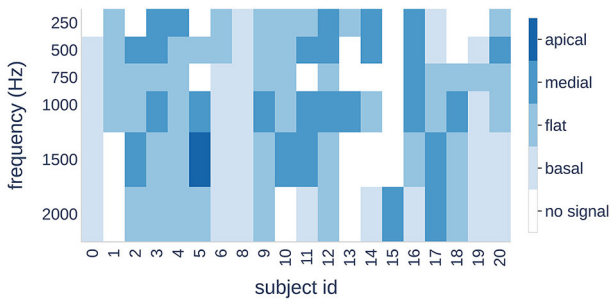

FIGURE 8
Four patterns (color bars) are shown for each subject (horizontal axis) and each stimulus frequency (vertical axis). A change in color indicates a shift of the maximum signal amplitude to a different cochlear region.

frequencies. Therefore, the supra-threshold group showed an increased variance. Additional data are needed to confirm this point.

As described by other researchers (9, 11, 12, 15, 16, 42) and our findings, ECochG recordings show a large, individual variance of amplitudes (4.56 μV_{pp} to 74.46 μV_{pp}). Small amplitudes in poor SNR situations may not be detected by the algorithm. The proposed open-access algorithm can be continuously improved in the future. Therefore, future refinement may improve this resolution.

4.2. Thresholds

In our data, we found a moderate to strong dependence between the CM/DIF and audiometric thresholds. These results are consistent with those of previous research and suggest that post-operative CM/DIF thresholds can be used as objective markers for estimating residual hearing (9, 10). Overall, higher relative stimulation levels resulted in a greater number of objectively detected CM/DIF responses. The mean relative stimulation level that elicited the response was 14.1 dB. Additionally, there was a large variance in the relative hearing threshold that elicited an ECochG response. In some cases, stimuli that were 30 dB below

the hearing threshold elicited an inner ear response (see Figure 3). Overall, the use of below-threshold stimuli resulted in detectable responses in 11.6% of the cases. However, the CM/DIF responses were not always elicited at stimulus levels well above the hearing threshold (up to 48 dB). These results were described in previous studies (10, 16, 42, 43).

The mean ECochG thresholds were above the pure-tone thresholds for all stimulus frequencies. Other groups stated that compared to the pure-tone audiogram, the ECochG threshold was overall lower (16, 43) or higher at lower frequencies and lower at higher frequencies (9, 10). When comparing the results from other studies, it is important to note that the study design may differ (e.g., measurement hardware and software, stimulation protocol, and the use of different scales dB nHL). Recordings were also made at the most apical electrode, whereas we chose the electrode with the lowest CM/DIF threshold (9, 10, 16, 43). Additionally, analysis were performed differently. The signals were evaluated visually (16) or a binning method using the FFT spectrum (4). In one case, the total signal was calculated (adding the SUM and DIF responses) and used instead (43). It should also be noted that some studies compared post-insertion ECochG thresholds with post-operative audiograms (16, 43). However, the residual hearing may have decreased during this period (19, 40).

A subjective loudness scale (instead of pure-tone thresholds) showed a strong correlation for all groups. As expected from the data in Table 2, the correlation was the highest for the *very soft* and *soft* groups. For the *cannot hear* and *medium* groups, we found more outliers reducing utility of a linear model. Outlier in the *cannot hear* group were mostly recorded at higher stimulus frequencies. Therefore, we assume that the subjects heard the repetition rate of the acoustic stimuli and not the actual stimulus frequency.

4.3. Tonotopy and patterns

With respect to the maximum signal amplitudes, we observed a tendency toward tonotopic allocation in our data. However, there was a large variance and the classification was not applicable to all study subjects. Published studies have shown that intracochlear ECochG amplitudes increase toward the tonotopic generator (13, 15, 17). However, some patterns did not follow this order (11–13, 17, 43). It should also be noted that intracochlear ECochG recordings were analyzed using electrode numbers but not the tonotopic locations of the measuring points (9, 11–13, 17). In our opinion, this approach is not optimal. Depending on the study, different electrode arrays (with corresponding variations in the length and inter-electrode spacing) were used. Additionally, the length of the cochlear duct can vary significantly, affecting the tonotopic position (35). Radiographic specification of the tonotopic position may be regarded as more accurate. If available, this information can be obtained using postoperative CT scans. If not available, impedance values or average insertion depths can be used to estimate the electrode positions (44). A possible explanation for the failure to maintain tonotopic organization could be the differences in the function of the hair cell segments within the cochlea. This may result in signal generators that lead to a divergence in the signal pattern (11–13, 17, 43).

In the present study, we observed a clear basal shift in the tonotopic allocation. When stimulated at 250 Hz, the weighted mean was ∼2.5 kHz. This tendency increased when stimulated at higher frequencies. Thus, a 2 kHz stimulus resulted in a weighted mean at ∼4.6 kHz (see Figure 6). There are several possible explanations for basal shift. High-intensity stimuli can activate basally located hair cell populations (3, 11, 15). Additionally, the electrode can touch the basilar membrane and alter the mechanical properties of the microstructures involved in the transduction process (e.g., increased stiffness) (12, 45). Similarly, trauma to the basilar membrane or intracochlear fibrosis as a result of the introduced foreign body could result in a deviation of the stimulation characteristics with a corresponding frequency shift (3, 46).

We divided the CM/DIF amplitudes into four patterns similar to those described in previous research (11, 12, 14, 17). Hypothetically, for a 500 Hz stimulus, we expected a maximum peak in the 500 Hz region (according to our frequency subdivision at the border of the apical and medial cochlear segments). In our study population, the flat pattern was the most common. This finding is consistent with those of Bester et al. (11, 12). One can only speculate on the reasons for the missing peaks. It is possible that poorly functioning hair cell populations are responsible for this phenomenon. If this pattern is already present at the time of electrode insertion, it would certainly be relevant. Many authors expect an apical peak to occur under intra-oberative conditions. Traumatic inner ear events are often suspected in the case of a drop. If a subject does not have a peak pattern (but rather a flat pattern or a basal peak), the CM/DIF amplitude will not increase or even decrease, and the surgeon may be misled into assuming an intracochlear traumatic event. Furthermore, we found that when a peak pattern was present, the tonotopic position of the peak was rarely congruent with the stimulation frequency. A basal shift in the peak patterns was observed with increasing frequency. At 1.5 and 2 kHz, the peaks were not located in the basal region but rather in the medial segment of the cochlea. Bester et al. described this a basal shift when ECochG recordings were repeated after 3 months (12). This could also explain our results because our data were recorded at least 6 months after implantation.

Finally, we examined the individual distribution of the patterns in response to different stimulus frequencies. Our results showed that three subjects had the same pattern for all frequencies, whereas the other subjects showed a transition from one pattern to another.

In conclusion, amplitude patterns can provide important information regarding inner ear function with the implant electrode in place. Further data analysis is necessary to determine which factors are responsible for these patterns.

4.4. Limitations

Our study population had relatively low residual hearing with a mean PTA of 88.7 dB HL (Table 1). However, we were able to measure the ECochG response over time in all but one subject. In our analysis, we focused on the CM/DIF signals. In future, other signal subtypes should be addressed (e.g., ANN/SUM, CAP,

SP potentials, latency measures) (47). These signal subtypes can be implemented using an improved DL algorithm. Finally, other intracochlear biomarkers should be included in the analysis (e.g., impedance measures) as they may reflect around the electrode carrier (12, 48, 49).

5. Conclusions

In this study, we successfully implemented an objective DL-based algorithm to evaluate post-operative intracochlear ECochG recordings. Using an objective analysis, we systematically evaluated and compared ECochG data. In our study, CM/DIF recordings showed substantial repeatability and may indicate the feasibility of using ECochG to monitor inner ear health over time. Additionally, the CM/DIF thresholds showed moderate to strong correlations with audiometric and subjective hearing levels. Finally, we found a basal shift in the tonotopic position of the CM/DIF responses as well as specific intracochlear peak patterns.

Our results help to identify signal patterns and thus better understand inner ear functions with the electrode in place. As a next step, the algorithm should be applied to intra-oberative recordings.

Data availability statement

The datasets presented in this study can be found in online repositories. The name of the repository and accession number can be found at: Dryad, https://datadryad.org/stash/share/hE4oniHffFhggCJzN36T9QnwMqw79nBMeo3A1WNsW3s.

Ethics statement

The studies involving human participants were reviewed and approved by the Cantonal Ethics Committee of Bern (BASEC ID 2019-01578). The patients/participants provided their written informed consent to participate in this study. Written informed consent was obtained from the individuals for the publication of any potentially identifiable data included in this article.

Author contributions

KS performed the measurements, analyzed the data, and wrote the software and paper. WW, CR, and MC provided interpretive analysis and critical revision. SW designed the experiment, analyzed the data, and provided interpretive analysis and critical revision. All authors contributed to this work.

Funding

This study was partly funded by the Department of Otorhinolaryngology, Head and Neck Surgery at the Inselspital Bern, the Clinical Trials Unit (CTU) Research Grant, and the MED-EL Company. Open access funding by University of Bern.

Acknowledgments

The authors would like to thank Marek Polak and his team from MED-EL, Austria, for their support. We would like to thank Editage (www.editage.com) for English language editing.

Conflict of interest

The authors declare that the research was conducted in the absence of any commercial or financial relationships that could be construed as a potential conflict of interest.

Publisher's note

Supplementary material

The Supplementary Material for this article can be found online at: https://www.frontiersin.org/articles/10.3389/fneur.2023.1181539/full#supplementary-material

References

1. Dallos P, Cheatham MA, Ferraro J. Cochlear mechanics, nonlinearities, and cochlear potentials. *J Acoust Soc Am*. (2005) 55:597. doi: 10.1121/1.1914570

2. Snyder RL, Schreiner CE. The auditory neurophonic: basic properties. *Hear Res*. (1984) 15:261–80. doi: 10.1016/0378-5955(84)90033-9

3. Forgues M, Koehn HA, Dunnon AK, Pulver SH, Buchman CA, Adunka OF, et al. Distinguishing hair cell from neural potentials recorded at the round window. *J Neurophysiol*. (2014) 111:580–93. doi: 10.1152/jn.00446.2013

4. Fitzpatrick DC, Campbell AT, Choudhury B, Dillon MP, Forgues M, Buchman CA, et al. Round window electrocochleography just before cochlear implantation: relationship to word recognition outcomes in adults. *Otol Neurotol*. (2014) 35:64–71. doi: 10.1097/MAO.0000000000000219

5. Weder S, Bester C, Collins A, Shaul C, Briggs RJ, O'Leary S. Toward a better understanding of electrocochleography: analysis of real-time recordings. *Ear Hear*. (2020) 41:1560–7. doi: 10.1097/AUD.0000000000000871

6. Weder S, Bester C, Collins A, Shaul C, Briggs RJ, O'Leary S. Real time monitoring during cochlear implantation: increasing the accuracy of predicting residual hearing outcomes. *Otol Neurotol*. (2021) 42:E1030–6. doi: 10.1097/MAO.0000000000003177

7. Wijewickrema S, Bester C, Gerard JM, Collins A, O'Leary S. Automatic analysis of cochlear response using electrocochleography signals during cochlear implant surgery. *PLoS ONE*. (2022) 17:e0269187. doi: 10.1371/journal.pone.0269187

8. O'leary S, Mylanus E, Venail F, Lenarz T, Birman C, Di Lella F, et al. Monitoring cochlear health with intracochlear electrocochleography during cochlear implantation: findings from an international clinical investigation. *Ear Hear*. (2022) 44:358–70. doi: 10.1097/AUD.0000000000001288

9. Haumann S, Imsiecke M, Bauernfeind G., Büchner A, Helmstaedter V, Lenarz T, et al. Monitoring of the inner ear function during and after cochlear implant insertion using electrocochleography. *Trends Hear*. (2019) 23:233121651983356. doi: 10.1177/2331216519833567

10. Koka K, Saoji AA, Litvak LM. Electrocochleography in cochlear implant recipients with residual hearing: comparison with audiometric thresholds. *Ear Hear*. (2017) 38:e161–7. doi: 10.1097/AUD.0000000000000385

11. Bester CW, Campbell L, Dragovic A, Collins A, O'Leary SJ. Characterizing electrocochleography in cochlear implant recipients with residual low-frequency hearing. *Front Neurosci*. (2017) 11:141. doi: 10.3389/fnins.2017.00141

12. Bester C, Dalbert A, Collins A, Razmovski T, Gerard JM, O'leary S. Electrocochleographic patterns predicting increased impedances and hearing loss after cochlear implantation. *Ear Hear*. (2022) 44:710–20. doi: 10.1097/AUD.0000000000001319

13. Calloway NH, Fitzpatrick DC, Campbell AP, Iseli C, Pulver S, Buchman CA, et al. Intracochlear electrocochleography during cochlear implantation. *Otol Neurotol*. (2014) 35:1451–7. doi: 10.1097/MAO.0000000000000451

14. Harris MS, Riggs WJ, Giardina CK, O'Connell BP, Holder JT, Dwyer RT, et al. Patterns seen during electrode insertion using intracochlear electrocochleography obtained directly through a cochlear implant. *Otol Neurotol*. (2017) 38:1415–20. doi: 10.1097/MAO.0000000000001559

15. Honrubia V, Ward PH. Longitudinal distribution of the cochlear microphonics inside the cochlear duct (guinea pig). *J Acoust Soc Am*. (1968) 44:951–8. doi: 10.1121/1.1911234

16. Campbell L, Kaicer A, Briggs R, O'Leary S. Cochlear response telemetry: intracochlear electrocochleography via cochlear implant neural response telemetry pilot study results. *Otol Neurotol*. (2015) 36:399–405. doi: 10.1097/MAO.0000000000000678

17. Campbell L, Bester C, Iseli C, Sly D, Dragovic A, Gummer AW, et al. Electrophysiological evidence of the basilar-membrane travelling wave and frequency place coding of sound in cochlear implant recipients. *Audiol Neurotol*. (2017) 22:180–9. doi: 10.1159/000478692

18. Schuerch K, Wimmer W, Dalbert A, Rummel C, Caversaccio M, Mantokoudis G, et al. Objectification of intracochlear electrocochleography using machine learning. *Front Neurol*. (2022) 13: 943816. doi: 10.3389/fneur.2022.943816

19. Wimmer W, Sclabas L, Caversaccio M, Weder S. Cochlear implant electrode impedance as potential biomarker for residual hearing. *Front Neurol*. (2022) 13:886171. doi: 10.3389/fneur.2022.886171

20. Rasetshwane DM, Trevino AC, Gombert JN, Liebig-Trehearn L, Kopun JG, Jesteadt W, et al. Categorical loudness scaling and equal-loudness contours in listeners with normal hearing and hearing loss. *J Acoust Soc Am*. (2015) 137:1899–913. doi: 10.1121/1.4916605

21. Schuerch K, Wimmer W, Dalbert A, Rummel C, Caversaccio M, Mantokoudis G, et al. An intracochlear electrocochleography dataset - from raw data to objective analysis using deep learning. *Sci Data*. (2023) 10:1–11. doi: 10.1038/s41597-023-02055-9

22. Schuerch K, Waser M, Mantokoudis G, Anschuetz L, Wimmer W, Caversaccio M, et al. Performing intracochlear electrocochleography during cochlear implantation. *J Vis Exp*. (2022) e63153. doi: 10.3791/63153

23. Schraivogel S, Aebischer P, Wagner F, Weder S, Mantokoudis G, Caversaccio M, et al. Postoperative impedance-based estimation of cochlear implant electrode insertion depth. *Ear Hear*. (2023). doi: 10.1097/AUD.0000000000001379. [Epub ahead of print].

24. Davila CE, Mobin MS. Weighted averaging of evoked potentials. *IEEE Trans Biomed Eng*. (1992) 39:338–45. doi: 10.1109/10.126606

25. Kumaragamage CL, Lithgow BJ, Moussavi ZK. Investigation of a new weighted averaging method to improve SNR of electrocochleography recordings. *IEEE Trans Biomed Eng*. (2016) 63:340–7. doi: 10.1109/TBME.2015.2457412

26. Van Drongelen W. *Signal Processing for Neuroscientists*. Amsterdam: Elsevier (2018).

27. Byrt T, Bishop J, Carlin JB. Bias, prevalence and kappa. *J Clin Epidemiol*. (1993) 46:423–9. doi: 10.1016/0895-4356(93)90018-V

28. Feinstein AR, Cicchetti DV. High agreement but low kappa: I. The problems of two paradoxes. *J Clin Epidemiol*. (1990) 43:543–9. doi: 10.1016/0895-4356(90)90158-L

29. Fleiss JL. Measuring nominal scale agreement among many raters. *Psychol Bull*. (1971) 76:378–82. doi: 10.1037/h0031619

30. Hallgren KA. Computing inter-rater reliability for observational data: an overview and tutorial. *Tutor Quant Methods Psychol*. (2012) 8:23. doi: 10.20982/tqmp.08.1.p023

31. Landis JR, Koch GG. The Measurement of observer agreement for categorical data. *Biometrics*. (1977) 33:174. doi: 10.2307/2529310

32. Plummer M, Carstensen B. Lexis: an R class for epidemiological studies with long-term follow-up. *J Stat Softw*. (2011) 38:1–12. doi: 10.18637/jss.v038.i05

33. Van Rossum G, Drake FL. *Python 3 Reference Manual*. Scotts Valley, CA: CreateSpace (2009).

34. McNemar Q. Note on the sampling error of the difference between correlated proportions or percentages. *Psychometrika*. (1947) 12:153–7. doi: 10.1007/BF02295996

35. Li H, Helpard L, Ekeroot J, Rohani SA, Zhu N, Rask-Andersen H, et al. Three-dimensional tonotopic mapping of the human cochlea based on synchrotron radiation phase-contrast imaging. *Sci Rep*. (2021) 11:1–8. doi: 10.1038/s41598-021-83225-w

36. Jamal FN, Arafat Dzulkarnain AA, Shahrudin FA, Marzuki MN. Test-retest reliability of level-specific CE-chirp auditory brainstem response in normal-hearing adults. *J Audiol Otol*. (2021) 25:14–21. doi: 10.7874/jao.2020.00073

37. Kavanagh KT, Crews PL, Domico WD, McCormick VA. Comparison of the intrasubject repeatability of auditory brain stem and middle latency responses elicited in young children. *Ann Otol Rhinol Laryngol*. (1988) 97:264–71. doi: 10.1177/000348948809700310

38. Schuerch K, Waser M, Mantokoudis G, Anschuetz L, Caversaccio M, Wimmer W, et al. Increasing the reliability of real-time electrocochleography during cochlear implantation: a standardized guideline. *Eur Arch Otorhinolaryngol*. (2022) 279:4655–65. doi: 10.1007/s00405-021-07204-7

39. Kompis M, Holzherr H, Pauciello G. *Audiologie*, Vol 14th ed. Göttingen: Hogrefe Verlagsgruppe (2016).

40. Gantz BJ, Hansen M, Dunn CC. Review: Clinical perspective on hearing preservation in cochlear implantation, the University of Iowa experience. *Hear Res*. (2022) 426:108487. doi: 10.1016/j.heares.2022.108487

41. Nadol JB, O'Malley JT, Burgess BJ, Galler D. Cellular immunologic responses to cochlear implantation in the human. *Hear Res*. (2014) 318:11–7. doi: 10.1016/j.heares.2014.09.007

42. Krüger B, Büchner A, Lenarz T, Nogueira W. Amplitude growth of intracochlear electrocochleography in cochlear implant users with residual hearing. *J Acoust Soc Am*. (2020) 147:1147–62. doi: 10.1121/10.0000744

43. Dalbert A, Sim JH, Gerig R, Pfiffner F, Roosli C, Huber A. Correlation of electrophysiological properties and hearing preservation in cochlear implant patients. *Otol Neurotol*. (2015) 36:1172–80. doi: 10.1097/MAO.0000000000000768

44. Aebischer P, Meyer S, Caversaccio M, Wimmer W. Intraoperative impedance-based estimation of cochlear implant electrode array insertion depth. *IEEE Trans Biomed Eng*. (2021) 68:545–55. doi: 10.1109/TBME.2020.3006934

45. Kiefer J. Böhnke F, Adunka O, Arnold W. Representation of acoustic signals in the human cochlea in presence of a cochlear implant electrode. *Hear Res*. (2006) 221:36–43. doi: 10.1016/j.heares.2006.07.013

46. Chole RA, Hullar TE, Potts LG. Conductive component after cochlear implantation in patients with residual hearing conservation. *Am J Audiol*. (2014) 23:359–64. doi: 10.1044/2014_AJA-14-0018

47. Bester C, Weder S, Collins A, Dragovic A, Brody K, Hampson A, et al. Cochlear microphonic latency predicts outer hair cell function in animal models and clinical populations. *Hear Res*. (2020) 398:108094. doi: 10.1016/j.heares.2020.108094

48. Shaul C, Bester CW, Weder S, Choi J, Eastwood H, Padmavathi KV, et al. Electrical impedance as a biomarker for inner ear pathology following lateral wall and peri-modiolar cochlear implantation. *Otol Neurotol*. (2019) 40:e518–26. doi: 10.1097/MAO.0000000000002227

49. Shepherd RK, Clark GM, Xu SA, Pyman BC. Cochlear pathology following reimplantation of a multichannel Scala tympani electrode array in the macaque. *Am J Otol*. (1995) 16:186–99.

frontiers | Frontiers in Neurology

TYPE Original Research
PUBLISHED 06 September 2023
DOI 10.3389/fneur.2023.1231403

OPEN ACCESS

EDITED BY
Armagan Incesulu,
Eskişehir Osmangazi University, Türkiye

REVIEWED BY
Merve Özbal Batuk,
Hacettepe University, Türkiye
Dongzhen Yu,
Shanghai Jiao Tong University, China

*CORRESPONDENCE
Marco D. Caversaccio
✉ Marco.caversaccio2@unibe.ch
Tom Gawliczek
✉ tom.gawliczek@insel.ch

RECEIVED 30 May 2023
ACCEPTED 21 August 2023
PUBLISHED 06 September 2023

CITATION
Gawliczek T, Mantokoudis G, Anschuetz L, Caversaccio MD and Weder S (2023) Comparison of auditory brainstem response and electrocochleography to assess the coupling efficiency of active middle ear implants. *Front. Neurol.* 14:1231403. doi: 10.3389/fneur.2023.1231403

Comparison of auditory brainstem response and electrocochleography to assess the coupling efficiency of active middle ear implants

Tom Gawliczek[1]*, Georgios Mantokoudis[1], Lukas Anschuetz[1], Marco D. Caversaccio[1,2]* and Stefan Weder[1]

[1]Department of ENT, Head and Neck Surgery, Bern University Hospital, University of Bern, Bern, Switzerland, [2]Hearing Research Laboratory, ARTORG Center for Biomedical Engineering Research, University of Bern, Bern, Switzerland

Aim: This study aimed to compare the effectiveness of auditory brainstem response (ABR) and extracochlear electrocochleography (ECochG) in objectively evaluating the coupling efficiency of floating mass transducer (FMT) placement during active middle ear implant (AMEI) surgery.

Methods: We enrolled 15 patients (mean age 58.5 ± 19.4 years) with mixed hearing loss who underwent AMEI implantation (seven ossicular chain and eight round window couplings). Before the surgical procedure, an audiogram was performed. We utilized a clinical measurement system to stimulate and record intraoperative ABR and ECochG recordings. The coupling efficiency of the VSB was evaluated through ECochG and ABR threshold measurements. Postoperatively, we conducted an audiogram and a vibrogram.

Results: In all 15 patients, ABR threshold testing successfully determined intraoperative coupling efficiency, while ECochG was successful in only eight patients. In our cohort, ABR measurements were more practical, consistent, and robust than ECochG measurements. Coupling efficiency, calculated as the difference between vibrogram thresholds and postoperative bone conduction thresholds, was found to be more accurately predicted by ABR measurements (p = 0.016, R^2 = 0.37) than ECochG measurements (p = 0.761, R^2 = 0.02). We also found a non-significant trend toward better results with ossicular chain coupling compared to round window coupling.

Conclusion: Our findings suggest that ABR measurements are more practical, robust, and consistent than ECochG measurements for determining coupling efficiency during FMT placement surgery. The use of ABR measurements can help to identify the optimal FMT placement, especially with round window coupling. Finally, we offer normative data for both techniques, which can aid other clinical centers in using intraoperative monitoring for AMEI placement.

KEYWORDS

active middle ear implant, coupling efficiency, objective measures, electrocochleography, auditory brainstem response, Vibrant Soundbridge

1. Introduction

Active middle ear implants (AMEIs) are medical devices intended for the treatment of hearing loss by direct stimulation of the middle ear structures. The Vibrant Soundbridge (MED-EL, Austria) is currently the most commonly used implant (1, 2). AMEIs are employed to provide amplification in individuals with hearing loss who are unable to use conventional hearing aids due to issues with their outer or middle ear (3). These include chronic infections of the outer or middle ear, atresia or stenosis of the ear canal, or problems with feedback when using conventional hearing aids. They may be recommended for patients with sensorineural, conductive, or mixed hearing loss (4).

The external component of the AMEI is a sound processor that transmits the auditory signal digitally to the implant. The implantable part comprises a coil, a magnet, a demodulator, and a floating mass transducer (FMT). One of the significant benefits of the MED-EL Soundbridge is its adaptability concerning surgical placement. Depending on the individual's anatomy and hearing loss characteristics, the FMT can be attached to the ossicular chain (i.e., the incus or stapes), the round window, or the oval window. However, suboptimal placement of the FMT can negatively affect sound amplification and patient satisfaction (4, 5). One major reason for poor coupling is the large number of degrees of freedom (for example, on the round window, the FMT can be placed differently into the niche (6, 7). There is a high number of reported subobtimal FMT placements with associated revisions surgeries (6, 8–10). Any solution offering to the surgeon an intraoperative objective evaluation of the coupling efficiency is therefore crucial.

Neurophysiological recordings, such as extracochlear electrocochleography (ECochG) and auditory brainstem response (ABR) measurements, can aid in identifying the optimal FMT placement. Prior research has demonstrated that ECochG recordings can enhance surgical techniques for round window placement (6), while ABR potentials have been utilized to evaluate FMT placement at different anatomical locations (9–11).

Despite these findings, a direct comparison between the two recording techniques, including signal analysis, is lacking. Therefore, our study aimed to address this gap and determine the feasibility, surgical aspects, and coupling efficiency of the two methods. We considered the technical setup, audiological assessment, and coupling modalities to determine whether ECochG and ABR are equivalent in terms of providing accurate and reliable information for optimizing FMT placement.

2. Materials and methods

2.1. Study design and demographics

Our exploratory study was executed in compliance with the principles outlined in the Declaration of Helsinki and the regulations established by the local ethics commission (BASEC-ID no. 2019-00555). Written informed consent was obtained from all participants. The study enrolled 15 patients who underwent implantation of a Vibrant Soundbridge VORP503 (MED-EL, Austria) between May 2021 and March 2023.

2.2. Pre-operative and postoperative assessments

Before the surgical procedure, an audiogram was performed on all participants within a sound attenuated acoustic chamber using a calibrated device (Interacoustics, Denmark). This evaluation included the assessments of air conduction (AC) and bone conduction (BC) thresholds in dB HL. Pure tone average (PTA) was calculated from measurements at 1,000, 2,000, and 4,000 Hz for the implanted side (8, 12). Four weeks after the implantation, we assessed BC and vibrogram thresholds with implant (latter in dB HL eq.). The demographic and audiological evaluations of the participants are presented in Table 1.

2.3. Intraoperative measurement setup

We utilized a clinical measurement system to stimulate and record all intraoperative electrophysiological recordings (Eclipse, EP version 4.6, Interacoustics A/S, Denmark). To facilitate stimulation, we connected a Vibrant Soundbridge audio processor to the implant by wrapping it in a sterile bag and attaching it to the coil of the implant, which had already been positioned and fixed in a subperiosteal pocket in its final location. At the opposite end, we connected the audio processor to an AcousticAP device (MED-EL, Innsbruck, Austria), which enabled us to connect the measurement system to the Eclipse system. The AcousticAP with audio processor generated a calibrated signal referenced to the in-ear headphones (IP30 insert phone speaker, 50 ohm) of the Eclipse system. To maintain consistency, we utilized the output/voltage intensity levels calibration as provided by the manufacturer. Figure 1 shows a schematic of the measurement setup.

For recording purposes, we positioned adhesive recording electrodes on the head, with a distance of approximately 1.5 cm between the "+" electrode and the ground "gr" electrode. The reference electrodes ("−") were positioned on the ipsilateral neck and contralateral mastoid, respectively. Prior to the start of the measurements, we ensured that all adhesive electrodes had an impedance lower than 3 kOhm. For measurements, we initially set a noise rejection level of 80 μV. In situations with significant background noise, a decision was made to increase the suppression level to 320 V in a specific case. This adjustment also resulted in an increase in the minimum number of sweeps to 2,500. The objective was to attain a residual noise level of 60–40 nV or lower, adhering to the manufacturer's system recommendation, in order to precisely assess thresholds.

2.4. Intraoperative data collection

We conducted intraoperative electrophysiological measurements immediately after placement of the FMT. For stimulation during ABR measurements, we used a broadband LS CE-Chirp with a stimulation frequency of 49.1 Hz at alternating polarities (condensation and rarefaction). We chose this approach because previous research has shown that it increases the amplitude of the signal (13). After the definitive placement of the FMT, the

TABLE 1 Characteristics of the 15 subjects.

No.	Sex	Side	Type	Coupler	Disease leading to hearing loss	Number of previous ear surgeries	Reasons for Soundbridge surgery	Surgery	Preoperative (dB HL)			Intraoperative (dB nHL)		Post-operative (dB HL eq.)
									BC	AC	ABG	ABR	ECochG	Vibrogram
1	m	Left	Imp	RW	Cholesteatoma	3	Infected radical cavity, increasing mixed hearing loss	Subtotal petresectomy with blind sack closure, RW coupling	47 (20–65)	98 (80–110)	51	60	Nm	45 (40-50)
2	f	Left	Imp	SH	Cholesteatoma	2	Increasing mixed hearing loss; extrusion of Partial Ossicular Chain Replacement (PROP)	Combined transcanal-transmastoid placement of SH stapes coupler	33 (15–45)	85 (75–105)	52	55	Nm	48 (35–70)
3	m	Left	Rev	RW	Complex petrous bone fracture with combined hearing loss	2	FMT dislocation	Transcanal revision of FMT placement RW niche	60 (55–65)	92 (90–95)	32	80	Nm	63 (55–75)
4	m	Left	Rev	RW	Chronic otitis media	4	FMT dislocation	Transcanal revision of FMT placement RW niche	28 (15–35)	85 (75–105)	57	60	50	42 (30–50)
5	m	Right	Imp	RW	Cholesteatoma	2	Infected radical cavity	Subtotal petresectomy with blind sack closure, RW coupling	38 (30–50)	62 (55–70)	24	60	70	67 (60–80)
6	f	Right	Imp	SH	Mucoepidermoid carcinoma of the parotid gland	0	Post-irradiation osteoradionecrosis of the petrous bone	Subtotal petresectomy with blind sack closure, SH stapes coupling	53 (45–60)	67 (60–75)	14	60	Nm	67 (60–75)
7	m	Right	Imp	SH	Nasopharyngeal carcinoma	0	Post-irradiation osteoradionecrosis of the petrous bone	Subtotal petresectomy with blind sack closure, SH stapes coupling	40 (10–55)	67 (30–100)	27	80	80	62 (45–75)
8	m	Left	Imp	SH	Cholesteatoma	5	Recurring Cholesteatoma and increasing mixed hearing loss	Subtotal petresectomy with blind sack closure, SH stapes coupling	40 (25–50)	98 (85–115)	58	50	70	53 (35–65)
9	m	Left	Imp	RW	Tympanosclerosis	4	Increasing mixed hearing loss	Transmastoid placement of RW coupling	40 (25–50)	80 (70–95)	40	70	80	60 (40–70)
10	m	Left	Imp	RW	Explosion trauma and subsequent cholesteatoma	1	Increasing mixed hearing loss	Revision radical cavity, RW coupling	20 (10–30)	78 (75–80)	58	40	50	30 (20–40)

(Continued)

10.3389/fneur.2023.1231403

TABLE 1 (Continued)

No.	Sex	Side	Type	Coupler	Disease leading to hearing loss	Number of previous ear surgeries	Reasons for Soundbridge surgery	Surgery	Preoperative (dB HL)			Intraoperative (dB nHL)		Post-operative (dB HL eq.)
									BC	AC	ABG	ABR	ECochG	Vibrogram
11	f	Left	Rev	SH	Inability to use conventional hearing aids	1	Increasing mixed hearing loss	Combined transcanal-transmastoid placement of SH stapes coupler	67 (55–75)	82 (75–95)	15	75	Nm	50 (45–60)
12	m	Left	Imp	RW	Tympanosclerosis	0	High degree of mixed hearing loss	Transmastoid placement of RW coupling	33 (15–45)	97 (75–115)	64	80	Nm	87 (80–95)
13	m	Right	Imp	SH	Nasopharyngeal carcinoma	1	Post-irradiation osteoradionecrosis of the petrous bone	Subtotal petresectomy with blind sack closure, SH stapes coupling	35 (10–60)	53 (35–90)	18	55	70	52 (35–80)
14	f	Right	Imp	RW	Tympanosclerosis	1	High degree of mixed hearing loss	Transmastoid placement of RW coupling	42 (35–50)	77 (75–80)	35	65	Nm	58 (50–65)
15	m	Left	Imp	INC	Sudden Sensineural Hearing Loss	0	No success with conventional hearing aids	Transmasoid placement of shot incus coupling	55 (50–60)	62 (55–65)	7	70	70	78 (75–85)

The AC, BC, and vibrogram thresholds show the average values across three frequencies (1, 2, and 4 kHz) with their minimum and maximum values. Improvement the coupling modalities consist of round window coupler (RW) and ossicular chain coupling, which involve the use of Stapes coupler (SH) and Incus coupler (INC). The types of surgery were referred to as implantation (Imp) and revision surgery (Rev). Preoperative air conduction (AC) and bone conduction (BC) thresholds, intraoperative thresholds (ABR and ECochG), air-bone gap (ABG) and postoperative *in situ* thresholds with implant (Vibrogram).

10.3389/fneur.2023.1231403

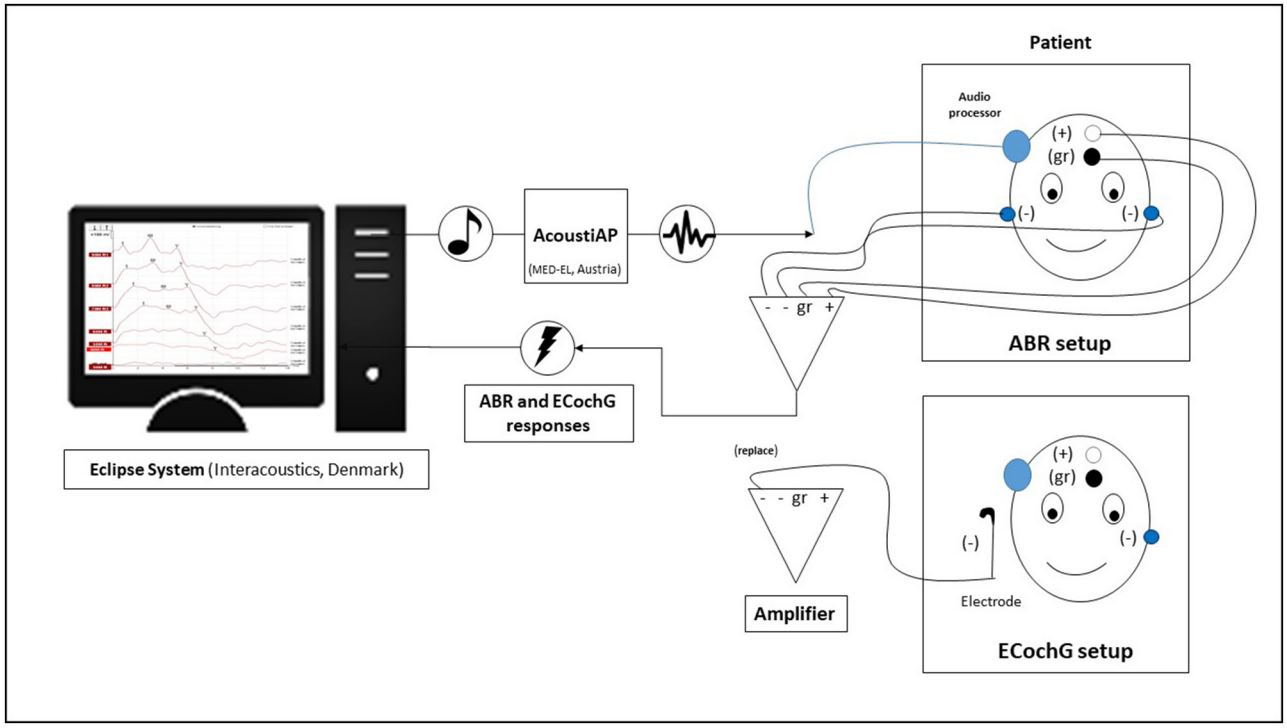

FIGURE 1
The diagram shows the intraoperative setup using the Eclipse system. The electrodes were taped differently for auditory brainstem response (ABR) and electrocochleography (ECochG) measurements.

ABR measurement procedure started with a stimulus intensity of 90 dB, followed by reduction in steps of 10 dB until no signal was visible (Figure 2A). In four cases, an additional measurement at the threshold level using a 5 dB step interval could be conducted due to time constraints during the surgical procedure (Table 1). The electrophysiological threshold was confirmed with a second measurement. If no electrophysiological response was observed at 90 dB or the threshold was high, the FMT was re-positioned and the ABR measurements were repeated until the clearest possible signal was obtained. If multiple ABR measurements were performed, only those values with the final FMT position were used in subsequent data analysis.

In a next step, we performed the extracochlear ECochG measurements (Figure 2B). The surgeon placed a sterile electrode (PromStim, MED-EL, Austria) on the promontory, connected to the ipsilateral channel of the preamplifier of the recording system. Impedance values were monitored and the electrode repositioned as required until a value of less than 20 kOhm was achieved. For stimulation, sinusoidal tone bursts at a frequency of 1.5 kHz (with a Blackman function) were used (8). As described above, ECochG measurements started at 90 dB and were lowered step-wise by 10 dB. However, the positioning of the FMT was not changed, as the final placement had previously been determined using the ABR method.

For both electrophysiological recordings, signal analysis was performed visually by two experts. In case of no consensus among experts, the higher threshold value was considered. Only signals with a response in both the condensation and rarefaction measurements were considered. During the ABR recordings, they paid attention to the occurrence and course of the wave V. For the ECcochG responses, they looked at the summation potential (summation of the response to the condensation and rarefaction stimulus).

2.5. Data analysis

We used GraphPad Prism 9.3.1 software (GraphPad Software, USA) for statistical analysis and data visualization. First, we assessed our data using Pearson correlation. Thereby, we compared intraoperative measurements (ABR and ECochG) to preoperative BC thresholds (Figures 3A, B). Figures 3C, D illustrate the relative coupling efficiency for both ABR and ECochG measurements. To create these graphs, we subtracted the postoperative BC threshold from the postoperative vibrogram threshold and plotted the resulting value against the difference between the intraoperative threshold and the preoperative bone conduction threshold. Finally, we compared subjects with ossicular chain (OC) and round window (RW) coupling modalities in respect to coupling efficiency. For this analysis a Mann-Whitney test was performed with a statistical significance level of 0.05.

3. Results

3.1. Patient demographics

We included 15 patients who underwent implant surgery (Vibrant Soundbridge VORP 503, MED-EL, Austria), including

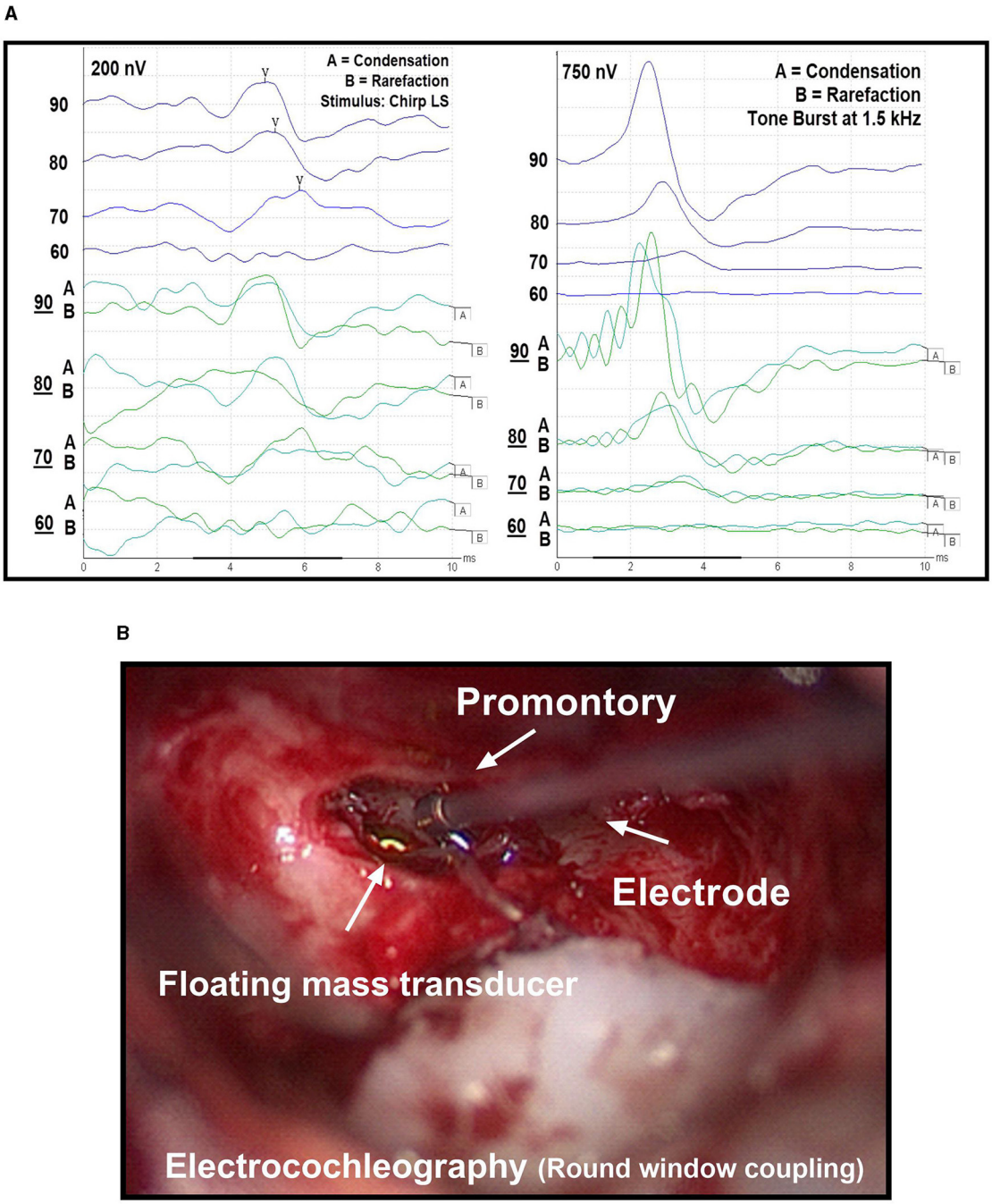

FIGURE 2
(A) Threshold measurement using auditory brainstem response (ABR, left) and electrocochleography (ECochG, right). In both methods, a 90 dB stimulus is gradually reduced in 10 dB steps until no response is visible. Rarefaction and condensation levels are represented by **(A, B)** curves, respectively. The average of the summation of both curves results in the overall curve. **(B)** Extracochlear electrocochleography (ECochG) measurement using a commercially available electrode, which is held on the promontory during recordings.

three revision cases (Table 1). Eleven males and four females were on average 58.5 years old (range 39–79 years). The FMT was connected in six cases to the OC (six stapes head couplers and one incus coupler) and eight times to the RW. The pure tone average hearing thresholds after surgery (BC 43.2 dB HL SD ± 13.7; AC 85.3 dB HL, SD ± 12.6) were almost identical to the preoperative BC threshold (42.1 dB HL, SD ± 12.4) and somewhat lower for the AC threshold (78.8 dB HL, SD ± 14.3).

3.2. Electrophysiological recordings

We were able to successfully measure an ABR response in all 15 cases. For the ECochG measurements, this was only the case in 8 subjects. In two cases, significant impedance fluctuations were observed. One possible reason is the entry of blood traces into the surgical site, which causes impedance changes. At the same time, stable electrode positioning is made more difficult.

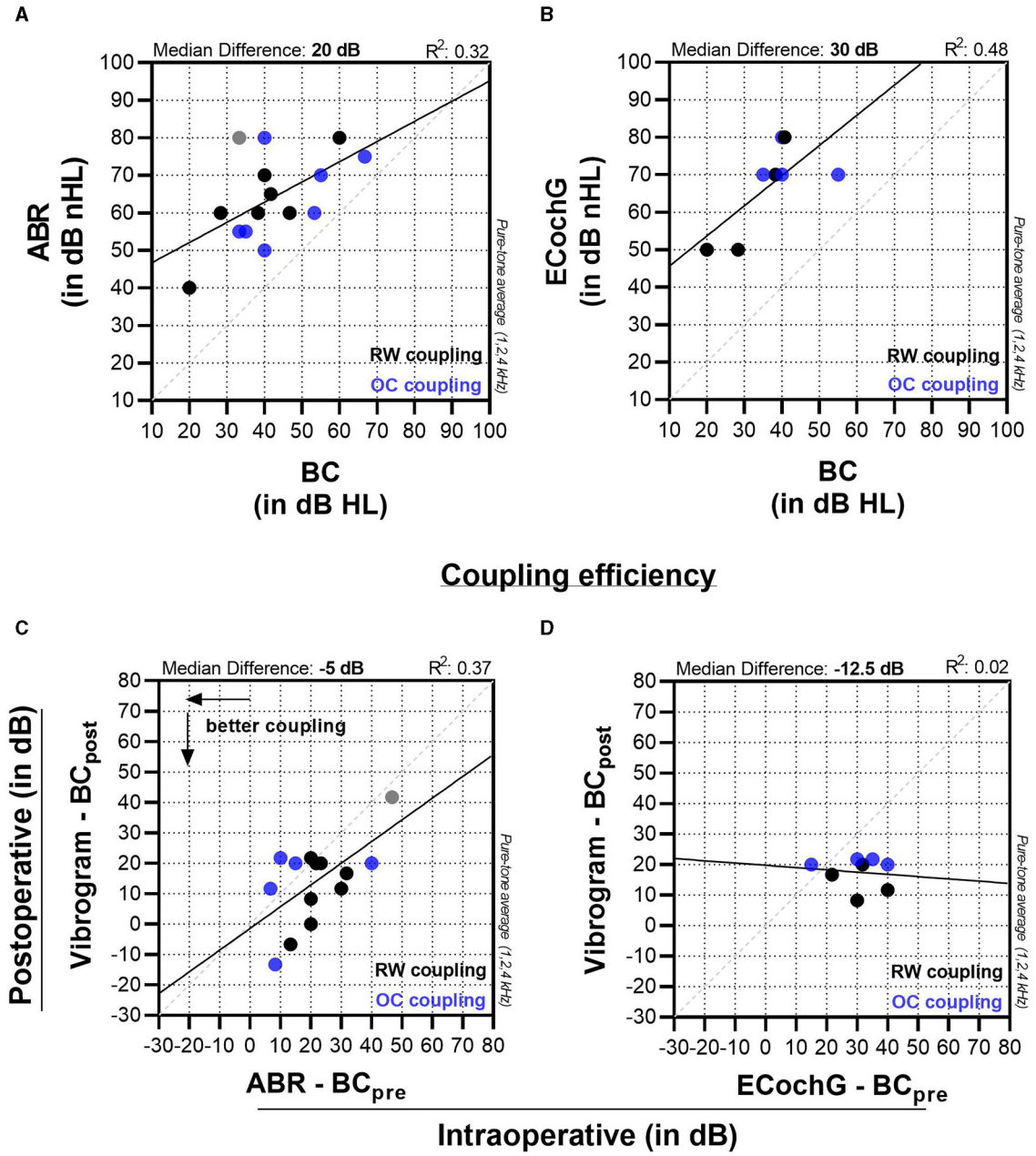

FIGURE 3
Panels **(A, B)** display the comparison of intraoperative ABR and ECochG measurements to preoperative bone conduction (BC) thresholds. Graphs **(C, D)** compare the coupling efficiency (vibrogram thresholds—postoperative BC thresholds) to the intraoperatively measured threshold (intraoperative ABR—preoperative BC threshold).

In three cases, the signal-to-noise ratio was too low to record meaningful measurements. In one of these cases, the ECochG traces were affected by a second synchronous signal, possibly due to the patient's pacemaker. Finally, in two patients, threshold measurements were started but could not be completed due to recurrent signal loss. After several attempts, the measurements were stopped in order not to prolong the anesthesia time unnecessarily.

For ABR measurements in our cohort, the experts detected a wave-V response with a median of 60 (55 to 75) dB nHL. This value was 20 dB higher than the preoperative BC thresholds, which were 40 (33.3 to 53.3) dB, and showed a moderate effect size (R^2 = 0.32, p = 0.029). The coupling efficiency on the other hand (Vibrogam threshold—postoperative BC threshold) was −5 (−20 to 2) dB (Figure 3C) with a moderate to strong effect size (R^2 = 0.37, p = 0.016). There was one outlier (patient no. 12, Table 1), where there was a marked ossification of the round window niche. A satisfactory intraoperative FMT coupling was not possible in this case, which was later confirmed by the postoperative coupling efficiency. ECochG measurement was not possible in this case due to poor SNR.

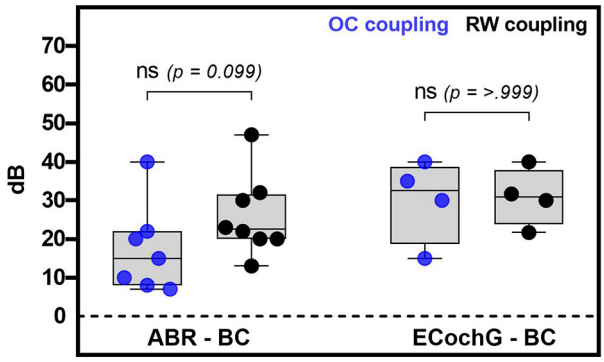

FIGURE 4
This figure shows the analysis of the coupling modality used in relation to the intraoperative electrophysiological (ABR or ECochG) minus the preoperative bone conduction thresholds. The blue dots in the graph represent coupling with the ossicular chain, while the black dots represent coupling with the round window. In this context, whiskers represent the minimum and maximum values, while boxes represent the median and quartiles. No significant difference was found between coupling with the ossicular chain and the round window for both methods.

For ECochG measurements, the median signal threshold was 70 (55–77.5) dB nHL and lay 30 dB higher (Figure 3B) compared to the preoperative BC threshold (near-significant moderate to strong effect size, R^2 = 0.48, p = 0.056). For ECochG (Figure 3D), the coupling efficiency showed no linear correlation (R^2 = 0.02, p = 0.761).

3.3. Coupling modalities

Figure 4 displays the measured ABR and ECochG thresholds comparing the ossicular chain and round window coupling. The results of the rank test comparison indicated no statistically significant difference between the two coupling modalities for measuring with ABR (p = 0.099) or EcochG ($p \geq 0.999$). However, looking at the ABR-BC thresholds, there was a trend toward better sound transmission when using a OC coupler. For both FMT placements, the ABR measurements lay 15 (8 to 22) dB (OC) and 22.5 (20 to 31.5) dB (RW) above the BC thresholds. For the EcochG recordings, these values were higher [32.5 (18.75 to 38.75) dB and 30.9 (23.8 to 37.9) dB, respectively], regardless of the coupling modality.

4. Discussion

The objective of this study was to compare the effectiveness of two electrophysiological methods, namely ECochG and ABR, in assessing the coupling efficiency during the implantation of AMEIs (Table 2). Our study yields three primary findings. First, intraoperative monitoring of coupling efficiency is feasible and can enhance the AMEI implantation procedure by enabling real-time feedback to the surgeon and a preliminary assessment of the patient's postoperative outcome. Second, we observed that ABR is a more sensitive method than ECochG for measuring coupling efficiency in middle ear implants, utilizing the same test setup, patient, and surgical environment. ABR also demonstrated higher feasibility and reliability in clinical application. Finally, we offer normative data for both techniques, which can aid other clinical centers in using intraoperative monitoring for AMEI placement.

4.1. Study cohort

In our cohort, we observed successful preservation of cochlear function in all 15 participants after AMEI implantation (as shown in Table 1). However, on average, there was a slight worsening of air conduction thresholds postoperatively, which was attributed to blind sack closure and reduced sound transmission. It is noteworthy that most study participants had a history of multiple ear surgeries or had been irradiated because of a malignancy. In these cases, efficient coupling of the FMT may be more difficult due to scar tissue formation. Furthermore, six study subjects had preoperative inner ear hearing thresholds near the implant's hearing indication range ($\geq$ 60 dB HL). In such cases, even minor differences in coupling efficiency can have a significant impact on postoperative outcomes, highlighting the importance of intraoperative monitoring. Poor coupling can result in patient dissatisfaction and non-use of the implant.

4.2. ECochG

In our study, the process of obtaining threshold estimations using EcochG proved to be challenging. Only 8 out of 15 cases yielded successful measurements due to issues such as fluctuating impedance values. It is worth noting that previous studies have not reported the number of failed measurements, but rather only the successful ones (6–8). The existing literature on evaluating coupling efficiency in AMEIs has primarily focused on ABR measurements (9–12, 14–16). It should be noted that the ECochG measurement has limitations, as it requires active participation from the surgeon and is only feasible if the promontory is accessible during surgery. Furthermore, postoperative measurements cannot be conducted in the same manner, and alternative methods such as ECochG measurement via a tympanic electrode may not provide an identical test setup. These limitations should be taken into account when interpreting the results.

Our experience suggests that intraoperative ECochG measurements are highly dependent on the positioning of the measuring electrode. Despite our efforts to place the electrode as close as possible to the round window niche, the surgical approach and type of coupler used can limit this positioning. The transmastoid round window coupling technique can pose challenges in terms of electrode placement, as the position of the electrode must not interfere with the placement of the FMT.

Furthermore, we found that the average thresholds of the ECochG measurements were 30 dB higher than the preoperative BC threshold and thus higher than the ABR measurements. The correlation between ECochG values and preoperative BC thresholds was slightly better than ABR, but worse with vibrogram

TABLE 2 Comparative analysis of intraoperative monitoring (i.e., auditory brainstem response/ABR and electrocochleography/ ECochG).

Auditory brainstem response (ABR)	*Electrocochleography (ECochG)*
Electrode location	
(−) Measurement distant to cochlea	(+) Measurement close to cochlea
Interferences	
(+) Adhesive electrodes have higher noise rejection	(−) Manual electrode placement increases the susceptibility to noise interference
Time of measurements	
(+) Shorter, measurement independent of surgeon	(−) Longer, measurement dependent on surgeon (additional positioning of electrode, i.e., 45 s to 3 min)
Coupling testing (reliability)	
(+) Measurements are possible during FMT coupling, after coupling (intraoperatively until wound closure) and at any point postoperatively (longitudinal comparison)	(−) Measurements can only be performed intraoperatively as long as the promontory is accessible (no longitudinal comparison)
Signal quality	
(+) Lower risk of surface impedance changes on reference electrodes (−) Far field increases risk of electrophysiological side effects (e.g., muscle contraction).	(+) Detection in the near field may result in higher signal amplitudes
Surgical handling	
(+) No risk of affecting the coupling of the FMT (+) ABR measurements are independent form surgeon (no additional operative steps, good reproducibility, as the measurements are always performed in the same way)	(−) The placement of the measuring electrode may affect the coupling of the FMT (in case of physical contact) (−) Body liquids (e.g., blood trickling) has impact on impedance (−) Variation in positioning the measurements electrode has impact on the recordings

For the two techniques, the positive (+) and negative (−) aspects are shown.

values. It is important to note, however, that caution should be exercised in interpreting these results, as the ECochG group in our study was relatively small.

4.3. ABR

We were able to successfully obtain ABR measurements from all participants in our cohort, both during and after surgery. In contrast to ECochG, we observed that ABR measurements could be more easily integrated into the surgical procedure, as they do not necessitate active intervention from the surgeon and are less prone to abrupt signal loss, such as that caused by impedance fluctuations.

In our study, the mean intraoperative ABR thresholds were found to be approximately 20 dB higher than the preoperative PTA of the bone conduction thresholds. Moreover, the coupling efficiency, which represents the difference between the vibrogram thresholds and postoperative bone conduction thresholds, showed a stronger correlation with the intraoperatively measured ABR thresholds compared to ECochG. Additionally, when comparing coupling efficiency values obtained intraoperatively and 4 weeks postoperatively, our results showed stable or slightly improved values with an average improvement of 5 dB in our study cohort. In terms of the various coupling modalities, there was a non-significant trend toward better outcomes with OC couplers, which is not surprising.

Comparison with previously published thresholds remains difficult due to the lack of consensus on measurement setup, stimulation type, and analysis methods. Geiger et al. (11) investigated the implantation of a Vibrant Soundbridge in 30 patients and reported that intraoperative thresholds were approximately 4 dB lower than the preoperative bone conduction threshold (median, pure tone mean of 0.5, 1, 2, and 4 kHz), which is in contrast to our results (Figure 3A, 20 dB). In a subsequent study, the same research group performed intraoperative monitoring in 14 revision cases and observed no significant correlation between preoperative bone conduction thresholds and intraoperative measurements (10). However, they did find a significant correlation between intraoperative measurements and postoperative vibrogram thresholds. It is challenging to draw direct comparisons between our results and theirs as they employed a different stimulus for intraoperative assessment and a prefitted audio processor.

Fröhlich et al. conducted a study of 18 patients with similar demographic and audiological characteristics to our cohort (17). They investigated the frequency-specific coupling efficiency and

found a range of postoperative coupling efficiency from approx. −10 to 40 dB and coupling efficiency ranging from −13.30 to 41.7 dB (Figure 3C), which is comparable to our findings. It should be noted, however, that direct comparisons between our study and that of Fröhlich et al. should be made with caution because Fröhlich et al. used a preprogrammed sound processor with an attached insert earphone for each implantation, resulting in different intraoperative ABR measurements. A recent study conducted by Sprinzl et al. presented findings similar to our study in terms of test design, measurements, cohort, and data analysis with 14 AMEI implantations (16). Our results showed an intraoperative ABR threshold almost identical to theirs. In the comparison between both studies, a discrepancy of 13 dB was observed specifically for the intraoperative threshold when compared to the preoperative bone conduction (BC) threshold. It is important to note that when making comparisons between studies, differences in the signal analysis methods employed and variations in individual hearing thresholds must be considered, even if the study design is similar.

In conclusion, our results suggest that electrophysiological measurement of coupling efficiency is useful when placing the FMT in AMEIs. This is particularly important for round window coupling, which increases the degrees of freedom of possible FMT placements. In comparing the two measurement methods (ABR and ECochG), we used available hard- and software without the need for additional programming. Our measurement setup can therefore be replicated by other centers.

When comparing the two measurement methods, ABR measurements were significantly more practical, could be better integrated into the surgical procedure, were more robust and consistent, and were less susceptible to interference. Furthermore, the ECochG measurements can be conducted in the post-operative setting, enabling the assessment of FMT coupling over time and the longitudinal evaluation of its performance.

4.4. Limitations

A major limitation of our study is the lack of technical calibration of the audio processor for the frequency-specific properties of the FMT in stimulus and related coupling modality. Such an evaluation would be valuable in interpreting the results and selecting the optimal stimulus for threshold determination. Additionally, for the two electrophysiological measurements, we used two different stimuli. These stimuli were selected based on previous research where they were evaluated and proposed accordingly (8, 14). Caution should be exercised when making a direct comparison between the two results. Lastly, our study was limited by a small cohort size, and future research with larger sample sizes will be necessary to validate our threshold values.

5. Conclusion

Monitoring the coupling efficiency of AMEIs is crucial, particularly in patients with a round window coupler. In our comparative study between ABR and ECochG measurements, ABR performed significantly better in terms of its seamless integration into the surgical workflow, higher success rate of measurements, threshold distance to the effective hearing threshold, and the feasibility of postoperative measurements. These findings highlight the importance of selecting the appropriate measurement technique to ensure accurate and reliable monitoring of coupling efficiency in AMEIs.

Data availability statement

The original contributions presented in the study are included in the article/supplementary material, further inquiries can be directed to the corresponding authors.

Ethics statement

The studies involving humans were approved by Swiss Association of Research Ethics Committee (BASEC-ID no. 2019-00555). The studies were conducted in accordance with the local legislation and institutional requirements. The participants provided their written informed consent to participate in this study.

Author contributions

TG, SW, and GM were involved in material preparation and data collection. Designed the study and data analysis were performed by TG and SW. TG performed the statistical analysis. MC, GM, LA, and SW provided resources and supervision. All authors contributed to this work and provided feedback on the final manuscript.

Funding

The author(s) declare that no financial support was received for the research, authorship, and/or publication of this article.

Acknowledgments

We express our gratitude to the Vibrant Research Team at MED-EL (Innsbruck, Austria), particularly to Hamidreza M., Bicego L., and Blanc S., for their valuable technical support and equipment provided during the study.

Conflict of interest

The authors declare that the research was conducted in the absence of any commercial or financial relationships that could be construed as a potential conflict of interest.

Publisher's note

All claims expressed in this article are solely those of the authors and do not necessarily represent those of their affiliated

organizations, or those of the publisher, the editors and the reviewers. Any product that may be evaluated in this article, or claim that may be made by its manufacturer, is not guaranteed or endorsed by the publisher.

References

1. Ball GR, Rose-Eichberger K. Design and development of the vibrant soundbridge–A 25-year perspective. *J Hear Sci.* (2021) 11:9–20. doi: 10.17430/JHS.2021.11.1.1

2. Labassi S, Beliaeff M, Péan V, Van de Heyning P. The Vibrant Soundbridge® middle ear implant: a historical overview. *Cochlear Implants Int.* (2017) 18:314–23. doi: 10.1080/14670100.2017.1358913

3. Pegan A, Ries M, Ajduk J, Bedeković V, Ivkić M, Trotić R. Active middle ear vibrant soundbridge sound implant. *Acta Clin Croat.* (2019) 58:348–53. doi: 10.20471/acc.2019.58.02.20

4. Ernst A, Todt I, Wagner J. Safety and effectiveness of the Vibrant Soundbridge in treating conductive and mixed hearing loss: a systematic review. *Laryngoscope.* (2016) 126:1451–7. doi: 10.1002/lary.25670

5. Sprinzl GM, Schoerg P, Muck S, Jesenko M, Speiser S, Ploder M, et al. Long-term stability and safety of the soundbridge coupled to the round window. *Laryngoscope.* (2021) 131:E1434–42. doi: 10.1002/lary.29269

6. Colletti V, Mandale M, Colletti L. Electrocochleography in round window vibrant soundbridge implantation. *Otolaryngol Head Neck Surg.* (2012) 146:633–40. doi: 10.1177/0194599811430808

7. Mandalà M, Colletti L, Colletti V. Treatment of the atretic ear with round window vibrant soundbridge implantation in infants and children: electrocochleography and audiologic outcomes. *Otol Neurotol.* (2011) 32:1250–5. doi: 10.1097/MAO.0b013e31822e9513

8. Radeloff A, Shehata-Dieler W, Rak K, Scherzed A, Tolsdorff B, Hagen R, et al. Intraoperative monitoring of active middle ear implant function in patients with normal and pathologic middle ears. *Otol Neurotol.* (2011) 32:104–7. doi: 10.1097/MAO.0b013e3181fcf167

9. Fröhlich L, Rahne T, Plontke SK, Oberhoffner T, Dziemba O, Gadyuchko M, et al. Intraoperative recording of auditory brainstem responses for monitoring of floating mass transducer coupling efficacy during revision surgery-proof of concept. *Otol Neurotol.* (2020) 41:e168–71. doi: 10.1097/MAO.0000000000002511

10. Rak K, Köstler C, Geiger U, Kaulitz S, Herrmann D, Shehata-Dieler W, et al. Application of an intraoperative auditory brainstem response measurement system in active middle ear implant revision surgery. *Otol Neurotol.* (2023) 44:483–92. doi: 10.1097/MAO.0000000000003851

11. Geiger U, Radeloff A, Hagen R, Cebulla M. Intraoperative estimation of the coupling efficiency and clinical outcomes of the vibrant soundbridge active middle ear implant using auditory brainstem response measurements. *Am J Audiol.* (2019) 28:553–9. doi: 10.1044/2019_AJA-18-0066

12. Verhaegen VJO, Mulder JJS, Noten JFP, Luijten BMA, Cremers CWRJ, Snik AFM. Intraoperative auditory steady state response measurements during Vibrant Soundbridge middle ear implantation in patients with mixed hearing loss: preliminary results. *Otol Neurotol.* (2010) 31:1365–8. doi: 10.1097/MAO.0b013e3181f0c612

13. Cargnelutti M, Cóser PL, Biaggio EPV. LS CE-Chirp(®) vs. click in the neuroaudiological diagnosis by ABR. *Braz J Otorhinolaryngol.* (2016) 83:313–7. doi: 10.1016/j.bjorl.2016.04.018

14. Cebulla M, Geiger U, Hagen R, Radeloff A. Device optimised chirp stimulus for ABR measurements with an active middle ear implant. *Int J Audiol.* (2017) 56:607–11. doi: 10.1080/14992027.2017.1314558

15. Cebulla M, Herrmann DP, Hagen R, Rak K. Intraoperative auditory brainstem response measurements via the vibrant soundbridge active middle ear implant: comparison of two methods. *Am J Audiol.* (2022) 31:261–7. doi: 10.1044/20227_AJA-21-00208

16. Sprinzl GM, Schorg P, Edlinger S, Ploder M, Magele A. Clinical feasibility of a novel test setup for objective measurements using the vibrant soundbridge. *Laryngosc Investig Otolaryngol.* (2022) 7:1113–9. doi: 10.1002/lio2.839

17. Fröhlich L, Rahne T, Plontke SK, Oberhoffner T, Dahl R, Mlynski R, et al. Intraoperative quantification of floating mass transducer coupling quality in active middle ear implants: a multicenter study. *Eur Arch Otorhinolaryngol.* (2021) 278:2277–88. doi: 10.1007/s00405-020-06313-z

Frontiers in Neurology

Explores neurological illness to improve patient care

The third most-cited clinical neurology journal explores the diagnosis, causes, treatment, and public health aspects of neurological illnesses. Its ultimate aim is to inform improvements in patient care.

Discover the latest Research Topics

See more →

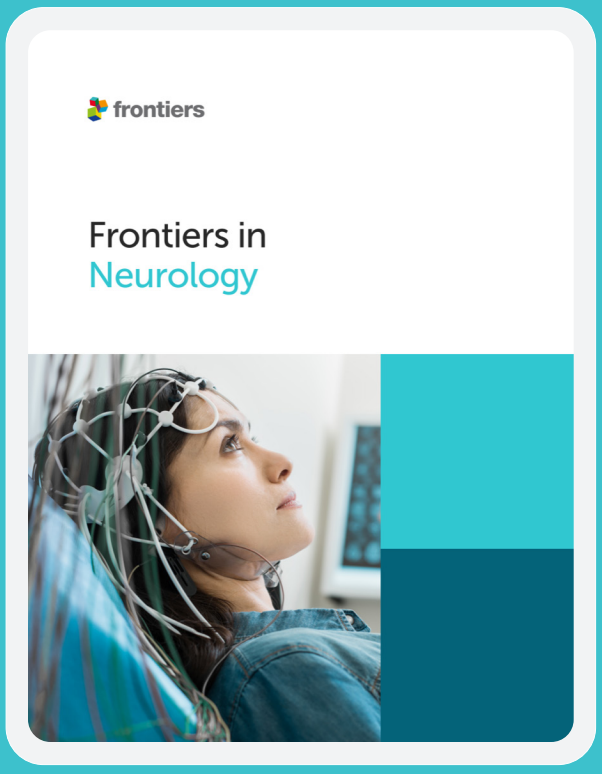

Frontiers

Avenue du Tribunal-Fédéral 34
1005 Lausanne, Switzerland
frontiersin.org

Contact us

+41 (0)21 510 17 00
frontiersin.org/about/contact